XIANWEN KONG

# TYPE SYNTHESIS AND KINEMATICS OF GENERAL AND ANALYTIC PARALLEL MECHANISMS

Thèse
présentée
à la Faculté des études supérieures
de l'Université Laval
pour l'obtention
du grade de Philosophiae Doctor (Ph.D.)

Département de génie mécanique
FACULTÉ DES SCIENCES ET DE GÉNIE
UNIVERSITÉ LAVAL
QUÉBEC

MARS 2003

# Abstract

Parallel mechanisms (PMs) have been and are being put into more and more use in motion simulators, parallel manipulators and parallel kinematic machines. To meet the needs for new, low-cost and simple PMs, a systematic study on the type synthesis and kinematics of general PMs and analytic PMs (APMs) is performed in this thesis. An APM is a PM for which the forward displacement analysis (FDA) can be solved using a univariate polynomial of degree 4 or lower. Firstly, a general approach is proposed to the type synthesis of PMs based on screw theory. Types of PMs generating 3-DOF translations, spherical motion and 4-DOF (3 translations and 1 rotation) motion are obtained. Full-cycle mobility conditions and validity conditions of the actuated joints are derived for these cases. Secondly, several approaches are proposed for the type synthesis of APMs. One class of the newly obtained APMs is linear PMs generating 3-DOF translations for which the FDA can be obtained by solving a set of linear equations. Thirdly, we present a comprehensive study, including the type synthesis, kinematic analysis and kinematic synthesis, on LTPMs. An LTPM is a PM generating 3-DOF translations with linear input-output equations and without constraint singularities. The proposed LTPMs may or may not contain some inactive joints and/or redundant joints. It is proved that an LTPM is free of uncertainty singularity. Isotropic conditions for the LTPMs are also revealed. An isotropic LTPM is globally isotropic. Fourthly, the FDA of several APMs is dealt with and the maximum number of real solutions is revealed for certain APMs. Finally, the singularity analysis of several typical PMs is dealt with. The one-to-one correspondence between the analytic expressions for four solutions to the FDA and the four singularity-free regions is revealed for a class of analytic planar PMs. This further simplifies the FDA since one can obtain directly the only

solution to the FDA once the singularity-free region in which the PM works is specified. The singularity analysis of a class of PMs is simplified based on the instability analysis of structures. The geometric characteristic is also revealed using linear algebra.

Xianwen Kong

Clément M. Gosselin

# Résumé

Les mécanismes parallèles (MPs) ont été et sont de plus en plus employés dans les simulateurs de mouvements, manipulateurs parallèles et machines-outils à cinématique parallèle. Afin de répondre aux besoins de nouveaux MPs à la fois simples et accessibles, une étude systématique de la synthèse architecturale et de la cinématique des MPs et MPs analytiques (MPAs) est proposée dans cette thèse. Un MPA est un MP pour lequel le problème géométrique direct (PGD) peut être résolu à l'aide d'un polynôme mono-variable de degré 4 ou moins. Premièrement, une approche générale pour la synthèse de MPs, basée sur la théorie des visseurs, est proposée. Des architectures de MPs ayant 3 ddl (degrés de liberté) en translation, ou en rotation (mouvement sphérique) ainsi qu'à 4 ddl (3 rotations et 1 translation) sont obtenues. Les conditions de mobilité globale et de validité des articulations actionnées sont décrites pour chaque cas. Deuxièmement, quelques approches sont proposées pour la synthèse de MPAs. Une classe parmi les nouveaux MPAs obtenus sont les MPs linéaires générant 3 ddl en translation, pour lesquels la solution du PGD est obtenue en résolvant un système d'équations linéaires. Troisièmement, nous présentons une étude complète, incluant la synthèse, l'analyse cinématique et la synthèse cinématique des MPTLs. Un MPTL est un MP ayant 3 ddl en translation ainsi que des équations d'entrées/sorties linéaires, sans aucune singularité de contrainte. Les MPTLs proposés peuvent contenir ou non des articulations inactives et/ou redondantes. Il est alors prouvé qu'un MPTL ne possède jamais de singularités incertaines. Les conditions d'isotropie des MPTLs sont elles aussi établies. Un MPLT isotropique est aussi globalement isotropique. Quatrièmement, le PGD de quelques MPAs est présenté ainsi que le nombre maximal de

solutions réelles de certains. Finalement, l'analyse des singularités de nombreux MPs typiques est présentée. La correspondance bijective entre les expressions analytiques des 4 solutions du PGD et les 4 régions sans singularités est révélée pour une classe particulière de MPAs plans. Ceci simplifie encore davantage le PGD car on peut alors obtenir directement la solution unique du PGD, une fois que la région exempte de singularités où le MP travaille est spécifiée. L'analyse des singularités d'une classe de MPs est simplifiée grâce à l'analyse d'instabilité des structures. Certaines caractéristiques géométriques sont aussi révélées en utilisant des résultats d'algèbre linéaire.

Xianwen Kong

Clément M. Gosselin

# Foreword

This thesis is completed at last, although there is still something to write.

I would like to express my gratitude to Prof. Clément M. Gosselin for his invaluable supervision, full support and critical review of the manuscript. I would like also to thank all my colleagues in the Robotics Laboratory for their help and cooperation. Thanks, in particular, go to Boris Mayer St-Onge for his help in using the laboratory facilities and Thierry Laliberté, Pierre-Luc Richard as well as Mathieu Goulet for the CAD and plastic models. I am also grateful to Drs. Just Herder and Dimiter Zlatanov as well as Prof. Jorge Angeles for their detailed remarks and suggestions in the revision of this thesis and to Lionel Birglen for his help in French translation.

I am deeply indebted to my wife, Hao Ma, and my son, Qingmiao Kong, for their understanding and support in my research during the past three years.

The financial support from NSERC and Innovatech through the PVR program is also acknowledged.

# Contents

# List of Tables

# List of Figures

# List of Symbols

| | |
|---|---|
| 3T1R-PKC | Parallel kinematic chain generating 3-DOF translations and 1-DOF rotation |
| 3T1R-PM | Parallel mechanism generating 3-DOF translations and 1-DOF rotation |
| APM | Analytic parallel mechanism |
| DOF | Degree of freedom |
| FDA | Forward displacement analysis |
| Linear TPM | Parallel mechanism generating 3-DOF translations for which the FDA can be obtained by solving a set of linear equations |
| LIO-TPM | Linear TPM with linear input-output relations |
| LTPM | Linear TPM with linear input-output relations and without constraint singularity |
| PKC | Parallel kinematic chain |
| PM | Parallel mechanism |
| PPKC | Parallel kinematic chain generating 3-DOF planar motion |
| PPM | Parallel mechanism generating 3-DOF planar motion |

| | |
|---|---|
| SPKC | Parallel kinematic chain generating 3-DOF spherical motion |
| SPM | Parallel mechanism generating 3-DOF spherical motion |
| TPKC | Parallel kinematic chain generating 3-DOF translations |
| TPM | Parallel mechanism generating 3-DOF translations |
| $\Delta$ | Number of over-constraints in a mechanism |
| $\Pi$ | Planar parallel parallelogram |
| $\$$ | Screw |
| $\$_0$ | Screw of zero-pitch |
| $\$_\infty$ | Screw of $\infty$ pitch |
| $\boldsymbol{\xi}$ | Twist |
| $\boldsymbol{\xi}_0$ | Twist of zero-pitch |
| $\boldsymbol{\xi}_\infty$ | Twist of $\infty$-pitch |
| $\boldsymbol{\zeta}$ | Wrench |
| $\boldsymbol{\zeta}_0$ | Wrench of zero-pitch |
| $\boldsymbol{\zeta}_\infty$ | Wrench of $\infty$-pitch |
| $\boldsymbol{\zeta}^i_{\not\supset j}$ | Effective wrench of joint $j$ in leg $i$ |
| $\boldsymbol{\zeta}^i_{t\not\supset j}$ | t-component of the effective wrench of joint $j$ in leg $i$ |
| $\boldsymbol{\zeta}^i_{w\not\supset j}$ | w-component of the effective wrench of joint $j$ in leg $i$ |
| $c$ | Order of the wrench system of a mechanism |
| $c^i$ | Order of the wrench system of leg $i$ in a parallel mechanism |
| $\mathcal{C}$ | Connectivity (or relative degree of freedom of motion between the moving platform and the base) of a parallel kinematic chain |
| C | Cylindrical joint |
| $\underline{\text{C}}$ | Cylindrical joint in which the translational degree of freedom is actuated |

| | |
|---|---|
| $f$ | Degree of freedom (also mobility) of a mechanism |
| $f^i$ | Degree of freedom of leg $i$ |
| $f_j$ | Degree of freedom of joint $j$ |
| H | Helical joint |
| P | Prismatic joint |
| $\underline{\mathrm{P}}$ | Actuated prismatic joint |
| R | Revolute joint |
| $\bar{\mathrm{R}}$ | Revolute joint with parallel axes within a same leg |
| $\dot{\mathrm{R}}$ | Revolute joint with parallel axes within a same leg |
| $\acute{\mathrm{R}}$ | Revolute joint with parallel axes within a parallel kinematic chain or a leg |
| $\ddot{\mathrm{R}}$ | Revolute joint with concurrent axes within a parallel kinematic chain or a leg |
| $\underline{\mathrm{R}}$ | Actuated revolute joint |
| $R^i$ | Redundant degree of freedom of motion of leg $i$ |
| $\overbrace{\mathrm{RRR}}$ | Three successive R joints with concurrent axes within a leg |
| $\widetilde{\mathrm{RRR}}$ | Three successive R joints which belong to a virtual Bennett mechanism within a leg |
| S | Spherical joint |
| $\mathcal{T}$ | Twist system |
| $\mathcal{T}^i$ | Twist system of leg $i$ |
| $\mathcal{T}_j^i$ | Twist system of joint $j$ in leg $i$ |
| $\mathcal{T}_j$ | Twist system of joint $j$ |
| U | Universal joint |
| V | Virtual joint with 3 translational degrees of freedom |

| | |
|---|---|
| W | Virtual joint with 3 translational degrees of freedom and 1 rotational degree of freedom |
| $\mathcal{W}$ | Wrench system |
| $\mathcal{W}_j$ | Wrench system of joint $j$ |
| $\mathcal{W}^i$ | Wrench system of leg $i$ |
| $\mathcal{W}_j^i$ | Wrench system of joint $j$ in leg $i$ |
| X | Any joint with single degree of freedom of motion |
| $\overline{\text{XXX}}$ | Three joints which are equivalent to a planar joint |

# Chapter 1

# Introduction

Parallel mechanisms (PMs) have been and are being put into use in a large variety of applications such as motion simulators and parallel manipulators. Type synthesis and kinematics are two fundamental and important issues in the study of PMs. They are also the two initial steps to develop motion simulators and parallel manipulators. In this chapter, the background and the subject of this thesis is presented. The state or the art of the research is also reviewed. Finally, the outline of this thesis is proposed.

## 1.1 Background

A parallel mechanism (PM) is a multi-DOF (degree of freedom) mechanism composed of one moving platform and one base connected by at least two serial kinematic chains

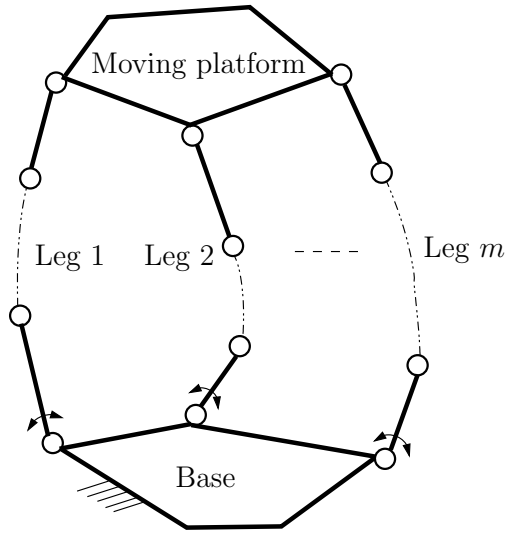


Figure 1.1: Schematic representation of a PM.

in-parallel (Fig. 1.1). These serial kinematic chains are called legs or limbs.

As compared with serial mechanisms, properly designed PMs have higher stiffness and higher accuracy, although their workspaces are smaller. PMs have been and are being put into use in a large variety of applications [1, 2, 3, 4, 5, 6, 7]. The first application of a six-legged PM dates back to the 1950's when a tire testing machine based on a PM was developed by Gough (Fig. 1.2(a)[2]). In the 1970's, flight simulators (Fig. 1.2(b)) based on PMs were put into practice. Since the 1980's, the research on parallel manipulators (Fig. 1.2(c)) has attracted the interest of many researchers and is still the focus of several important research projects. Parallel manipulators alone also cover a wide range of applications in assembly, inspection and others. Some parallel manipulators, such as the Gough-Stewart platform and the Delta robot, have been put into practice. In the past decade, PMs have also been used in machine tools, also referred to as parallel kinematic machines (see Fig. 1.2(d)), haptic devices (Fig. 1.2(e)), medical robots (Fig. 1.2(f)[7]), alignment devices (Fig. 1.2(g)[7]), coordinate measuring machines as well as force sensors.

So far, many types of PMs have been proposed, and several approaches have also been proposed for the type synthesis of PMs [11, 12, 13, 14, 15, 16, 17, 18, 19, 20, 21, 22, 23, 24, 25, 26, 27, 28, 29, 30, 31]. In [32] and [33], a comprehensive list of PMs has been presented. Due to the large variety of applications of PMs, the motion patterns of the moving platform required by different applications vary to a great extent. There is

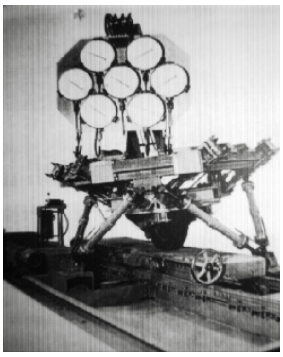

(a) Gough's original tire testing machine

(b) Flight simulator from CAE Electronics Ltd of Canada.

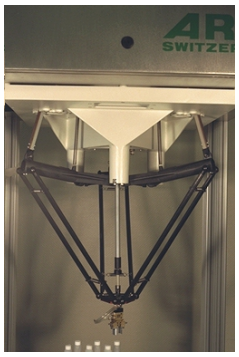

(c) Delta robot from Demaurex SA

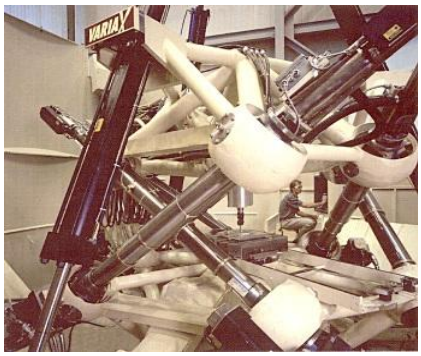


(d) Parallel kinematic machine (Variax from Giddings & Lewis).

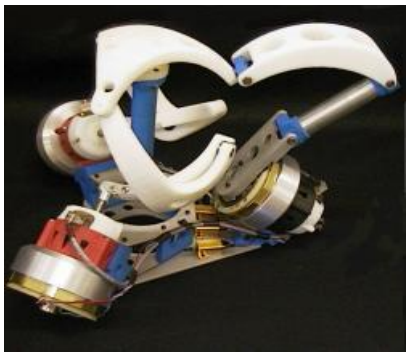

(e) Haptic device (courtesy of the Laval University Robotics Lab).

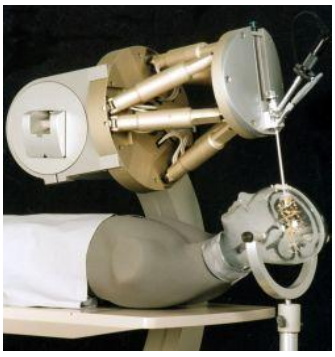

(f) Medical robot (courtesy of IPA)

(g) Active secondary mirror for Telescope from IPA

Figure 1.2: Applications of PMs.

still a great need to find new PMs [8, 9] generating desired motion patterns. This will also facilitate the development of hybrid kinematic machine tools in which two PMs are used cooperatively. However, due to the complexity of PMs, the type synthesis of PMs has not been well studied. All the current approaches to the type synthesis of PMs have some restrictions (for details, see section 1.2).

Usually the inverse kinematics of PMs is very simple, while their forward displacement analysis (FDA) is very complex. The FDA of a PM consists in finding the pose (position and orientation) of the moving platform for a set of specified values of the inputs. For the general 6-U$\underline{\text{P}}$S [1] (6-S$\underline{\text{P}}$S or Gough-Stewart platform) PM, the FDA can have up to 40 solutions [34]. In addition, the singularity-free trajectory planning of PMs is also very complicated [35]. Due to the complexity of PMs, it is logical to start with some simple PMs. Hence, the investigation on analytic parallel mechanisms (APMs) began a few years ago [36, 37, 38, 39, 40, 41, 42, 43, 44, 45, 46, 47]. APMs are PMs with a characteristic polynomial of fourth degree or lower. The FDA of APMs can be performed analytically and efficiently since the roots of a polynomial equation of fourth degree or lower can be obtained as algebraic functions of its coefficients while for a polynomial equation of degree higher than 4, in general, no such algebraic function of roots can be found [48]. It is necessary to rely on algorithmic numerical methods to obtain the roots of a polynomial equation of degree higher than 4. Unlike more complex PMs, no additional sensors are needed in APMs in order to solve the FDA in real time. The cost of APMs is thus reduced in this respect. As reported in [8], the high non-linearity of PMs is one of the reasons which prevents the end-users from better understanding and adopting PMs. The research on APMs may help to remove such a burden.

Up to now, most of the existing APMs have been proposed following an intuitive approach. One APM, the Delta PM, has been put into practical use [36]. Several prototypes of some APMs, such as the Agile Eye (Fig. 1.3) [44], have been built. As in the case of general PMs, little work [39, 40] has been performed on the systematic type synthesis of APMs.

In short, new PMs and APMs are needed and the research on PMs does not meet this need.

[1] R, P, C, U, S, $\underline{\text{R}}$ and $\underline{\text{P}}$ are used to denote a revolute joint, a prismatic joint, a cylindrical joint, a universal joint, a spherical joint, an actuated revolute joint and an actuated prismatic joint respectively.

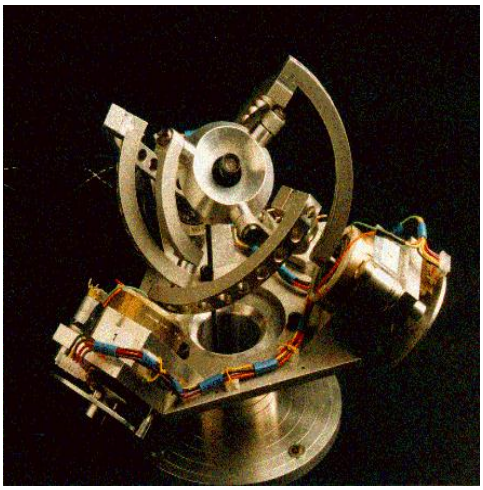

Figure 1.3: Agile Eye (courtesy of the Laval University Robotics Lab).

## 1.2 Literature review

Given the context presented above on the research on PMs, in this thesis, a systematic type synthesis of general PMs and APMs will be performed and the kinematics of PMs will be studied. Type synthesis and kinematics are two fundamental and important issues in the study of PMs. They are also the two initial steps to develop motion simulators and parallel manipulators. Here, the research on the kinematics of PMs is confined to issues such as the FDA, the instantaneous kinematics, the singularity analysis, the workspace analysis as well as the kinematic design.

### 1.2.1 Type synthesis of parallel mechanisms

PMs are a class of multi-loop spatial mechanisms. In the review of the type synthesis of PMs, the work on the type synthesis of multi-loop spatial mechanisms should also be taken into consideration. Type synthesis of $f$-DOF mechanisms can be roughly divided into two stages. The first is to perform the type synthesis of $f$-DOF kinematic chains and the second is to select $f$ actuated joints in an $f$-DOF kinematic chain to obtain $f$-DOF mechanisms.

**Type synthesis of multi-loop spatial mechanisms**

The type synthesis of multi-loop spatial mechanisms deals with the generation of all types (architectures) of multi-loop spatial mechanisms for a specified DOF. The type synthesis of multi-loop spatial mechanisms began in the 1960's and was perhaps the least explored area of research in the science of mechanisms until 1991 [49]. Since 1991, some progress has been made in this aspect. The type synthesis of multi-loop spatial mechanisms is usually based on the mobility criterion of a mechanism which takes one of the following forms [11, 12, 15, 50].

$$f = d(n - g - 1) + \sum_{j=1}^{g} f_j \tag{1.1}$$

where $f$ is the mobility or relative DOF of a kinematic chain, $n$ is the number of links including the base, $g$ is the number of joints, $f_j$ is the freedom of the $j$-th joint, $d$ is the the number of independent constraint equations within a loop, or

$$f = \sum_{j=1}^{g} f_j - dv \tag{1.2}$$

where $v$ is the number of independent loops in the mechanism, or

$$f = \sum_{j=1}^{g} f_j - \min \sum_{i=1}^{v} d_i \tag{1.3}$$

where $d_i$ is the number of independent constraint equations within loop $i$, $\sum_{i=1}^{v} d_i$ is the sum of $d_i$ in a set of $v$ independent loops, $min\sum_{i=1}^{v} d_i$ is the minimum of $\sum_{i=1}^{v} d_i$ of all the sets of $v$ independent loops.

Equation (1.1) is usually referred to as the Chebychev-Grübler-Kutzbach criterion or the general mobility criterion.

The type synthesis of multi-loop spatial mechanisms in which all the loops have the same number of independent constraint equations has been dealt with by several authors (such as [51]) based on the mobility equation (Eq. (1.2)). In 1994, the type synthesis of spatial mechanisms involving R and P joints in which all the loops have 6 independent constraint equations was dealt with in [52, 53]. Spatial kinematic chains with inactive joints due to P joints were revealed. In 1998, the type synthesis of spatial mechanisms in which not all the loops have the same number of independent constraint equations (Eq.(1.3)) was dealt with in [54].

The selection of actuated joints has been overlooked for a long time. One reason is that most works on the type synthesis of spatial linkages focus on 1-DOF kinematic chains. For a 1-DOF kinematic chain, any one of the joints can be actuated. There is no invalid actuated joint appearing in 1-DOF mechanisms. The other reason is that the validity condition of actuated joints has been proposed (see for example [50]) and stated in the following fashion:

For an $f$-DOF mechanism, a set of $f$ actuated joints is valid if the DOF of the kinematic chain obtained from the mechanism by blocking all the actuated joints is 0.

However, in the selection of actuated joints using the above condition, the calculation of DOF encountered is in fact very difficult. In 1999, a validity condition of actuated joints was proposed in [55] for spatial mechanisms involving R and P joints in which each loop has six independent constraint equations.

At present, both the type synthesis of spatial kinematic chains and the selection of actuated joints of spatial kinematic chains are not yet fully solved.

**Type synthesis of PMs**

The type synthesis of PMs deals with the generation of all types (architectures) of PMs for a specified DOF or a specified motion pattern of the moving platform. The motion pattern of the moving platform contains more information than the mobility of the moving platform. Most works proposed new PMs on a case by case basis while a few [10, 11, 12, 13, 14, 15, 16, 17, 18, 19, 20, 21, 22, 27, 28] presented systematic approaches for the type synthesis of PMs.

The type synthesis of parallel kinematic chains began in 1970's [10]. Some progress has been made in [11, 12, 13, 14, 15, 16, 17, 18, 19, 20, 21, 22, 23, 24, 25, 26, 27, 28, 29, 30, 31].

The type synthesis of PMs with a specified number of DOF is performed based on the mobility equation (Eqs. (1.1) and (1.3)). In [11], the type synthesis of PMs has been solved for the case of $d$=2, 3, 4 and 6. Some PMs generating two translations, three translations, planar motions, spherical motions and 3T1R (three translations and 1 rotations) motions were obtained. In [12, 15], type synthesis of PMs for the case

of $d$=6 are dealt with. This approach is most appropriate for the type synthesis of PMs with full-DOF (6 for spatial PM and 3 for spherical and planar PMs). However, PMs that do not satisfy the current mobility criteria could not be obtained using this approach.

The type synthesis of PMs with a specified motion pattern has been performed in [10, 13, 14, 17, 18, 19, 20, 21, 22, 27, 28, 29, 30, 31]. In [13, 14], the type synthesis of TPMs (PMs with three translational DOFs) has been performed using displacement group theory. All the TPKCs (translational parallel kinematic chains) with 3- or 4-DOF legs have been proposed. In [10], where a TPKC is used as a constant-velocity coupling connecting two parallel axes, Hunt proposed an approach based on screw theory for the type synthesis of 3-legged TPKCs with 5-DOF legs and all the types of 5-DOF legs have been obtained. However, Hunt himself did not mention his work on the type synthesis of TPKCs in [11]. An unfortunate consequence of this omission was that his work on TPKCs has been neglected for a long time. Several authors worked independently on the type synthesis of TPKCs with 5-DOF legs [17, 18, 22] and the same results were re-obtained. The contribution of [17, 18, 22] lies in that the full-cycle mobility conditions, which are given in [10] without detailed explanations, were derived algebraically. It was thus implicitly proved that there are no 5-DOF legs composed of R and P joints for TPKCs except those identified in [10]. The type synthesis of 3-DOF SPMs (spherical parallel manipulator) was dealt with in [16, 28]. The type synthesis of 4-DOF (three rotations and 1 translation) PMs was dealt with in [19]. The type synthesis of 4-DOF (three translations and 1 rotation) PMs was dealt with in [20, 31]. The type synthesis of 5-DOF (three translations and 2 rotations) PMs was dealt with in [21]. The type synthesis of 5-DOF (two translations and 3 rotations) PMs was dealt with in [23]. Some 3-DOF PMs with peculiar characteristics were proposed in [58].

The approaches to the type synthesis of PKCs generating a specified motion pattern fall into four classes that will be described in the following.

(1) The approach based on screw theory [10, 17, 18, 27, 28, 29].

This approach is general. It is most appropriate for the type synthesis of PMs with prescribed motion patterns, such as 3-DOF translation, spherical motion and so on. One of the key issues in using the approach based on screw theory is to find the condition of full-cycle mobility. This problem is still not fully solved.

(2) The approach based on the displacement group theory [13, 14, 16, 30, 31].

Like the approach based on screw theory, this approach is also general. It is also most appropriate for the type synthesis of PMs with prescribed motion patterns, such as 3-DOF translation, spherical motion and so on. The characteristic of this approach is that PMs obtained have full-cycle mobility. However, this approach may encounter some difficulties in the type synthesis of PMs with 5-DOF legs.

(3) The approach based on kinematics [22].

This approach was applied to the type synthesis of TPMs with 5-DOF legs. The derivation needed is very complicated. This approach has no advantage as compared with the approach based on screw theory.

(4) The approach based on single-opened-chain units [20, 21].

Some types of 3T1R-PMs and 5-DOF PMs have been obtained using this approach. However, using this approach in its current state of development, not all the types of PMs generating the desired motion patterns can be obtained. Only the PMs that satisfy the general mobility criterion (see Eq. (1.3)) with variable $d$ can be obtained.

Little work has been done on the selection of actuated joints for PMs. The reason is that for most of the proposed $f$-DOF PMs, any set of $f$ joints can be actuated. In [56], a validity condition of actuated joints was proposed based on screw theory and the selection of actuated joints for a 2-DOF PPM (planar PM) was discussed in detail. In [57], an alternative validity condition of actuated joints was proposed based on screw theory, and the selection of actuated joints for a 3-DOF PM and a 4-DOF PM was discussed in detail. For a spatial PM, the validity detection of the actuated joints requires the calculation of a $6 \times 6$ determinant when the above approaches are applied. The above works laid the foundation for the selection of actuated joints for PMs. For a given PKC, the selection of actuated joints should be dealt with individually. Once new PKCs appear, the selection of actuated joints should be considered to obtain new PMs.

So far, both stages of the type synthesis of PMs, namely (1) the type synthesis of PKCs and (2) finding the validity condition of actuated joints of PMs have not been

well studied. The research at the current state of development does not meet the needs to develop new PMs,

Except in the works on the type synthesis of PKCs based on the displacement group theory, the mobility criteria shown in Eqs. (1.1), (1.2) or (1.3) are used. This mobility criterion cannot cover those overconstained PMs that do not satisfy these mobility criteria. On the other hand, the approach based on the displacement group theory may encounter some difficulties in the type synthesis of PMs with 5-DOF legs. Screw theory provides a way of solving these problems.

As a first objective, this thesis tries to solve the above problems encountered in the type synthesis of PMs and proposes a general approach, based on screw theory, to the type synthesis of PMs. In addition, type synthesis of PMs with the most commonly used motion patterns will be performed. The key issue in the type synthesis of PKCs using screw theory is to derive the full-cycle mobility conditions.

### 1.2.2 Type synthesis of analytic parallel mechanisms

An APM is a PM which has characteristic polynomial of fourth degree or lower. The FDA of APMs can be performed analytically and efficiently. APMs are suitable for fast PMs design from the kinematic point of view. The type synthesis of APMs consists of revealing the topological conditions, the constraints on joint types and/or the dimensional conditions for a given type of PM which reduce the degree of the characteristic polynomial of the PM to four or lower.

The first APM is the Delta PM [36]. The joint type conditions for analytic PPMs have been investigated in [42]. References [39, 41] studied the dimensional conditions for analytic PPMs. Reference [44] revealed the dimensional conditions for a class of analytic SPMs (spherical PMs) with actuated R joints. Reference [46] revealed the dimensional conditions for a class of analytic SPMs with actuated P joints. References [37, 38, 40, 45, 47] revealed some dimensional conditions of 6-S$\underline{\text{P}}$S APMs. So far, two systematic approaches have been proposed to the type synthesis of APMs, i.e., the component approach [40] and the algebraic FDA-based approach [39]. Overall, the problem of the type synthesis of APMs is far from being solved. One reason is that

there is many link parameters in a PM [59], the other reason is that new types of PMs are being proposed with the progress in the type synthesis of general PMs.

The type synthesis of APMs in this thesis will focus on the development of methods for the type synthesis of APMs and the generation of new APMs.

### 1.2.3 Forward displacement analysis of parallel mechanisms

For a PM, the inverse displacement analysis is usually very easy while the FDA is usually very complex.

Many papers have been published on the FDA of PMs and different approaches have been proposed. The approaches to the FDA fall into the following classes, (1) the iterative approach, (2) the elimination approach [60, 61], (3) the continuation approach [62] and (4) the sensor based approach [63, 64, 65, 66, 67, 68].

Since the FDA of an APM can be reduced to the solution of a univariate equation of degree 4 of lower, it is suitable to perform the FDA of the APM using the elimination approach. In this thesis, we focus on the FDA of some APMs using the elimination approach.

### 1.2.4 Instantaneous kinematics of parallel mechanisms

The instantaneous kinematics of PMs deals with the velocity analysis of the PMs. It includes the inverse velocity analysis and the forward velocity analysis.

Several general approaches have been proposed to solve the instantaneous kinematics of PMs. For example, the conventional approach [69], the approach based on screw theory [56, 70, 71, 72], and the kinematic influence coefficient approach [73, 74, 75, 76, 77, 78].

Usually, an efficient method should be proposed for a PM or APM by taking into consideration its specific characteristics. In this thesis, we focus on finding efficient

methods for the determination of the instantaneous kinematics of some APMs.

### 1.2.5 Kinematic singularity analysis of parallel mechanisms

Kinematic singularity analysis is an important issue in the design and control of PMs. When kinematic singularities occur, the moving platform may lose or gain some DOFs of motion when the inputs are specified. Kinematic singularities are classified into the following two basic classes [79], namely, the inverse kinematic singularity and the forward kinematic singularity. When the inverse kinematic singularities occur, the moving platform loses one or more DOFs of motion. When the forward kinematic singularities occur, the moving platform gains some DOFs of motion when the inputs are specified. Forward kinematic singularities can be further classified [80] into two sub-classes, the singularities in which the PM undergoes infinitesimal motion and the singularities in which the PM undergoes finite motion when the inputs are given. A PM is called architecturally singular [80] or permanently singular [32] if each of its configurations is a singular configuration in which the moving platform can undergo finite motion when the inputs are specified. The classification of singularities has been further studied in [81, 82] and [83].

The inverse kinematic singularity analysis of a PM is the same as the inverse singularity analysis of serial mechanisms. This problem has been well solved. The forward kinematic singularity analysis of a PM is usually very complex. It is difficult to analyze and has received much attention from many researchers over the past two decades.

Different approaches have been proposed for the forward kinematic singularity analysis of PMs. For example, the method based on line geometry or screw theory [71, 81, 83, 84, 85, 86, 87, 88, 89, 90, 91, 92], the algebraic method based on the Jacobian matrix [79, 80, 93], the method based on a differentiation of the closure equations [94, 95] and the component approach [96, 97]. Some results have also been obtained on the generation of architecturally singular Gough-Stewart platforms [97, 98, 99, 100, 101, 102]. Using the method based on line geometry or screw theory, the geometric meaning of singularity conditions is clear while the forward kinematic singularity analysis of PMs is reduced to a $6 \times 6$ determinant. Using the other approaches, the forward kinematic singularity analysis of PMs is reduced to an $N \times N$ ($N \leq 6$) determinant while input

velocities appear in the derivation. According to the physical meaning of the forward kinematic singularity analysis of PMs, there is no need for the input velocities to appear in the derivation. Thus, the approaches to the forward kinematic singularity analysis of PMs should be simplified.

In addition, the characteristics of forward kinematic singularities of a planar APM is partially revealed in [41] numerically and in [103] using the condition of singular-free change of assembly modes. The characteristic of the planar APM should be revealed fully using an algebraic approach.

In this thesis, the forward kinematic singularity analysis of some APMs will be performed in order to reveal the characteristics of the singularity loci of APMs as compared with PMs of the general form. In addition, an approach based on the instability analysis of structures is proposed to simplify the forward kinematic singularity analysis of PMs. The geometric interpretation of the singular conditions is also re-obtained for a broad class of PMs using linear algebra.

### 1.2.6 Workspace analysis of parallel mechanisms

Workspaces are defined as regions which can be reached by a reference frame located on the moving platform. Different types of workspaces are defined in [104] for PMs. Up to now, different approaches [78, 105] have been proposed for the determination of the workspace of a PM.

In this thesis, we focus on the workspace analysis of some new APMs with great application potential using the geometric approach [105].

### 1.2.7 Kinematic synthesis of parallel mechanisms

The kinematic synthesis of PMs has been investigated from different points of view, and a great number of papers on this issue have been published [8, 32]. Different criteria, such as the global dexterity or the specified workspace [106], have been proposed for the kinematic synthesis of PMs. Meanwhile, different approaches have been proposed

to solve the problem [8, 107, 108].

This thesis tries to extend the global dexterity based approach [106] to the kinematic synthesis of some new APMs of great application potential. To verify the theoretical results, obtained especially in the type synthesis of APMs, physical models are built using a commercial CAD software and an FDM (Fused Deposition Modeling) rapid prototyping machine as proposed in [109].

## 1.3 Thesis scope

Due to the comprehensive topics of this thesis, the subject of this thesis has been given in the literature review. For clarity, the scope of the thesis is summarized as follows.

1. Type synthesis of PMs.

   As a first objective, this thesis aims at solving the not-fully solved problems encountered in the type synthesis of PMs. A general approach will be proposed, based on screw theory, to the type synthesis of PMs generating a specified motion pattern. In addition, type synthesis of PMs with the most commonly used motion patterns will be performed.

2. Type synthesis of APMs.

   An APM has a characteristic polynomial of fourth degree or lower and the FDA of APMs can be performed analytically and efficiently. APMs are suitable for fast PMs from the kinematic point of view. As a second objective, this thesis will propose methods for the type synthesis of APMs. New APMs will also be generated.

3. Kinematics of APMs.

   As a third objective, this thesis will deal with the kinematics of a class of PMs with linear input-output relations we obtained which has a great potential application. The kinematics includes the FDA, the instantaneous kinematics, the workspace analysis and the kinematic design of these APMs.

4. Kinematic singularity analysis of PMs.

As the last objective, this thesis will focus on revealing the kinematic characteristics of APMs from the perspective of kinematic singularities and simplifying the forward kinematic singularity analysis of a class of PMs used in practice.

## 1.4 Thesis organization

This thesis includes mainly three parts.

Part 1 deals with the type synthesis of PMs. This part includes Chapters 2–6. Chapter 2 provides the theoretical framework required for the type synthesis of PMs. A review of important results from screw theory is given. In Chapter 3, a method for the type synthesis of PMs based on screw theory is proposed. The proposed approach is used to the type synthesis of 3-DOF TPMs (translational PMs), 3-DOF SPMs (spherical PMs) and 4-DOF 3T1R-PMs (3 translations and 1 rotation PMs) in Chapters 4, 5 and 6, respectively. Many new PMs are proposed.

Part 2 includes only Chapter 7. This part deals mainly with the generation of APMs from PMs obtained in Part 1. APMs are PMs with a characteristic polynomial of fourth degree or lower. The FDA of APMs can be performed analytically and efficiently. Several approaches, namely the decomposition approach, the geometric approach and the algebraic approach, are proposed for the type synthesis of APMs. Using these approaches, some APMs are generated from the PMs obtained in Part 1. An approach is also proposed to generate some APMs directly from analytic components, without first performing the type synthesis of PMs using the general approach. A brief comparison of the different approaches is also presented.

Part 3 discusses some kinematic issues on APMs and general PMs. Part 3 is composed of three chapters (Chapters 8–10). Chapter 8 deals with the type synthesis, the kinematic analysis and the kinematic synthesis of LTPMs (TPMs with linear input-output equations and without constraint singularities). LTPMs are a subset of analytic TPMs obtained in Part 2. In Chapter 9, we deal with the FDA of several APMs generated in Part 2. The FDA of the APMs dealt with in this chapter is more complex than the LTPMs dealt with in Chapter 8. In Chapter 10, the forward kinematic singularity analysis of several typical PMs are dealt with. At first, we discuss the forward

kinematic singularity analysis of an APM. The results are used to further simplify the FDA. The characteristic of this APM is revealed from the perspective of kinematic singularities. A new method is proposed for the singularity analysis of a broad class of PMs. The geometric characteristics of the forward kinematic singularities are revealed using a method based on linear algebra.

Finally, conclusions are drawn and future work is suggested in Chapter 11.

# Chapter 2

# Theoretical background

This chapter provides the theoretical framework required for the type synthesis of parallel mechanisms. First, a review of important results from screw theory is given. Screw theory will prove to be extremely useful in the type synthesis of parallel kinematic chains. Especially the principle of reciprocity of screws will be fruitful in the type synthesis of the legs and the composition of legs into a parallel kinematic chain. Subsequently, a mobility equation for parallel mechanisms is proposed that is different from existing ones, and which will facilitate the type synthesis of parallel kinematic chains. Finally, for use in the development of a parallel kinematic chain into a parallel mechanism, a validity condition is proposed for the selection of the actuated joints.

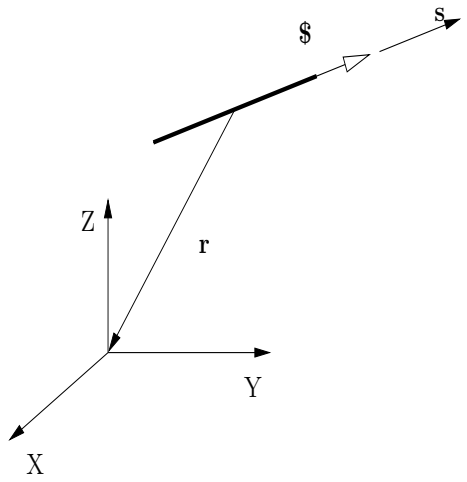


Figure 2.1: Screw.

## 2.1 Screw theory

In this section, the relevant results of screw theory are given for a better understanding of this thesis [71, 110].

### 2.1.1 Screws

A (normalized) screw is defined by (See Fig. 2.1)

$$\$ = \begin{bmatrix} \$_F \\ \$_S \end{bmatrix} = \begin{cases} \begin{bmatrix} \mathbf{s} \\ \mathbf{s} \times \mathbf{r} + h\mathbf{s} \end{bmatrix} & \text{if } h \text{ is finite} \\ \begin{bmatrix} \mathbf{0} \\ \mathbf{s} \end{bmatrix} & \text{if } h = \infty \end{cases} \tag{2.1}$$

where $\mathbf{s}$ is a unit vector along the axis of the screw $\$$, $\mathbf{r}$ is the vector directed from any point on the axis of the screw to the origin of the reference frame O-XYZ, and $h$ is called the pitch. It is noted that there are two vector components or six scalar components in the above presentation of the screw.

For convenience, $\$_0$ and $\$_\infty$ are used to represent a screw of 0-pitch and a screw of $\infty$-pitch respectively.

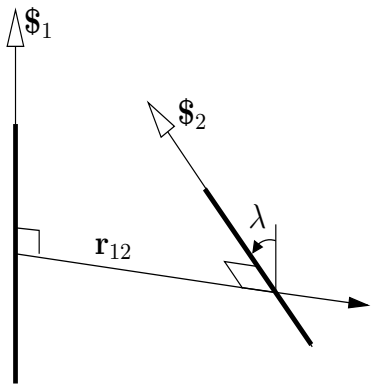


Figure 2.2: Reciprocal screws.

### 2.1.2 Reciprocal screws

Two screws, $\$_1$ and $\$_2$, are said to be reciprocal if they satisfy the following condition (Fig. 2.2):

$$\$_1 \circ \$_2 = [\mathbf{\Pi}\$_1]^T \$_2 = 0 \tag{2.2}$$

where

$$\mathbf{\Pi} = \begin{bmatrix} \mathbf{0} & \mathbf{I}_3 \\ \mathbf{I}_3 & \mathbf{0} \end{bmatrix} \tag{2.3}$$

where $\mathbf{I}_3$ is the $3 \times 3$ identity matrix and $\mathbf{0}$ is the $3 \times 3$ zero matrix.

The reciprocity condition can be derived as

$$\begin{cases} \text{no constraint} & \text{if } h_1 \text{ and } h_2 \text{ are both } \infty \\ \cos\lambda = 0 & \text{if } h_1 \text{ or } h_2 \text{ is } \infty \\ (h_1 + h_2)\cos\lambda - r_{12}\sin\lambda = 0 & \text{if } h_1 \text{ and } h_2 \text{ are both finite} \end{cases} \tag{2.4}$$

where $r_{12}$ is the offset distance along the common perpendicular leading from screw $\$_1$ to screw $\$_2$ and $\lambda$ is the angle between the axes of $\$_1$ and $\$_2$, measured from $\$_1$ to $\$_2$ about the common perpendicular according to the right-hand rule as shown in Fig. 2.2.

It can be concluded from Eq. (2.4) that 1) Two $\$_\infty$'s are always reciprocal to each other; 2) An $\$_\infty$ is reciprocal to a $\$_0$ if and only if their axes are perpendicular to each other; and 3) Two $\$_0$'s are reciprocal to each other if and only if their axes are coplanar.

### 2.1.3 Screw systems and reciprocal screw systems

A screw system of order $n$ ($0 \leq n \leq 6$) comprises all the screws that are linearly dependent on $n$ given linearly independent screws. A screw system of order $n$ is also called an $n$-system. Any set of $n$ linearly independent screws within an $n$-system forms a basis of the $n$-system. Usually, the basis of an $n$-system can be chosen in different ways. Given an $n$-system, there is a unique reciprocal screw system of order $(6-n)$ which comprises all the screws reciprocal to the original screw system. Let $\mathcal{T}$ and $\mathcal{T}^{\perp}$ denote a screw system and its reciprocal screw system. We have

$$\mathcal{T} = (\mathcal{T}^{\perp})^{\perp} \tag{2.5}$$

where $()^{\perp}$ denotes the reciprocal screw system of the screw system within the parentheses.

### 2.1.4 Twist systems and wrench systems of kinematic chains

A screw $\$$ multiplied by a scalar $\rho$, $\rho\$$, is called a twist if it represents an instantaneous motion of a rigid body, and a wrench if it represents a system of forces and couples acting on a rigid body. The reciprocity condition (Eq. (2.4)) can be stated as the virtual power developed by a wrench about one screw along a twist about another screw being equal to zero.

The twist system of a kinematic chain, in the form of a kinematic joint, serial kinematic chain or PKC, is an $f$-system where $f \leq F$ and $F$ denotes the DOF of the kinematic chain. The wrench system of a kinematic chain is a $(6-f)$-system. The twist system of a kinematic chain is the reciprocal screw system of its wrench system, and vice versa.

In the following, $\boldsymbol{\xi}$ and $\boldsymbol{\zeta}$ are used to represent a twist and one of its wrenches, while $\mathcal{T}$ and $\mathcal{W}$ are used to represent a twist system and its wrench system. Equation (2.5) can be rewritten as

$$\begin{cases} \mathcal{W} = \mathcal{T}^{\perp} \\ \mathcal{T} = \mathcal{W}^{\perp} \end{cases} \tag{2.6}$$

Similarly to the notation for $\$_0$ and $\$_\infty$, the symbols $\boldsymbol{\xi}_0$, $\boldsymbol{\xi}_\infty$, $\boldsymbol{\zeta}_0$ and $\boldsymbol{\zeta}_\infty$ are used to represent a normalized twist of 0-pitch, a normalized twist of $\infty$-pitch, a normalized wrench of 0-pitch and a normalized wrench of $\infty$-pitch, respectively.

**Kinematic joints**

The commonly used kinematic joints are R, P, C, U and S joints. The twist systems and wrench systems of R and P kinematic joints are presented below.

- R (Revolute) joint

  The twist system of an R joint is a 1-system. The twist in the 1-system is a $\boldsymbol{\xi}_0$ directed along the joint axis. The wrench system is a 5-system which includes all the $\boldsymbol{\zeta}_0$'s whose axes intersect with the joint axis and all the $\boldsymbol{\zeta}_\infty$'s whose axes are perpendicular to the axis of the R joint.

- P (Prismatic) joint

  The twist system of a P joint is a 1-system. The twist in the 1-system is a $\boldsymbol{\xi}_\infty$ in the direction of the joint axis. The wrench system is a 5-system which includes all the $\boldsymbol{\zeta}_0$'s whose axes are perpendicular to the joint axis and all the $\boldsymbol{\zeta}_\infty$'s.

**Serial kinematic chains**

For simplicity and without loss of generality, we make the assumption that a serial kinematic chain is composed of 1-DOF joints since an $l$-DOF joint can be treated as a serial kinematic chain of $l$ 1-DOF joints. The output twist of the moving platform in a serial kinematic chain (Fig. 2.3) is

$$\boldsymbol{\xi} = \sum_{j=1}^{f} \boldsymbol{\xi}_j \dot{\theta}_j \tag{2.7}$$

where $\boldsymbol{\xi}_j$ and $\dot{\theta}_j$ are, respectively, the twist and the velocity of the $j$-th joint and $f$ denotes the DOF of the serial kinematic chain.

From Eq. (2.7), we can conclude that the twist system $\mathcal{T}$ of (the moving platform in) a serial kinematic chain is the union (linear combination) of the twist systems $\mathcal{T}_j$ of all

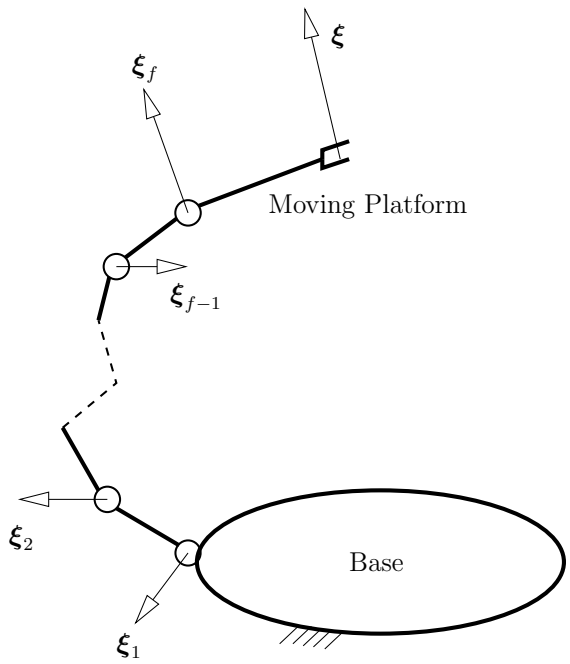


Figure 2.3: Serial kinematic chain.

the joints in the serial kinematic chain, i.e.

$$\mathcal{T} = \sum_{j=1}^{f} \mathcal{T}_j \tag{2.8}$$

where the subscript, $j$, denotes the $j$-th kinematic joint. From Eqs. (2.8) and (2.6), we obtain

$$\mathcal{W} = \bigcap_{j=1}^{f} \mathcal{W}_j \tag{2.9}$$

Equation (2.9) states that the wrench system $\mathcal{W}$ of (the moving platform in) a serial kinematic chain is the intersection of the wrench systems $\mathcal{W}_j$ of all the joints in the serial kinematic chain.

Let us take the PR serial kinematic chain as an example. The twist system of the PR serial kinematic chain is the union of the twist systems of the P and R joints, which is a 2-system. One possible basis for this system is composed of a $\boldsymbol{\xi}_0$ along the axis of the R joint and a $\boldsymbol{\xi}_\infty$ along the axis of the P joint. The wrench system of the PR serial kinematic chain is the intersection of the wrench system of the R joint with that of the P joint. This is a 4-system which includes all the $\boldsymbol{\zeta}_\infty$'s whose axes are perpendicular to the axis of the R joint and all the $\boldsymbol{\zeta}_0$'s whose axes are perpendicular to the axis of the P joint and intersect with the axis of the R joint.

**Parallel kinematic chains** [72]

For a PKC (Fig. 2.4), the output twist of the moving platform is

$$\boldsymbol{\xi} = \sum_{j=1}^{f^i} \boldsymbol{\xi}_j^i \dot{\theta}_j^i \quad i = 1, 2, \cdots, m \tag{2.10}$$

where the subscript and superscript, ${}_j^i$, denote the $j$-th joint in the $i$-th leg, $m$ and $f^i$ respectively denote the number of legs in the PKC and the DOF of the $i$-th leg.

From Eq. (2.10), we can conclude that the twist system $\mathcal{T}$ of (the moving platform in) a PKC is the intersection of the twist systems $\mathcal{T}^i$ of all its legs, i.e.,

$$\mathcal{T} = \bigcap_{i=1}^{m} \mathcal{T}^i \tag{2.11}$$

where

$$\mathcal{T}^i = \sum_{j=1}^{f^i} \mathcal{T}_j^i$$

and $\mathcal{T}_j^i$ denotes the twist system of joint $j$ in leg $i$.

From Eqs. (2.11) and (2.6), we obtain

$$\mathcal{W} = \sum_{i=1}^{m} \mathcal{W}^i \tag{2.12}$$

where

$$\mathcal{W}^i = \bigcap_{j=1}^{f^i} \mathcal{W}_j^i$$

and $\mathcal{W}_j^i$ denotes the wrench system of joint $j$ in leg $i$. Equation (2.12) states that the wrench system $\mathcal{W}$ of (the moving platform in) a PKC is the union of the wrench systems $\mathcal{W}^i$ of all its legs.

## 2.2 Mobility analysis of parallel kinematic chains

Consider an $m$-legged PKC. Let $c$ and $f$ denote the order of the wrench system $\mathcal{W}$ and mobility (DOF) of the PKC, and $c^i$ and $f^i$ denote the order of the wrench system $\mathcal{W}^i$ and DOF of leg $i$.

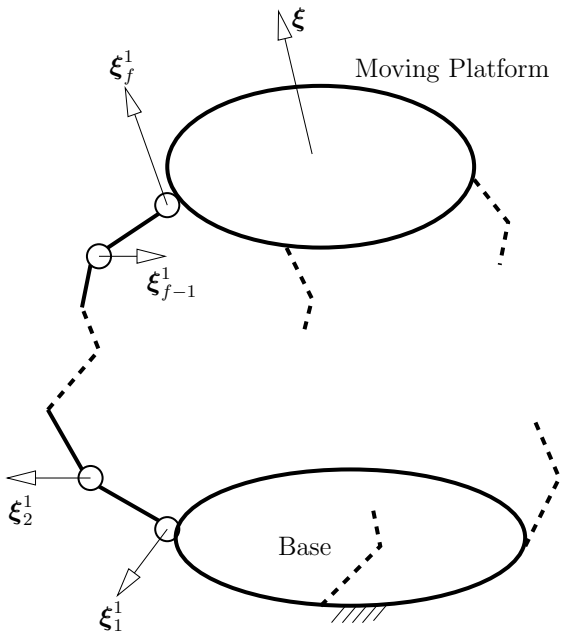


Figure 2.4: PKC.

Since the mobility (DOF) of a kinematic chain is the number of independent parameters to determine the relative configuration of all its links, the mobility $f$ of a PKC is the sum of (1) the number of independent parameters to determine the relative configuration of the moving platform and (2) the number of independent parameters to determine the configuration of all the links in all the legs with the relative configuration of the moving platform specified.

The number of independent parameters to determine the relative configuration of the moving platform is equal to the connectivity $\mathcal{C}$ (also the relative DOF of the moving platform with respect to the base) of the PKC. $\mathcal{C}$ can be calculated using

$$\mathcal{C} = 6 - c \tag{2.13}$$

Since the order of the twist system of leg $i$ is $(6 - c^i)$, the number of independent parameters to determine the configuration of all the links in leg $i$ with the relative configuration of the moving platform specified can be determined using

$$R^i = f^i - (6 - c^i) = f^i - 6 + c^i \tag{2.14}$$

where $R^i$ is called the redundant DOF of leg $i$.

The number of independent parameters to determine the configuration of all the

links in all legs with the relative configuration of the moving platform specified is

$$R = \sum_{i=1}^{m} R^i \tag{2.15}$$

where $R$ is called the redundant DOF of the PKC. Then, we obtain the mobility (or the degree of freedom) $f$ of the PKC

$$f = \mathcal{C} + R = 6 - c + \sum_{i=1}^{m} R^i \tag{2.16}$$

The mobility obtained using Eqs. (2.16) is usually instantaneous. When $c$, $c^i$ and $R^i$ are the same at different general configurations, the DOF is full-cycle.

In addition to the mobility, another important index of PKCs is

$$\Delta = \sum_{i=1}^{m} c^i - c \tag{2.17}$$

where $\Delta$ is called number of overconstraints (also passive constraints or redundant constraints) if $\Delta > 0$.

As an example, consider the 3-$\underline{\text{P}}$RRRR PKC (Fig. 2.5). In this PKC, all the axes of the R joints within a same leg are parallel. The axis of a P joint is not perpendicular to the axes of the R joints within the same leg. The axes of the R joints on the moving platform are not parallel to a plane. The wrench system of each leg is 2-$\boldsymbol{\zeta}_\infty$-system. The wrench system of the PM is a 3-$\boldsymbol{\zeta}_\infty$-system. In addition, the order of the twist-system of the four R joints within a same leg is 3. We have $c^i = 2$, $c = 3$, $R^i = 1$. Then

$$\mathcal{C} = 6 - c = 3$$

and

$$f = \mathcal{C} + \sum_{i=1}^{3} R^i = 6$$

It is noted that the axes of successive R joints with parallel axes are always parallel in the process of motion. Hence, $c$, $c^i$ and $R^i$ do not change when the moving platform undergoes a small displacement from a general configuration and the mobility obtained is thus full-cycle. The number of overconstraints of the 3-legged PKC is

$$\Delta = \sum_{i=1}^{3} c^i - c = 6 - 3 = 3$$

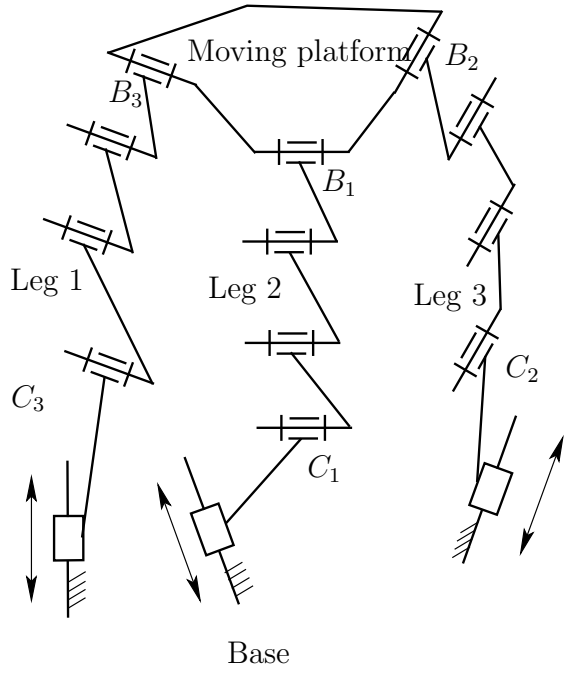


Figure 2.5: 3-$\underline{\text{P}}\bar{\text{R}}\bar{\text{R}}\bar{\text{R}}\bar{\text{R}}\bar{\text{R}}$ PKC.

To facilitate the type synthesis of PMs, we can substitute Eq. (2.17) into Eq. (2.16). We obtain

$$f = \mathcal{C} + R = 6 - \sum_{i=1}^{m} c^i + \Delta + R \tag{2.18}$$

Equation (2.18) is the mobility equation to be applied in the type synthesis of PMs. In addition to Eq. (2.18), Eqs. (2.14) and (2.15) will also be used in the type synthesis.

In this thesis, we focus on non-redundant PMs for which

$$R = R^i = 0 \quad i = 1, 2, \cdots, m \tag{2.19}$$

In this case, Eqs. (2.18) and (2.14) are reduced to

$$f = \mathcal{C} = 6 - \sum_{i=1}^{m} c^i + \Delta \tag{2.20}$$

and

$$f^i = 6 - c^i \tag{2.21}$$

Equations (2.20) and (2.21) will be used in the type synthesis of PMs in Chapters 3–6.

## 2.3 Validity condition of actuated joints in parallel mechanisms

For an $f$-DOF mechanism, $f$ actuated joints should be selected. There are many different ways of selecting the actuated joints for the mechanism. Usually, the actuated joints cannot be selected arbitrarily. The selection of actuated joints should ensure that, in a general configuration, the DOF of the mechanism with the $f$ actuated joints locked should be zero. In other words, in a general configuration, any load on the output link can be balanced by the torques/forces of the actuated joints. Relatively little work has been done on the validity condition of actuated joints for PMs as well as conventional mechanisms. In [55], a method based on the generalized kinematic joints and generalized kinematic loops is proposed to detect the validity of actuated joints for a class of multi-loop spatial kinematic chains. In the case of PMs, the validity condition of actuated joints can be obtained using screw theory.

### 2.3.1 Actuation wrenches

Let $\mathcal{W}^i_{\not\partial j}$ be the set of all the wrenches which are not reciprocal to the twist of joint $j$ and reciprocal to all the twists of the other joints within leg $i$. Physically speaking, $\mathcal{W}^i_{\not\partial j}$ is the set of wrenches that could be exerted on the moving platform through the actuation of joint $j$ in leg $i$. This set of wrenches has been defined previously by several authors (such as [70, 111]). Here, it is called the actuation wrench of the actuated joint $j$ in leg $i$.

Let $\boldsymbol{\zeta}^i_j$ denote a basis of the wrench system $\mathcal{W}^i$ of leg $i$ and $\boldsymbol{\zeta}'^i_{\not\partial j}$ denote any one arbitrary wrench which belongs to $\mathcal{W}^i_{\not\partial j}$. Then, any wrench in $\mathcal{W}^i_{\not\partial j}$ can be expressed as

$$\boldsymbol{\zeta}^i_{\not\partial j} = \alpha \boldsymbol{\zeta}'^i_{\not\partial j} + \sum_{k=1}^{c^i} (\beta^i_k \boldsymbol{\zeta}^i_k), \quad \alpha \neq 0 \tag{2.22}$$

### 2.3.2 Validity condition of actuated joints

The validity condition of actuated joints for PMs is similar to the static singularity condition proposed [56, 70]. In [56], the selection of actuated joints for a PPM was dealt with. It can be stated as follows:

**For an $f$-DOF PM in which all the twists within the same leg are linearly independent in a general configuration, a set of $f$ actuated joints is valid if and only if, in a general configuration, all the actuation wrenches, $\boldsymbol{\zeta}^i_{\not\oslash j}$, of the $f$ actuated joints together with the wrench system $\mathcal{W}$ of the PKC constitute a 6-system.**

The validity condition of actuated joints for PMs is different from the static singularity condition in that the former deals with the case of general configurations while the latter deals with the case of singular configurations.

Unlike the work presented in [57] which deals with the selection of actuated joints for a PKC with specific geometry, in this thesis, the validity condition of a set of actuated joints of a PM with the general geometry is revealed.

# Chapter 3

# General procedure for the type synthesis of parallel mechanisms

In this chapter, a method for the type synthesis of PMs based on screw theory is developed. A general procedure is proposed which consists of four main steps: the decomposition of the wrench system of a PKC, the type synthesis of legs, the combination of legs to generate PKCs, and the selection of the actuated joints. These steps will be discussed successively in separate sections.

## 3.1 Introduction

Most of the works on the type synthesis of PMs start with a specified DOF of a PM, while a few works start with a specified motion pattern. The type synthesis of PMs in this thesis starts with a specified motion pattern and a specified number of overconstraints (also redundant constraints or passive constraints) $\Delta$. The reasons why the starting point is chosen in this way are that (1) In many applications, PMs generating a specified motion pattern are required. A specified motion pattern contains more information than a specified DOF; and (2) The number of overconstraints $\Delta$ is also an important index of PMs. The complexity, the cost and the performance of PMs generating the same motion pattern varies with the change of $\Delta$.

The mobility criterion (see Eq. (2.20)) proposed in Chapter 2 as well as Eq. (2.21) will be used in the type synthesis of PMs generating a specified motion pattern. In addition, $\Delta$ takes all the possible values during the type synthesis of PMs for the completeness of the results in Chapters 3–6.

## 3.2 Motion patterns of the moving platform

There are many types of motion patterns of the moving platform. The DOF itself is not sufficient to describe a motion pattern. A 3-DOF motion may be a 3-DOF translational motion, 3-DOF spherical motion, a 3-DOF planar motion or any other 3-DOF motion.

In this thesis, the following three types of motion patterns, which cover a wide range of applications, are considered.

- Three-DOF translational motion: In this type of motion pattern, the moving platform can translate arbitrarily with respect to the base while its orientation must be invariant.
- Three-DOF spherical motion: In this type of motion pattern, there must be an invariant common point between the moving platform and the base while the moving platform can rotate arbitrarily with respect to the base.

- Four-DOF 3T1R motion: In this type of motion pattern, the moving platform can translate arbitrarily and rotate about axes with a given direction. 3T1R motion is also called Schönflies motion [31].

The above motion patterns are, respectively, the motion patterns of the Cartesian (or gantry) robots, 3-DOF wrists and the SCARA robots, which are widely used in a large variety of applications.

In any general configuration, the twist system of a PKC generating a specified motion pattern is an $f$-system. The wrench system of the PKC is a $c = (6-f)$-system. As the wrench system of a PKC is the union of those of all its legs in any configuration, it is then concluded that the wrench system of any leg in a PKC is a subset of the $(6-f)$-system in any general configuration.

To facilitate the type synthesis of PMs, the above result can be expressed in the following way.

A PKC is a desired PKC if it satisfies the following four conditions:

(1) The wrench system of any leg in the PKC is a subset of the $(6-f)$-system in a general configuration;

(2) The moving platform can undergo arbitrary small desired motion;

(3) The wrench system of a leg in a PKC is still a subset of the $(6-f)$-system when the moving platform is undergoing arbitrary small desired motion;

(4) The PKC is composed of a set of legs satisfying Conditions (1)–(3). The PKC is assembled is a way such that (1) The desired motion is permitted by all the legs and (2) The wrench system of the PKC is a $(6-f)$-system in a general configuration.

Conditions (1)–(3) are the conditions that a leg for a desired PKC should satisfy. Conditions (2)–(3) together constitute actually the full-cycle mobility condition of legs for PKCs. Condition (4) guarantees that the DOF of the PKC is not greater than expected.

## 3.3 Main steps for the type synthesis of parallel mechanisms

A general procedure can be proposed for the type synthesis of PMs as follows.

**Step 1.** To perform the decomposition of the wrench system of a PKC (See Section 3.4).

**Step 2.** To perform the type synthesis of legs for PKCs. Here, a leg for PKCs refers to a leg satisfying conditions (1), (2) and (3) for PKCs. In order to achieve this, two sub-steps are proposed.

Step 2a. To perform the type synthesis of legs with a specific wrench system (See section 3.5.1.2 and 3.5.1.3).

Step 2b. To find the conditions which guarantee that a leg with a specific wrench system satisfies conditions (2) and (3) for PKCs.

Step 2c. To generate types of legs for TPKCs.

**Step 3.** To generate PKCs.

PKCs can be generated by taking two or more legs for PKCs, obtained in Step 2, such that the union of their wrench systems constitutes a $(6-f)$-system (condition (4) for PKCs). These conditions can be easily satisfied by inspection.

**Step 4.** To generate PMs by selecting actuated joints in different ways for each PKC (Section 2.3), obtained in Step 3.

The steps 1 through 4 will be elaborated in the following sections.

## 3.4 Step 1: Decomposition of the wrench system of parallel kinematic chains

Decomposition of the wrench system of PKCs generating a specified motion pattern consists in finding all the leg wrench systems and all the combinations of leg systems for a specified motion pattern of the moving platform and a specified $\Delta$.

For the commonly used motion patterns considered, all the wrenches in the wrench systems are of the same pitch. The leg wrench systems are $c^i (0 \leq c^i \leq c)$-systems of the same pitch. The combination of leg wrench systems can be simply represented by the combination of the orders, $c^i$, of leg wrench systems.

The combination of the orders, $c^i$, of leg wrench systems can be determined as follows.

Equation (2.20) can be rewritten as

$$\sum_{i=1}^{m} c^i = 6 - f + \Delta \tag{3.1}$$

By solving Eq. (3.1), the combinations of constraint numbers of legs for $f$-DOF PKCs generating a specified motion pattern can be obtained. It should be noted that $0 \leq c^i \leq c$. Table 3.1 shows the set of $c^i$ for $m(m = f)$-legged PKCs generating a specified motion pattern. In Table 3.1, the sets of $c^i$ corresponding to all the possible values of $\Delta$ have been listed for completeness. For an $m$-legged $f$-DOF PKC generating a specified motion pattern, $\Delta$ varies from 0 to $(m-1)(6-f)$.

## 3.5 Step 2: Type synthesis of legs

### 3.5.1 Step 2a: Type synthesis of legs with a specific wrench system

Based on the fact that the wrench system of a leg is the intersection of the wrench systems of all its joints, a general method can be proposed for the type synthesis of legs

Table 3.1: Combinations of $c^i$ for $m$-legged $f$-DOF PKCs (Case $m = f$)

| $f$ | $c$ | $\Delta$ | $c^1$ | $c^2$ | $c^3$ | $c^4$ | $c^5$ | $c^6$ |
|---|---|---|---|---|---|---|---|---|
| 2 | 4 | 4 | 4 | 4 | | | | |
| | | 3 | 4 | 3 | | | | |
| | | 2 | 4 | 2 | | | | |
| | | | 3 | 3 | | | | |
| | | 1 | 4 | 1 | | | | |
| | | | 3 | 2 | | | | |
| | | 0 | 4 | 0 | | | | |
| | | | 3 | 1 | | | | |
| | | | 2 | 2 | | | | |
| 3 | 3 | 6 | 3 | 3 | 3 | | | |
| | | 5 | 3 | 3 | 2 | | | |
| | | 4 | 3 | 3 | 1 | | | |
| | | | 3 | 2 | 2 | | | |
| | | 3 | 3 | 3 | 0 | | | |
| | | | 3 | 2 | 1 | | | |
| | | | 2 | 2 | 2 | | | |
| | | 2 | 3 | 2 | 0 | | | |
| | | | 3 | 1 | 1 | | | |
| | | | 2 | 2 | 1 | | | |
| | | 1 | 3 | 1 | 0 | | | |
| | | | 2 | 2 | 0 | | | |
| | | | 2 | 1 | 1 | | | |
| | | 0 | 3 | 0 | 0 | | | |
| | | | 2 | 1 | 0 | | | |
| | | | 1 | 1 | 1 | | | |
| 4 | 2 | 6 | 2 | 2 | 2 | 2 | | |
| | | 5 | 2 | 2 | 2 | 1 | | |
| | | 4 | 2 | 2 | 2 | 0 | | |
| | | | 2 | 2 | 1 | 1 | | |
| | | 3 | 2 | 2 | 1 | 0 | | |
| | | | 2 | 1 | 1 | 1 | | |
| | | 2 | 2 | 2 | 0 | 0 | | |
| | | | 2 | 1 | 1 | 0 | | |
| | | | 1 | 1 | 1 | 1 | | |
| | | 1 | 2 | 1 | 0 | 0 | | |
| | | | 1 | 1 | 1 | 0 | | |
| | | 0 | 1 | 1 | 0 | 0 | | |
| 5 | 1 | 4 | 1 | 1 | 1 | 1 | 1 | |
| | | 3 | 1 | 1 | 1 | 1 | 0 | |
| | | 2 | 1 | 1 | 1 | 0 | 0 | |
| | | 1 | 1 | 1 | 0 | 0 | 0 | |
| | | 0 | 1 | 0 | 0 | 0 | 0 | |
| 6 | 0 | 0 | 0 | 0 | 0 | 0 | 0 | 0 |

with a specific wrench system. A specific leg wrench system will be denoted as a $c^i$-$\boldsymbol{\zeta}$-system. It is not easy to do so directly starting from the wrench systems of kinematic joints. This section presents a simple and efficient approach to the type synthesis of legs with a $c^i$-$\boldsymbol{\zeta}_\infty$-system and a $c^i$-$\boldsymbol{\zeta}_0$-system. In a 2- or 3-$\boldsymbol{\zeta}_0$-system in this thesis, the axes of all the $\boldsymbol{\zeta}_0$'s intersect at one point. The intersection of the axes of the $\boldsymbol{\zeta}_0$'s is referred to as the center of the 2- or 3-$\boldsymbol{\zeta}_0$-system.

Considering that each of the U, C and S joints can be regarded as a combination of R and P joints and the sequence of the R and P joints within a leg has no influence on the wrench system of the leg instantaneously, it is reasonable to make the assumption that legs with a $c^i$-$\boldsymbol{\zeta}$-system are composed of R and P joints. The types of legs with a $c^i$-$\boldsymbol{\zeta}$-system can be represented by the number of R and P joints in the leg in sequence. For example, the 3R-1P leg with a 2-$\boldsymbol{\zeta}$-system is composed of 3 R joints and 1 P joint.

#### 3.5.1.1 Number of joints within a leg

The number of R and P joints within a leg, which is equal to the DOF of the leg, can be calculated using Eq. (2.21) as

$$f^i = 6 - c^i$$

It is noted that for non-redundant PKCs, all the twists within the same leg are linearly independent in a general configuration. Table 3.2 shows joint numbers of legs for $f$-legged $f$-DOF PKCs.

#### 3.5.1.2 Type synthesis of legs with a $c^i$-$\boldsymbol{\zeta}_\infty$-system

The type synthesis of 6-DOF legs or legs with $c^i = 0$ is well documented (see [11] for example). In this section, the type synthesis of legs with a $c^i (c^i > 0)$-$\boldsymbol{\zeta}_\infty$-system is discussed.

**Kinematic joints whose twist systems are reciprocal to $n$ $\boldsymbol{\zeta}_\infty$'s**

The kinematic joints whose twist system is reciprocal to 3 (linearly independent) $\boldsymbol{\zeta}_\infty$'s are P joints. The kinematic joints whose twist system is reciprocal to 2 $\boldsymbol{\zeta}_\infty$'s are R and C joints whose axes are perpendicular to the axes of the two $\boldsymbol{\zeta}_\infty$'s.

Table 3.2: Joint numbers of legs for $m$-legged $f$-DOF PKCs (Case $m = f$)

| $f$ | $c$ | $\Delta$ | $f^1$ | $f^2$ | $f^3$ | $f^4$ | $f^5$ | $f^6$ |
|---|---|---|---|---|---|---|---|---|
| 2 | 4 | 4 | 2 | 2 | | | | |
| | | 3 | 2 | 3 | | | | |
| | | 2 | 2 | 4 | | | | |
| | | | 3 | 3 | | | | |
| | | 1 | 2 | 5 | | | | |
| | | | 3 | 4 | | | | |
| | | 0 | 2 | 6 | | | | |
| | | | 3 | 5 | | | | |
| | | | 4 | 4 | | | | |
| 3 | 3 | 6 | 3 | 3 | 3 | | | |
| | | 5 | 3 | 3 | 4 | | | |
| | | 4 | 3 | 3 | 5 | | | |
| | | | 3 | 4 | 4 | | | |
| | | 3 | 3 | 3 | 6 | | | |
| | | | 3 | 4 | 5 | | | |
| | | | 4 | 4 | 4 | | | |
| | | 2 | 3 | 4 | 6 | | | |
| | | | 3 | 5 | 5 | | | |
| | | | 4 | 4 | 5 | | | |
| | | 1 | 3 | 5 | 6 | | | |
| | | | 4 | 4 | 6 | | | |
| | | | 4 | 5 | 5 | | | |
| | | 0 | 3 | 6 | 6 | | | |
| | | | 4 | 6 | 6 | | | |
| | | | 5 | 5 | 5 | | | |
| 4 | 2 | 6 | 4 | 4 | 4 | 4 | | |
| | | 5 | 4 | 4 | 4 | 5 | | |
| | | 4 | 4 | 4 | 4 | 6 | | |
| | | | 4 | 4 | 5 | 5 | | |
| | | 3 | 4 | 4 | 5 | 6 | | |
| | | | 4 | 5 | 5 | 5 | | |
| | | 2 | 4 | 4 | 6 | 6 | | |
| | | | 4 | 5 | 5 | 6 | | |
| | | | 5 | 5 | 5 | 5 | | |
| | | 1 | 4 | 5 | 6 | 6 | | |
| | | | 5 | 5 | 5 | 6 | | |
| | | 0 | 5 | 5 | 6 | 6 | | |
| 5 | 1 | 4 | 5 | 5 | 5 | 5 | 5 | |
| | | 3 | 5 | 5 | 5 | 5 | 6 | |
| | | 2 | 5 | 5 | 5 | 6 | 6 | |
| | | 1 | 5 | 5 | 6 | 6 | 6 | |
| | | 0 | 5 | 6 | 6 | 6 | 6 | |
| 6 | 0 | 0 | 6 | 6 | 6 | 6 | 6 | 6 |

Table 3.3: Legs with a $c^i$-$\boldsymbol{\zeta}_\infty$-system.

| $c^i$ | Type | Geometric conditions |
|---|---|---|
| 3 | 3P | |
| 2 | 3R-1P | The axes of all the R joints are parallel to a line which is perpendicular to all the axes of the $\boldsymbol{\zeta}_\infty$'s in the 2-$\boldsymbol{\zeta}_\infty$-system. |
| | 2R-2P | |
| | 1R-3P | |
| 1 | 5R | The axes of all the R joints are parallel to a plane which is perpendicular to the $\boldsymbol{\zeta}_\infty$. |
| | 4R-1P | |
| | 3R-2P | |
| | 2R-3P | |
| 0 | Omitted | |

**Geometric conditions for legs with a $c^i$-$\boldsymbol{\zeta}_\infty$-system**

From the result given in Section 2.1.4, we obtain that a leg reciprocal to $c^i$ $\boldsymbol{\zeta}_\infty$'s is composed of joints whose twist systems are respectively reciprocal to $k(k > c^i)$ $\boldsymbol{\zeta}_\infty$'s. For example, a leg with a 3-$\boldsymbol{\zeta}_\infty$-system is composed of only P joints, while a leg with a $c^i(c^i < 3)$-$\boldsymbol{\zeta}_\infty$-system is composed of R and P joints.

Using the reciprocity condition (Section 2.1.2) and the twist systems of kinematic joints (Section 2.1.4), the geometric conditions which guarantee the leg to be reciprocal to $c^i$ $\boldsymbol{\zeta}_\infty$'s can be obtained (see Column 3 of Table 3.3).

As we have made the assumption that the twists of joints within a leg are linearly independent, a leg being reciprocal to $c^i$ $\boldsymbol{\zeta}_\infty$'s is actually a leg with a $c^i$-$\boldsymbol{\zeta}_\infty$-system.

All the legs with a $c^i$-$\boldsymbol{\zeta}_\infty$-system obtained are shown in Table 3.3.

#### 3.5.1.3 Type synthesis of legs with a $c^i$-$\boldsymbol{\zeta}_0$-system

**Kinematic joints whose twist systems are reciprocal to a $c^i$-$\boldsymbol{\zeta}_0$-system**

The kinematic joint whose twist system is reciprocal to a 3-$\boldsymbol{\zeta}_0$-system is an R joint

with its axis passing through the center of the 3-$\boldsymbol{\zeta}_0$-system. The kinematic joint whose twist system is reciprocal to a 2-$\boldsymbol{\zeta}_0$-system is a P joint whose axis is perpendicular to the axes of $\boldsymbol{\zeta}_0$'s within the 2-$\boldsymbol{\zeta}_0$-system.

**Geometric conditions for legs with a $c^i$-$\boldsymbol{\zeta}_0$-system**

Considering that the wrench system of a serial kinematic chain is the intersection of the wrench systems of all its joints [72], we obtain that a leg with a $c^i$-$\boldsymbol{\zeta}_0$-system is composed of joints whose twist systems are respectively reciprocal to an $k(k \geq c^i)$-$\boldsymbol{\zeta}_0$-system. For example, a leg with a 3-$\boldsymbol{\zeta}_0$-system is composed of only R joints, while a leg with a $c^i(c^i < 3)$-$\boldsymbol{\zeta}_0$-system is composed of R and P joints.

It is known that (a) a $\boldsymbol{\zeta}_0$ is reciprocal to an R joint if and only if the axis of the $\boldsymbol{\zeta}_0$ intersects with the axis of the R joint and (b) a $\boldsymbol{\zeta}_0$ is reciprocal to a P joint if and only if the axis of the $\boldsymbol{\zeta}_0$ is perpendicular to the axis of the P joint [71, 110]. The geometric conditions for legs with a $c^i$-$\boldsymbol{\zeta}_0$-system are given in Table 3.4.

Table 3.4: Legs with a $c^i$-$\boldsymbol{\zeta}_0$-system.

| $c^i$ | Type | Geometric conditions |
|---|---|---|
| 3 | 3R | The axes of all the R joints intersect at the center of the 3-$\boldsymbol{\zeta}_0$-system |
| 2 | 4R | The axes of at least one and at most three R joints are located on the plane containing all the axes of the $\boldsymbol{\zeta}_0$'s in the 2-$\boldsymbol{\zeta}_0$-system, while the axes of the other R joints pass through the center of the 2-$\boldsymbol{\zeta}_0$-system |
| | 3R-1P | The axis of the P joint is perpendicular to the plane containing all the axes of the $\boldsymbol{\zeta}_0$'s in the 2-$\boldsymbol{\zeta}_0$-system, while the axes of the R joints are either located on the above plane or passing through the center of the 2-$\boldsymbol{\zeta}_0$-system. |
| 1 | 5R | All the axes of the five R joints intersect with the axis of the $\boldsymbol{\zeta}_0$ |
| | 4R-1P | All the axes of the four R joints intersect with the axis of the $\boldsymbol{\zeta}_0$, while the axis of the P joint is perpendicular to the axis of the $\boldsymbol{\zeta}_0$ |
| | 3R-2P | All the axes of the three R joints intersect with the axis of the $\boldsymbol{\zeta}_0$, while the axes of the two P joints are perpendicular to the axis of the $\boldsymbol{\zeta}_0$ |
| 0 | Omitted | |

### 3.5.2 Step 2b: Derivation of the full-cycle mobility condition

For a leg with a specified leg wrench system obtained in Step 2a, its wrench system is the specified leg wrench system instantaneously or at one configuration. In this section, two approaches are proposed to the derivation of full-cycle mobility conditions of legs for for PKCs. Under the full-cycle mobility conditions, the wrench system of the leg with a specified leg wrench system will still be the specified leg wrench system when the moving platform undergoes finite motion according the desired motion pattern.

#### 3.5.2.1 Small-motion approach

The full-cycle mobility conditions of legs for PMs can be derived directly from conditions (2) and (3) for TPKCs (Section 3.2). This approach to derive the full-cycle mobility conditions of legs for PMs is called the small-motion approach.

In the derivation, the displacement analysis of a leg undergoing small joint motion is needed.

Let a leg be composed of $n_R$ R joints and $n_P$ P joints where $n_P = (f - n_R)$. The superscript denoting the leg is omitted in this section for brevity. For the purposes of simplification, in the sequence from the base to the moving platform, the R joints are labeled from 1 to $n_R$, while the P joints are labeled from $(n_R + 1)$ to $f$.

**Small change of orientation of the moving platform in a leg**

The small change of orientation of the moving platform in a leg (Fig. 2.3) undergoing small joint motion is

$$\Delta R = \sum_{i=1}^{n_R} \Delta\theta_i \mathbf{s}_i \tag{3.2}$$

where $\Delta R$ denotes the small change of orientation of the moving platform; $\Delta\theta_i$ denote the small joint motion of R joint $i$; and $\mathbf{s}_i$ denotes the unit vector along the axis of R joint $i$ before the small motion.

**Small displacement of the moving platform in a leg**

The small displacement of the moving platform in a leg (Fig. 2.3) undergoing small joint motion is

$$\Delta\mathbf{p} = \sum_{i=1}^{n_R} \Delta\theta_i \mathbf{s}_i \times \mathbf{r}_i + \sum_{j=n_R+1}^{f} \Delta S_j \mathbf{s}_j \tag{3.3}$$

where $\Delta\mathbf{p}$ denotes the small change of the position $\mathbf{p}$ of the moving platform; $\Delta S_j$ denotes the small joint motion of P joint $j$; and $\mathbf{r}_i$ denotes the vector directed from a point on the axis of R joint $i$ to the point considered.

**Unit vector along the axis of an R joint**

The unit vector along the axis of R joint $i$ in a leg (Fig. 2.3), after the small joint motion, is

$$\mathbf{s}_i' = \mathbf{s}_i + \sum_{j=1}^{i-1} \Delta\theta_i \mathbf{s}_j \times \mathbf{s}_i \tag{3.4}$$

where $\mathbf{s}_i'$ denotes the unit vector along the axis of R joint $i$ after the small joint motion.

**Main steps for deriving the full-cycle mobility condition**

With the aid of the results of the displacement analysis of a leg undergoing small joint motion, full-cycle mobility conditions of PKCs can be derived. The main steps for deriving the full-cycle mobility conditions of a leg are

**Step 2b1** To derive the conditions on the small joint motions and/or the link parameters to guarantee that the wrench system of the leg is still the specified wrench system after undergoing small joint motions.

**Step 2b2** Under the conditions obtained in step 2b1, further derive the conditions on the small joint motions and/or the link parameters to guarantee that the moving platform undergoes no motion outside the specified motion pattern.

**Step 2b3** To verify whether the moving platform can undergo arbitrary small motions within the specified motion pattern under the conditions on link parameters and/or the

small joint motion obtained in Steps 2b1 and 2b2. If yes, the conditions are full-cycle mobility conditions; if no, the conditions on link parameters are not full-cycle mobility conditions and are discarded.

#### 3.5.2.2 Virtual joint approach

A virtual-joint is a joint generating the same motion pattern as the moving platform of a PKC. The full-cycle mobility conditions of legs for PMs can be derived based on the type synthesis of single-loop kinematic chains involving a virtual-joint. This approach to derive the full-cycle mobility conditions of legs for PMs is called the virtual-joint approach.

Let us consider a PKC generating a motion pattern of $f$-DOF. When we connect the base and the moving platform of a PKC by an appropriate virtual-joint, the function of the PKC is not affected. Any of its legs and the virtual-joint will construct an $f$-DOF single loop kinematic chain. When the orders of the leg-wrench system and the wrench system of the virtual-joint are both greater than 0, the single-loop kinematic chain constructed must be an overconstrained kinematic chain.

The type synthesis of $f$-DOF single-loop overconstrained kinematic chains involving a virtual-joint can be performed using the displacement group theory [30], screw theory [112] or other approaches [113].

As will be seen in the following chapters, the small-motion approach is general and complicated, while the virtual-joint approach is simple.

### 3.5.3 Step 2c: Generation of types of legs

In the derivation of full-cycle mobility equations, the sequence of some or all the joints in the leg may not have been determined. As a last sub-step in the type synthesis of legs for PKCs, all the types of legs of PKCs are obtained by determining the sequence of all the joints within a leg which satisfy the full-cycle mobility condition of PKCs.

## 3.6 Step 3: Combination of legs to generate parallel kinematic chains

The type synthesis of PKCs consists of obtaining the types of PKCs by assembling the combination of legs obtained in Step 2 selected according to the combinations of leg wrench systems shown in Table 3.1. In assembling PKCs, the following condition should be met: The union of the wrench systems of all the legs should constitute the desired wrench system.

In the generation of PKCs with a specified motion pattern, the condition which guarantees that the union of the wrench systems of all the legs will constitute the desired wrench system will be revealed for the PKCs with invariant leg wrench systems, i.e., the leg wrench system is invariant with respect to the base and/or the moving platform. For those PKCs with variant leg wrench systems, we make the assumption that the union of the wrench systems of all the legs readily constitutes the desired wrench system.

The degeneracy of the wrench system of a PKC is termed as constraint singularity of a PM in [114, 115]. Since the constraint singularity analysis of a PM is input independent, it is more accurate to refer to it as the constraint singularity analysis of the PKC corresponding to the PM. The constraint singularity surfaces of a PKC comprise the open boundary of the workspace of the PMs corresponding to the PKC.

## 3.7 Step 4: Selection of actuated joints to generate parallel mechanisms

In Section 2.3, the validity conditions of actuated joints for PMs has been proposed. The validity detection of the actuated joints for PMs requires to calculate a $6 \times 6$ determinant. In fact, for an $f$-DOF PM with a specified motion pattern, the validity detection of the actuated joints can be reduced to the calculation of an $f \times f$ determinant when the characteristics of actuation wrenches are revealed. In the following, we only give the outline of the procedure used in Chapters 4–6, while a general proof of the above result is omitted in order to avoid more symbols. For details, please refer to

Sections 4.6, 5.5 and 6.5.

Since the linear dependency of screws is frame-independent, we can select a frame to represent a wrench system $\mathcal{W}$ for convenience. Firstly, for a wrench system $\mathcal{W}$ of order $c$, the frame can be selected in such a way that $(6-c)$ of the six scalar components in the same position are zero for each of the wrenches of the wrench system $\mathcal{W}$. Let $\boldsymbol{\zeta}^i_{t\not\emptyset j}$ denote a vector consisted of the $(6-c)$ scalar components of the actuation wrench $\boldsymbol{\zeta}^i_{\not\emptyset j}$ in the same position as the $(6-c)$ vanishing scalar components of a wrench of the wrench system $\mathcal{W}$. $\boldsymbol{\zeta}^i_{t\not\emptyset j}$ is called the t-component of the actuation wrench $\boldsymbol{\zeta}^i_{\not\emptyset j}$, while the vector $\boldsymbol{\zeta}^i_{w\not\emptyset j}$ consisted of the other components of $\boldsymbol{\zeta}^i_{\not\emptyset j}$ is called the w-component of $\boldsymbol{\zeta}^i_{\not\emptyset j}$. From Eqs. (2.22) and (2.12), we conclude that all the t-components of actuation wrenches $\boldsymbol{\zeta}^i_{\not\emptyset j}$ are proportional to one another. Then, the linear dependency of all the actuation wrenches and the wrench systems is equivalent to the linear dependency of the $f(=6-c)$ t-components of the actuation wrenches. Thus, the validity detection of the actuated joints is reduced to the calculation of the determinant of an $f \times f$ matrix each column of which is composed of a t-component of an actuation wrench.

The procedure for the validity detection of the actuated joints is proposed as follows:

**Step 4a.** If one or more of the actuated joints of a possible PM are inactive, the set of actuated joints are invalid and the possible PM should be discarded.

An inactive joint is a joint in a mechanism which always loses its degree of freedom. When an inactive joint is removed from a mechanism, the relative motion within the mechanism is unchanged. In deriving the full-cycle mobility conditions using the small-motion approach, if the small joint motion of a joint is required to be 0, then the joint is inactive. In addition, the actuation wrenches of an inactive joint belong to the wrench system of the PKC. This provides another way to detect inactive joints in a PM.

It is noted that for a PKC with inactive joints and its kinematic equivalent PKC without inactive joints, the number of overconstraints as well as the reaction forces in the joints are different, although the inactive joints in a PKC make no contribution to the movement of the moving platform.

**Step 4b.** If more than one joints in a dependent joint group belong to the set of actuated joints of a possible PM and the t-components of the actuation wrenches of

the actuated joints in the dependent joint group are linearly dependent, the set of actuated joints is invalid and the possible PM should be discarded.

A dependent joint group is composed of all the joints within a leg of PKC the t-components of the actuation wrenches of which are linearly dependent. Within a dependent joint group, the number of joints that can be actuated is less than or equal to the number of independent t-components of the actuation wrenches. In the case that the full-cycle mobility conditions of a leg are derived using the virtual-joint approach, dependent joint groups will be identified by the linear dependency of the t-components of their actuation wrench. In addition, the motions of the joints within a dependent joint group are also dependent. The dependent joint groups will be identified in this way by deriving the full-cycle mobility conditions using the small-motion approach.

**Step 4c.** If the elements of the $f \times f$ matrix are constant and its determinant is zero, the set of actuated joints is invalid. In this case, the possible PM should be discarded. The PMs for which the elements of the $f \times f$ matrix are constant and the determinant is not zero are valid and they have no constraint singularities. It is noted that in the case that there are no inactive joints and dependent joint groups among the set of actuated joints, we make the assumption that the set of actuated joints is valid if the elements of the $f \times f$ matrix are variant.

# Chapter 4

# Type synthesis of 3-DOF translational parallel mechanisms

In this chapter, the type synthesis of 3-DOF TPMs (translational parallel mechanisms) is dealt with using the general approach proposed in Chapter 3. A TPM is a PM generating 3-DOF translational motion which covers a wide range of applications. Four steps of the type synthesis of TPMs are presented in detail. The four steps are the decomposition of the wrench system of TPKC, the type synthesis of legs of TPKCs, the combination of legs to generate TPKCs and the selection of actuated joints. TPKCs with and without inactive joints are synthesized. The phenomenon of dependent joint groups in a TPKC is revealed systematically for the first time. The validity check of actuated joints of TPMs is also simplified.

## 4.1 Introduction

A TPM (translational parallel mechanism) is a PM generating 3-DOF translational motion. TPMs have a wide range of applications such as assembly and machining. Several types of TPMs have been proposed [13, 14, 15, 18, 22, 36, 71, 116, 117, 118, 119, 120]. A systematic approach is proposed in [13, 14] to generate TPMs based on the displacement group. Systematic studies on the generation of 3-DOF TPMs are performed using screw algebra and screw theory in [17, 18] respectively.

In fact, previous works on the systematic type synthesis of TPMs [13, 17, 18, 22] deal mainly with the systematic type synthesis of translational parallel kinematic chains (TPKCs). The results on TPKCs with 5-DOF legs published in [13, 17, 18, 22] were published in [10] in 1973. Hunt's work [10] is in fact not easy to read and has been neglected for a long time. Some important issues in obtaining TPMs such as the selection of actuated joints for TPMs are not dealt with systematically. It is pointed out in [13] that for all the actuated joints to be located on the base, three legs should be used in a TPM. In fact, this is only a necessary condition that a 3-DOF TPM with fixed motors should meet. It does not guarantee that any set of three actuated joints located on the base is valid. For example, for the 3-CRR TPKC with planar base and moving platform, the three R joints on the 3R platform can be actuated [118]. However, the three translational degrees of freedom of the C joints of the mechanism cannot be actuated simultaneously. A proof of this result is given later in this chapter. The 3-CRR TPKC is composed of three CRR legs which were first proposed in [13]. The CRR leg is a serial kinematic chain composed of one C joint and two R joints in sequence. In a CRR leg, the axes of the C and R joints are parallel. A TPM composed of two CRR legs was also proposed in [13].

Using the general approach to the type synthesis of PMs proposed in Chapter 3, the type synthesis of TPMs is dealt with in this chapter. The decomposition of wrench systems of TPKCs is dealt with in section 4.2. The type synthesis of legs for TPKCs is performed in Section 4.3 using the small-motion approach and in Section 4.4 using the virtual joint approach. In Section 4.5, the combination of legs to generate TPKCs is dealt with. The selection of actuated joints for TPMs is discussed in Section 4.6. Finally, conclusions are drawn.

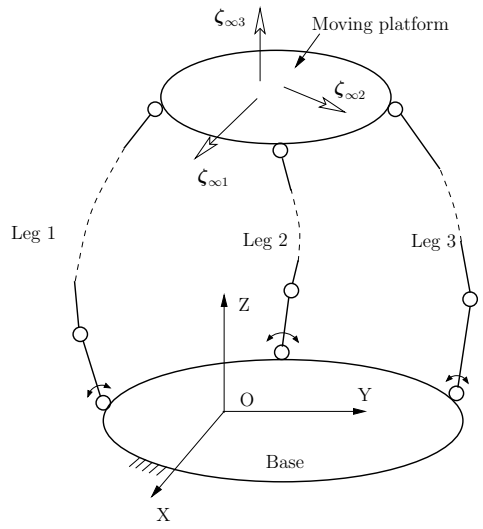


Figure 4.1: Wrench system of a TPKC.

## 4.2 Step 1: Decomposition of the wrench system of translational parallel kinematic chains

In any general configuration, the twist system of a TPKC is a 3-$\boldsymbol{\xi}_\infty$-system. It can be found without difficulty that its wrench system is also a 3-$\boldsymbol{\zeta}_\infty$-system (Fig. 4.1). As the wrench system of a PKC is the union of those of all its legs in any configuration, it is then concluded that the wrench system of any leg in a TPKC is a $c^i(0 \leq c^i \leq 3)$-$\boldsymbol{\zeta}_\infty$-system in any general configuration.

Since all the wrenches within a leg wrench system are of the same pitch, the combination of leg-wrench systems can be simply represented by the combination of the orders, $c^i$, of leg-wrench systems. The combinations of the orders $c^i$ of leg wrench systems are listed in Table 3.1.

## 4.3 Step 2: Type synthesis of legs using the small-motion approach

The specified conditions that a TPKC satisfies are given below.

(1) The wrench system of any leg in the parallel kinematic chain is a $c^i$-$\boldsymbol{\zeta}_\infty$-system in a general configuration;

(2) The moving platform can undergo arbitrary small translation;

(3) The wrench system of a leg in a PKC is still a $c^i$-$\boldsymbol{\zeta}_\infty$-system when the moving platform undergoes an arbitrary small translation.

(4) The PKC is composed of a set of legs satisfying Conditions (1)–(3). The PKC is assembled is a way such that the wrench system for the PKC is a 3-$\boldsymbol{\zeta}_\infty$-system in a general configuration.

Conditions (1)–(3) are the conditions that a leg for TPKC should satisfy. Conditions (2)–(3) constitute actually the full-cycle mobility condition of legs for TPKCs. Conditions (4) guarantees that the PKC is a TPKC.

A leg for TPKCs is a leg satisfying Conditions (1), (2) and (3) for TPKCs. The type synthesis of legs for TPKCs can be performed in three steps.

**Step 2a** To perform the type synthesis of legs with a $c^i$-$\boldsymbol{\zeta}_\infty$-system, i.e., a leg satisfying Condition (1) for TPKCs. This was done in Section 3.5.1.2 and is, therefore, not repeated here.

**Step 2b** To find the full-cycle mobility conditions for the legs for TPKCs, namely, the specific geometric condition which makes a leg with a $c^i$-$\boldsymbol{\zeta}_\infty$-system satisfy conditions (2) and (3) for TPKCs and thus be a leg for TPKCs. In this section, the full-cycle mobility conditions will be derived using the small-motion approach.

**Step 2c** To generate the types of legs for TPKCs corresponding to each of the full-cycle mobility conditions for the legs for TPKCs.

### 4.3.1 Step 2b: Full-cycle mobility conditions, inactive joints, and dependent joint groups of legs

This section applies the small-motion approach (see Section 3.5.2) to find the full-cycle mobility conditions for a leg for TPKCs. As full-cycle mobility conditions, inactive

Table 4.1: Legs for TPKCs

| $c^i$ | Class | No | Type | Full cycle mobility | Inactive joints | Dependent joint groups |
|---|---|---|---|---|---|---|
| 3 | 3P | 1 | PPP | condition | | |
| 2 | 3R-1P | 2 | $\bar{R}\bar{R}\bar{R}P$ | | | |
| | | 3 | $\bar{R}\bar{R}P\bar{R}$ | | | |
| | | 4 | $\bar{R}P\bar{R}\bar{R}$ | | | |
| | | 5 | $P\bar{R}\bar{R}\bar{R}$ | | | |
| | 2R-2P | 6 | $\bar{R}\bar{R}PP$ | | | |
| | | 7 | $\bar{R}P\bar{R}P$ | | | |
| | | 8 | $\bar{R}PP\bar{R}$ | | | |
| | | 9 | $P\bar{R}\bar{R}P$ | | | |
| | | 10 | $P\bar{R}P\bar{R}$ | | | |
| | | 11 | $PP\bar{R}\bar{R}$ | | | |
| | 1R-3P | 12 | $\bar{R}PPP$ | | The only R joint | |
| | | 13 | $P\bar{R}PP$ | | | |
| | | 14 | $PP\bar{R}P$ | | | |
| | | 15 | $PPP\bar{R}$ | | | |
| 1 | 5R | 16 | $\dot{R}\dot{R}\bar{R}\bar{R}\bar{R}$ | The axes of two or three successive R joints are parallel, while the axes of the other R joints are also parallel | | Each of the two groups of R joints whose axes are parallel. |
| | | 17 | $\bar{R}\bar{R}\bar{R}\dot{R}\dot{R}$ | | | |
| | | 18 | $\dot{R}\bar{R}\bar{R}\bar{R}\dot{R}$ | | | |
| | | 19 | $\bar{R}\dot{R}\dot{R}\bar{R}\bar{R}$ | | | |
| | | 20 | $\bar{R}\bar{R}\dot{R}\dot{R}\bar{R}$ | | | |
| | 4R-1P | 21 | $\dot{R}\dot{R}\bar{R}\bar{R}P$ | The axes of two successive R joints or two R joints connected by the P joint are parallel to each other, the axes of the other two R joints are parallel to each other | | |
| | | 22 | $\dot{R}\dot{R}\bar{R}P\bar{R}$ | | | |
| | | 23 | $\dot{R}\dot{R}P\bar{R}\bar{R}$ | | | |
| | | 24 | $\dot{R}P\dot{R}\bar{R}\bar{R}$ | | | |
| | | 25 | $P\dot{R}\dot{R}\bar{R}\bar{R}$ | | | |
| | | 26 | $\dot{R}\bar{R}\bar{R}\dot{R}P$ | | | |
| | | 27 | $\dot{R}\bar{R}\bar{R}P\dot{R}$ | | | |
| | | 28 | $\dot{R}\bar{R}P\bar{R}\dot{R}$ | | | |
| | | 29 | $\dot{R}P\bar{R}\bar{R}\dot{R}$ | | | |
| | | 30 | $P\dot{R}\bar{R}\bar{R}\dot{R}$ | | | |
| | | 31-50 | Permutation of $\bar{R}\bar{R}\bar{R}\dot{R}P$ | The axes of three R joints are parallel | The only R joint whose axis is not parallel to the axes of the other R joints | The three R joints whose axes are parallel |
| | 3R-2P | 51-80 | Permutation of $\bar{R}\bar{R}\dot{R}PP$ | The axes of two R joints are parallel to each other | | The two R joints whose axes are parallel to each other |
| | 2R-3P | 81-90 | Permutation of $\bar{R}\dot{R}PPP$ | | All the R joints | |
| 0 | Omitted | Omitted | Omitted | | Omitted | Omitted |

joints, and dependent joint groups of a leg for TPKCs are interrelated, they will be discussed simultaneously. The inactive joints and the dependent joint groups of a leg for TPKCs are also revealed and will be used in Step 4.

The legs for TPKCs are classified according to the types of their corresponding legs with a $c^i$-$\boldsymbol{\zeta}_\infty$-system. For example, the legs for TPKCs of Class 4R-1P are those corresponding to the 4R-1P leg with a 1-$\boldsymbol{\zeta}_\infty$-system. In deriving the full-cycle mobility conditions of legs of Class 4R-1P, the R joints are labeled in sequence by 1, 2, 3 and 4 from the base to the moving platform. The P joint is labeled by 5. The full-cycle mobility conditions, inactive joints, and dependent joint groups of all the legs for TPKCs will be derived below and are listed in Table 4.1.

In the following, the full-cycle mobility conditions, inactive joints, and dependent joint groups of the legs for TPKCs of Class 4R-1P are derived to illustrate the application of the proposed approach.

A leg for TPKCs of Class 4R-1P has a 1-$\boldsymbol{\zeta}_\infty$-system. The axes of all the four R joints are parallel to one plane in a general configuration. This condition can be expressed as[1]

Case 1

$$\begin{cases} \mathbf{s}_2 = a\mathbf{s}_1 + b\mathbf{s}_4 \\ \mathbf{s}_3 = c\mathbf{s}_1 + d\mathbf{s}_4 \end{cases} \tag{4.1}$$

if

$$\mathbf{s}_1 \neq \mathbf{s}_4 \tag{4.2}$$

or Case 2

$$\mathbf{s}_3 = e\mathbf{s}_1 + f\mathbf{s}_2 \tag{4.3}$$

if

$$\mathbf{s}_4 = \mathbf{s}_1 \neq \mathbf{s}_2 \tag{4.4}$$

[1]For simplicity reasons and without loss of generality, here and throughout this section, we make the assumption that $\mathbf{s}_i = \mathbf{s}_j$ if two axes $i$ and $j$ are parallel to each other and $\mathbf{s}_i \neq \mathbf{s}_j$ if two axes $i$ and $j$ are not parallel to each other.

or Case 3

$$\mathbf{s}_4 = \mathbf{s}_2 = \mathbf{s}_1 \neq \mathbf{s}_3 \tag{4.5}$$

After a set of small joint motions, we obtain from Eq. (3.4)

$$\mathbf{s}_1' = \mathbf{s}_1 \tag{4.6}$$

$$\mathbf{s}_2' = \mathbf{s}_2 + \Delta\theta_1 \mathbf{s}_1 \times \mathbf{s}_2 \tag{4.7}$$

$$\mathbf{s}_3' = \mathbf{s}_3 - \Delta\theta_4 \mathbf{s}_4 \times \mathbf{s}_3 \tag{4.8}$$

$$\mathbf{s}_4' = \mathbf{s}_4 \tag{4.9}$$

In the following, we will derive case-by-case the full-cycle mobility conditions of legs for TPKCs following the procedure given in Section 3.5.2.

Step 2b1. To derive the conditions on the small joint motion and/or the link parameters to guarantee that the wrench system of the leg is still a 1-$\boldsymbol{\zeta}_\infty$-system. This requires that the axes of all the four R joints are parallel to a common plane after a small joint motion. From Condition (3) for TPKCs, the orientation of the moving platform should not change. This implies that a vector along the axis of the R joint located on or connected to — through P joints — the moving platform or the base is constant. The unit vector along the axis of any other R joint after small joint motion can be calculated using Eq. (3.4).

Step 2b2. Under the conditions obtained in step 2b1, further derive the conditions on the small joint motion and/or the link parameters to guarantee that the moving platform undergoes no motion outside the specified motion pattern. This requires that the small change of orientation of the moving platform should be zero (see Eq. (3.2)), i.e.,

$$\Delta R = \sum_{i=1}^{n_R} \Delta\theta_i \mathbf{s}_i = 0 \tag{4.10}$$

Step 2b3. To verify whether the moving platform can undergo arbitrary small translation (see Eq. (3.3)) under the conditions on link parameters obtained in Steps 2b1 and

2b2. If yes, the conditions are full-cycle mobility conditions; if not, the conditions are not full-cycle mobility conditions and the solution is discarded.

**Case 1**. Equation (4.2) is satisfied.

The substitution of the 1st equation in Eq. (4.1) as well as Eqs. (4.6) and (4.9) into Eq. (4.7) yields

$$\mathbf{s}_2' = a\mathbf{s}_1' + b\mathbf{s}_4' + b\Delta\theta_1\mathbf{s}_1 \times \mathbf{s}_4 \tag{4.11}$$

The substitution of the 2nd equation in Eq. (4.1) as well as Eqs. (4.6) and (4.9) into Eq. (4.8) yields

$$\mathbf{s}_3' = c\mathbf{s}_1' + d\mathbf{s}_4' - c\Delta\theta_4\mathbf{s}_4 \times \mathbf{s}_1 \tag{4.12}$$

As each of $\mathbf{s}_2'$ and $\mathbf{s}_3'$ should be a linear combination of $\mathbf{s}_1'$ and $\mathbf{s}_4'$, the last term in Eq. (4.11) and that in Eq. (4.12) should vanish. This leads to the four cases below:

**Case 1a**.

$$\begin{cases} b = 0 \\ c = 0 \end{cases} \tag{4.13}$$

Substituting Eq. (4.13) into Eq. (4.1), we obtain

$$\begin{cases} \mathbf{s}_2 = \mathbf{s}_1 \\ \mathbf{s}_3 = \mathbf{s}_4 \end{cases} \tag{4.14}$$

Substituting Eq. (4.14) into Eq. (4.10), we obtain

$$\Delta R = \sum_{i=1}^{4} \mathbf{s}_i \Delta\theta_i = (\Delta\theta_1 + \Delta\theta_2)\mathbf{s}_1 + (\Delta\theta_3 + \Delta\theta_4)\mathbf{s}_4 = 0 \tag{4.15}$$

Solving Eq. (4.15), we obtain

$$\begin{cases} \Delta\theta_1 + \Delta\theta_2 = 0 \\ \Delta\theta_3 + \Delta\theta_4 = 0 \end{cases} \tag{4.16}$$

Substituting Eqs. (4.14) and (4.16) into Eq. (3.3), we obtain

$$\Delta\mathbf{p} = \begin{bmatrix} \mathbf{s}_1 \times (\mathbf{r}_1 - \mathbf{r}_2) & \mathbf{s}_3 \times (\mathbf{r}_3 - \mathbf{r}_4) & \mathbf{s}_5 \end{bmatrix} \begin{bmatrix} \Delta\theta_1 \\ \Delta\theta_3 \\ \Delta S_5 \end{bmatrix} \tag{4.17}$$

It is verified that the coefficient matrix in Eq. (4.17) is of full rank. Hence, this system of equations has a solution for arbitrary $\Delta\mathbf{p}$. It is then proved that Eq. (3.3) is met for arbitrary $\Delta\mathbf{p}$ under Eq. (4.14). Thus, the first full-cycle mobility condition for the leg of Class 4R-1P is Eq. (4.14). Equation (4.16) shows that there exist two dependent joint groups. The first is composed of R joints 1 and 2, while the second is composed of R joints 3 and 4.

**Case 1b**.

$$\begin{cases} b = 0 \\ \Delta\theta_4 = 0 \end{cases} \tag{4.18}$$

The substitution of the 1st equation in Eq. (4.18) into the 1st equation in Eq. (4.1) gives

$$\mathbf{s}_2 = \mathbf{s}_1 \tag{4.19}$$

Substituting Eq. (4.19) and the 2nd equation in Eq. (4.18) into Eq. (4.10), we obtain

$$\Delta R = \sum_{i=1}^{4} \mathbf{s}_i \Delta\theta_i = (\Delta\theta_1 + \Delta\theta_2)\mathbf{s}_1 + \Delta\theta_3 \mathbf{s}_3 = 0 \tag{4.20}$$

As $\Delta\theta_4 = 0$, $\Delta\theta_3$ should have non-zero solutions. Otherwise, Eq. (3.3) cannot be met for arbitrary $\Delta\mathbf{p}$. We then obtain from Eq. (4.20) that

$$\mathbf{s}_3 = \mathbf{s}_1 \tag{4.21}$$

The substitution of Eq. (4.21) into Eq. (4.20) yields

$$\Delta\theta_1 + \Delta\theta_2 + \Delta\theta_3 = 0 \tag{4.22}$$

Similarly to the derivation of Eq. (4.17), it can be verified that Eq. (3.3) is met for arbitrary $\Delta\mathbf{p}$ under the conditions of Eqs. (4.19) and (4.21). Thus, the second full-cycle mobility condition for the leg of Class 4R-1P is given by Eqs. (4.19) and (4.21). Equation (4.22) shows that R joints 1, 2, and 3 constitute a dependent joint group, while the 2nd equation in Eq. (4.18) shows that R joint 4 is inactive.

**Case 1c**.

$$\begin{cases} c = 0 \\ \Delta\theta_1 = 0 \end{cases} \tag{4.23}$$

The substitution of the 1st equation in Eq. (4.23) into the 2nd equation in Eq. (4.1) yields

$$\mathbf{s}_3 = \mathbf{s}_4 \tag{4.24}$$

Substituting Eq. (4.24) and the 2nd equation in Eq. (4.23) into Eq. (4.10), we obtain

$$\Delta R = \sum_{i=1}^{4} \mathbf{s}_i \Delta\theta_i = \Delta\theta_2 \mathbf{s}_2 + (\Delta\theta_3 + \Delta\theta_4)\mathbf{s}_4 = 0 \tag{4.25}$$

As $\Delta\theta_1 = 0$, $\Delta\theta_2$ should have non-zero solutions. Otherwise, Eq. (3.3) cannot be met for arbitrary $\Delta\mathbf{p}$. We then obtain from Eq. (4.25) that

$$\mathbf{s}_2 = \mathbf{s}_4 \tag{4.26}$$

The substitution of Eq. (4.26) into Eq. (4.25) yields

$$\Delta\theta_2 + \Delta\theta_3 + \Delta\theta_4 = 0 \tag{4.27}$$

Similarly to the derivation of Eq. (4.17), it can be verified that Eq. (3.3) is met for arbitrary $\Delta\mathbf{p}$ under the conditions of Eqs. (4.26) and (4.24). Thus, the third full-cycle mobility condition for the leg of Class 4R-1P is given by Eqs. (4.26) and (4.24). Equation (4.27) shows that R joints 2, 3, and 4 constitute a dependent joint group, while the 2nd equation in Eq. (4.23) shows that R joint 1 is inactive.

**Case 1d**.

$$\begin{cases} \Delta\theta_1 = 0 \\ \Delta\theta_4 = 0 \end{cases} \tag{4.28}$$

Substituting Eq. (4.28) into Eq. (4.10), we obtain

$$\Delta R = \sum_{i=1}^{4} \mathbf{s}_i \Delta\theta_i = \Delta\theta_2 \mathbf{s}_2 + \Delta\theta_3 \mathbf{s}_3 = 0 \tag{4.29}$$

In this case, Eq. (3.3) cannot be met for arbitrary $\Delta\mathbf{p}$. There is thus no leg of Class 4R-1P with full-cycle mobility in case 1d.

**Case 2**. Eqs. (4.4) is satisfied.

Substituting Eq. (4.4) into Eqs. (4.8) and (4.9), we have

$$\mathbf{s}_3' = \mathbf{s}_3 - \Delta\theta_4 \mathbf{s}_1 \times \mathbf{s}_3 \tag{4.30}$$

$$\mathbf{s}'_4 = \mathbf{s}_1 \tag{4.31}$$

From Eqs. (4.8) and (4.9), we obtain

$$\mathbf{s}'_1 \neq \mathbf{s}'_2 \tag{4.32}$$

The substitution of Eqs. (4.3), (4.6) and (4.7) into Eq. (4.30) yields

$$\mathbf{s}'_3 = e\mathbf{s}'_1 + f\mathbf{s}'_2 - f(\Delta\theta_1 + \Delta\theta_4)\mathbf{s}_1 \times \mathbf{s}_2 \tag{4.33}$$

As $\mathbf{s}'_3$ is a linear combination of $\mathbf{s}'_1$ and $\mathbf{s}'_2$, the last term in Eq. (4.33) should vanish. This leads to the two cases below.

**Case 2a.**

$$f = 0 \tag{4.34}$$

Substituting Eq. (4.34) into Eq. (4.3), we obtain

$$\mathbf{s}_3 = \mathbf{s}_1 \tag{4.35}$$

Substituting Eqs. (4.4) and (4.35) into Eq. (4.10), we obtain

$$\Delta R = \sum_{i=1}^{4} \mathbf{s}_i \Delta\theta_i = (\Delta\theta_1 + \Delta\theta_3 + \Delta\theta_4)\mathbf{s}_1 + \Delta\theta_2\mathbf{s}_2 = 0 \tag{4.36}$$

Solving Eq. (4.36), we obtain

$$\begin{cases} \Delta\theta_1 + \Delta\theta_3 + \Delta\theta_4 = 0 \\ \Delta\theta_2 = 0 \end{cases} \tag{4.37}$$

Similarly to the derivation of Eq. (4.17), it can be verified that Eq. (3.3) is met for arbitrary $\Delta\mathbf{p}$ under the conditions of Eqs. (4.4) and (4.35). Thus, the fourth full-cycle mobility condition for the leg of Class 4R-1P is given by Eqs. (4.4) and (4.35). Equation (4.37) shows that R joint 2 is an inactive joint and joints 1, 3, and 4 constitute a dependent joint group.

**Case 2b**.

$$\Delta\theta_1 + \Delta\theta_4 = 0 \tag{4.38}$$

Substituting Eqs. (4.4) and (4.38) into Eq. (4.10), we obtain

$$\Delta R = \sum_{i=1}^{4} \mathbf{s}_i \Delta\theta_i = (\Delta\theta_1 + \Delta\theta_4)\mathbf{s}_1 + \Delta\theta_2\mathbf{s}_2 + \Delta\theta_3\mathbf{s}_3 = \Delta\theta_2\mathbf{s}_2 + \Delta\theta_3\mathbf{s}_3 = 0 \tag{4.39}$$

As $\Delta\theta_2$ and $\Delta\theta_3$ should have non-vanishing solutions, we thus obtain

$$\mathbf{s}_3 = \mathbf{s}_2 \tag{4.40}$$

The substitution of Eq. (4.40) into (4.39) gives

$$\Delta\theta_2 + \Delta\theta_3 = 0 \tag{4.41}$$

Similarly to the derivation of Eq. (4.17), it can be verified that Eq. (3.3) is met for arbitrary $\Delta\mathbf{p}$ under the condition of Eqs. (4.4) and (4.40). Thus, the fifth full-cycle mobility condition for the leg of Class 4R-1P is given by Eqs. (4.4) and (4.40). Eqs. (4.38) and (4.41) show that there exist two dependent joint groups. The first is composed of R joints 1 and 4, while the second is composed of R joints 2 and 3.

**Case 3**. Equation (4.5) is met.

From Eq. (4.10), we obtain

$$\Delta R = \sum_{i=1}^{4} \mathbf{s}_i \Delta\theta_i = (\Delta\theta_1 + \Delta\theta_2 + \Delta\theta_4)\mathbf{s}_1 + \Delta\theta_3\mathbf{s}_3 = 0 \tag{4.42}$$

Solving Eq. (4.42), we obtain

$$\begin{cases} \Delta\theta_1 + \Delta\theta_2 + \Delta\theta_4 = 0 \\ \Delta\theta_3 = 0 \end{cases} \tag{4.43}$$

Similarly to the derivation of Eq. (4.17), it can be verified that Eq. (3.3) is met for arbitrary $\Delta\mathbf{p}$. Thus, the sixth full-cycle mobility condition for the leg of Class 4R-1P is given by Eq. (4.5). Equation (4.43) shows that R joint 3 is an inactive joint and R joints 1, 2 and 4 constitute a dependent joint group.

It is noted that in the above derivation, there are no conditions on the sequence of the P joint in the legs of class 4R-1P.

In summary, the full-cycle mobility conditions for legs of Class 4R-1P can be stated as (1) The axes of two successive R joints or two R joints connected by the P joint are parallel to each other, and the axes of the other two R joints are also parallel to each other or (2) The axes of three R joints are parallel.

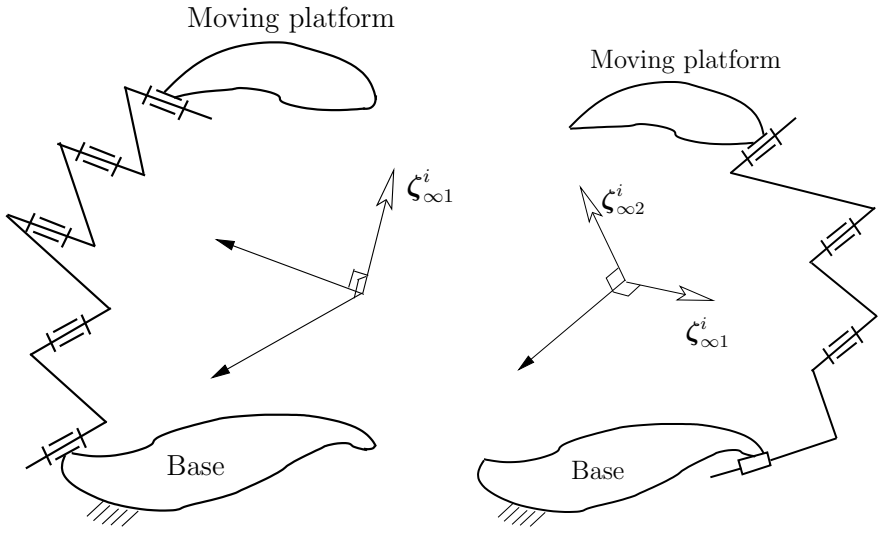


(a) $\dot{\mathrm{R}}\dot{\mathrm{R}}\bar{\mathrm{R}}\bar{\mathrm{R}}\bar{\mathrm{R}}$ leg. (b) $\mathrm{P}\bar{\mathrm{R}}\bar{\mathrm{R}}\bar{\mathrm{R}}$ leg.

Figure 4.2: Some legs for TPKCs.

### 4.3.2 Step 2c: Generation of types of legs

In the representation of types of legs for TPKCs, the axes of the R joints corresponding to the same symbols, $\bar{\mathrm{R}}$ or $\dot{\mathrm{R}}$, are parallel while the axes of the R joints corresponding to different symbols are not.

Fig. 4.2 shows two legs for TPKCs taken from Table 4.1. In the $\dot{\mathrm{R}}\dot{\mathrm{R}}\bar{\mathrm{R}}\bar{\mathrm{R}}\bar{\mathrm{R}}$ leg shown in Fig. 4.2(a), the axes of the first two R joints are parallel to each other while the axes of the other three R joints are also parallel. This leg has a 1-$\boldsymbol{\zeta}_\infty$-system. The $\boldsymbol{\zeta}_\infty$ is perpendicular to the axes of all the R joints. In the $\mathrm{P}\dot{\mathrm{R}}\dot{\mathrm{R}}\dot{\mathrm{R}}$ leg shown in Fig. 4.2(b), all the axes of the R joints are parallel. This leg has a 2-$\boldsymbol{\zeta}_\infty$-system which constitutes all $\boldsymbol{\zeta}_\infty$'s whose axes are perpendicular to all the axes of the R joints.

All the types of legs for TPKCs of each class should satisfy the full-cycle mobility conditions shown in Column 5 of Table 4.1. Thus, it is proved that there are no 5-DOF legs for TPKCs involving R and P joints except for those proposed in [10].

## 4.4 Step 2V: Type synthesis of legs using a virtual joint approach

In this section, the type synthesis of legs for TPKCs will be performed using the virtual joint approach (Section 3.5.2). As will be seen later, less derivations are needed using this approach as compared to the small-motion approach.

A leg for TPKCs is a leg satisfying Conditions (1), (2) and (3) for TPKCs (Section 4.3). The type synthesis of legs for TPKCs can be performed in three steps.

**Step 2Va** To perform the type synthesis of legs with a $c^i(0 \leq c^i \leq 3)$-$\boldsymbol{\zeta}_\infty$-system, i.e., a leg satisfying Condition (1a) for TPKCs (Section 3.5.1.2).

**Step 2Vb** To find the full-cycle mobility conditions for the legs for TPKCs, namely, the specific geometric condition which makes a leg with a $c^i$-$\boldsymbol{\zeta}_\infty$-system satisfy conditions (2) and (3) for TPKCs and thus be a leg for TPKCs. In this section, the full-cycle mobility conditions will be derived using the virtual joint approach (3.5.2.2).

**Step 2Vc** To generate the types of legs for TPKCs corresponding to each of the full-cycle mobility conditions for the legs for TPKCs.

### 4.4.1 Step 2Vb: Type synthesis of 3-DOF single-loop kinematic chains with a V joint

A V joint is a virtual joint that has the same motion pattern as the desired TPKC. For a TPKC, the V joint and one of its legs will constitute a 3-DOF single-loop kinematic chain.

From the types of legs with a $c^i(0 \leq c^i \leq 3)$-$\boldsymbol{\zeta}_\infty$-system, the possible types of 3-DOF single-loop kinematic chains are PPPV, RRRPV, RRPPV, RPPPV, RRRRRV, RRRRPV, RRRPPV and RRPPPV. It is noted that the wrench system of the V joint is a 3-$\boldsymbol{\zeta}_\infty$-system. To obtain a 3-DOF single-loop kinematic chain with a V joint, the leg with a $c^i(0 \leq c^i \leq 3)$-$\boldsymbol{\zeta}_\infty$-system must be arranged in such a way that the union of

the two wrench systems constitute a 3-$\boldsymbol{\zeta}_\infty$-system.

For the 3-DOF single-loop kinematic chains of classes PPPV, RRRPV, RRPPV and RPPPV, no condition needs to be met, except for the condition for a leg with a $c^i$-$\boldsymbol{\zeta}_\infty$-system. The types of 3-DOF single-loop kinematic chains of classes RRRPV, RRPPV and RPPPV are (1) PPPV, (2) $\bar{\text{R}}\bar{\text{R}}\bar{\text{R}}$PV, (3) $\bar{\text{R}}\bar{\text{R}}$PPV, and (4) $\bar{\text{R}}$PPPV.

It is noted that for a group of successive R joints or R joints connected by P joints in which the axes of these R joints are parallel in any one configuration, the axes of the R joints will always be parallel. Thus, for the 3-DOF single-loop kinematic chains of classes RRRRRV, RRRRPV, RRRPPV and RRPPPV, the R joints should be divided into two groups. In each group of R joints, the R joints are successively connected or connected by P joints and their axes are parallel.

The types of the 4-DOF single-loop kinematic chains of classes RRRRRV, RRRRPV, RRRPPV and RRPPPV are (1) $\bar{\text{R}}\bar{\text{R}}\bar{\text{R}}\dot{\text{R}}\dot{\text{R}}$V, (2) $\bar{\text{R}}\bar{\text{R}}\dot{\text{R}}\dot{\text{R}}\bar{\text{R}}$V, (3) $\bar{\text{R}}\bar{\text{R}}\bar{\text{R}}\dot{\text{R}}$PV, (4) $\bar{\text{R}}\bar{\text{R}}\dot{\text{R}}\dot{\text{R}}$PV, (5) $\bar{\text{R}}\dot{\text{R}}\dot{\text{R}}\bar{\text{R}}$PV, (6) $\bar{\text{R}}\bar{\text{R}}\dot{\text{R}}$PPV, and (7) $\bar{\text{R}}\dot{\text{R}}$PPPV.

It is pointed out that the P joints and the only $\dot{\text{R}}$ joint can be put anywhere in the single-loop kinematic chain. For brevity, we list only the 3-DOF single-loop kinematic chains from which all 3-DOF single-loop kinematic chains can be obtained through the above operations. For example, $\bar{\text{R}}\bar{\text{R}}\text{P}\bar{\text{R}}$V single-loop kinematic chain can be obtained by changing the position of the P joint in $\bar{\text{R}}\bar{\text{R}}\bar{\text{R}}$PV single-loop kinematic chain (Fig. 4.3(b)) while P$\dot{\text{R}}\bar{\text{R}}\bar{\text{R}}\bar{\text{R}}$V single-loop kinematic chain can be obtained by changing the position of the combination of $\dot{\text{R}}$ joints in the $\bar{\text{R}}\bar{\text{R}}\bar{\text{R}}\dot{\text{R}}$PV single-loop kinematic chain (Fig. 4.3(g)).

In the representation of types of 3-DOF single-loop kinematic chains involving a V joint, the axes of R joints denoted by the same symbols, $\bar{\text{R}}$ or $\dot{\text{R}}$, are parallel, while the axes of the R joints denoted by different symbols are not.

### 4.4.2 Step 2Vc: Generation of types of legs

By removing the V joint in a 3-DOF single-loop kinematic chain involving a V joint, one or two legs for TPMs can be obtained. For example, by removing the V joint in a

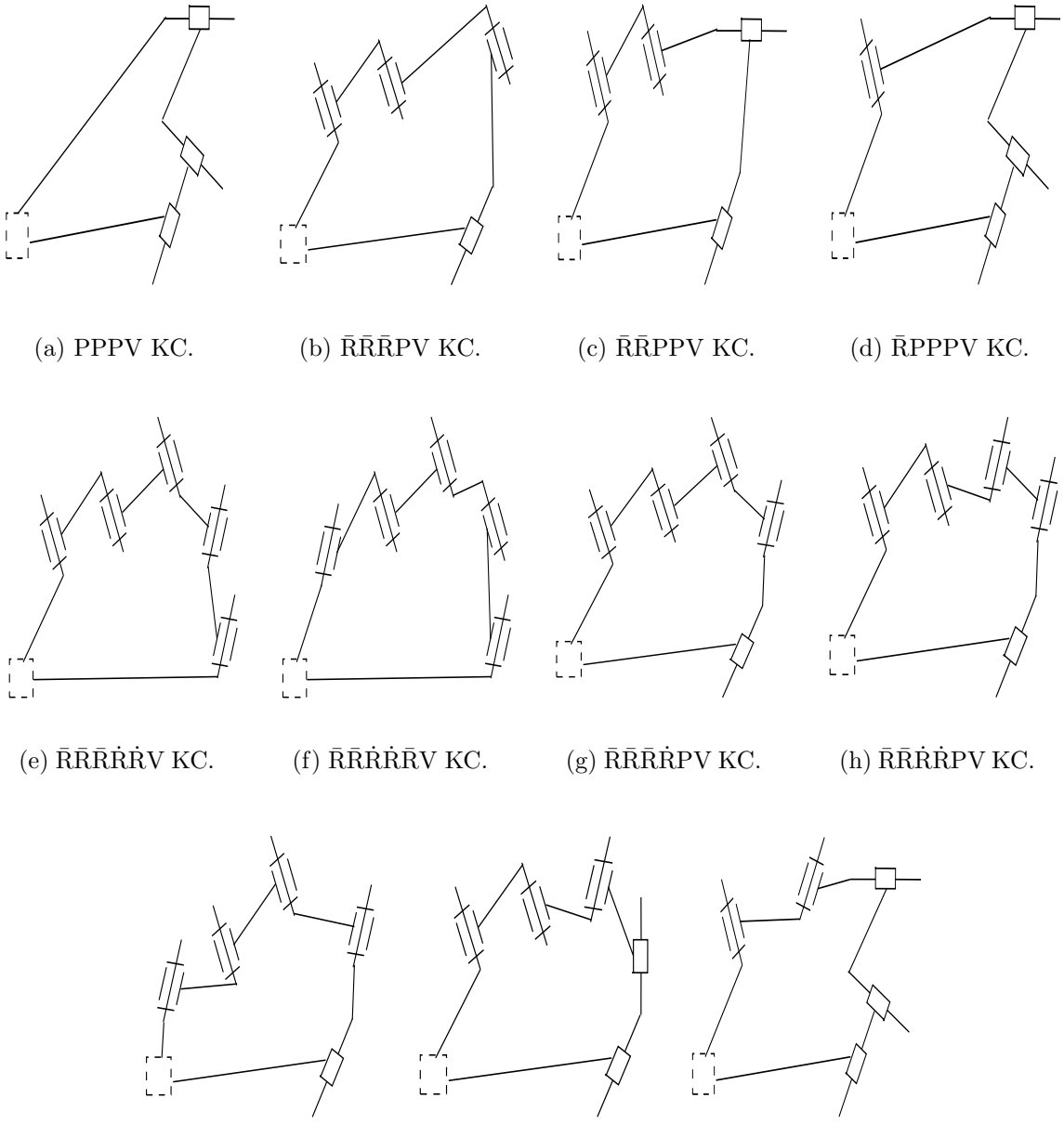

(a) PPPV KC. (b) $\bar{\mathrm{R}}\bar{\mathrm{R}}\bar{\mathrm{R}}$PV KC. (c) $\bar{\mathrm{R}}\bar{\mathrm{R}}$PPV KC. (d) $\bar{\mathrm{R}}$PPPV KC.

(e) $\bar{\mathrm{R}}\bar{\mathrm{R}}\bar{\mathrm{R}}\dot{\mathrm{R}}\dot{\mathrm{R}}$V KC. (f) $\bar{\mathrm{R}}\bar{\mathrm{R}}\dot{\mathrm{R}}\dot{\mathrm{R}}\bar{\mathrm{R}}$V KC. (g) $\bar{\mathrm{R}}\bar{\mathrm{R}}\bar{\mathrm{R}}\dot{\mathrm{R}}$PV KC. (h) $\bar{\mathrm{R}}\bar{\mathrm{R}}\dot{\mathrm{R}}\dot{\mathrm{R}}$PV KC.

(i) $\bar{\mathrm{R}}\dot{\mathrm{R}}\dot{\mathrm{R}}\bar{\mathrm{R}}$PV KC. (j) $\bar{\mathrm{R}}\bar{\mathrm{R}}\dot{\mathrm{R}}$PPV KC. (k) $\bar{\mathrm{R}}\dot{\mathrm{R}}$PPPV KC.

Figure 4.3: Some 3-DOF single-loop kinematic chains involving a V joint.

$\bar{\mathrm{R}}\bar{\mathrm{R}}\bar{\mathrm{R}}\dot{\mathrm{R}}\dot{\mathrm{R}}\mathrm{V}$ kinematic chain (Fig. 4.3(e)), a $\dot{\mathrm{R}}\dot{\mathrm{R}}\bar{\mathrm{R}}\bar{\mathrm{R}}\bar{\mathrm{R}}$ (Fig. 4.2(a)) and a $\bar{\mathrm{R}}\bar{\mathrm{R}}\bar{\mathrm{R}}\dot{\mathrm{R}}\dot{\mathrm{R}}$ leg can be obtained. The legs for TPMs obtained are the same as those obtained in section 4.3 (see Table 4.1).

## 4.5 Step 3: Combination of legs to generate translational parallel kinematic chains

TPKCs can be generated by assembling a set of legs for TPKCs shown in Table 4.1 selected according to the combinations of the leg wrench systems shown in Table 3.1. In assembling PKCs, the following condition should be met: The union of their wrench systems constitutes a 3-$\boldsymbol{\zeta}_\infty$-system (see Condition (4) for TPKCs in Section 4.3).

For a TPKC in which not all the leg wrench systems of are invariant with respect to the base or the moving platform, the union of their leg wrench systems usually constitutes a 3-$\boldsymbol{\zeta}_\infty$-system. For a TPKC in which all the leg wrench systems are invariant with respect to the base or the moving platform, the base or the moving platform should meet certain conditions to guarantee that the union of their leg wrench systems constitutes a 3-$\boldsymbol{\zeta}_\infty$-system.

For example, by taking one $\dot{\mathrm{R}}\dot{\mathrm{R}}\bar{\mathrm{R}}\bar{\mathrm{R}}\bar{\mathrm{R}}$ leg (Fig. 4.2(a)) and one $\mathrm{P}\bar{\mathrm{R}}\bar{\mathrm{R}}\bar{\mathrm{R}}$ leg (Fig. 4.2(b)), a 2-legged $\dot{\mathrm{R}}\dot{\mathrm{R}}\bar{\mathrm{R}}\bar{\mathrm{R}}\bar{\mathrm{R}}$-$\mathrm{P}\bar{\mathrm{R}}\bar{\mathrm{R}}\bar{\mathrm{R}}$ TPKC (Fig. 4.4) can be obtained. The two leg wrench systems are both invariant with respect to the base or the moving platform, hence the axes of all the R joints within the TPKC should not be parallel to a plane in order to guarantee that the union of their leg wrench systems constitutes a 3-$\boldsymbol{\zeta}_\infty$-system.

Due to the large number of TPKCs, only three-legged TPKC with identical legs are listed in Table 4.2.

It is noted that the inactive joints in a TPKC make no contribution to the movement of the moving platform. This may be the reason why TPKCs with inactive joints have been discarded in previous work on the type synthesis of TPMs [17, 18, 30]. TPKCs with inactive joints are kept here as for a TPKC with inactive joints and its kinematic equivalent TPKC without inactive joints, the number of overconstraints as well as the

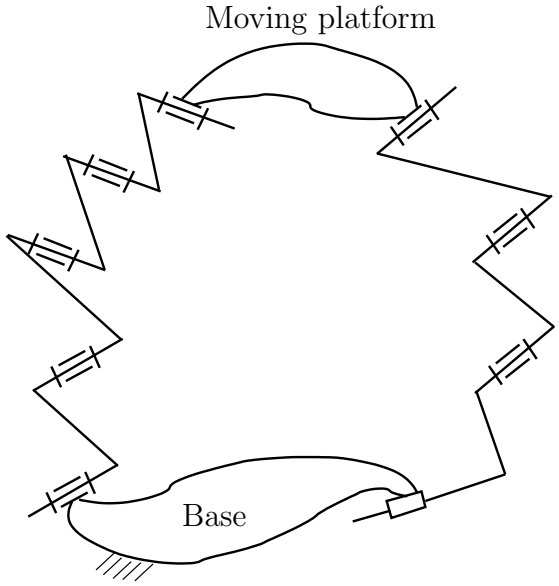


Figure 4.4: $\dot{\mathrm{R}}\dot{\bar{\mathrm{R}}}\bar{\mathrm{R}}\bar{\mathrm{R}}\bar{\mathrm{R}}$-P$\bar{\mathrm{R}}\bar{\mathrm{R}}\bar{\mathrm{R}}$ TPKC.

reaction forces in the joints are different.

## 4.6 Step 4: Selection of actuated joints to generate translational parallel mechanisms

In this section, a simplified approach is proposed for the validity check of actuated joints for TPMs. All the types of TPMs are then obtained.

### 4.6.1 Characteristics of actuation wrenches

Since the wrench system of a leg for TPMs is a $c^i$-$\boldsymbol{\zeta}_\infty$ system, from Eq. (2.22), we can conclude that all the $\boldsymbol{\zeta}^i_{\not 0 j}$'s corresponding to the same actuated joint are in the same direction if $\boldsymbol{\zeta}^i_{\not 0 j}$ is not a $\boldsymbol{\zeta}_\infty$.

Figure 4.5 shows the actuation wrenches of actuated joints in some legs for TPMs. In the $\underline{\dot{\mathrm{R}}}\dot{\bar{\mathrm{R}}}\bar{\mathrm{R}}\bar{\mathrm{R}}\bar{\mathrm{R}}$ leg (Fig. 4.5(a)), the first R joint is actuated. The actuation wrench is any $\boldsymbol{\zeta}_0$ whose axis is parallel to the axes of the last three R joints and intersects with

Table 4.2: Three-legged TPKCs

| Class | No | Type | Geometric condition |
|---|---|---|---|
| 3P | 1 | 3-PPP | |
| 3R-1P | 2-3 | 3-$\bar{R}\bar{R}\bar{R}P$ 3-$\bar{R}\bar{R}P\bar{R}$ | The axes of R joints are not all parallel |
| | 4-5 | 3-$\bar{R}P\bar{R}\bar{R}$ 3-$P\bar{R}\bar{R}\bar{R}$ | |
| 2R-2P | 6-7 | 3-$\bar{R}\bar{R}PP$ 3-$\bar{R}P\bar{R}P$ | |
| | 8-9 | 3-$\bar{R}PP\bar{R}$ 3-$P\bar{R}\bar{R}P$ | |
| | 10-11 | 3-$P\bar{R}P\bar{R}$ 3-$PP\bar{R}\bar{R}$ | |
| 1R-3P | 12-13 | 3-$\bar{R}PPP$ 3-$P\bar{R}PP$ | |
| | 14-15 | 3-$PP\bar{R}P$ 3-$PPP\bar{R}$ | |
| 5R | 16-17 | 3-$\dot{R}\bar{R}\bar{R}\bar{R}\bar{R}$ 3-$\bar{R}\bar{R}\bar{R}\dot{R}\dot{R}$ | Three lines each perpendicular to all the axes of R joints within a leg are not parallel to a plane. |
| | 18-19 | 3-$\dot{R}\bar{R}\bar{R}\bar{R}\dot{R}$ 3-$\bar{R}\dot{R}\dot{R}\bar{R}\bar{R}$ | |
| | 20 | 3-$\bar{R}\bar{R}\dot{R}\dot{R}\bar{R}$ | |
| 4R-1P | 21-22 | 3-$\dot{R}\dot{R}\bar{R}\bar{R}P$ 3-$\dot{R}\dot{R}\bar{R}P\bar{R}$ | The same condition for types 16 and 17. |
| | 23-24 | 3-$\dot{R}\dot{R}P\bar{R}\bar{R}$ 3-$\dot{R}P\dot{R}\bar{R}\bar{R}$ | |
| | 25-26 | 3-$P\dot{R}\dot{R}\bar{R}\bar{R}$ 3-$\dot{R}\bar{R}\bar{R}\dot{R}P$ | |
| | 27-28 | 3-$\dot{R}\bar{R}\bar{R}P\dot{R}$ 3-$\dot{R}\bar{R}P\bar{R}\dot{R}$ | |
| | 29-30 | 3-$\dot{R}P\bar{R}\bar{R}\dot{R}$ 3-$P\dot{R}\bar{R}\bar{R}\dot{R}$ | |
| | 31-40 | see Table 4.3 | |
| | 41-50 | | The same condition for types 16 and 17. |
| 3R-2P | 51-70 | | |
| | 71-80 | | |
| 2R-3P | 81-90 | | The same condition for types 16 and 17. |

Table 4.3: Types of TPKCs (No. 31-90)

| No | Type |
|---|---|
| 31-35 | 3-$\bar{\text{R}}\dot{\text{R}}\bar{\text{R}}\bar{\text{R}}\text{P}$ 3-$\bar{\text{R}}\bar{\text{R}}\dot{\text{R}}\bar{\text{R}}\text{P}$ 3-$\bar{\text{R}}\dot{\text{R}}\bar{\text{R}}\text{P}\bar{\text{R}}$ 3-$\bar{\text{R}}\bar{\text{R}}\dot{\text{R}}\text{P}\bar{\text{R}}$ 3-$\bar{\text{R}}\bar{\text{R}}\text{P}\dot{\text{R}}\bar{\text{R}}$ |
| 36-40 | 3-$\bar{\text{R}}\dot{\text{R}}\text{P}\bar{\text{R}}\bar{\text{R}}$ 3-$\bar{\text{R}}\text{P}\dot{\text{R}}\bar{\text{R}}\bar{\text{R}}$ 3-$\bar{\text{R}}\text{P}\bar{\text{R}}\dot{\text{R}}\bar{\text{R}}$ 3-$\text{P}\bar{\text{R}}\dot{\text{R}}\bar{\text{R}}\bar{\text{R}}$ 3-$\text{P}\bar{\text{R}}\bar{\text{R}}\dot{\text{R}}\bar{\text{R}}$ |
| 41-45 | 3-$\dot{\text{R}}\text{P}\bar{\text{R}}\bar{\text{R}}\bar{\text{R}}$ 3-$\dot{\text{P}}\bar{\text{R}}\bar{\text{R}}\bar{\text{R}}$ 3-$\text{P}\bar{\text{R}}\bar{\text{R}}\bar{\text{R}}\dot{}$ 3-$\dot{\text{R}}\bar{\text{R}}\text{P}\bar{\text{R}}\bar{\text{R}}$ 3-$\bar{\text{R}}\text{P}\bar{\text{R}}\bar{\text{R}}\dot{}$ |
| 46-50 | 3-$\dot{\text{R}}\bar{\text{R}}\bar{\text{R}}\text{P}\bar{\text{R}}$ 3-$\bar{\text{R}}\bar{\text{R}}\text{P}\bar{\text{R}}\dot{}$ 3-$\dot{\text{R}}\bar{\text{R}}\bar{\text{R}}\bar{\text{R}}\text{P}$ 3-$\bar{\text{R}}\bar{\text{R}}\bar{\text{R}}\dot{\text{R}}\text{P}$ 3-$\bar{\text{R}}\bar{\text{R}}\bar{\text{R}}\text{P}\dot{\text{R}}$ |
| 51-55 | 3-$\dot{\text{R}}\bar{\text{R}}\bar{\text{R}}\text{PP}$ 3-$\bar{\text{R}}\bar{\text{R}}\dot{\text{R}}\text{PP}$ 3-$\bar{\text{R}}\bar{\text{R}}\text{P}\dot{\text{R}}\text{P}$ 3-$\bar{\text{R}}\bar{\text{R}}\text{PP}\dot{\text{R}}$ 3-$\dot{\text{R}}\bar{\text{R}}\text{P}\bar{\text{R}}\text{P}$ |
| 56-60 | 3-$\bar{\text{R}}\text{P}\bar{\text{R}}\dot{\text{R}}\text{P}$ 3-$\bar{\text{R}}\text{P}\bar{\text{R}}\text{P}\dot{\text{R}}$ 3-$\dot{\text{R}}\bar{\text{R}}\text{PP}\bar{\text{R}}$ 3-$\bar{\text{R}}\text{PP}\bar{\text{R}}\dot{\text{R}}$ 3-$\dot{\text{R}}\text{P}\bar{\text{R}}\bar{\text{R}}\text{P}$ |
| 61-65 | 3-$\text{P}\dot{\text{R}}\bar{\text{R}}\bar{\text{R}}\text{P}$ 3-$\text{P}\bar{\text{R}}\bar{\text{R}}\dot{\text{R}}\text{P}$ 3-$\text{P}\bar{\text{R}}\bar{\text{R}}\text{P}\dot{\text{R}}$ 3-$\dot{\text{R}}\text{P}\bar{\text{R}}\text{P}\bar{\text{R}}$ 3-$\text{P}\dot{\text{R}}\text{P}\bar{\text{R}}$ |
| 66-70 | 3-$\text{P}\bar{\text{R}}\text{P}\bar{\text{R}}\dot{\text{R}}$ 3-$\dot{\text{R}}\text{PP}\bar{\text{R}}\bar{\text{R}}$ 3-$\text{P}\dot{\text{R}}\text{P}\bar{\text{R}}\bar{\text{R}}$ 3-$\text{PP}\dot{\text{R}}\bar{\text{R}}\bar{\text{R}}$ 3-$\text{PP}\bar{\text{R}}\bar{\text{R}}\dot{\text{R}}$ |
| 71-75 | 3-$\text{PP}\bar{\text{R}}\dot{\text{R}}\bar{\text{R}}$ 3-$\text{P}\bar{\text{R}}\dot{\text{R}}\text{P}\bar{\text{R}}$ 3-$\text{P}\bar{\text{R}}\text{P}\dot{\text{R}}\bar{\text{R}}$ 3-$\text{P}\bar{\text{R}}\dot{\text{R}}\bar{\text{R}}\text{P}$ 3-$\bar{\text{R}}\dot{\text{R}}\text{PP}\bar{\text{R}}$ |
| 76-80 | 3-$\bar{\text{R}}\text{P}\dot{\text{R}}\text{P}\bar{\text{R}}$ 3-$\bar{\text{R}}\text{PP}\dot{\text{R}}\bar{\text{R}}$ 3-$\bar{\text{R}}\dot{\text{R}}\text{P}\bar{\text{R}}\text{P}$ 3-$\bar{\text{R}}\text{P}\dot{\text{R}}\bar{\text{R}}\text{P}$ 3-$\bar{\text{R}}\dot{\text{R}}\bar{\text{R}}\text{PP}$ |
| 81-85 | 3-$\text{P}\bar{\text{R}}\dot{\text{R}}\text{PP}$ 3-$\text{P}\bar{\text{R}}\text{P}\dot{\text{R}}\text{P}$ 3-$\text{P}\bar{\text{R}}\text{PP}\dot{\text{R}}$ 3-$\text{PP}\bar{\text{R}}\dot{\text{R}}\text{P}$ 3-$\text{PP}\bar{\text{R}}\text{P}\dot{\text{R}}$ |
| 86-90 | 3-$\text{PPP}\bar{\text{R}}\dot{\text{R}}$ 3-$\bar{\text{R}}\dot{\text{R}}\text{PPP}$ 3-$\bar{\text{R}}\text{P}\dot{\text{R}}\text{PP}$ 3-$\bar{\text{R}}\text{PP}\dot{\text{R}}\text{P}$ 3-$\bar{\text{R}}\text{PPP}\dot{\text{R}}$ |

the axis of the second R joint. In the $\dot{\text{R}}\underline{\dot{\text{R}}}\bar{\text{R}}\bar{\text{R}}\bar{\text{R}}$ leg (Fig. 4.5(b)), the second R joint is actuated. The actuation wrench is any $\boldsymbol{\zeta}_0$ whose axes are parallel to the axes of the last three R joints and intersect with the axis of the first R joint. In the $\underline{\text{P}}\dot{\text{R}}\dot{\text{R}}\dot{\text{R}}$ leg (Fig. 4.5(c)), the first P joint is actuated. The actuation wrench is any $\boldsymbol{\zeta}_0$ whose axis is parallel to the axes of the three R joints.

### 4.6.2 Simplified validity condition of actuated joints

Following the validity condition of actuated joints for PMs (Section 2.3), we know that a set of three actuated joints for a 3-DOF TPM is valid if and only if, in a general configuration, the actuation wrenches $\boldsymbol{\zeta}^i_{\not\partial j}$, of the three actuated joints, together with the wrench system, $\mathcal{W}$, of the TPM constitute a 6-system. Let $[\mathbf{0} \quad \mathbf{i}^T]^T$, $[\mathbf{0} \quad \mathbf{j}^T]^T$, $[\mathbf{0} \quad \mathbf{k}^T]^T$ denote a basis of $\mathcal{W}$, $[\boldsymbol{\zeta}^i_{F\not\partial j} \quad \boldsymbol{\zeta}^i_{S\not\partial j}]^T$ represents $\boldsymbol{\zeta}^i_{\not\partial j}$. Here, $\mathbf{i}$, $\mathbf{j}$ and $\mathbf{k}$ denote respectively the unit vectors along the $X$-, $Y$- and $Z$-axes. The validity condition of

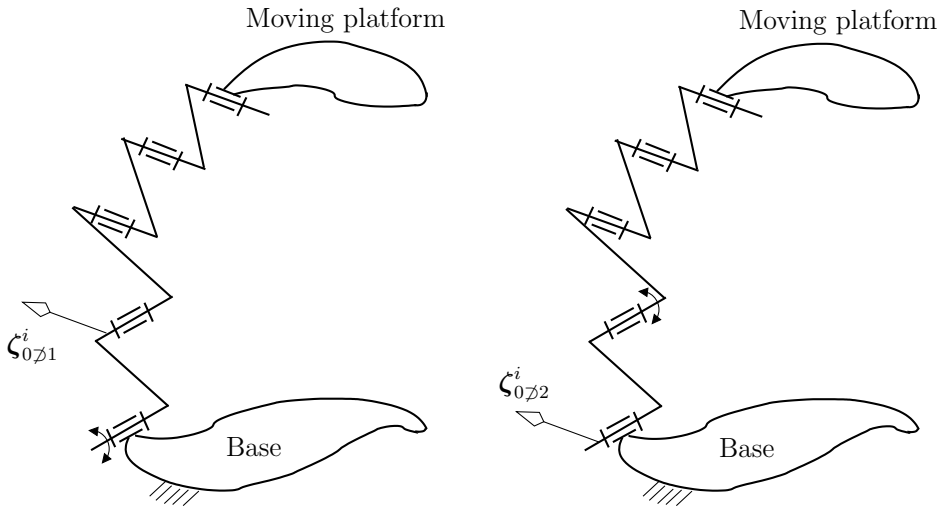


(a) $\underline{\dot{\mathrm{R}}}\dot{\mathrm{R}}\bar{\mathrm{R}}\bar{\mathrm{R}}\bar{\mathrm{R}}$ leg. (b) $\dot{\mathrm{R}}\underline{\dot{\mathrm{R}}}\bar{\mathrm{R}}\bar{\mathrm{R}}\bar{\mathrm{R}}$ leg.

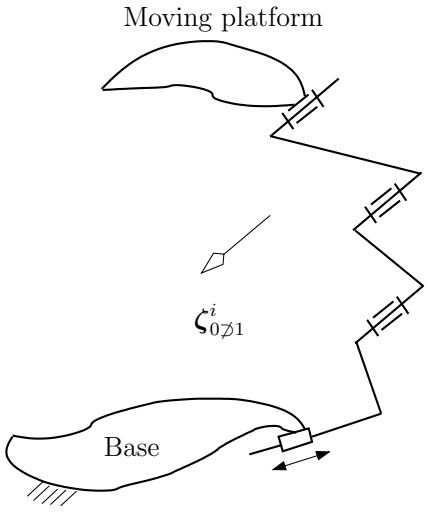


(c) $\underline{\mathrm{P}}\bar{\mathrm{R}}\bar{\mathrm{R}}\bar{\mathrm{R}}$ leg.

Figure 4.5: Actuation wrenches of some legs for TPMs.

actuated joints of a TPM can be expressed as

$$\begin{vmatrix} \boldsymbol{\zeta}^1_{F\not\partial j} & \boldsymbol{\zeta}^2_{F\not\partial j} & \boldsymbol{\zeta}^3_{F\not\partial j} & \mathbf{0} & \mathbf{0} & \mathbf{0} \\ \boldsymbol{\zeta}^1_{S\not\partial j} & \boldsymbol{\zeta}^2_{S\not\partial j} & \boldsymbol{\zeta}^3_{S\not\partial j} & \mathbf{i} & \mathbf{j} & \mathbf{k} \end{vmatrix} = \begin{vmatrix} \mathbf{i} & \mathbf{j} & \mathbf{k} \end{vmatrix} \begin{vmatrix} \boldsymbol{\zeta}^1_{F\not\partial j} & \boldsymbol{\zeta}^2_{F\not\partial j} & \boldsymbol{\zeta}^3_{F\not\partial j} \end{vmatrix} \neq 0 \tag{4.44}$$

As $\begin{vmatrix} \mathbf{i} & \mathbf{j} & \mathbf{k} \end{vmatrix} = 1$, Eq. (4.44) can be reduced to

$$\begin{vmatrix} \boldsymbol{\zeta}^1_{F\not\partial j} & \boldsymbol{\zeta}^2_{F\not\partial j} & \boldsymbol{\zeta}^3_{F\not\partial j} \end{vmatrix} \neq 0 \tag{4.45}$$

Equation (4.45) shows that the validity condition of actuated joints for TPMs can be stated as follows:

**A set of 3 actuated joints is valid for a 3-DOF TPM if and only if, in a general configuration, none of the actuation wrenches of the actuated joints is a $\boldsymbol{\zeta}_\infty$ and the unit vectors along the axes of the actuation wrenches of the three actuated joints $\boldsymbol{\zeta}^i_{\not\partial j}$ are linearly independent.**

From Eq. (4.44), we obtain the t-component $\boldsymbol{\zeta}^i_{t\not\partial j}$ and the w-component $\boldsymbol{\zeta}^i_{w\not\partial j}$ of the actuation wrench $\boldsymbol{\zeta}^i_{\not\partial j}$ are respectively $\boldsymbol{\zeta}^i_{F\not\partial j}$ and $\boldsymbol{\zeta}^i_{S\not\partial j}$. To keep the geometric insight clear, the notations $\boldsymbol{\zeta}^i_{F\not\partial j}$ and $\boldsymbol{\zeta}^i_{S\not\partial j}$ are used in this section.

### 4.6.3 Procedure for the validity detection of actuated joints

The validity detection of actuated joints of TPMs can thus be simplified using the following steps.

**Step 3a.** If one or more of the actuated joints of a possible TPM are inactive, the set of actuated joints is invalid and the possible TPM should be discarded. The inactive joints of TPKCs were revealed in Section 4.3.1.

**Step 3b.** If all the joints of a dependent joint group belong to the set of actuated joints of a possible TPM, the set of actuated joints is invalid and the possible TPM should be discarded. The dependent joint groups of TPKCs were revealed in Section 4.3.1.

**Step 3c.** If the unit vectors along the axes of all the actuation wrenches of actuated joints $\boldsymbol{\zeta}^i_{\not\partial j}$ are linearly dependent in a general configuration for a possible TPM, the set of actuated joints is invalid. In this case, the possible TPM should be discarded.

For practical reasons, the selection of actuated joints for $m$-legged TPMs should satisfy the following criteria:

(1) The actuated joints should be distributed among all the legs as evenly as possible.

(2) The actuated joints should preferably be on the base or close to the base.

Following the above criteria and the procedure for the detection of the validity of actuated joints, all the $n(n \geq 2)$-legged TPMs corresponding to each TPKC can be generated.

For example, the possible TPMs corresponding to the 2-legged TPKC, $\dot{\mathrm{R}}\dot{\mathrm{R}}\bar{\mathrm{R}}\bar{\mathrm{R}}\bar{\mathrm{R}}$-$\mathrm{P}\bar{\mathrm{R}}\bar{\mathrm{R}}\bar{\mathrm{R}}$, satisfying the above criteria are $\underline{\dot{\mathrm{R}}\dot{\mathrm{R}}}\bar{\mathrm{R}}\bar{\mathrm{R}}\bar{\mathrm{R}}$-$\underline{\mathrm{P}}\bar{\mathrm{R}}\bar{\mathrm{R}}\bar{\mathrm{R}}$, $\underline{\dot{\mathrm{R}}}\dot{\mathrm{R}}\bar{\mathrm{R}}\bar{\mathrm{R}}\bar{\mathrm{R}}$-$\underline{\mathrm{P}\bar{\mathrm{R}}}\bar{\mathrm{R}}\bar{\mathrm{R}}$ and $\dot{\mathrm{R}}\underline{\dot{\mathrm{R}}}\bar{\mathrm{R}}\bar{\mathrm{R}}\bar{\mathrm{R}}$-$\underline{\mathrm{P}\bar{\mathrm{R}}}\bar{\mathrm{R}}\bar{\mathrm{R}}$ TPMs (Fig. 4.6). Following the procedure for the validity detection of actuated joints, the $\underline{\dot{\mathrm{R}}\dot{\mathrm{R}}}\bar{\mathrm{R}}\bar{\mathrm{R}}\bar{\mathrm{R}}$-$\underline{\mathrm{P}}\bar{\mathrm{R}}\bar{\mathrm{R}}\bar{\mathrm{R}}$ TPM should be discarded as all the joints within a dependent joint group, which is composed of R joints 1 and 2 in the $\underline{\dot{\mathrm{R}}\dot{\mathrm{R}}}\bar{\mathrm{R}}\bar{\mathrm{R}}\bar{\mathrm{R}}$ leg, belong to the set of actuated joints. Thus, the TPMs corresponding to the 2-legged TPKC, $\dot{\mathrm{R}}\dot{\mathrm{R}}\bar{\mathrm{R}}\bar{\mathrm{R}}\bar{\mathrm{R}}$-$\mathrm{P}\bar{\mathrm{R}}\bar{\mathrm{R}}\bar{\mathrm{R}}$, are the $\underline{\dot{\mathrm{R}}}\dot{\mathrm{R}}\bar{\mathrm{R}}\bar{\mathrm{R}}\bar{\mathrm{R}}$-$\underline{\mathrm{P}\bar{\mathrm{R}}}\bar{\mathrm{R}}\bar{\mathrm{R}}$ and $\dot{\mathrm{R}}\underline{\dot{\mathrm{R}}}\bar{\mathrm{R}}\bar{\mathrm{R}}\bar{\mathrm{R}}$-$\underline{\mathrm{P}\bar{\mathrm{R}}}\bar{\mathrm{R}}\bar{\mathrm{R}}$ TPMs.

Due to the large number of TPKCs, a large number of TPMs can be generated. Here, we only give 3-legged TPMs with identical legs all actuated joints located on the base (Table 4.4).

## 4.7 Presentation of new translational parallel mechanisms

There are many new TPMs among those listed in Table 4.4. Two of them, namely, the 3-$\underline{\mathrm{P}}\bar{\mathrm{R}}\bar{\mathrm{R}}\bar{\mathrm{R}}\dot{\mathrm{R}}$ and 3-$\underline{\mathrm{P}}\bar{\mathrm{R}}\bar{\mathrm{R}}\bar{\mathrm{R}}$ TPMs, are shown in Fig. 4.7. It will be revealed in Chapter 7 that both of them belong to a class of analytic TPMs. A comprehensive kinematic study of the class of analytic TPMs will be presented in Chapter 8.

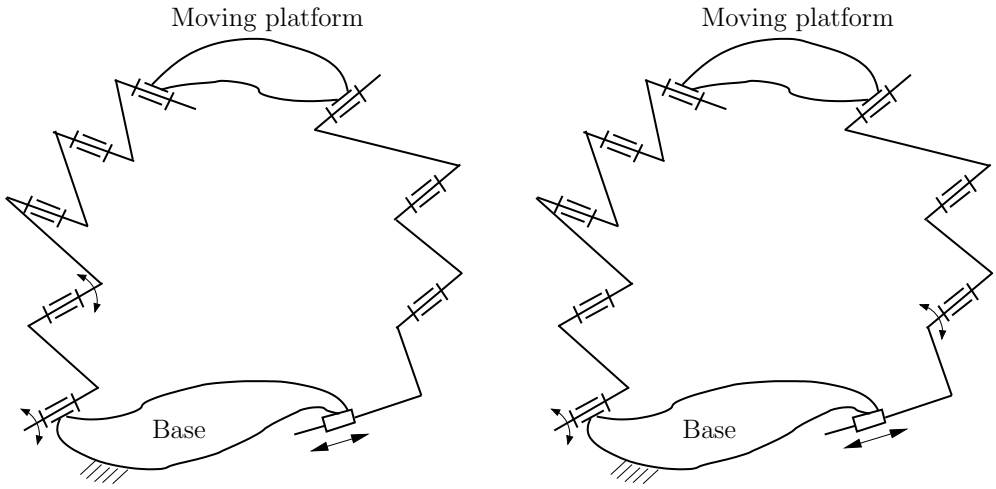


(a) $\underline{\text{R}}\dot{\text{R}}\bar{\text{R}}\bar{\text{R}}\bar{\text{R}}$-$\underline{\text{P}}\bar{\text{R}}\bar{\text{R}}\bar{\text{R}}$ TPM.

(b) $\underline{\dot{\text{R}}}\dot{\text{R}}\bar{\text{R}}\bar{\text{R}}\bar{\text{R}}$-$\underline{\text{P}\bar{\text{R}}}\bar{\text{R}}\bar{\text{R}}$ TPM.

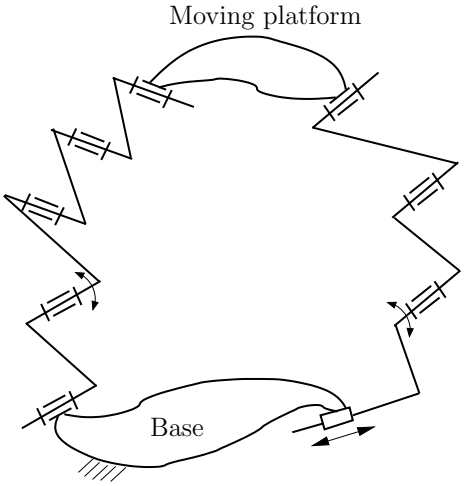


(c) $\dot{\text{R}}\underline{\dot{\text{R}}}\bar{\text{R}}\bar{\text{R}}\bar{\text{R}}$-$\underline{\text{P}\bar{\text{R}}}\bar{\text{R}}\bar{\text{R}}$ TPM.

Figure 4.6: Selection of actuated joints for the $\text{P}\bar{\text{R}}\bar{\text{R}}\bar{\text{R}}$-$\dot{\text{R}}\dot{\text{R}}\bar{\text{R}}\bar{\text{R}}\bar{\text{R}}$ TPKC.

Table 4.4: Three-legged TPMs

| Class | No | Type | Geometric condition |
|---|---|---|---|
| 3P | 1 | 3-$\underline{\text{P}}$PP | Three lines each perpendicular to the axes of two unactuated P joints within a leg are not parallel to a plane. |
| 3R-1P | 2-3 | 3-$\underline{\bar{\text{R}}}\bar{\text{R}}\bar{\text{R}}$P 3-$\underline{\bar{\text{R}}}\bar{\text{R}}$P$\bar{\text{R}}$ | |
| | 4 | 3-$\underline{\bar{\text{R}}}$P$\bar{\text{R}}\bar{\text{R}}$ | |
| | 5 | 3-$\underline{\text{P}}\bar{\text{R}}\bar{\text{R}}\bar{\text{R}}$ | All the axes of $\bar{\text{R}}$ joints are not parallel to a plane. |
| 2R-2P | 6 | 3-$\underline{\bar{\text{R}}}\bar{\text{R}}$PP | The same condition as type 1. |
| | 7-8 | 3-$\underline{\bar{\text{R}}}$P$\bar{\text{R}}$P 3-$\underline{\bar{\text{R}}}$PP$\bar{\text{R}}$ | |
| | 9-10 | 3-$\underline{\text{P}}\bar{\text{R}}\bar{\text{R}}$P 3-$\underline{\text{P}}\bar{\text{R}}$P$\bar{\text{R}}$ | |
| | 11 | 3-$\underline{\text{P}}$P$\bar{\text{R}}\bar{\text{R}}$ | |
| 1R-3P | 12-13 | 3-$\underline{\text{P}}$PP$\bar{\text{R}}$ 3-$\underline{\text{P}}$P$\bar{\text{R}}$P | The same condition as type 1. |
| | 14-15 | 3-$\underline{\text{P}}\bar{\text{R}}$PP 3-$\bar{\text{R}}\underline{\text{P}}$PP | |
| 5R | 16 | 3-$\underline{\dot{\text{R}}}\dot{\bar{\text{R}}}\bar{\text{R}}\bar{\text{R}}$ | The same condition as type 5. |
| | 17-18 | 3-$\underline{\bar{\text{R}}}\bar{\text{R}}\bar{\text{R}}\dot{\text{R}}\dot{\text{R}}$ 3-$\underline{\dot{\text{R}}}\bar{\text{R}}\bar{\text{R}}\bar{\text{R}}\dot{\text{R}}$ | |
| | 19-20 | 3-$\underline{\bar{\text{R}}}\dot{\text{R}}\dot{\bar{\text{R}}}\bar{\text{R}}$ 3-$\underline{\bar{\text{R}}}\bar{\text{R}}\dot{\text{R}}\dot{\bar{\text{R}}}$ | |
| 4R-1P | 21-22 | 3-$\underline{\dot{\text{R}}}\dot{\bar{\text{R}}}\bar{\text{R}}\bar{\text{R}}$P 3-$\underline{\dot{\text{R}}}\dot{\bar{\text{R}}}\bar{\text{R}}$P$\bar{\text{R}}$ | |
| | 23-24 | 3-$\underline{\dot{\text{R}}}\dot{\text{R}}$P$\bar{\text{R}}\bar{\text{R}}$ 3-$\underline{\dot{\text{R}}}$P$\dot{\text{R}}\bar{\text{R}}\bar{\text{R}}$ | |
| | 25-26 | 3-$\underline{\text{P}}\dot{\text{R}}\dot{\text{R}}\bar{\text{R}}\bar{\text{R}}$ 3-$\underline{\dot{\text{R}}}\bar{\text{R}}\bar{\text{R}}\dot{\text{R}}$P | |
| | 27-28 | 3-$\underline{\dot{\text{R}}}\bar{\text{R}}\bar{\text{R}}$P$\dot{\text{R}}$ 3-$\underline{\dot{\text{R}}}\bar{\text{R}}$P$\bar{\text{R}}\dot{\text{R}}$ | |
| | 29-30 | 3-$\underline{\dot{\text{R}}}$P$\bar{\text{R}}\bar{\text{R}}\dot{\text{R}}$ 3-$\underline{\text{P}}\dot{\text{R}}\bar{\text{R}}\bar{\text{R}}\dot{\text{R}}$ | |
| | 31-38 | see Table 4.5 | |
| | 39-43 | | The same condition as type 5. |
| | 44-50 | | |
| 3R-2P | 51-54 | | The same condition as type 1. |
| | 55-79 | | |
| | 80 | | The same condition as type 1. |
| 2R-3P | 81-90 | | |

Table 4.5: Types of TPMs (No. 31-90)

| No | Type |
|---|---|
| 31-35 | 3-$\underline{\bar{R}}\dot{\bar{R}}\bar{R}\bar{R}P$ 3-$\underline{\bar{R}}\bar{R}\dot{\bar{R}}\bar{R}P$ 3-$\underline{\bar{R}}\dot{\bar{R}}\bar{R}P\bar{R}$ 3-$\underline{\bar{R}}\bar{R}\dot{\bar{R}}P\bar{R}$ 3-$\underline{\bar{R}}\bar{R}P\dot{\bar{R}}\bar{R}$ |
| 36-40 | 3-$\underline{\bar{R}}\dot{\bar{R}}P\bar{R}\bar{R}$ 3-$\underline{\bar{R}}P\dot{\bar{R}}\bar{R}\bar{R}$ 3-$\underline{\bar{R}}P\bar{R}\dot{\bar{R}}\bar{R}$ 3-$\underline{P}\bar{R}\dot{\bar{R}}\bar{R}\bar{R}$ 3-$\underline{P}\bar{R}\bar{R}\dot{\bar{R}}\bar{R}$ |
| 41-45 | 3-$\dot{R}\underline{P}\bar{R}\bar{R}\bar{R}$ 3-$\underline{P}\dot{\bar{R}}\bar{R}\bar{R}\bar{R}$ 3-$\underline{P}\bar{R}\bar{R}\bar{R}\dot{\bar{R}}$ 3-$\dot{R}\underline{\bar{R}}P\bar{R}\bar{R}$ 3-$\underline{\bar{R}}P\bar{R}\bar{R}\dot{\bar{R}}$ |
| 46-50 | 3-$\dot{R}\underline{\bar{R}}\bar{R}P\bar{R}$ 3-$\underline{\bar{R}}\bar{R}P\bar{R}\dot{\bar{R}}$ 3-$\dot{R}\underline{\bar{R}}\bar{R}\bar{R}P$ 3-$\underline{\bar{R}}\bar{R}\bar{R}\dot{R}P$ 3-$\underline{\bar{R}}\bar{R}\bar{R}P\dot{\bar{R}}$ |
| 51-55 | 3-$\dot{R}\underline{\bar{R}}\bar{R}PP$ 3-$\underline{\bar{R}}\bar{R}\dot{R}PP$ 3-$\underline{\bar{R}}\bar{R}P\dot{R}P$ 3-$\underline{\bar{R}}\bar{R}PP\dot{R}$ 3-$\dot{R}\underline{\bar{R}}P\bar{R}P$ |
| 56-60 | 3-$\underline{\bar{R}}P\bar{R}\dot{R}P$ 3-$\underline{\bar{R}}P\bar{R}P\dot{R}$ 3-$\dot{R}\underline{\bar{R}}PP\bar{R}$ 3-$\underline{\bar{R}}PP\bar{R}\dot{R}$ 3-$\dot{R}\underline{P}\bar{R}\bar{R}P$ |
| 61-65 | 3-$\underline{P}\dot{\bar{R}}\bar{R}\bar{R}P$ 3-$\underline{P}\bar{R}\bar{R}\dot{R}P$ 3-$\underline{P}\bar{R}\bar{R}P\dot{R}$ 3-$\dot{R}\underline{P}\bar{R}P\bar{R}$ 3-$\underline{P}\dot{\bar{R}}\bar{R}P\bar{R}$ |
| 66-70 | 3-$\underline{P}\bar{R}P\bar{R}\dot{R}$ 3-$\dot{R}\underline{P}P\bar{R}\bar{R}$ 3-$\underline{P}\dot{R}P\bar{R}\bar{R}$ 3-$\underline{P}P\dot{\bar{R}}\bar{R}\bar{R}$ 3-$\underline{P}P\bar{R}\bar{R}\dot{R}$ |
| 71-75 | 3-$\underline{P}PP\bar{R}\dot{\bar{R}}\bar{R}$ 3-$\underline{P}\bar{R}\dot{\bar{R}}P\bar{R}$ 3-$\underline{P}\bar{R}P\dot{\bar{R}}\bar{R}$ 3-$\underline{P}\bar{R}\dot{\bar{R}}\bar{R}P$ 3-$\bar{\underline{R}}\dot{\bar{R}}PP\bar{R}$ |
| 76-80 | 3-$\bar{\underline{R}}P\dot{\bar{R}}P\bar{R}$ 3-$\bar{\underline{R}}PP\dot{\bar{R}}\bar{R}$ 3-$\bar{\underline{R}}\dot{\bar{R}}P\bar{R}P$ 3-$\bar{\underline{R}}P\dot{\bar{R}}\bar{R}P$ 3-$\bar{\underline{R}}\dot{\bar{R}}\bar{R}PP$ |
| 81-85 | 3-$\underline{P}\bar{R}\dot{\bar{R}}PP$ 3-$\underline{P}\bar{R}P\dot{\bar{R}}P$ 3-$\underline{P}\bar{R}PP\dot{\bar{R}}$ 3-$\underline{P}P\bar{R}\dot{\bar{R}}P$ 3-$\underline{P}P\bar{R}P\dot{\bar{R}}$ |
| 86-90 | 3-$\underline{P}PP\bar{R}\dot{\bar{R}}$ 3-$\bar{R}\dot{\bar{R}}\underline{P}PP$ 3-$\bar{R}\underline{P}\dot{\bar{R}}PP$ 3-$\bar{R}\underline{P}P\dot{\bar{R}}P$ 3-$\bar{R}\underline{P}PP\dot{\bar{R}}$ |

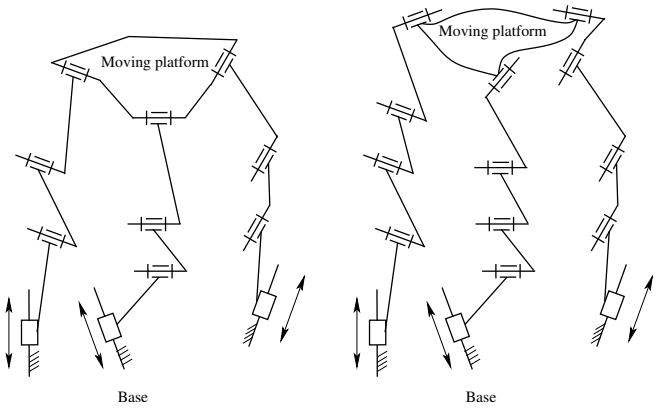


(a) 3-$\underline{P}\bar{R}\bar{R}\bar{R}$ TPM. (b) 3-$\underline{P}\bar{R}\bar{R}\bar{R}\dot{R}$ TPM.

Figure 4.7: Some new TPMs.

## 4.8 Conclusions

The type synthesis of TPMs has been well solved using the general approach to the type synthesis of PMs proposed in Chapter 3. TPKCs which were proposed in [10, 13] have been re-obtained. TPKCs with inactive joints have also been obtained. Either overconstrained or not-overconstrained 3T1R-PKCs can be obtained. It has been proved that there are no TPKCs which are composed of R and P joints and have no inactive joints except for those TPKCs proposed in [10, 13]. The validity check of actuated joints of TPMs has been reduced to the calculation of a $3 \times 3$ determinant. Some new TPMs have also been revealed. The phenomenon of dependent joint groups of a leg for TPMs is revealed systematically.

The small-motion approach to the derivation of the full-cycle-mobility conditions of TPKCs is general. It is more concise than the approaches reported in [17, 22]. The virtual joint approach is simpler than the small-motion approach although it cannot guarantee in theory that all the legs for TPKCs can be obtained.

It should be pointed out that in any TPKC generated in this chapter, any R joint can be replaced with an H (helical) joint, while any P joint can be replaced with a parallelogram. Some variations of the TPMs can be obtained in this way.

# Chapter 5

# Type synthesis of 3-DOF spherical parallel mechanisms

In this chapter, the type synthesis of 3-DOF spherical parallel mechanisms (SPMs) is dealt with using the general approach proposed in Chapter 3. An SPM refers to a 3-DOF PM generating 3-DOF spherical motion. Four steps of the type synthesis of SPMs are presented in detail. The four steps are the decomposition of the wrench system of SPKC, the type synthesis of legs of SPKCs, the combination of legs to generate SPKCs and the selection of actuated joints. SPKCs with and without inactive joints are synthesized. The phenomenon of dependent joint groups in a SPKC is revealed systematically for the first time. The validity check of actuated joints of SPMs is also simplified.

## 5.1 Introduction

An SPM (spherical parallel mechanism) refers to a 3-DOF PM generating 3-DOF spherical motion. SPMs have a wide range of applications such as orienting devices and wrists.

The SPMs fall into two categories, namely, overconstrained and non-overconstrained (also statically determined) SPMs. The 3-legged SPM, in which each leg is composed of three R joints whose axes all pass through the center of rotation, is one of the most typical overconstrained SPMs [106, 121, 122]. Several non-overconstrained SPMs proposed so far include (a) SPMs in which one of its legs is composed of only one unactuated S joint; (b) SPMs in which each of the three legs is composed of two R joints whose axes pass through the center of rotation of the moving platform and are connected by a kinematic chain equivalent to a planar joint [16]; (c) SPMs in which each of the three legs is composed of two R joints in series with parallel axes, and three R joints whose axes intersect at the center of rotation of the moving platform [123]; and (d) SPMs in which each of the three legs is composed of an R, $\Pi$ (parallelogram), and S joints [124].

An approach based on displacement group theory is proposed in [16] for the type synthesis of SPMs. Some new types of SPKCs and SPMs have been obtained using this approach [16, 125]. Unfortunately, the number of overconstraints of SPMs has not been revealed. The selection of the actuated joints has not been dealt with systematically either.

Using the general approach proposed in Chapter 3, the type synthesis of SPMs is dealt with in this chapter. The decomposition of wrench systems of SPKCs is dealt with in section 5.2. The type synthesis of legs for SPKCs is performed in Section 5.3 using the virtual joint approach. In Section 5.4, the combination of legs to generate SPKCs is dealt with. The selection of actuated joints for SPMs is discussed in Section 5.5. Finally, conclusions are drawn.

## 5.2 Decomposition of the wrench system of spherical parallel kinematic chains

In any general configuration, the twist system of an SPKC is a 3-$\boldsymbol{\xi}_0$-system whose center is at the center of rotation of the moving platform. It can be found without difficulty that its wrench system is also a 3-$\boldsymbol{\zeta}_0$-system whose center is at the center of rotation of the moving platform (Fig. 5.1). As the wrench system, $\mathcal{W}$, of a PKC is the union of those of all its legs, $\mathcal{W}_i$, in any configuration [72], it is then concluded that the wrench system of any leg in an SPKC is a $c^i(0 \leq c^i \leq 3)$-$\boldsymbol{\zeta}_0$-system in any general configuration.

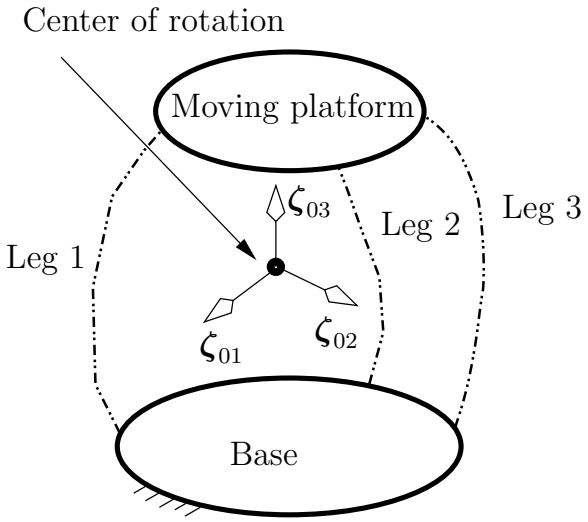


Figure 5.1: Wrench system of an SPKC.

Since all the wrenches within a leg wrench system are of the same pitch, the combination of leg-wrench systems can be simply represented by the combination of the orders $c^i$ of the leg-wrench systems. The combinations of the orders of leg wrench systems are listed in Table 3.1.

## 5.3 Type synthesis of legs using the virtual joint approach

The specified conditions that an SPKC satisfies are given below.

**(1)** The wrench system of any leg in the PKC is a $c^i(0 \leq c^i \leq 3)$-$\boldsymbol{\zeta}_0$-system in a general configuration;

**(2)** The moving platform can undergo arbitrary small rotations;

**(3)** The wrench system of a leg in a PKC is still a $c^i(0 \leq c^i \leq 3)$-$\boldsymbol{\zeta}_0$-system when the moving platform undergoes arbitrary small rotations.

**(4)** The PKC is composed of a set of legs satisfying Conditions (1)–(3). The PKC is assembled is a way such that (1) Arbitrary small arbitrary rotations are permitted by all the legs and (2) The wrench system of the PKC is a 3-$\boldsymbol{\zeta}_0$-system in a general configuration.

Conditions (1)–(3) are the conditions that a leg for SPKC should satisfy. Conditions (2)–(3) are actually the full-cycle mobility condition of legs for SPKCs. Condition (4) guarantees that the PKC is an SPKC.

A leg for SPKCs is a leg satisfying Conditions (1), (2) and (3) for SPKCs. The type synthesis of legs for SPKCs can be performed by first finding legs with a $c^i$-$\boldsymbol{\zeta}_0$-system, i.e., a leg satisfying Condition (1) for SPKCs, and then finding legs with a $c^i$-$\boldsymbol{\zeta}_0$-system that further satisfy Conditions (2) and (3) for SPKCs.

The type synthesis of legs for SPKCs can be performed in three steps.

**Step 2a** To perform the type synthesis of legs with a $c^i$-$\boldsymbol{\zeta}_0$-system, i.e., a leg satisfying Condition (1) for SPKCs. Legs with a $c^i$-$\boldsymbol{\zeta}_0$-system have been obtained in Section 3.5.1.3.

**Step 2b** To find the full-cycle mobility conditions for the legs for SPKCs, namely, the specific geometric condition which makes a leg with a $c^i$-$\boldsymbol{\zeta}_0$-system satisfy conditions (2) and (3) for SPKCs and thus be a leg for SPKCs. In this section, the full-cycle mobility conditions for SPKCs will be derived using the virtual joint approach (3.5.2). The type synthesis of legs for SPKCs involving $\Pi$ joints, such as the R$\Pi$S leg proposed in [124], is out of the scope of this thesis.

**Step 2c** To generate the types of legs for SPKCs corresponding to each of the 3-DOF single-loop kinematic chains.

### 5.3.1 Step 2b: Type synthesis of 3-DOF single-loop kinematic chains involving an S joint

An S joint has the same motion pattern as an SPKC. For an SPKC, the S joint and one of its legs will constitute virtually a 3-DOF single-loop kinematic chain. The axes of the wrenches of the $c^i$-$\boldsymbol{\zeta}_0$-system of the leg always pass through the center of the S joint.

From the types of legs with a $c^i(c^i > 0)$-$\boldsymbol{\zeta}_0$-system (Table 3.4), the possible types of 3-DOF single-loop kinematic chains are RRRS, RRRRS, RRRPS, RRRRRS, RRRRPS and RRRPPS 3-DOF single-loop kinematic chains.

Based on the 3-DOF single-loop spherical kinematic chain, the following 3-DOF single-loop kinematic chains involving an S joint can be obtained:

$\ddot{\text{R}}\ddot{\text{R}}\ddot{\text{R}}$S, $\ddot{\text{R}}\ddot{\text{R}}\ddot{\text{R}}$RS, $\ddot{\text{R}}\ddot{\text{R}}\ddot{\text{R}}$RS, $\ddot{\text{R}}\ddot{\text{R}}\ddot{\text{R}}$PS, $\ddot{\text{R}}\ddot{\text{R}}\text{P}\ddot{\text{R}}$S, $\ddot{\text{R}}\ddot{\text{R}}\ddot{\text{R}}$RRS, $\ddot{\text{R}}\ddot{\text{R}}\ddot{\text{R}}$RRS, $\ddot{\text{R}}\ddot{\text{R}}\ddot{\text{R}}$RRS, R$\ddot{\text{R}}\ddot{\text{R}}\ddot{\text{R}}$RRS, $\ddot{\text{R}}\ddot{\text{R}}$RRR$\ddot{\text{R}}$S, $\ddot{\text{R}}\ddot{\text{R}}$RR$\ddot{\text{R}}$RS, $\ddot{\text{R}}\ddot{\text{R}}\ddot{\text{R}}$RPS, $\ddot{\text{R}}\ddot{\text{R}}$RR$\ddot{\text{R}}$PS, $\ddot{\text{R}}$RR$\ddot{\text{R}}\ddot{\text{R}}$PS, R$\ddot{\text{R}}\ddot{\text{R}}\ddot{\text{R}}$PS, $\ddot{\text{R}}\ddot{\text{R}}\text{RP}\ddot{\text{R}}$S, $\ddot{\text{R}}$RR$\ddot{\text{R}}\ddot{\text{R}}$PS, $\ddot{\text{R}}\ddot{\text{R}}\ddot{\text{R}}$PRS, $\ddot{\text{R}}\ddot{\text{R}}\text{P}\ddot{\text{R}}$RS, $\ddot{\text{R}}\text{P}\ddot{\text{R}}\ddot{\text{R}}$RS, $\ddot{\text{R}}\ddot{\text{R}}$PR$\ddot{\text{R}}$S, $\ddot{\text{R}}\ddot{\text{R}}\ddot{\text{R}}$PPS, $\ddot{\text{R}}\ddot{\text{R}}\text{P}\ddot{\text{R}}$PS, $\ddot{\text{R}}\text{P}\ddot{\text{R}}\ddot{\text{R}}$PS, P$\ddot{\text{R}}\ddot{\text{R}}\ddot{\text{R}}$PS, $\ddot{\text{R}}\ddot{\text{R}}$PPP$\ddot{\text{R}}$S and $\ddot{\text{R}}\text{P}\ddot{\text{R}}\text{P}\ddot{\text{R}}$S 3-DOF single-loop kinematic chains.

In the representation of types of 3-DOF single-loop kinematic chains involving an S joint, SPKCs, SPMs and their legs, $\ddot{\text{R}}$'s denote R joints whose axes intersect at the center of the S joint or the center of rotation of the moving platform, $\overline{\text{XXX}}$ (X represents an R or a P joint) denotes an equivalent planar joint formed by three successive joints, and $\overbrace{\text{RRR}}$ denotes an equivalent spherical joint formed by three successive R joints. $\widetilde{\text{RRR}}$ is used to denote that the three R joints belong to a Bennett linkage [1] while the center of the S joint or the intersection of $\ddot{\text{R}}$ joints is located on the axis of the fourth R joint. All the axes of the R joints within the $\overline{\text{XXX}}$ or $\overbrace{\text{RRR}}$ do not pass through the intersection of the axes of the $\ddot{\text{R}}$ joints.

The geometric characteristic of these 3-DOF single-loop kinematic chains involving an S joint is that the axes of three of the R joints, i.e., $\ddot{\text{R}}$ joints, pass through the center of the S joint. The kinematic characteristic of these 3-DOF single-loop kinematic chains involving an S joint is that all the R and P joint except for the S and $\ddot{\text{R}}$ joints

[1] For a review on the research on the Bennett linkage, see [126]

are inactive. A joint in a mechanism is said to be inactive when its joint variable is invariant during the motion of the mechanism.

Based on displacement group theory [16] or screw theory [112], the following 3-DOF single-loop kinematic chains involving an S joint can be obtained:

$\ddot{\mathrm{R}}\overline{\mathrm{RRRR}}\ddot{\mathrm{R}}\mathrm{S}$, $\ddot{\mathrm{R}}\overline{\mathrm{RRRP}}\ddot{\mathrm{R}}\mathrm{S}$, $\ddot{\mathrm{R}}\overline{\mathrm{RRPR}}\ddot{\mathrm{R}}\mathrm{S}$, $\ddot{\mathrm{R}}\overline{\mathrm{RRPP}}\ddot{\mathrm{R}}\mathrm{S}$, $\ddot{\mathrm{R}}\overline{\mathrm{RPRP}}\ddot{\mathrm{R}}\mathrm{S}$, $\ddot{\mathrm{R}}\ddot{\mathrm{R}}\overline{\mathrm{RRRR}}\mathrm{S}$, $\ddot{\mathrm{R}}\ddot{\mathrm{R}}\overline{\mathrm{RRRP}}\mathrm{S}$, $\ddot{\mathrm{R}}\ddot{\mathrm{R}}\overline{\mathrm{RRPR}}\mathrm{S}$, $\ddot{\mathrm{R}}\ddot{\mathrm{R}}\overline{\mathrm{PRRR}}\mathrm{S}$, $\ddot{\mathrm{R}}\ddot{\mathrm{R}}\overline{\mathrm{RRPP}}\mathrm{S}$, $\ddot{\mathrm{R}}\ddot{\mathrm{R}}\overline{\mathrm{PRPR}}\mathrm{S}$, $\ddot{\mathrm{R}}\ddot{\mathrm{R}}\overline{\mathrm{PPRR}}\mathrm{S}$, $\ddot{\mathrm{R}}\ddot{\mathrm{R}}\overbrace{\mathrm{RRRR}}\ddot{\mathrm{R}}\mathrm{S}$, $\ddot{\mathrm{R}}\ddot{\mathrm{R}}\overbrace{\mathrm{RRRR}}\mathrm{S}$, $\ddot{\mathrm{R}}\mathrm{R}\widetilde{\mathrm{RRR}}\ddot{\mathrm{R}}\mathrm{S}$ and $\ddot{\mathrm{R}}\ddot{\mathrm{R}}\widetilde{\mathrm{RRR}}\mathrm{RS}$ 3-DOF single-loop kinematic chains.

Of these 3-DOF single-loop kinematic chains involving an S joint, the first three are proposed in [16], the fourth and the fifth are implicitly proposed in [16], while the others are new (Fig. 5.2).

The characteristic of these 3-DOF single-loop kinematic chains involving an S joint is that the axes of two R joints pass through the center of the S joint.

### 5.3.2 Type 2c: Generation of types of legs

By removing the S joint in a 3-DOF single-loop kinematic chain involving an S joint, one or two legs for SPMs can be obtained. For example, by removing the S joint in a $\ddot{\mathrm{R}}\ddot{\mathrm{R}}\overline{\mathrm{RRRR}}\mathrm{S}$ kinematic chain (Fig. 5.2(b)), a $\overline{\mathrm{RRRR}}\ddot{\mathrm{R}}\ddot{\mathrm{R}}$ leg (Fig. 3(a)) and a $\ddot{\mathrm{R}}\ddot{\mathrm{R}}\overline{\mathrm{RRR}}$ leg can be obtained. The legs for SPMs obtained are listed in Table 5.1.

## 5.4 Step 3: Combination of legs to generate spherical parallel kinematic chains

SPKCs can be generated by assembling a set of legs for SPKCs shown in Table 5.1 selected according to the combinations of the leg wrench systems shown in Table 3.1. In assembling SPKCs, the following condition should be met: The union of their wrench systems constitutes a 3-$\boldsymbol{\zeta}_0$-system (see Condition (4) for SPKCs in Section 5.3).

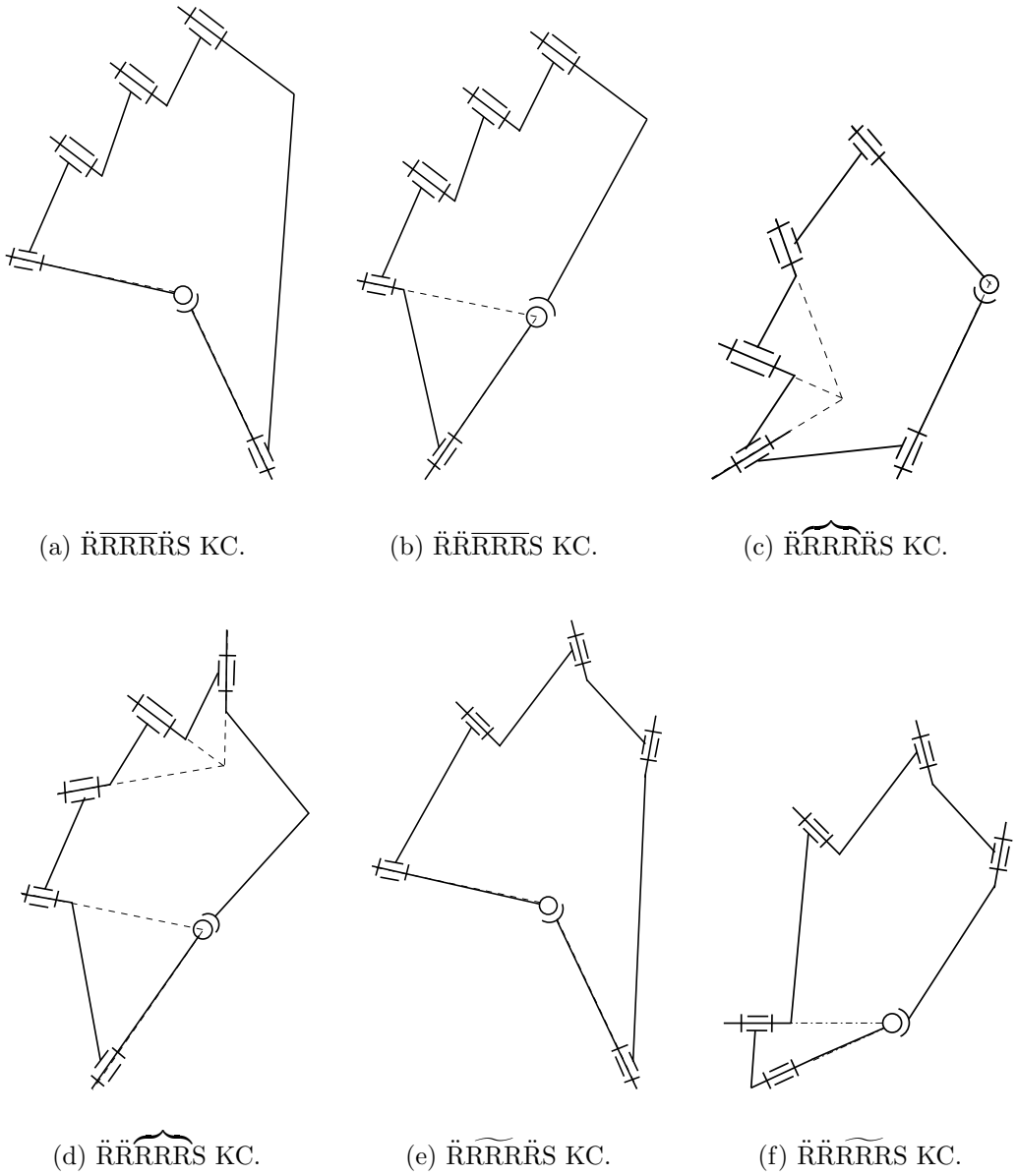

(a) $\ddot{\mathrm{R}}\overline{\mathrm{RRRR}}\ddot{\mathrm{R}}\mathrm{S}$ KC. (b) $\ddot{\mathrm{R}}\ddot{\mathrm{R}}\overline{\mathrm{RRRR}}\mathrm{S}$ KC. (c) $\ddot{\mathrm{R}}\overbrace{\mathrm{RRRR}}\ddot{\mathrm{R}}\mathrm{S}$ KC.

(d) $\ddot{\mathrm{R}}\ddot{\mathrm{R}}\overbrace{\mathrm{RRR}}\mathrm{S}$ KC. (e) $\ddot{\mathrm{R}}\mathrm{R}\widetilde{\mathrm{RRR}}\ddot{\mathrm{R}}\mathrm{S}$ KC. (f) $\ddot{\mathrm{R}}\ddot{\mathrm{R}}\mathrm{R}\widetilde{\mathrm{RRR}}\mathrm{S}$ KC.

Figure 5.2: 3-DOF single-loop kinematic chains involving an S joint.

Table 5.1: Legs for SPKCs.

| $c^i$ | Class | No. | Type |
|---|---|---|---|
| 3 | 3R | 1 | $\ddot{R}\ddot{R}\ddot{R}$ |
| 2 | 4R | 2 | $\ddot{R}\ddot{R}\ddot{R}R$ |
| | | 3 | $\ddot{R}\ddot{R}R\ddot{R}$ |
| | | 4 | $\ddot{R}R\ddot{R}\ddot{R}$ |
| | | 5 | $R\ddot{R}\ddot{R}\ddot{R}$ |
| | 3R1P | 6 | $\ddot{R}\ddot{R}\ddot{R}P$ |
| | | 7 | $\ddot{R}\ddot{R}P\ddot{R}$ |
| | | 8 | $\ddot{R}P\ddot{R}\ddot{R}$ |
| | | 9 | $P\ddot{R}\ddot{R}\ddot{R}$ |
| 1 | 5R | 10-19 | Permutation of $\ddot{R}\ddot{R}\ddot{R}RR$ |
| | | 20 | $\ddot{R}\ddot{R}\overline{RRR}$ |
| | | 21 | $\ddot{R}\overline{RRR}\ddot{R}$ |
| | | 22 | $\overline{RRR}\ddot{R}\ddot{R}$ |
| | | 23 | $\ddot{R}\ddot{R}\overbrace{RRR}$ |
| | | 24 | $\ddot{R}\overbrace{RRR}\ddot{R}$ |
| | | 25 | $\overbrace{RRR}\ddot{R}\ddot{R}$ |
| | | 26 | $\ddot{R}\ddot{R}\widetilde{RRR}$ |
| | | 27 | $\ddot{R}\widetilde{RRR}\ddot{R}$ |
| | | 28 | $\widetilde{RRR}\ddot{R}\ddot{R}$ |
| | 4R1P | 29-48 | Permutation of $\ddot{R}\ddot{R}\ddot{R}RP$ |
| | | 49 | $\ddot{R}\ddot{R}\overline{RRP}$ |
| | | 50 | $\ddot{R}\ddot{R}\overline{RPR}$ |
| | | 51 | $\ddot{R}\ddot{R}\overline{PRR}$ |
| | | 52 | $\ddot{R}\overline{RRP}\ddot{R}$ |
| | | 53 | $\ddot{R}\overline{RPR}\ddot{R}$ |
| | | 54 | $\ddot{R}\overline{PRR}\ddot{R}$ |
| | | 55 | $\overline{RRP}\ddot{R}\ddot{R}$ |
| | | 56 | $\overline{RPR}\ddot{R}\ddot{R}$ |
| | | 57 | $\overline{PRR}\ddot{R}\ddot{R}$ |
| | 3R2P | 58-67 | Permutation of $\ddot{R}\ddot{R}\ddot{R}PP$ |
| | | 68 | $\ddot{R}\ddot{R}\overline{RPP}$ |
| | | 69 | $\ddot{R}\ddot{R}\overline{PRP}$ |
| | | 70 | $\ddot{R}\ddot{R}\overline{PPR}$ |
| | | 71 | $\ddot{R}\overline{RPP}\ddot{R}$ |
| | | 72 | $\ddot{R}\overline{PRP}\ddot{R}$ |
| | | 73 | $\ddot{R}\overline{PPR}\ddot{R}$ |
| | | 74 | $\overline{RPP}\ddot{R}\ddot{R}$ |
| | | 75 | $\overline{PRP}\ddot{R}\ddot{R}$ |
| | | 76 | $\overline{PPR}\ddot{R}\ddot{R}$ |
| 0 | omitted | omitted | omitted |

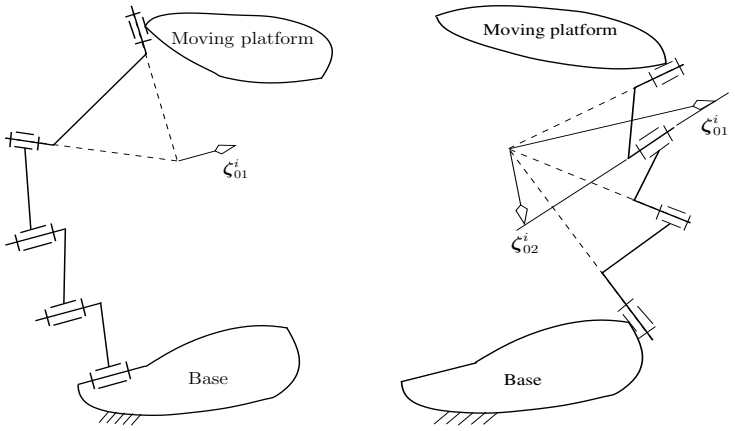


(a) $\overline{\text{RRRR}}\ddot{\text{R}}\ddot{\text{R}}$ leg. (b) $\ddot{\text{R}}\ddot{\text{R}}\text{RR}\ddot{\text{R}}$ leg.

Figure 5.3: Some legs for SPKCs.

In constructing an SPKC, it is usually sufficient to ensure that all the $\ddot{\text{R}}$ joints in the SPKCs intersect at one point. For an SPKC the wrench systems of whose legs are all invariant with respect to the base or the moving platform, additional constraints should be imposed on the base or the moving platform.

Figure 5.3 shows two legs for SPKCs. In the $\overline{\text{RRRR}}\ddot{\text{R}}\ddot{\text{R}}$ leg shown in Fig. 5.3(a), the axes of the first three R joints are parallel while the axes of the last two R joints intersect with each other. This leg has a 1-$\boldsymbol{\zeta}_0$-system. The $\boldsymbol{\zeta}_0$ passes through the common point of the axes of two $\ddot{\text{R}}$ joint and is parallel to the axes of the first three R joints. In the $\ddot{\text{R}}\ddot{\text{R}}\text{RR}\ddot{\text{R}}$ leg shown in Fig. 5.3(b), all the axes of the $\ddot{\text{R}}$ joints intersect at a point. This leg has a 2-$\boldsymbol{\zeta}_0$-system which comprises all $\boldsymbol{\zeta}_0$'s whose axes pass through the common point of all the axes of the $\ddot{\text{R}}$ joints and intersect with the axis of the R joint. By taking one $\overline{\text{RRRR}}\ddot{\text{R}}\ddot{\text{R}}$ leg and one $\ddot{\text{R}}\ddot{\text{R}}\text{RR}\ddot{\text{R}}$ leg, a 2-legged $\overline{\text{RRRR}}\ddot{\text{R}}\ddot{\text{R}}$-$\ddot{\text{R}}\ddot{\text{R}}\text{RR}\ddot{\text{R}}$ SPKC (Fig. 5.4) can be obtained. In the SPKC, all the $\ddot{\text{R}}$ joints in the SPKCs intersect at one point.

Due to the large number of SPKCs, only the three-legged SPKCs with legs of the same type are listed in Table 5.2.

The wrench system of each leg of the 3-$\overline{\text{RRRR}}\ddot{\text{R}}\ddot{\text{R}}$, 3-$\overbrace{\text{RRRR}}\ddot{\text{R}}\ddot{\text{R}}$, 3-$\overline{\text{RRPR}}\ddot{\text{R}}\ddot{\text{R}}$, 3-$\overline{\text{RPRR}}\ddot{\text{R}}\ddot{\text{R}}$, 3-$\overline{\text{PRRR}}\ddot{\text{R}}\ddot{\text{R}}$, 3-$\overline{\text{RPPR}}\ddot{\text{R}}\ddot{\text{R}}$, 3-$\overline{\text{PRPR}}\ddot{\text{R}}\ddot{\text{R}}$, 3-$\overline{\text{PPRR}}\ddot{\text{R}}\ddot{\text{R}}$ are invariant with respect to the base. To guarantee that the union of the wrench systems of three legs within an SPKC

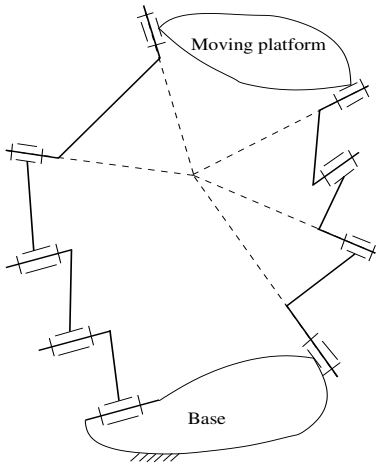


Figure 5.4: $\overline{\text{RRR}}\ddot{\text{R}}\ddot{\text{R}}$-$\ddot{\text{R}}\ddot{\text{R}}\text{R}\ddot{\text{R}}$ SPKC.

constitutes a 3-$\boldsymbol{\zeta}_0$-system, the base should be designed in such a way that the normals to the equivalent planar joints of all legs are not parallel to a plane or that the center of rotation of the moving platform and the centers of the three equivalent spherical joints are not located on a same plane. The wrench system of each leg of the 3-$\ddot{\text{R}}\ddot{\text{R}}\overline{\text{RRR}}$, 3-$\ddot{\text{R}}\ddot{\text{R}}\overbrace{\text{RRR}}$, 3-$\ddot{\text{R}}\ddot{\text{R}}\overline{\text{RRP}}$, 3-$\ddot{\text{R}}\ddot{\text{R}}\overline{\text{RPR}}$, 3-$\ddot{\text{R}}\ddot{\text{R}}\overline{\text{PRR}}$, 3-$\ddot{\text{R}}\ddot{\text{R}}\overline{\text{RPP}}$, 3-$\ddot{\text{R}}\ddot{\text{R}}\overline{\text{PRP}}$, 3-$\ddot{\text{R}}\ddot{\text{R}}\overline{\text{PPR}}$ are invariant with respect to the moving platform. To guarantee that the union of the wrench systems of three legs within an SPKC constitutes a 3-$\boldsymbol{\zeta}_0$-system, the moving platform should be designed in such a way that the normals to the equivalent planar joints of all legs are not parallel to a plane or that the center of rotation of the moving platform and the centers of the three equivalent spherical joints are not located on a same plane.

## 5.5 Step 4: Selection of actuated joints to generate spherical parallel mechanisms

In this section, the characteristic of the actuation wrenches of actuated joints for an SPM is first revealed. A simplified validity condition of actuated joints for SPMs is then proposed.

Considering that the order of a screw system is coordinate free and for simplicity reasons, all the actuation wrenches and wrenches are expressed in a coordinate system

Table 5.2: Three-legged SPKCs.

| $c^i$ | Class | No. | Type | Number of overconstraints |
|---|---|---|---|---|
| 3 | 3R | 1 | 3-$\ddot{\mathrm{R}}\ddot{\mathrm{R}}\ddot{\mathrm{R}}$ | 6 |
| 2 | 4R | 2 | 3-$\ddot{\mathrm{R}}\ddot{\mathrm{R}}\ddot{\mathrm{R}}\mathrm{R}$ | 3 |
| | | 3 | 3-$\ddot{\mathrm{R}}\ddot{\mathrm{R}}\mathrm{R}\ddot{\mathrm{R}}$ | |
| | | 4 | 3-$\ddot{\mathrm{R}}\mathrm{R}\ddot{\mathrm{R}}\ddot{\mathrm{R}}$ | |
| | | 5 | 3-$\mathrm{R}\ddot{\mathrm{R}}\ddot{\mathrm{R}}\ddot{\mathrm{R}}$ | |
| | 3R1P | 6 | 3-$\ddot{\mathrm{R}}\ddot{\mathrm{R}}\ddot{\mathrm{R}}\mathrm{P}$ | |
| | | 7 | 3-$\ddot{\mathrm{R}}\ddot{\mathrm{R}}\mathrm{P}\ddot{\mathrm{R}}$ | |
| | | 8 | 3-$\ddot{\mathrm{R}}\mathrm{P}\ddot{\mathrm{R}}\ddot{\mathrm{R}}$ | |
| | | 9 | 3-$\mathrm{P}\ddot{\mathrm{R}}\ddot{\mathrm{R}}\ddot{\mathrm{R}}$ | |
| 1 | 5R | 10-19 | 3-Permutation of $\ddot{\mathrm{R}}\ddot{\mathrm{R}}\ddot{\mathrm{R}}\mathrm{RR}$ | 0 |
| | | 20 | 3-$\ddot{\mathrm{R}}\ddot{\mathrm{R}}\overline{\mathrm{RRR}}$ | |
| | | 21 | 3-$\ddot{\mathrm{R}}\overline{\mathrm{RRR}}\ddot{\mathrm{R}}$ | |
| | | 22 | 3-$\overline{\mathrm{RRR}}\ddot{\mathrm{R}}\ddot{\mathrm{R}}$ | |
| | | 23 | 3-$\ddot{\mathrm{R}}\ddot{\mathrm{R}}\overbrace{\mathrm{RRR}}$ | |
| | | 24 | 3-$\ddot{\mathrm{R}}\overbrace{\mathrm{RRR}}\ddot{\mathrm{R}}$ | |
| | | 25 | 3-$\overbrace{\mathrm{RRR}}\ddot{\mathrm{R}}\ddot{\mathrm{R}}$ | |
| | | 26 | 3-$\ddot{\mathrm{R}}\ddot{\mathrm{R}}\widetilde{\mathrm{RRR}}$ | |
| | | 27 | 3-$\ddot{\mathrm{R}}\widetilde{\mathrm{RRR}}\ddot{\mathrm{R}}$ | |
| | | 28 | 3-$\widetilde{\mathrm{RRR}}\ddot{\mathrm{R}}\ddot{\mathrm{R}}$ | |
| | 4R1P | 29-48 | 3-Permutation of $\ddot{\mathrm{R}}\ddot{\mathrm{R}}\ddot{\mathrm{R}}\mathrm{RP}$ | |
| | | 49 | 3-$\ddot{\mathrm{R}}\ddot{\mathrm{R}}\overline{\mathrm{RRP}}$ | |
| | | 50 | 3-$\ddot{\mathrm{R}}\ddot{\mathrm{R}}\overline{\mathrm{RPR}}$ | |
| | | 51 | 3-$\ddot{\mathrm{R}}\ddot{\mathrm{R}}\overline{\mathrm{PRR}}$ | |
| | | 52 | 3-$\ddot{\mathrm{R}}\overline{\mathrm{RRP}}\ddot{\mathrm{R}}$ | |
| | | 53 | 3-$\ddot{\mathrm{R}}\overline{\mathrm{RPR}}\ddot{\mathrm{R}}$ | |
| | | 54 | 3-$\ddot{\mathrm{R}}\overline{\mathrm{PRR}}\ddot{\mathrm{R}}$ | |
| | | 55 | 3-$\overline{\mathrm{RRP}}\ddot{\mathrm{R}}\ddot{\mathrm{R}}$ | |
| | | 56 | 3-$\overline{\mathrm{RPR}}\ddot{\mathrm{R}}\ddot{\mathrm{R}}$ | |
| | | 57 | 3-$\overline{\mathrm{PRR}}\ddot{\mathrm{R}}\ddot{\mathrm{R}}$ | |
| | 3R2P | 58-67 | 3-Permutation of $\ddot{\mathrm{R}}\ddot{\mathrm{R}}\ddot{\mathrm{R}}\mathrm{PP}$ | |
| | | 68 | 3-$\ddot{\mathrm{R}}\ddot{\mathrm{R}}\overline{\mathrm{RPP}}$ | |
| | | 69 | 3-$\ddot{\mathrm{R}}\ddot{\mathrm{R}}\overline{\mathrm{PRP}}$ | |
| | | 70 | 3-$\ddot{\mathrm{R}}\ddot{\mathrm{R}}\overline{\mathrm{PPR}}$ | |
| | | 71 | 3-$\ddot{\mathrm{R}}\overline{\mathrm{RPP}}\ddot{\mathrm{R}}$ | |
| | | 72 | 3-$\ddot{\mathrm{R}}\overline{\mathrm{PRP}}\ddot{\mathrm{R}}$ | |
| | | 73 | 3-$\ddot{\mathrm{R}}\overline{\mathrm{PPR}}\ddot{\mathrm{R}}$ | |
| | | 74 | 3-$\overline{\mathrm{RPP}}\ddot{\mathrm{R}}\ddot{\mathrm{R}}$ | |
| | | 75 | 3-$\overline{\mathrm{PRP}}\ddot{\mathrm{R}}\ddot{\mathrm{R}}$ | |
| | | 76 | 3-$\overline{\mathrm{PPR}}\ddot{\mathrm{R}}\ddot{\mathrm{R}}$ | |

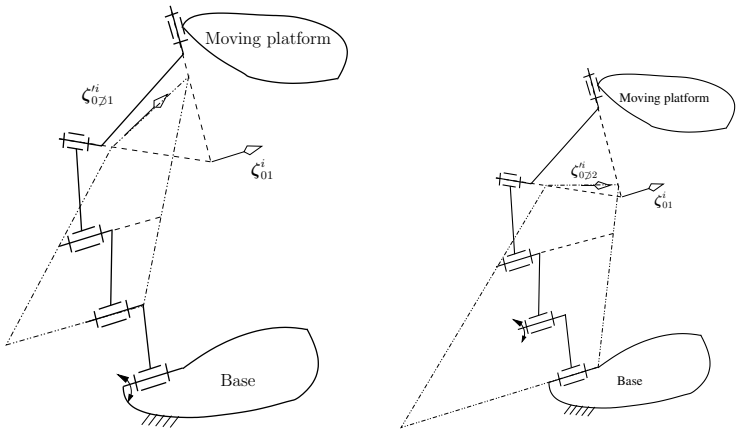


(a) $\overline{\underline{\text{R}}\text{RR}}\dot{\text{R}}\dot{\text{R}}$ leg. (b) $\overline{\text{R}\underline{\text{R}}\text{R}}\dot{\text{R}}\dot{\text{R}}$ leg.

Figure 5.5: Actuation wrenches of some legs for SPKCs.

with its origin at the center of the wrench system. Inactive joints and dependent joint groups of an SPKC are introduced to further simplify the validity check of actuated joints.

### 5.5.1 Characteristics of actuation wrenches

Considering that all the axes of $\boldsymbol{\zeta}_j^i$'s pass through the origin of the coordinate system, we have

$$\boldsymbol{\zeta}_{Sj}^i = 0 \tag{5.1}$$

The substitution of Eq. (5.1) into Eq. (2.22) yields

$$\boldsymbol{\zeta}_{S\not\parallel j}^i = \alpha \boldsymbol{\zeta}_{S\not\parallel j}'^i, \quad \alpha \neq 0 \tag{5.2}$$

From Eq. (5.2), we can conclude that all the $\boldsymbol{\zeta}_{S\not\parallel j}^i$'s corresponding to the same actuated joint are in the same direction if $\boldsymbol{\zeta}_{S\not\parallel j}'^i \neq \mathbf{0}$.

### 5.5.2 Simplified validity condition of actuated joints

Following the validity condition of actuated joints for PMs (Section 2.3), we know that a set of 3 actuated joints for a 3-DOF SPM is valid if and only if, in a general

configuration, the actuation wrenches $\boldsymbol{\zeta}^i_{\not\partial j}$, of the 3 actuated joints, together with the wrench system, $\mathcal{W}$, of the SPM constitute a 6-system.

Let $[\mathbf{i} \quad \mathbf{0}]^T$, $[\mathbf{j} \quad \mathbf{0}]^T$, $[\mathbf{k} \quad \mathbf{0}]^T$ denote a basis of $\mathcal{W}$, $[\boldsymbol{\zeta}^i_{F\not\partial j} \quad \boldsymbol{\zeta}^i_{S\not\partial j}]^T$ represents $\boldsymbol{\zeta}^i_{\not\partial j}$. The validity condition of actuated joints of an SPM can be expressed as

$$\begin{vmatrix} \boldsymbol{\zeta}^1_{F\not\partial j} & \boldsymbol{\zeta}^2_{F\not\partial j} & \boldsymbol{\zeta}^3_{F\not\partial j} & \mathbf{i} & \mathbf{j} & \mathbf{k} \\ \boldsymbol{\zeta}^1_{S\not\partial j} & \boldsymbol{\zeta}^2_{S\not\partial j} & \boldsymbol{\zeta}^3_{S\not\partial j} & \mathbf{0} & \mathbf{0} & \mathbf{0} \end{vmatrix} = \begin{vmatrix} \mathbf{i} & \mathbf{j} & \mathbf{k} \end{vmatrix} \begin{vmatrix} \boldsymbol{\zeta}^1_{S\not\partial j} & \boldsymbol{\zeta}^2_{S\not\partial j} & \boldsymbol{\zeta}^3_{S\not\partial j} \end{vmatrix} \neq 0 \tag{5.3}$$

As $\begin{vmatrix} \mathbf{i} & \mathbf{j} & \mathbf{k} \end{vmatrix} = 1$, Eq. (5.3) can be reduced to

$$\begin{vmatrix} \boldsymbol{\zeta}^1_{S\not\partial j} & \boldsymbol{\zeta}^2_{S\not\partial j} & \boldsymbol{\zeta}^3_{S\not\partial j} \end{vmatrix} \neq 0 \tag{5.4}$$

Equation (5.4) shows that a simplified validity condition of actuated joints for SPMs can be stated as follows:

**A set of 3 actuated joints is valid for a 3-DOF SPM if and only if, in a general configuration, none of the second vector components of the actuation wrenches of the actuated joints is 0 and the second vector components of the actuation wrenches of the three actuated joints $\boldsymbol{\zeta}^i_{\not\partial j}$ are linearly independent.**

From Eq. (5.3), we obtain the t-component $\boldsymbol{\zeta}^i_{t\not\partial j}$ and the w-component $\boldsymbol{\zeta}^i_{w\not\partial j}$ of the actuation wrench $\boldsymbol{\zeta}^i_{\not\partial j}$ are respectively $\boldsymbol{\zeta}^i_{S\not\partial j}$ and $\boldsymbol{\zeta}^i_{F\not\partial j}$. To keep to geometric insight clear, the notations $\boldsymbol{\zeta}^i_{S\not\partial j}$ and $\boldsymbol{\zeta}^i_{F\not\partial j}$ are used in this section.

### 5.5.3 Procedure for the validity detection of actuated joints

The validity detection of actuated joints of SPMs can thus be performed using the following steps.

**Step 4a** If one or more of the actuated joints of a possible SPM are inactive, the set of actuated joints is invalid and the possible SPM should be discarded.

Although different approaches can be used to detect inactive joints, an alternative approach is proposed below.

A joint in an SPKC is inactive if the second vector component of its actuation wrenches, $\boldsymbol{\zeta}^i_{S\not\partial j}$'s, is $\mathbf{0}$. In other words, a joint in an SPKC is inactive if its

actuation wrenches belong to the 3-$\boldsymbol{\zeta}_0$-system of the SPKC. Physically speaking, the actuation wrenches of the inactive joint will not restrict the motion of the moving platform within its twist system.

For example, the actuation wrenches of the $\ddot{\mathrm{R}}\ddot{\mathrm{R}}\underline{\mathrm{R}}\ddot{\mathrm{R}}$ leg for SPMs when the R joint is selected as actuated joint are the $\boldsymbol{\zeta}_0$'s whose axes pass through the common points of the axes of the three $\ddot{\mathrm{R}}$ joints and do not pass through the axis of the R joint. The second vector component of all its actuation wrenches is $\mathbf{0}$, thus the R joint is inactive and cannot be selected as actuated joint. In fact, for a leg involving three $\ddot{\mathrm{R}}$ joints, all the joints in the leg except the $\ddot{\mathrm{R}}$ joints are inactive.

**Step 4b** If more than one joints of a dependent joint group belong to the set of actuated joints of a possible SPM, the set of actuated joints is invalid and the possible SPM should be discarded.

It is found that dependent joint groups include the joints with an $\overline{\mathrm{XXX}}$ joint or the R joints within an $\overbrace{\mathrm{RRR}}$ joint. For a leg with an $\overline{\mathrm{XXX}}$ joint, the axes of the actuation wrenches of different joints within the $\overline{\mathrm{XXX}}$ joint are all located on the plane passing through the axes of the two $\ddot{\mathrm{R}}$ joints of the same leg (Fig. 5.5). The second vector components of these actuation wrenches are all perpendicular to the above plane and thus parallel. The three joints in the $\overline{\mathrm{RRR}}$ joint comprise a dependent joint group. Thus, only one of the three joints in the $\overline{\mathrm{XXX}}$ joint can be actuated. For a leg with an $\overbrace{\mathrm{RRR}}$ joint, the axes of the actuation wrenches of different R joints within the $\overbrace{\mathrm{RRR}}$ joint are all located on the plane passing through the axes of the two $\ddot{\mathrm{R}}$ joints of the same leg. The second vector components of these actuation wrenches are all perpendicular to the above plane and thus parallel. The three R joints in the $\overbrace{\mathrm{RRR}}$ joint comprise a dependent joint group. Thus, only one of the three R joints in the $\overbrace{\mathrm{RRR}}$ joint can be actuated. One of the joints within a dependent joint group can be actuated.

**Step 4c** If the second vector components of the actuation wrenches of actuated joints $\boldsymbol{\zeta}^i_{\not\partial j}$ are linearly dependent in a general configuration for a possible SPM, the set of actuated joints is invalid. In this case, the possible SPM should be discarded.

For practical reasons, the selection of actuated joints for $m$-legged SPMs should satisfy the following criteria:

**(1)** The actuated joints should be distributed among all the legs as evenly as possible.

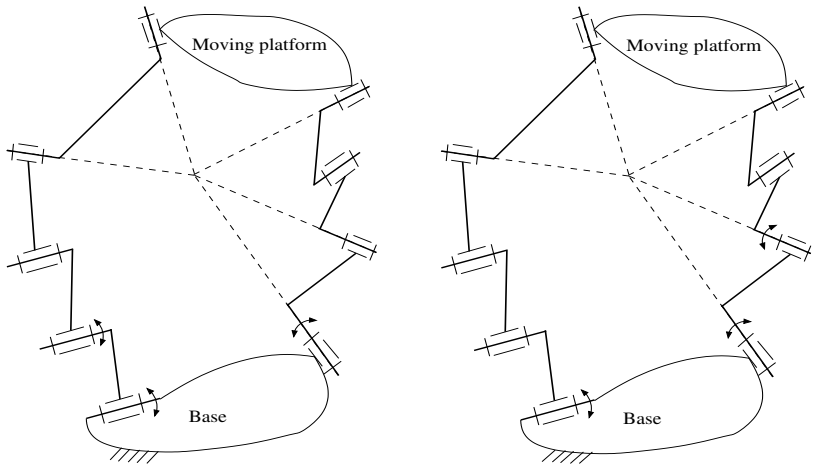


(a) $\overline{\underline{\mathrm{RR}}\mathrm{RR}}\ddot{\mathrm{R}}\ddot{\mathrm{R}}$-$\underline{\ddot{\mathrm{R}}}\ddot{\mathrm{R}}\mathrm{R}\ddot{\mathrm{R}}$ SPM. (b) $\overline{\underline{\mathrm{R}}\mathrm{RR}}\ddot{\mathrm{R}}\ddot{\mathrm{R}}$-$\underline{\ddot{\mathrm{R}}\ddot{\mathrm{R}}}\mathrm{R}\ddot{\mathrm{R}}$ SPM.

Figure 5.6: Selection of actuated joints for the RRR$\ddot{\mathrm{R}}\ddot{\mathrm{R}}$-$\ddot{\mathrm{R}}\ddot{\mathrm{R}}\mathrm{R}\ddot{\mathrm{R}}$ SPKC.

**(2)** The actuated joints should preferably be on the base or close to the base.

**(3)** No unactuated P joint exists.

For example, the possible SPMs corresponding to the 2-legged SPKC, $\overline{\mathrm{RRR}}\ddot{\mathrm{R}}\ddot{\mathrm{R}}$-$\ddot{\mathrm{R}}\ddot{\mathrm{R}}\mathrm{R}\ddot{\mathrm{R}}$ satisfying the above criteria are $\overline{\underline{\mathrm{RR}}\mathrm{RR}}\ddot{\mathrm{R}}\ddot{\mathrm{R}}$-$\underline{\ddot{\mathrm{R}}}\ddot{\mathrm{R}}\mathrm{R}\ddot{\mathrm{R}}$ and $\overline{\underline{\mathrm{R}}\mathrm{RR}}\ddot{\mathrm{R}}\ddot{\mathrm{R}}$-$\underline{\ddot{\mathrm{R}}\ddot{\mathrm{R}}}\mathrm{R}\ddot{\mathrm{R}}$ (Fig. 5.6). Following the procedure for the detection of the validity of actuated joints, the $\overline{\underline{\mathrm{RR}}\mathrm{RR}}\ddot{\mathrm{R}}\ddot{\mathrm{R}}$-$\underline{\ddot{\mathrm{R}}}\ddot{\mathrm{R}}\mathrm{R}\ddot{\mathrm{R}}$ SPM should be discarded as more than one of the joints within a dependent joint group, which is composed of the first three R joints in the $\overline{\mathrm{RRR}}\ddot{\mathrm{R}}\ddot{\mathrm{R}}$ leg, belong to the set of actuated joints. Thus, there is only one SPM corresponding to the 2-legged SPKC, i.e., the $\overline{\underline{\mathrm{R}}\mathrm{RR}}\ddot{\mathrm{R}}\ddot{\mathrm{R}}$-$\underline{\ddot{\mathrm{R}}\ddot{\mathrm{R}}}\mathrm{R}\ddot{\mathrm{R}}$ SPM.

Following the above criteria and the procedure for the validity detection of actuated joints, all the $m(m \geq 2)$-legged SPMs corresponding to each SPKC can be generated. Due to the large number of SPMs, only 3-legged SPMs with all legs of the same type satisfying the above criteria are listed in Table 5.3. By substituting a combination of an R joint and a P joint with parallel axes, a combination of two R joints whose axes are not parallel and a combination of three R joints whose axes are not parallel with a C, U, and S joint respectively, all the special cases of SPMs can be obtained. For example, the RUU SPM [123] is a special case of the 3-$\underline{\ddot{\mathrm{R}}}\ddot{\mathrm{R}}\mathrm{R}\ddot{\mathrm{R}}$ SPM. To make the conditions for SPMs clear in their representation and for simplicity reasons, these special cases

are not listed in Table 5.3.

## 5.6 Presentation of new spherical parallel mechanisms

There are 11 new SPMs in Table 5.3 (see No. 16, 18–27). Four of the new SPMs, namely the 3-$\overline{\underline{\mathrm{R}}\mathrm{RRR}}\ddot{\mathrm{R}}\ddot{\mathrm{R}}$, 3-$\overbrace{\underline{\mathrm{R}}\mathrm{RRR}}^{}\ddot{\mathrm{R}}\ddot{\mathrm{R}}$, 3-$\underline{\ddot{\mathrm{R}}}\mathrm{S}\ddot{\mathrm{R}}$ and 3-$\underline{\ddot{\mathrm{R}}}\ddot{\mathrm{R}}\mathrm{S}$ SPMs, are shown in Fig. 5.7. All the four new SPMs are not overconstrained. The 3-$\underline{\ddot{\mathrm{R}}}\mathrm{S}\ddot{\mathrm{R}}$ SPM is a special case of the 3-$\underline{\ddot{\mathrm{R}}}\overbrace{\mathrm{RRR}}^{}\ddot{\mathrm{R}}$, 3-$\underline{\ddot{\mathrm{R}}}\ddot{\mathrm{R}}\mathrm{RRR}\ddot{\mathrm{R}}$, 3-$\underline{\ddot{\mathrm{R}}}\mathrm{R}\ddot{\mathrm{R}}\mathrm{RR}\ddot{\mathrm{R}}$ or 3-$\underline{\ddot{\mathrm{R}}}\mathrm{RRR}\ddot{\mathrm{R}}\ddot{\mathrm{R}}$ SPMs, while the 3-$\underline{\ddot{\mathrm{R}}}\ddot{\mathrm{R}}\mathrm{S}$ SPM is a special case of the 3-$\underline{\ddot{\mathrm{R}}}\ddot{\mathrm{R}}\overbrace{\mathrm{RRR}}^{}$, 3-$\underline{\ddot{\mathrm{R}}}\ddot{\mathrm{R}}\ddot{\mathrm{R}}\mathrm{RR}$, 3-$\underline{\ddot{\mathrm{R}}}\ddot{\mathrm{R}}\mathrm{R}\ddot{\mathrm{R}}\mathrm{R}$ or 3-$\underline{\ddot{\mathrm{R}}}\ddot{\mathrm{R}}\mathrm{RRR}\ddot{\mathrm{R}}$ SPMs.

Based on the above four new SPMs, some variations (Fig. 5.8) of the agile eye [44] are under investigation. Compared with the agile eye, the arrangement of the location of the actuated joints on the base is more flexible for the 3-$\overline{\underline{\mathrm{R}}\mathrm{RRR}}\ddot{\mathrm{R}}\ddot{\mathrm{R}}$ and 3-$\overbrace{\underline{\mathrm{R}}\mathrm{RRR}}^{}\ddot{\mathrm{R}}\ddot{\mathrm{R}}$ SPMs. In the case of the 3-$\overbrace{\underline{\mathrm{R}}\mathrm{RR}}^{}\ddot{\mathrm{R}}\ddot{\mathrm{R}}$ SPM, the axes of three actuated joints can be parallel (Fig 5.8(a)). However, the new SPMs are more complex in structure than the agile eye.

## 5.7 Conclusions

The type synthesis of SPMs has been well solved using the general approach to the type synthesis of PMs proposed in Chapter 3. SPKCs with inactive joints as well as SPKCs without inactive joints have been obtained. Either overconstrained or non-overconstrained SPKCs can be obtained. The validity check of actuated joints of SPMs has been reduced to the calculation of a $3 \times 3$ determinant. The phenomenon of dependent joint groups of a leg for SPMs is revealed for the first time.

The SPKCs obtained include some new SPKCs as well as all the known SPKCs involving R, P, U and C joints. Some new SPMs have also been proposed. Most of the results in this section have been published in [28]. At almost the same time, Hervé and Karouia have also published several papers [127, 128] on type synthesis of SPMs

Table 5.3: Three-legged SPMs.

| $c^i$ | Class | No. | Type |
|---|---|---|---|
| 3 | 3R | 1 | 3-$\underline{\ddot{R}}\ddot{R}\ddot{R}$ |
| 2 | 4R | 2 | 3-$\underline{\ddot{R}}\ddot{R}\ddot{R}R$ |
| | | 3 | 3-$\underline{\ddot{R}}\ddot{R}R\ddot{R}$ |
| | | 4 | 3-$\underline{\ddot{R}}R\ddot{R}\ddot{R}$ |
| | | 5 | 3-$R\underline{\ddot{R}}\ddot{R}\ddot{R}$ |
| 1 | 5R | 6-15 | 3-Permutation of $\underline{\ddot{R}}\ddot{R}\ddot{R}RR$ |
| | | 16 | 3-$\underline{\ddot{R}}\ddot{R}\overline{RRR}$ |
| | | 17 | 3-$\underline{\ddot{R}}\overline{RRR}\ddot{R}$ |
| | | 18 | 3-$\overline{\underline{R}RR}\ddot{R}\ddot{R}$ |
| | | 19 | 3-$\underline{\ddot{R}}\ddot{R}\overbrace{RRR}$ |
| | | 20 | 3-$\underline{\ddot{R}}\overbrace{RRR}\ddot{R}$ |
| | | 21 | 3-$\overbrace{\underline{R}RR}\ddot{R}\ddot{R}$ |
| | | 22 | 3-$\underline{\ddot{R}}\ddot{R}\widetilde{RRR}$ |
| | | 23 | 3-$\underline{\ddot{R}}\widetilde{RRR}\ddot{R}$ |
| | | 24 | 3-$\underline{\widetilde{R}}\widetilde{R}R\ddot{R}\ddot{R}$ |
| | 4R-1P | 25 | 3-$\overline{RR\underline{P}}\ddot{R}\ddot{R}$ |
| | | 26 | 3-$\overline{R\underline{P}R}\ddot{R}\ddot{R}$ |
| | | 27 | 3-$\overline{\underline{P}RR}\ddot{R}\ddot{R}$ |

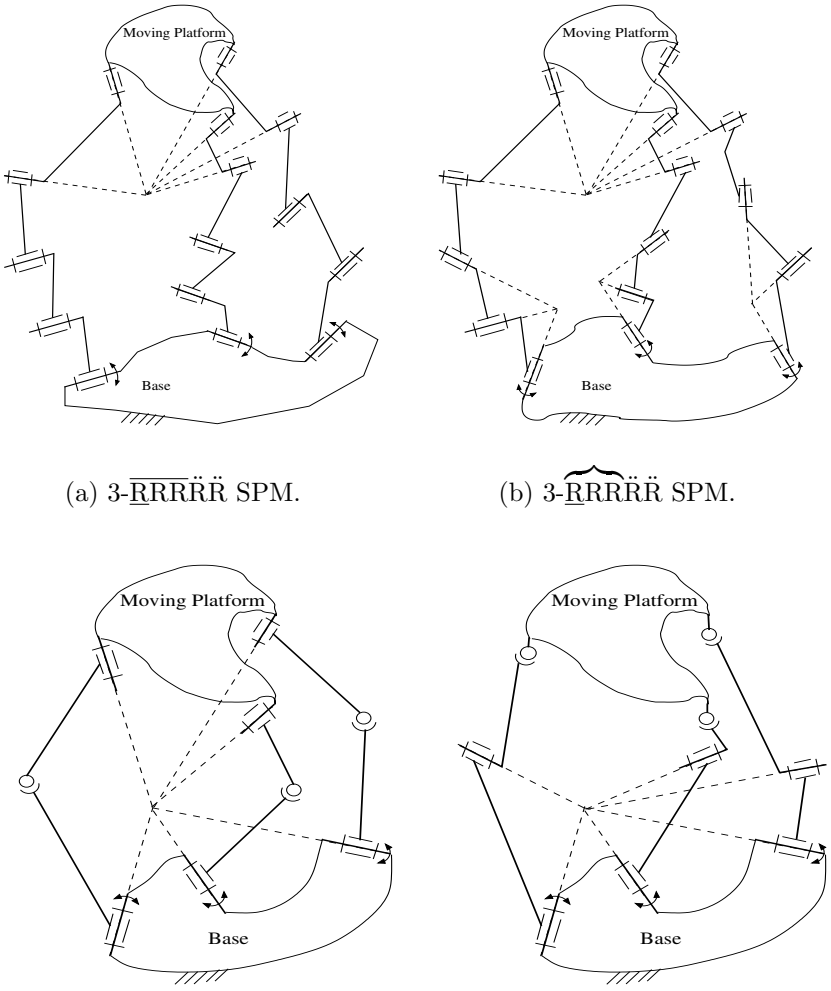


(a) 3-$\underline{\overline{\mathrm{R}}\mathrm{RR}}\ddot{\mathrm{R}}\ddot{\mathrm{R}}$ SPM. (b) 3-$\underline{\overbrace{\mathrm{R}\mathrm{RR}}}\ddot{\mathrm{R}}\ddot{\mathrm{R}}$ SPM.

(c) 3-$\underline{\ddot{\mathrm{R}}}\mathrm{S}\ddot{\mathrm{R}}$ SPM. (d) 3-$\underline{\ddot{\mathrm{R}}}\ddot{\mathrm{R}}\mathrm{S}$ SPM.

Figure 5.7: Four new SPMs.

using displacement group theory in which similar results were obtained. Up to now, the 3-$\ddot{\mathrm{R}}\ddot{\mathrm{R}}\widetilde{\mathrm{RRR}}$, 3-$\ddot{\mathrm{R}}\widetilde{\mathrm{RRR}}\ddot{\mathrm{R}}$ and 3-$\widetilde{\mathrm{RRR}}\ddot{\mathrm{R}}\ddot{\mathrm{R}}$ SPKCs have not been found in the literature.

It is still open to find new non-overconstrained SPKCs or to prove that there are no SPKCs, except those given in this section.

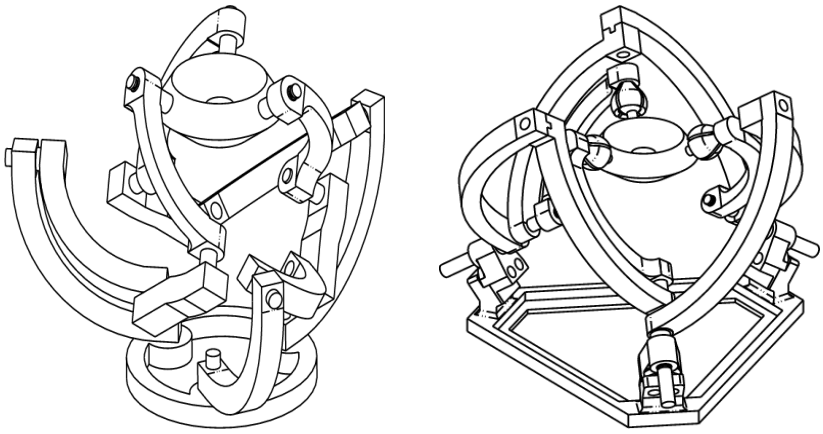

(a) 3-$\underline{\underline{\widetilde{\mathrm{R}}}}\mathrm{RRR}\ddot{\mathrm{R}}\ddot{\mathrm{R}}$ SPM. (b) 3-$\underline{\underline{\ddot{\mathrm{R}}}}\ddot{\mathrm{R}}\mathrm{S}$ SPM.

Figure 5.8: Some variations of the Agile eye.

# Chapter 6

# Type synthesis of 4-DOF parallel mechanisms generating 3 translations and 1 rotation

In this chapter, the type synthesis of 4-DOF 3T1R parallel mechanisms (3T1R-PMs) is dealt with using the general approach proposed in Chapter 3. A 4-DOF 3T1R-PM is a PM generating 3T1R motion (also called Schönflies motion) which includes 3 translations and 1 rotation. A 3T1R-PM covers a wide range of applications. Four steps of the type synthesis of 3T1R-PMs are presented in detail. The four steps are the decomposition of the wrench system of 3T1R-PKC, the type synthesis of legs of 3T1R-PKCs, the combination of legs to generate 3T1R-PKCs and the selection of actuated joints. 3T1R-PKCs with and without inactive joints are synthesized. The phenomenon of dependent joint groups in a 3T1R-PKC is revealed systematically for the first time. The validity check of actuated joints of 3T1R-PMs is also simplified.

## 6.1 Introduction

SCARA robots are 4-DOF serial robots and are widely used in tasks such as assembly, pick-and-place and machine loading as well as haptic devices. 3T1R-PMs are the parallel counterparts of the SCARA robot. In a 3T1R-PM (3T1R parallel mechanism), the moving platform can undergo arbitrary translations as well as rotations about axes with a given direction. This type of motion pattern is termed as 3T1R motion (also called Schönflies motion [31]). Unfortunately, only a few 3T1R-PMs have been proposed so far. The 3T1R-PMs proposed in [36, 129, 130] contain either four legs in different structures or S joints. A 3-UPU 4-DOF 3T1R-PM is proposed in [24]. Recently, a systematic study on the type synthesis of 3T1R-PMs is presented in [20]. Three types of 4-legged 3T1R-PMs with legs of the same type and no unactuated P joint are proposed. It is also claimed that all actuated joints are located on the base. However, only two types of PMs are functional, while the other one, in which the four translational degrees of freedom of the C joints are actuated, is flawed. In the latter case, the four translational degrees of freedom of the C joints cannot control the translational degree of freedom along the direction perpendicular to all the axes of the four C joints. The reason is that the selection of the actuated joints has not been well solved. In addition, the number of overconstraints of 3T1R-PMs has not been revealed.

Using the general approach proposed in Chapter 3, the type synthesis of 3T1R-PMs is dealt with in this chapter. The decomposition of wrench systems of 3T1R-PKCs is dealt with in section 6.2. The type synthesis of legs for 3T1R-PKCs is performed in Section 6.3 using the virtual joint approach. In Section 6.4, the combination of legs to generate 3T1R-PKCs is dealt with. The selection of actuated joints for 3T1R-PMs is discussed in Section 6.5. Meanwhile, the detection of inactive joints and dependent joint groups is dealt with. Finally, conclusions are drawn.

## 6.2 Step 1: Decomposition of the wrench system of 4-DOF parallel kinematic chains generating 3 translations and 1 rotation

In any general configuration, the twist system of a 3T1R-PKC is a 3-$\boldsymbol{\xi}_\infty$-1-$\boldsymbol{\xi}_0$-system. It can be found without difficulty that its wrench system is a 2-$\boldsymbol{\zeta}_\infty$-system. As the wrench system of a PKC is the union of those of all its legs in any configuration [72], it is then concluded that the wrench system of any leg in a 3T1R-PKC is a $c^i(0 \leq c^i \leq 2)$-$\boldsymbol{\zeta}_\infty$-system in any general configuration.

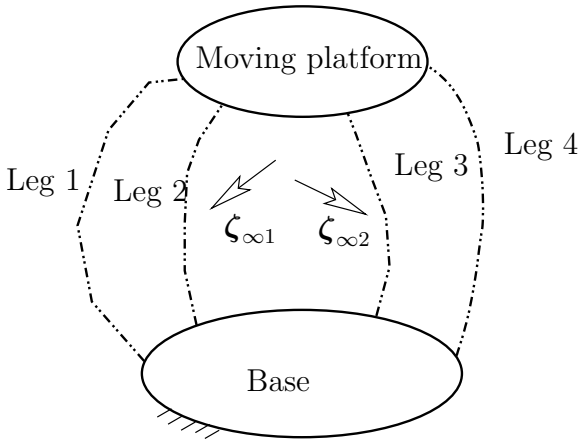


Figure 6.1: Wrench system of a 3T1R-PKC.

Since all the wrenches within a leg wrench system are of the same pitch, the combination of leg-wrench systems can be simply represented by the combination of the orders $c^i$ of leg-wrench systems. The combinations of the orders of leg wrench systems are listed in Table 3.1.

## 6.3 Step 2: Type synthesis of legs

A PKC is a 3T1R-PKC if it satisfies the following four conditions.

(1) The wrench system of any leg in the PKC is a $c^i(0 \leq c^i \leq 2)$-$\boldsymbol{\zeta}_\infty$-system in a general configuration;

(2) The moving platform can undergo arbitrary small 3T1R motions;

(3) The wrench system of a leg in a PKC is still a $c^i(0 \leq c^i \leq 2)$-$\boldsymbol{\zeta}_\infty$-system when the moving platform undergoes arbitrary small 3T1R motion;

(4) The PKC is composed of a set of legs satisfying Conditions (1)–(3). The PKC is assembled is a way such that (1) Arbitrary small 3T1R motions are permitted by all the legs and (2) The wrench system of the PKC is a 2-$\boldsymbol{\zeta}_\infty$-system in a general configuration.

Conditions (1)–(3) are the conditions that a leg for 3T1R-PKC should satisfy. Conditions (2)–(3) constitute actually the full-cycle mobility condition for legs for 3T1R-PKCs. Condition (4) guarantees that the PKC is a 3T1R-PKC.

A leg for 3T1R-PKCs is a leg satisfying Conditions (1), (2) and (3) for 3T1R-PKCs. Type synthesis of legs for 3T1R-PKCs can be performed in three steps.

**Step 2a** To perform the type synthesis of legs with a $c^i(0 \leq c^i \leq 2)$-$\boldsymbol{\zeta}_\infty$-system, i.e., a leg satisfying Condition (1) for 3T1R-PKCs. This was done in Section 3.5.1.2 and is therefore not repeated here.

**Step 2b** To find the full-cycle mobility conditions for the legs for 3T1R-PKCs, namely, the specific geometric condition which makes a leg with a $c^i$-$\boldsymbol{\zeta}_\infty$-system satisfy conditions (2) and (3) for 3T1R-PKCs and thus be a leg for 3T1R-PKCs. This problem can be solved using either the small-motion approach or the virtual joint approach (Section 3.5.2). The derivation needed for the small-motion-approach is very complex and similar to that used in the case of legs for 3T1R-PMs (Section 4.3). Since the results obtained using both the small-motion approach and the virtual-joint approach are the same, only the derivation using the virtual joint approach is presented in this section.

**Step 2c** To generate the types of legs for 3T1R-PKCs corresponding to each of the full-cycle mobility conditions for the legs for 3T1R-PKCs.

### 6.3.1 Step 2b Type synthesis of 4-DOF single-loop kinematic chains with a W joint

A W joint is a virtual joint having 4 DOFs (three translations and one rotation). It has the same motion pattern as a 3T1R-PKC. For a 3T1R-PKC, the W joint and one of its legs will constitute a 4-DOF single-loop kinematic chain.

From the types of legs with a $c^i(0 \leq c^i \leq 2)$-$\boldsymbol{\zeta}_\infty$-system, the possible types of 4-DOF single-loop kinematic chains are RRRPW, RRPPW, RPPPW, RRRRRW, RRRRPW, RRRPPW and RRPPPW. It is noted that the wrench system of the W joint is a 2-$\boldsymbol{\zeta}_\infty$-system. To obtain a 4-DOF single-loop kinematic chain with a W joint, the leg with a $c^i(0 \leq c^i \leq 2)$-$\boldsymbol{\zeta}_\infty$-system must be arranged in such a way that the union of the two wrench systems comprise a 2-$\boldsymbol{\zeta}_\infty$-system.

For the 4-DOF single-loop kinematic chains of classes RRRPW, RRPPW and RPPPW, the axis of the R joint within the W joint and the axes of the other R joints must be parallel. The types of 4-DOF single-loop kinematic chains of classes RRRPW, RRPPW and RPPPW are (1) $\acute{\mathrm{R}}\acute{\mathrm{R}}\acute{\mathrm{R}}\mathrm{P}\acute{\mathrm{W}}$, (2) $\acute{\mathrm{R}}\acute{\mathrm{R}}\mathrm{P}\mathrm{P}\acute{\mathrm{W}}$, and (3) $\acute{\mathrm{R}}\mathrm{P}\mathrm{P}\mathrm{P}\acute{\mathrm{W}}$.

In the representation of types of 4-DOF single-loop kinematic chains involving a W joint, 3T1R-PKCs, 3T1R-PMs and their legs, $\acute{\mathrm{R}}$'s denote R joints whose axes are all parallel, $\dot{\mathrm{R}}$'s denote R joints within the same leg whose axes are all parallel.

It is noted that for a group of successive R joints or R joints connected by P joints in which the axes of these R joints are parallel in any one configuration, the axes of the R joints will always be parallel. Thus, for the 4-DOF single-loop kinematic chains of classes RRRRRW, RRRRPW, RRRPPW and RRPPPW, the R joints should be divided into two groups. In each group of R joints, the R joints are successively connected or connected by P joints and their axes are parallel.

The types of the 4-DOF single-loop kinematic chains of classes RRRRRW, RRRRPW, RRRPPW and RRPPPW are (1) $\acute{\mathrm{R}}\acute{\mathrm{R}}\acute{\mathrm{R}}\acute{\mathrm{R}}\dot{\mathrm{R}}\acute{\mathrm{W}}$, (2) $\acute{\mathrm{R}}\acute{\mathrm{R}}\acute{\mathrm{R}}\dot{\mathrm{R}}\dot{\mathrm{R}}\acute{\mathrm{W}}$, (3) $\acute{\mathrm{R}}\acute{\mathrm{R}}\dot{\mathrm{R}}\dot{\mathrm{R}}\dot{\mathrm{R}}\acute{\mathrm{W}}$, (4) $\acute{\mathrm{R}}\dot{\mathrm{R}}\dot{\mathrm{R}}\dot{\mathrm{R}}\dot{\mathrm{R}}\acute{\mathrm{W}}$, (5) $\acute{\mathrm{R}}\acute{\mathrm{R}}\acute{\mathrm{R}}\dot{\mathrm{R}}\mathrm{P}\acute{\mathrm{W}}$, (6) $\acute{\mathrm{R}}\acute{\mathrm{R}}\dot{\mathrm{R}}\dot{\mathrm{R}}\mathrm{P}\acute{\mathrm{W}}$, (7) $\acute{\mathrm{R}}\dot{\mathrm{R}}\dot{\mathrm{R}}\dot{\mathrm{R}}\mathrm{P}\acute{\mathrm{W}}$, (8) $\acute{\mathrm{R}}\acute{\mathrm{R}}\dot{\mathrm{R}}\mathrm{P}\mathrm{P}\acute{\mathrm{W}}$, (9) $\acute{\mathrm{R}}\dot{\mathrm{R}}\dot{\mathrm{R}}\mathrm{P}\mathrm{P}\acute{\mathrm{W}}$, and (10) $\acute{\mathrm{R}}\dot{\mathrm{R}}\mathrm{P}\mathrm{P}\mathrm{P}\acute{\mathrm{W}}$.

It is pointed out that the P joints and the only $\dot{\mathrm{R}}$ joint can be put anywhere in the single-loop kinematic chain, the combination of $\dot{\mathrm{R}}$ joints can also be put anywhere in the kinematic chain. For brevity, we list only the 4-DOF single-loop kinematic chains from which all 4-DOF single-loop kinematic chains can be obtained through the above operations. For example, $\mathrm{\acute{R}\acute{R}P\acute{R}\acute{W}}$ single-loop kinematic chain can be obtained by changing the position of the P joint in $\mathrm{\acute{R}\acute{R}\acute{R}P\acute{W}}$ single-loop kinematic chain (Fig. 6.2(a)) while $\mathrm{\acute{R}\acute{R}\dot{R}\dot{R}\acute{R}\acute{W}}$ single-loop kinematic chain can be obtained by changing the position of the combination of $\dot{\mathrm{R}}$ joints in the $\mathrm{\acute{R}\acute{R}\acute{R}\dot{R}\dot{R}\acute{W}}$ single-loop kinematic chain (Fig. 6.2(e)).

### 6.3.2 Step 2c: Generation of types of legs

By removing the W joint in a 4-DOF single-loop kinematic chain involving a W joint, one or two legs for 3T1R-PMs can be obtained. For example, by removing the W joint in an $\mathrm{\acute{R}\acute{R}\acute{R}\dot{R}\dot{R}\acute{W}}$ kinematic chain (Fig. 6.2(e)), an $\mathrm{\dot{R}\dot{R}\acute{R}\acute{R}\acute{R}}$ (Fig. 6.5(a)) and an $\mathrm{\acute{R}\acute{R}\acute{R}\dot{R}\dot{R}}$ (Fig. 6.5(b)) leg can be obtained. The legs for 3T1R-PMs obtained are listed in Table 6.1.

It is noted that there are no legs corresponding to the $\mathrm{\acute{R}\acute{R}\acute{R}\acute{R}\dot{R}\acute{W}}$, $\mathrm{\acute{R}\acute{R}\acute{R}\dot{R}\acute{R}\acute{W}}$, $\mathrm{\acute{R}\acute{R}\dot{R}\acute{R}\acute{R}\acute{W}}$, and $\mathrm{\dot{R}\dot{R}\dot{R}\acute{R}\acute{W}}$ 4-DOF single-loop kinematic chain involving a W joint since the five twists of the joints in the serial kinematic chains obtained are linearly dependent.

## 6.4 Step 3: Combination of legs to generate parallel kinematic chains generating 3 translations and 1 rotation

3T1R-PKCs can be generated by assembling a set of legs for 3T1R-PKCs shown in Table 6.1 selected according to the combinations of the leg wrench systems shown in Table 3.1. In assembling 3T1R-PKCs, the following condition should be met: The union of their wrench systems constitutes a 2-$\boldsymbol{\zeta}_\infty$-system (see Condition (4) for 3T1R-PKCs in Section 6.3).

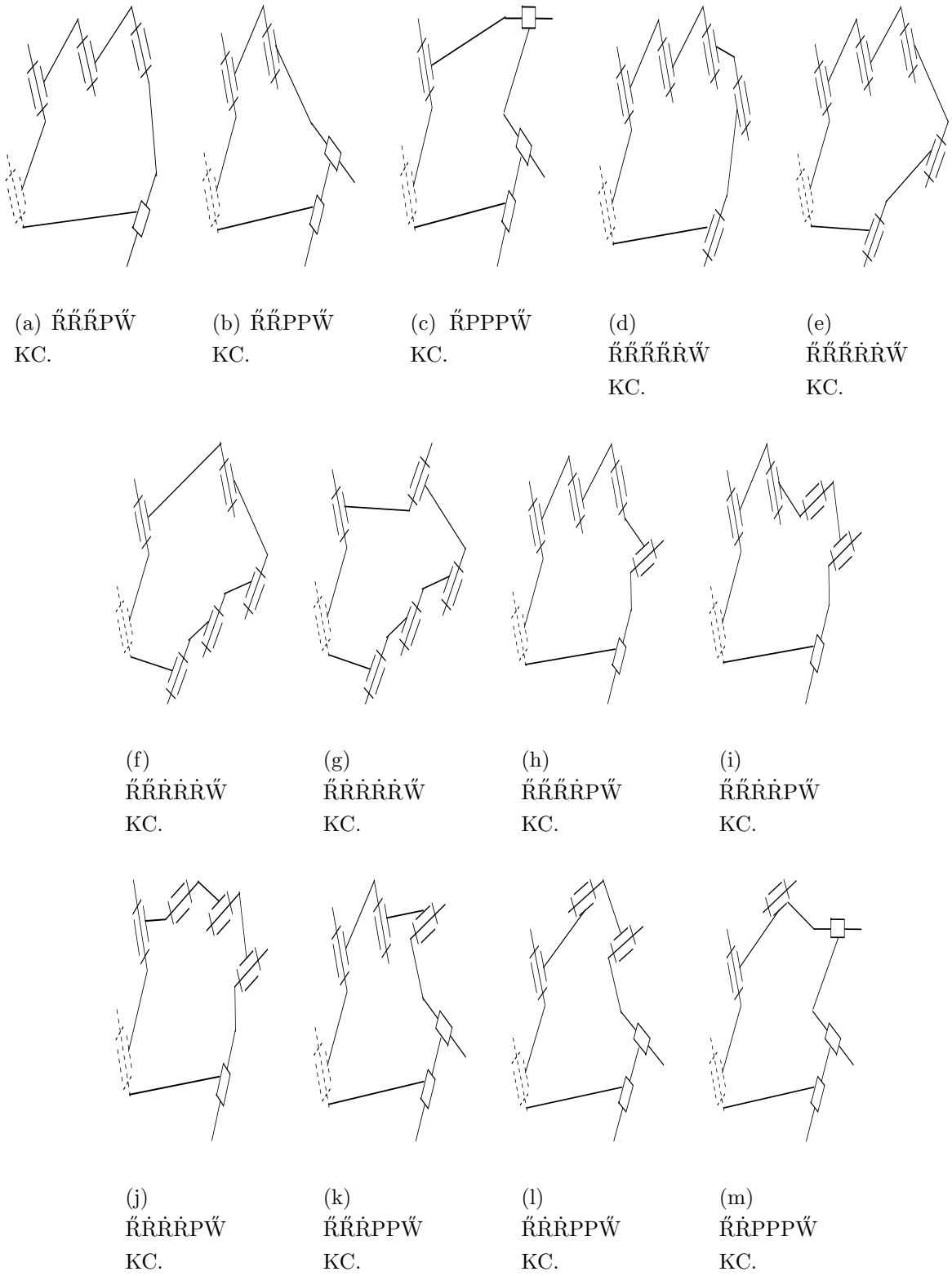

(a) $\acute{R}\acute{\acute{R}}\acute{\acute{R}}P\acute{\acute{W}}$ KC.

(b) $\acute{R}\acute{\acute{R}}PP\acute{\acute{W}}$ KC.

(c) $\acute{R}PPP\acute{\acute{W}}$ KC.

(d) $\acute{R}\acute{\acute{R}}\acute{\acute{R}}\dot{R}\acute{\acute{W}}$ KC.

(e) $\acute{R}\acute{\acute{R}}\acute{\acute{R}}\dot{R}\acute{\acute{W}}$ KC.

(f) $\acute{R}\acute{\acute{R}}\dot{R}\dot{R}\acute{\acute{W}}$ KC.

(g) $\acute{R}\dot{R}\dot{R}\dot{R}\acute{\acute{W}}$ KC.

(h) $\acute{R}\acute{\acute{R}}\acute{\acute{R}}P\acute{\acute{W}}$ KC.

(i) $\acute{R}\acute{\acute{R}}\dot{R}P\acute{\acute{W}}$ KC.

(j) $\acute{R}\dot{R}\dot{R}P\acute{\acute{W}}$ KC.

(k) $\acute{R}\acute{\acute{R}}PP\acute{\acute{W}}$ KC.

(l) $\acute{R}\dot{R}PP\acute{\acute{W}}$ KC.

(m) $\acute{R}\dot{R}PPP\acute{\acute{W}}$ KC.

Figure 6.2: Some 4-DOF single-loop kinematic chains involving a W joint.

Table 6.1: Legs for 3T1R-PKCs.

| $c^i$ | Class | No. | Type |
|---|---|---|---|
| 2 | 3RP | 1 | PR̋R̋R̋ |
| | | 2 | R̋PR̋R̋ |
| | | 3 | R̋R̋PR̋ |
| | | 4 | R̋R̋R̋P |
| | 2R-2P | 5-10 | permutation of PPR̋R̋ |
| | 1R-3P | 11 | PPPR̋ |
| | | 12 | PPR̋P |
| | | 13 | PR̋PP |
| | | 14 | R̋PPP |
| 1 | 5R | 15 | R̋R̋R̋Ṙ |
| | | 16 | R̋R̋Ṙ R̋ |
| | | 17 | R̋Ṙ R̋R̋ |
| | | 18 | Ṙ R̋R̋R̋ |
| | | 19 | R̋R̋Ṙ Ṙ |
| | | 20 | R̋Ṙ Ṙ R̋ |
| | | 21 | Ṙ R̋R̋R̋ |
| | 4R-1P | 22-41 | Permutation of R̋R̋R̋ṘP |
| | | 42 | R̋R̋Ṙ P |
| | | 43 | R̋R̋ṘPR̋ |
| | | 44 | R̋R̋PṘ Ṙ |
| | | 45 | R̋PR̋Ṙ Ṙ |
| | | 46 | PR̋R̋Ṙ Ṙ |
| | | 47 | R̋R̋Ṙ P |
| | | 48 | PR̋Ṙ R̋ |
| | | 49 | R̋Ṙ PR̋ |
| | | 50 | R̋ṘPR̋ |
| | | 51 | R̋PṘ R̋ |
| | | 52 | Ṙ R̋R̋P |
| | | 53 | Ṙ R̋PR̋ |
| | | 54 | Ṙ PR̋R̋ |
| | | 55 | ṘPR̋R̋ |
| | | 56 | PṘ R̋R̋ |
| | | 57 | R̋Ṙ P |
| | | 58 | R̋ṘPR̋ |
| | | 59 | R̋PṘ Ṙ |
| | | 60 | R̋PṘ Ṙ |
| | | 61 | PR̋Ṙ Ṙ |
| | | 62 | Ṙ R̋P |
| | | 63 | Ṙ R̋PR̋ |
| | | 64 | Ṙ PR̋R̋ |
| | | 65 | ṘPṘ R̋ |
| | | 66 | PṘ R̋R̋ |
| | 3R-2P | 67-96 | Permutation of R̋R̋ṘPP |
| | | 97-112 | Permutation of R̋Ṙ PP |
| | 2R-3P | 113-132 | Permutation of R̋ṘPPP |
| 0 | omitted | omitted | omitted |

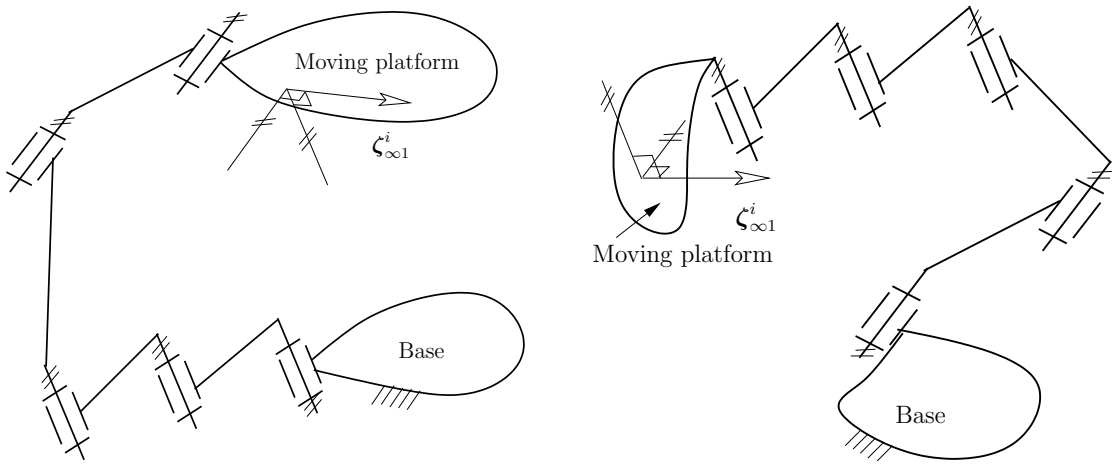


(a) $\acute{\mathrm{R}}\acute{\mathrm{R}}\acute{\mathrm{R}}\dot{\mathrm{R}}\dot{\mathrm{R}}$ leg. (b) $\dot{\mathrm{R}}\dot{\mathrm{R}}\acute{\mathrm{R}}\acute{\mathrm{R}}\acute{\mathrm{R}}$ leg.

Figure 6.3: Some legs for 3T1R-PKCs.

In constructing a 3T1R-PKC, it is usually sufficient to ensure that all the $\acute{\mathrm{R}}$ joints in the 3T1R-PKCs are parallel.

Figure 6.3 shows two legs for 3T1R-PKCs. In the $\acute{\mathrm{R}}\acute{\mathrm{R}}\acute{\mathrm{R}}\dot{\mathrm{R}}\dot{\mathrm{R}}$ leg shown in Fig. 6.3(a), the axes of the first three R joints are parallel while the axes of the last two R joints are also parallel to each other. This leg has a 1-$\boldsymbol{\zeta}_\infty$-system. The $\boldsymbol{\zeta}_\infty$ is perpendicular to the axes of all the R joints. In the $\dot{\mathrm{R}}\dot{\mathrm{R}}\acute{\mathrm{R}}\acute{\mathrm{R}}\acute{\mathrm{R}}$ leg shown in Fig. 6.3(b), the axes of the first two R joints are parallel to each other while the axes of the last three R joints are also parallel. The $\boldsymbol{\zeta}_\infty$ is perpendicular to the axes of all the R joints. Using these two legs, an $\acute{\mathrm{R}}\acute{\mathrm{R}}\acute{\mathrm{R}}\dot{\mathrm{R}}\dot{\mathrm{R}}$-$\dot{\mathrm{R}}\dot{\mathrm{R}}\acute{\mathrm{R}}\acute{\mathrm{R}}\acute{\mathrm{R}}$ 3T1R-PKC can be obtained.

Due to the large number of 3T1R-PKCs, only the 4-legged 3T1R-PKCs with legs of the same type are listed in Table 6.2. However, there are many more possible 3T1R-PKCs, one of which is shown in Fig. 6.4.

It is noted that for a 3T1R-PKC with inactive joints and its kinematic equivalent 3T1R-PKC without inactive joints, the number of overconstraints as well as the reaction forces in the joints are different, although the inactive joints in a 3T1R-PKC make no contribution to the movement of the moving platform.

Table 6.2: Four-legged 3T1R-PKCs.

| $c^i$ | Class | No. | Type | Number of overconstraints |
|---|---|---|---|---|
| 2 | 3RP | 1 | 4-P$\check{R}\check{R}\check{R}$ | 6 |
| | | 2 | 4-$\check{R}$P$\check{R}\check{R}$ | |
| | | 3 | 4-$\check{R}\check{R}$P$\check{R}$ | |
| | | 4 | 4-$\check{R}\check{R}\check{R}$P | |
| | 2R-2P | 5-10 | 4-permutation of PP$\check{R}\check{R}$ | |
| | 1R-3P | 11 | 4-PPP$\check{R}$ | |
| | | 12 | 4-PP$\check{R}$P | |
| | | 13 | 4-P$\check{R}$PP | |
| | | 14 | 4-$\check{R}$PPP | |
| 1 | 5R | 15 | 4-$\check{R}\check{R}\check{R}\dot{R}\dot{R}$ | 2 |
| | | 16 | 4-$\check{R}\check{R}\dot{R}\dot{R}\check{R}$ | |
| | | 17 | 4-$\check{R}\dot{R}\dot{R}\check{R}\check{R}$ | |
| | | 18 | 4-$\dot{R}\dot{R}\check{R}\check{R}\check{R}$ | |
| | | 19 | 4-$\check{R}\check{R}\dot{R}\dot{R}\dot{R}$ | |
| | | 20 | 4-$\check{R}\dot{R}\dot{R}\dot{R}\check{R}$ | |
| | | 21 | 4-$\dot{R}\dot{R}\dot{R}\check{R}\check{R}$ | |
| | 4R-1P | 22-41 | 4-Permutation of $\check{R}\check{R}\check{R}\dot{R}$P | |
| | | 42 | 4-$\check{R}\check{R}\dot{R}\dot{R}$P | |
| | | 43 | 4-$\check{R}\check{R}\dot{R}$P$\dot{R}$ | |
| | | 44 | 4-$\check{R}\check{R}$P$\dot{R}\dot{R}$ | |
| | | 45 | 4-$\check{R}$P$\check{R}\dot{R}\dot{R}$ | |
| | | 46 | 4-P$\check{R}\check{R}\dot{R}\dot{R}$ | |
| | | 47 | 4-$\check{R}\check{R}\dot{R}\dot{R}$P | |
| | | 48 | 4-P$\check{R}\dot{R}\dot{R}\check{R}$ | |
| | | 49 | 4-$\check{R}\dot{R}\dot{R}$P$\check{R}$ | |
| | | 50 | 4-$\check{R}\dot{R}$P$\dot{R}\check{R}$ | |
| | | 51 | 4-$\check{R}$P$\dot{R}\dot{R}\check{R}$ | |
| | | 52 | 4-$\dot{R}\dot{R}\check{R}\check{R}$P | |
| | | 53 | 4-$\dot{R}\dot{R}\check{R}$P$\check{R}$ | |
| | | 54 | 4-$\dot{R}\dot{R}$P$\check{R}\check{R}$ | |
| | | 55 | 4-$\dot{R}$P$\dot{R}\check{R}\check{R}$ | |
| | | 56 | 4-P$\dot{R}\dot{R}\check{R}\check{R}$ | |
| | | 57 | 4-$\check{R}\dot{R}\dot{R}\dot{R}$P | |
| | | 58 | 4-$\check{R}\dot{R}\dot{R}$P$\dot{R}$ | |
| | | 59 | 4-$\check{R}\dot{R}$P$\dot{R}\dot{R}$ | |
| | | 60 | 4-$\check{R}$P$\dot{R}\dot{R}\dot{R}$ | |
| | | 61 | 4-P$\check{R}\dot{R}\dot{R}\dot{R}$ | |
| | | 62 | 4-$\dot{R}\dot{R}\dot{R}\check{R}$P | |
| | | 63 | 4-$\dot{R}\dot{R}\dot{R}$P$\check{R}$ | |
| | | 64 | 4-$\dot{R}\dot{R}$P$\dot{R}\check{R}$ | |
| | | 65 | 4-$\dot{R}$P$\dot{R}\dot{R}\check{R}$ | |
| | | 66 | 4-P$\dot{R}\dot{R}\dot{R}\check{R}$ | |
| | 3R-2P | 67-96 | 4-Permutation of $\check{R}\check{R}\dot{R}$PP | |
| | | 97-112 | 4-Permutation of $\check{R}\dot{R}\dot{R}$PP | |
| | 2R-3P | 113-132 | 4-Permutation of $\check{R}\dot{R}$PPP | |

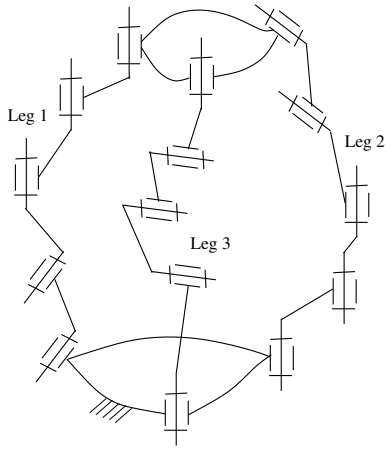


Figure 6.4: $\dot{\mathrm{R}}\dot{\mathrm{R}}\bar{\bar{\mathrm{R}}}\bar{\bar{\mathrm{R}}}$-$\bar{\bar{\mathrm{R}}}\bar{\bar{\mathrm{R}}}\dot{\mathrm{R}}\dot{\mathrm{R}}$-$\bar{\bar{\mathrm{R}}}\dot{\mathrm{R}}\dot{\mathrm{R}}\bar{\bar{\mathrm{R}}}$ 3T1R-PKC.

## 6.5 Step 4: Selection of actuated joints to generate parallel mechanisms generating 3 translations and 1 rotation

In this section, the characteristic of the actuation wrenches of actuated joints for a 3T1R-PM is first revealed. A simplified validity condition of actuated joints for 3T1R-PMs is proposed. The types of 3T1R-PMs are then obtained.

Considering that the order of a screw system is coordinate free and for simplicity reasons, all the actuation wrenches and wrenches are expressed in a coordinate system with its X-axis parallel to the axis of the rotational degree of freedom of the moving platform. Inactive joints and dependent joint groups of a 3T1R-PKC are introduced to further simplify the validity check of actuated joints.

### 6.5.1 Characteristics of actuation wrenches

Considering that all the $\boldsymbol{\zeta}_j^i$'s are with $\infty$ pitch and their axes are all perpendicular to the X-axis, we have

$$\boldsymbol{\zeta}_{Fj}^i = 0 \tag{6.1}$$

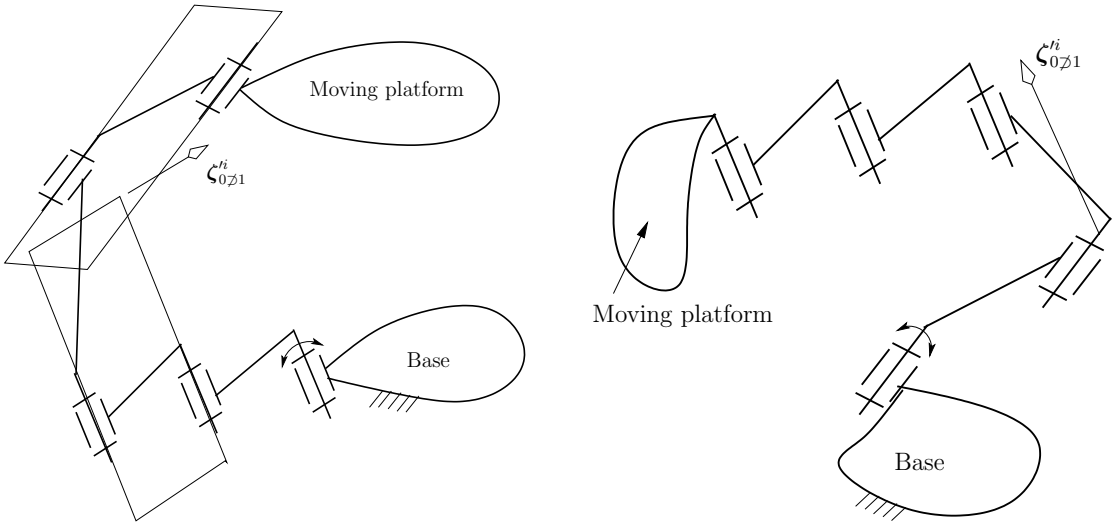


(a) $\underline{\text{R}}\text{R}''\text{R}''\dot{\text{R}}\dot{\text{R}}$ leg. (b) $\underline{\text{R}}\dot{\text{R}}\dot{\text{R}}''\text{R}''\text{R}''$ leg.

Figure 6.5: Actuation wrenches of some legs for 3T1R-PKCs.

In addition, the component of $\boldsymbol{\zeta}^i_{Sj}$ along the X-axis is also 0. Thus, we have

$$\boldsymbol{\zeta}^i_{fj} = 0 \tag{6.2}$$

Thus, the t-component $\boldsymbol{\zeta}^i_{t\not\partial j}$ is composed of the first four scalar components of the actuation wrench $\boldsymbol{\zeta}^i_{\not\partial j}$ while the w-component $\boldsymbol{\zeta}^i_{w\not\partial j}$ is composed of the last two scalar components $\boldsymbol{\zeta}^i_{\not\partial j}$.

The substitution of Eqs. (6.1) and (6.2) into Eq. (2.22) yields

$$\boldsymbol{\zeta}^i_{t\not\partial j} = \alpha \boldsymbol{\zeta}'^i_{t\not\partial j}, \quad \alpha \neq 0 \tag{6.3}$$

From Eq. (6.3), we can conclude that all the $\boldsymbol{\zeta}^i_{t\not\partial j}$'s corresponding to the same actuated joint are proportional to one another.

Figure 6.5 shows the actuation wrenches of actuated joints in some legs for 3T1R-PMs. In the $\underline{\text{R}}\dot{\text{R}}\text{R}''\text{R}''\text{R}''$ leg (Fig. 6.5(a)), the first R joint is actuated. The actuation wrench is any $\boldsymbol{\zeta}_0$ whose axis is parallel to the axes of the last three R joints and intersect with the axis of the second R joint. In the $\underline{\text{R}}''\text{R}''\text{R}''\dot{\text{R}}\dot{\text{R}}$ leg (Fig. 6.5(b)), the first R joint is actuated. The actuation wrench is a $\boldsymbol{\zeta}_0$ whose axes is the intersection of the plane passing through the axes of two unactuated $\text{R}''$ joints and the plane passing through the axes of the two $\dot{\text{R}}$ joints.

### 6.5.2 Simplified validity condition of actuated joints

Following the validity condition of actuated joints for PMs (Section 2.3), we know that a set of four actuated joints for a 4-DOF 3T1R-PM is valid if and only if, in a general configuration, the actuation wrenches $\boldsymbol{\zeta}^i_{\not\partial j}$, of the four actuated joints, together with the wrench system, $\mathcal{W}$, of the 3T1R-PM constitute a 6-system. To perform the validity check of actuated joints for 3T1R-PMs using the above approach directly is very complex.

Let $[\mathbf{0} \quad \mathbf{j}^T]^T$, $[\mathbf{0} \quad \mathbf{k}^T]^T$ denote a basis of $\mathcal{W}$. Here, $\mathbf{j}^T = \{1 \quad 0\}^T$ and $\mathbf{k}^T = \{0 \quad 1\}^T$. The validity condition of actuated joints of a 3T1R-PM can be expressed as

$$\begin{aligned} &\left| \begin{array}{cccccc} \boldsymbol{\zeta}^1_{t\not\partial j} & \boldsymbol{\zeta}^2_{t\not\partial j} & \boldsymbol{\zeta}^3_{t\not\partial j} & \boldsymbol{\zeta}^4_{t\not\partial j} & \mathbf{0} & \mathbf{0} \\ \boldsymbol{\zeta}^1_{w\not\partial j} & \boldsymbol{\zeta}^2_{w\not\partial j} & \boldsymbol{\zeta}^3_{w\not\partial j} & \boldsymbol{\zeta}^4_{w\not\partial j} & \mathbf{j} & \mathbf{k} \end{array} \right| \\ &= \left| \begin{array}{cc} \mathbf{j} & \mathbf{k} \end{array} \right| \left| \begin{array}{cccc} \boldsymbol{\zeta}^1_{t\not\partial j} & \boldsymbol{\zeta}^2_{t\not\partial j} & \boldsymbol{\zeta}^3_{t\not\partial j} & \boldsymbol{\zeta}^4_{t\not\partial j} \end{array} \right| \neq 0 \end{aligned} \tag{6.4}$$

As $\left| \begin{array}{cc} \mathbf{j} & \mathbf{k} \end{array} \right| \neq 0$, Eq. (6.4) can be reduced to

$$\left| \begin{array}{cccc} \boldsymbol{\zeta}^1_{t\not\partial j} & \boldsymbol{\zeta}^2_{t\not\partial j} & \boldsymbol{\zeta}^3_{t\not\partial j} & \boldsymbol{\zeta}^4_{t\not\partial j} \end{array} \right| \neq 0 \tag{6.5}$$

Equation (6.5) shows that a simplified validity condition of actuated joints for 3T1R-PMs can be stated as follows:

**A set of four actuated joints is valid for a 4-DOF 3T1R-PM if and only if, in a general configuration, the t-components of the actuation wrenches of the four actuated joints $\boldsymbol{\zeta}^i_{\not\partial j}$ are linearly independent.**

Three cases for which a set of actuated joints is invalid are (1) One or more actuation wrenches belong to the wrench system of the 3T1R-PM, (2) The axes of two or more $\boldsymbol{\zeta}^i_{\not\partial j}$'s are parallel to the X-axis and (3) The axes of the actuation wrenches of the four actuated joints $\boldsymbol{\zeta}^i_{\not\partial j}$ are all perpendicular to the X-axis.

### 6.5.3 Procedure for the validity detection of actuated joints

The validity detection of actuated joints of 3T1R-PMs can thus be performed using the following steps.

**Step 4a.** If one or more of the actuated joints of a possible 3T1R-PM are inactive, the set of actuated joints is invalid and the possible 3T1R-PM should be discarded.

Although different approaches can be used to detect inactive joints, an alternative approach is proposed below.

A joint in a 3T1R-PKC is inactive if its actuation wrenches, $\boldsymbol{\zeta}_{\not\varnothing j}$'s, belong to the wrench system of the 3T1R-PKC. Physically speaking, the actuation wrenches of the inactive joint will not restrict the motion of the moving platform within its twist system.

For example, the actuation wrenches of the $\dot{\mathrm{R}}$ joint in the $\underline{\dot{\mathrm{R}}}\mathrm{P}\check{\mathrm{R}}\check{\mathrm{R}}\check{\mathrm{R}}$ leg for 3T1R-PMs are the $\boldsymbol{\zeta}_{\infty}$'s whose axes are perpendicular to the axes of all the R joints except the $\dot{\mathrm{R}}$ joint. The $\dot{\mathrm{R}}$ joint is thus an inactive joint. In fact, for a leg involving one and only one $\dot{\mathrm{R}}$ joint, the $\dot{\mathrm{R}}$ joint in the leg is inactive.

**Step 4b.** If all the joints of a dependent joint group belong to the set of actuated joints of a possible 3T1R-PM, the set of actuated joints are invalid and the possible 3T1R-PM should be discarded.

The minimum set of $n_d$ (more than one) joints in the same leg for 3T1R-PMs are termed as a dependent joint group if the t-components $\boldsymbol{\zeta}^i_{t\not\varnothing j}$ of their actuation wrenches are linearly dependent. According to the validity condition of actuated joints for 3T1R-PMs in Section 6.5.2, no more than $(n_d - 1)$ joints within the same dependent joint group can be actuated.

For a leg composed of two $\dot{\mathrm{R}}$ joints and three $\check{\mathrm{R}}$ joints, the axes of the actuation wrenches of different $\dot{\mathrm{R}}$ joints are all parallel to the axes of the $\check{\mathrm{R}}$ joints. The two $\boldsymbol{\zeta}^i_{f\not\varnothing j}$'s are linearly dependent. The two $\dot{\mathrm{R}}$ joints comprise a dependent joint group. Thus, only one of the two $\dot{\mathrm{R}}$ joints can be actuated. Similarly, three $\dot{\mathrm{R}}$ joints within a same leg also comprise a dependent joint group in which at most two of them can be actuated.

**Step 4c.** If the t-components of the actuation wrenches of actuated joints, $\boldsymbol{\zeta}^i_{f\not\varnothing j}$, are linearly dependent in a general configuration for a possible 3T1R-PM, the set of actuated joints is invalid. In this case, the possible 3T1R-PM should be discarded.

For practical reasons, the selection of actuated joints for $m$-legged 3T1R-PMs should

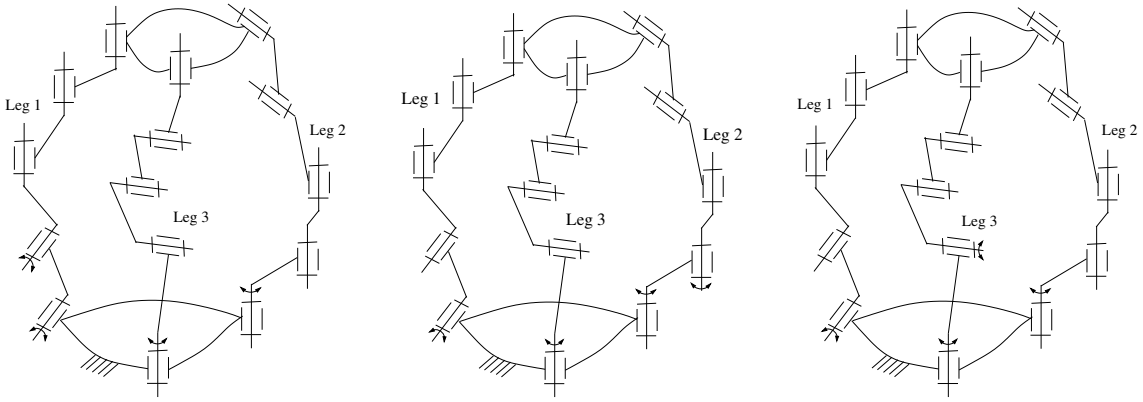


(a) $\underline{\dot{R}\dot{R}}\ddot{R}\ddot{R}\ddot{R}$-$\underline{\ddot{R}}\ddot{R}\dot{R}\dot{R}\dot{R}$-$\underline{\ddot{R}}\dot{R}\dot{R}\dot{R}\ddot{R}$ 3T1R-PM.

(b) $\underline{\dot{R}}\dot{R}\ddot{R}\ddot{R}\ddot{R}$-$\underline{\ddot{R}\ddot{R}}\dot{R}\dot{R}\dot{R}$-$\underline{\ddot{R}}\dot{R}\dot{R}\dot{R}\ddot{R}$ 3T1R-PM.

(c) $\underline{\dot{R}}\dot{R}\ddot{R}\ddot{R}\ddot{R}$-$\underline{\ddot{R}}\ddot{R}\dot{R}\dot{R}\dot{R}$-$\underline{\ddot{R}\dot{R}}\dot{R}\dot{R}\ddot{R}$ 3T1R-PM.

Figure 6.6: Selection of actuated joints for the $\dot{R}\dot{R}\ddot{R}\ddot{R}\ddot{R}$-$\ddot{R}\ddot{R}\ddot{R}\dot{R}\dot{R}$-$\ddot{R}\dot{R}\dot{R}\dot{R}\ddot{R}$ 3T1R-PKC.

satisfy the following criteria:

**(1)** The actuated joints should be distributed among all the legs as evenly as possible.

**(2)** The actuated joints should preferably be on the base or close to the base.

**(3)** No unactuated P joint exists.

For example, the possible 3T1R-PMs corresponding to the 3-legged 3T1R-PKC $\dot{R}\dot{R}\ddot{R}\ddot{R}\ddot{R}$-$\ddot{R}\ddot{R}\ddot{R}\dot{R}\dot{R}$-$\ddot{R}\dot{R}\dot{R}\dot{R}\ddot{R}$ satisfying the above criteria are $\underline{\dot{R}\dot{R}}\ddot{R}\ddot{R}\ddot{R}$-$\underline{\ddot{R}}\ddot{R}\ddot{R}\dot{R}\dot{R}$-$\underline{\ddot{R}}\dot{R}\dot{R}\dot{R}\ddot{R}$, $\underline{\dot{R}}\dot{R}\ddot{R}\ddot{R}\ddot{R}$-$\underline{\ddot{R}\ddot{R}}\dot{R}\dot{R}\dot{R}$-$\underline{\ddot{R}}\dot{R}\dot{R}\dot{R}\ddot{R}$, and $\underline{\dot{R}}\dot{R}\ddot{R}\ddot{R}\ddot{R}$-$\underline{\ddot{R}}\ddot{R}\ddot{R}\dot{R}\dot{R}$-$\underline{\ddot{R}\dot{R}}\dot{R}\dot{R}\ddot{R}$ (Fig. 6.6). Following the procedure for the detection of the validity of actuated joints, the $\underline{\dot{R}\dot{R}}\ddot{R}\ddot{R}\ddot{R}$-$\underline{\ddot{R}}\ddot{R}\ddot{R}\dot{R}\dot{R}$-$\underline{\ddot{R}}\dot{R}\dot{R}\dot{R}\ddot{R}$ 3T1R-PM should be discarded as all the joints within a dependent joint group, which is composed of the first two $\dot{R}$ joints in the $\dot{R}\dot{R}\ddot{R}\ddot{R}\ddot{R}$ leg, belong to the set of actuated joints. Thus, there are only two 3T1R-PMs corresponding to the 3-legged 3T1R-PKC, i.e., the $\underline{\dot{R}}\dot{R}\ddot{R}\ddot{R}\ddot{R}$-$\underline{\ddot{R}\ddot{R}}\ddot{R}\dot{R}\dot{R}$-$\underline{\ddot{R}}\dot{R}\dot{R}\dot{R}\ddot{R}$, and $\underline{\dot{R}}\dot{R}\ddot{R}\ddot{R}\ddot{R}$-$\underline{\ddot{R}}\ddot{R}\ddot{R}\dot{R}\dot{R}$-$\underline{\ddot{R}\dot{R}}\dot{R}\dot{R}\ddot{R}$ 3T1R-PM.

Following the above criteria and the procedure for the detection of the validity of actuated joints, all the $m(m \geq 2)$-legged 3T1R-PMs corresponding to each 3T1R-PKC can be generated. By substituting a combination of an R joint and a P joint with parallel axes, a combination of two R joints with intersecting non-parallel axes and a

combination of three R joints with concurrent axes with a C, U, and S joint respectively, replacing one or more R joints each with an H joint whose axis is parallel to the axis of the R joint replaced, and/or replacing a P joint with a Π joint, all the special cases of 3T1R-PMs can be obtained. To make the conditions for 3T1R-PMs clear in their representation and due to the large number of 3T1R-PMs, only 4-legged 3T1R-PMs with all legs of the same type which are composed of R and P joints and satisfy the above criteria are listed in Table 6.3 and also shown in Figs. 6.7 and 6.8.

## 6.6 Presentation of new 4-DOF parallel mechanisms generating 3 translations and 1 rotation

Among the 11 types of 3T1R-PMs, nine of them are new while some specific cases of No. 6 and No. 9 3T1R-PMs have been proposed in [20]. Figure 6.9 shows the CAD model of the No. 2 (Fig. 6.7(b)) 3T1R-PM, which is one of the 3T1R-PMs under our investigation.

For the 4-$\underline{\text{R}}\''\dot{\text{R}}\dot{\text{R}}\dot{\text{R}}$ and the 4-$\underline{\text{P}}\''\dot{\text{R}}\dot{\text{R}}\dot{\text{R}}$ 3T1R-PMs, the validity condition of actuated joints is that the axes of the $\dot{\text{R}}$ joints are not all parallel to a same plane. For the 4-$\underline{\text{R}}\''\dot{\text{R}}\dot{\text{R}}\''$ and the 4-$\underline{\text{P}}\dot{\text{R}}\dot{\text{R}}\''$ 3T1R-PMs, the validity condition of actuated joints is that not all the axes of the $\dot{\text{R}}$ joints are perpendicular to the axes of the $\''$R joints.

The 3T1R-PKC discussed in [57] is actually is a specific case of 4-$\''\dot{\text{R}}\dot{\text{R}}\dot{\text{R}}\''$ 3T1R-PKC in which all the axes of the $\dot{\text{R}}$ joints are perpendicular to the axes of the $\''$R joints. It was also pointed out in [57] that in this case all the $\''$R joints on the base cannot be actuated simultaneously. However, the conditions for all the $\''$R joints on the base of the general 4-$\''\dot{\text{R}}\dot{\text{R}}\dot{\text{R}}\''$ 3T1R-PKC can be actuated simultaneously were not obtained in [57].

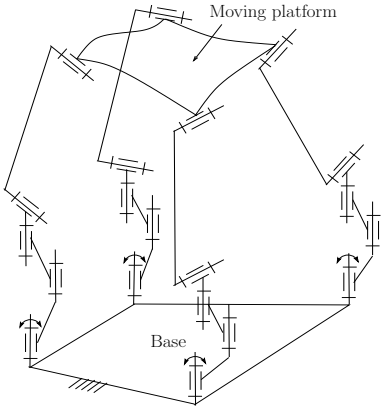


(a) 4-$\underline{\text{R}}\dot{\text{R}}\dot{\text{R}}\dot{\text{R}}\dot{\text{R}}$ 3T1R-PM.

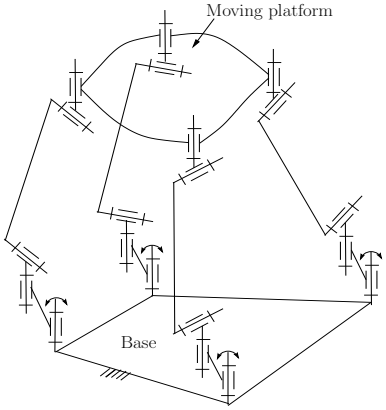


(b) 4-$\underline{\text{R}}\dot{\text{R}}\dot{\text{R}}\dot{\text{R}}\dot{\text{R}}$ 3T1R-PM.

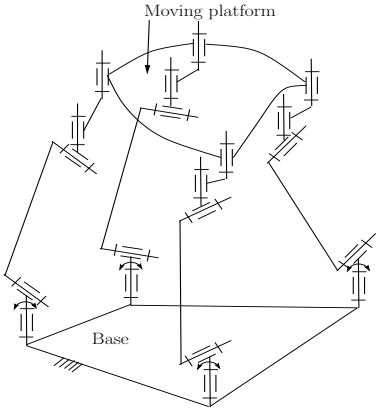


(c) 4-$\underline{\text{R}}\dot{\text{R}}\dot{\text{R}}\dot{\text{R}}\dot{\text{R}}$ 3T1R-PM.

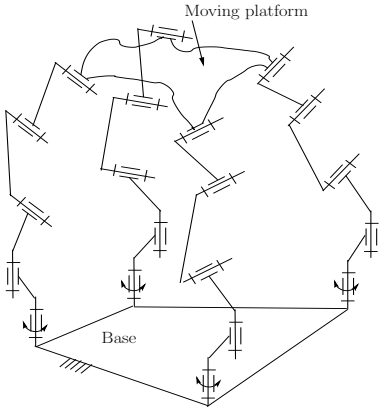


(d) 4-$\underline{\text{R}}\dot{\text{R}}\dot{\text{R}}\dot{\text{R}}\dot{\text{R}}$ 3T1R-PM.

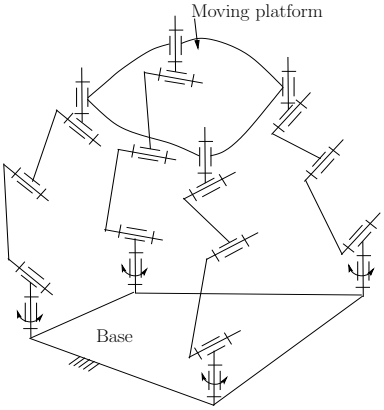


(e) 4-$\underline{\text{R}}\dot{\text{R}}\dot{\text{R}}\dot{\text{R}}\dot{\text{R}}$ 3T1R-PM.

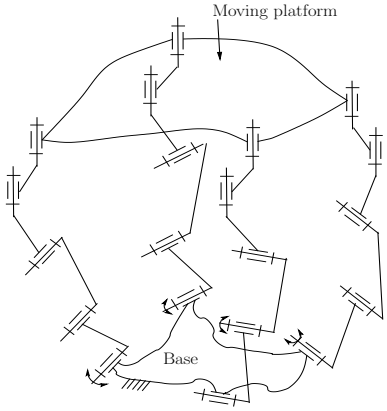


(f) 4-$\underline{\text{R}}\dot{\text{R}}\dot{\text{R}}\dot{\text{R}}\dot{\text{R}}$ 3T1R-PM.

Figure 6.7: Eleven 3T1R-PMs (to be continued).

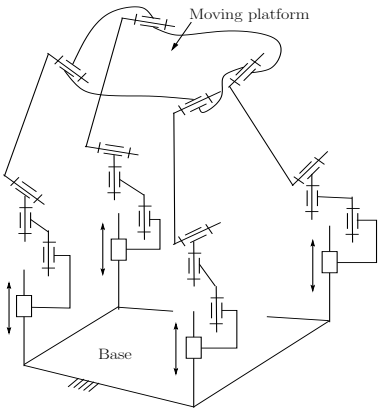


(a) 4-$\underline{\text{P}}\overset{''}{\text{R}}\overset{''}{\text{R}}\dot{\text{R}}\dot{\text{R}}$ 3T1R-PM.

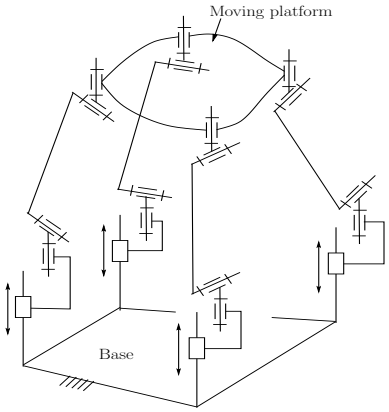


(b) 4-$\underline{\text{P}}\overset{''}{\text{R}}\dot{\text{R}}\dot{\text{R}}\overset{''}{\text{R}}$ 3T1R-PM.

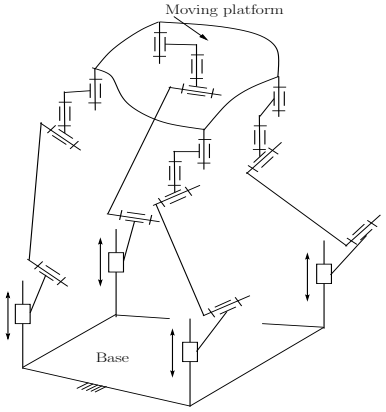


(c) 4-$\underline{\text{P}}\dot{\text{R}}\dot{\text{R}}\overset{''}{\text{R}}\overset{''}{\text{R}}$ 3T1R-PM.

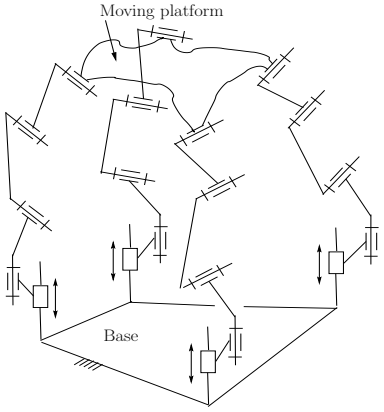


(d) 4-$\underline{\text{P}}\overset{''}{\text{R}}\dot{\text{R}}\dot{\text{R}}\dot{\text{R}}$ 3T1R-PM.

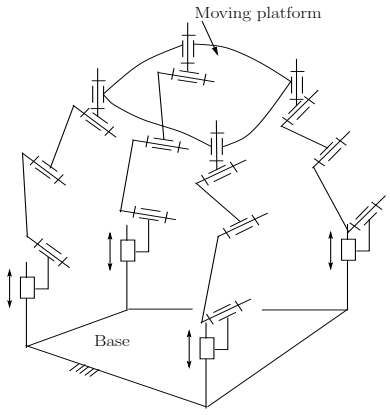


(e) 4-$\underline{\text{P}}\dot{\text{R}}\dot{\text{R}}\dot{\text{R}}\overset{''}{\text{R}}$ 3T1R-PM.

Figure 6.8: Eleven 3T1R-PMs (continued).

Table 6.3: Four-legged 3T1R-PMs.

| $c^i$ | Class | No. | Type |
|---|---|---|---|
| 1 | 5R | 1 | 4-$\underline{\text{R}}\text{R}''\text{R}''\dot{\text{R}}\dot{\text{R}}$ |
| | | 2 | 4-$\underline{\text{R}}\text{R}''\dot{\text{R}}\dot{\text{R}}\text{R}''$ |
| | | 3 | 4-$\underline{\text{R}}\dot{\text{R}}\dot{\text{R}}\text{R}''\text{R}''$ |
| | | 4 | 4-$\underline{\text{R}}\text{R}''\dot{\text{R}}\dot{\text{R}}\dot{\text{R}}$ |
| | | 5 | 4-$\underline{\text{R}}\dot{\text{R}}\dot{\text{R}}\dot{\text{R}}\text{R}''$ |
| | | 6 | 4-$\dot{\underline{\text{R}}}\dot{\text{R}}\dot{\text{R}}\text{R}''\text{R}''$ |
| | 4R-1P | 7 | 4-$\underline{\text{P}}\text{R}''\text{R}''\dot{\text{R}}\dot{\text{R}}$ |
| | | 8 | 4-$\underline{\text{P}}\text{R}''\dot{\text{R}}\dot{\text{R}}\text{R}''$ |
| | | 9 | 4-$\underline{\text{P}}\dot{\text{R}}\dot{\text{R}}\text{R}''\text{R}''$ |
| | | 10 | 4-$\underline{\text{P}}\text{R}''\dot{\text{R}}\dot{\text{R}}\dot{\text{R}}$ |
| | | 11 | 4-$\underline{\text{P}}\dot{\text{R}}\dot{\text{R}}\dot{\text{R}}\text{R}''$ |

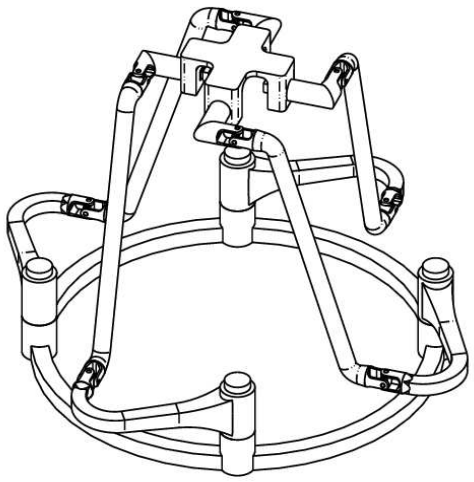

Figure 6.9: CAD model of a 4-$\underline{\text{R}}\text{R}''\dot{\text{R}}\dot{\text{R}}\text{R}''$ 3T1R-PM.

## 6.7 Conclusions

The type synthesis of 3T1R-PMs has been well solved using the general approach to the type synthesis of PMs proposed in Chapter 3. 3T1R-PKCs with inactive joints as well as 3T1R-PKCs without inactive joints have been obtained. Either overconstrained or non-overconstrained 3T1R-PKCs can be obtained. The validity check of actuated joints of 3T1R-PMs has been reduced to the calculation of a $4 \times 4$ determinant. Eleven types of 3T1R-PMs with identical legs and actuated joints located on the base have been proposed. The phenomenon of dependent joint group of a leg for 3T1R-PKCs is revealed for the first time.

Using the virtual joint approach (Section Section 3.5.2), the same types of legs for 3T1R-PKCs can be obtained. It is thus proved that there are no 3T1R-PKCs composed of R and P joints except the 3T1R-PKCs proposed in this chapter.

# Chapter 7

# Type synthesis of analytic parallel mechanisms

In Chapters 3–6, a general approach has been proposed for the type synthesis of PMs generating a specified motion pattern. PMs generated may or may not be APMs. APMs refer to PMs with a characteristic polynomial of fourth degree or lower. The FDA of APMs can be performed analytically and efficiently since the roots of a polynomial equation of fourth degree or lower can be obtained as algebraic functions of its coefficients. In this chapter, we dealt with the type synthesis of APMs. Several approaches are proposed for the type synthesis of APMs. These approaches are the component approach, the geometric approach and the algebraic FDA-based approach. The component approach further includes the composition approach and the decomposition approach. Using the decomposition approach, the geometric approach and the algebraic FDA-based approach, APMs can be generated from the PMs which can be obtained using the general approach to the type synthesis of PMs proposed in Chapter 3. Using the composition approach, APMs can be obtained directly without the need to perform the type synthesis of general PMs in advance. Several new APMs have been proposed using the proposed approaches. Among the new APMs, linear TPMs —TPMs whose FDA can be solved by linear equations — are the most promising ones.

## 7.1 Introduction

APMs are PMs with a characteristic polynomial of fourth degree or lower. The FDA of APMs can be performed analytically and efficiently since the roots of a polynomial equation of fourth degree or lower can be obtained as algebraic functions of its coefficients. It is known that for a polynomial equation of degree higher than 4, in general, no such algebraic function of roots can be found [48]. It is necessary to rely on algorithmic numerical methods to obtain the roots of a polynomial equation of degree higher than 4. Unlike more complex PMs, no additional sensors are needed in APMs in order to solve the FDA in real time. The cost of APMs is thus reduced in this respect. As reported in [8], the high non-linearity of PMs is one of the reasons which prevents the end-users from better understanding and adopting PMs. The research on APMs may help to remove such a burden.

Up to now, most of the existing APMs have been proposed following an intuitive approach. One APM, the Delta PM, has been put into practical use [36]. Several prototypes of some APMs, such as the agile eye (Fig. 1.3) [44], have been built. As in the case of general PMs, little work [39, 40] has been performed on the systematic type synthesis of APMs.

In this chapter, several approaches to the type synthesis of APMs are proposed and several new APMs are generated.

## 7.2 Component approach

In this section, a method is proposed for the type synthesis of APMs. The types of analytic components are listed. This approach is applied to the 3-R$\underline{P}$R and 3-R$\underline{P}$R-PR-R$\underline{P}$R PPMs, as well as the 6-S$\underline{P}$S PM. Several APMs are generated.

### 7.2.1 Introduction

In the literature, a mechanism is regarded to be composed of one or more components [132] in order to simplify its displacement analysis. A component is a link or an irreducible closed kinematic chain with 0 DOF when all of its actuators are locked. The component approach has been well-documented in the displacement analysis of multi-loop planar and spatial mechanisms. Using this approach, the displacement analysis of a multi-loop mechanism is reduced to the analysis of its components.

In [40], a component approach is first extended to the type synthesis of 6-S$\underline{\text{P}}$S APMs and several APMs are obtained. The component approach proposed in [40] is in fact the decomposition approach in Section 7.2.4. The contribution of this section lies in (1) further application of the decomposition approach and (2) the development of the composition approach (Section 7.2.3).

The component approach for the type synthesis of APMs is based on the following fact.

**A mechanism is analytic if and only if all of its components are analytic. Here, an analytic component refers to a component for which the displacement analysis can be performed by solving a univariate equation of degree 4 or lower.**

### 7.2.2 Analytic components

There are many types of analytic components. In the following, a preliminary classification of analytic components is proposed and the types of analytic components will be presented. For brevity, analytic components with more than 2 DOF are omitted.

#### 7.2.2.1 Simple components

A simple component is a serial chain whose joints are all actuated. For example the $\underline{\text{R}}$, $\underline{\text{P}}$, $\underline{\text{RR}}$ and $\underline{\text{PR}}$ components are simple components (Fig. 7.1).

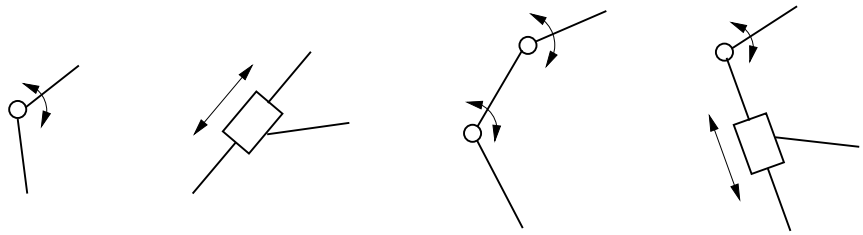

Figure 7.1: Simple components.

#### 7.2.2.2 Single-loop components

**Single-loop planar components** The single-loop planar components include the RRR, RRP, RPP (Fig. 7.2(a)), RRRR, PRRR, RPRR (Fig. 7.2(b)), RRRRR, RPRRR and the PPRRR(Fig. 7.2(c)) components. The configuration analysis of the above components is equivalent to the displacement analysis of planar four-bar linkages which are well documented in many textbooks on kinematics.

The components for planar mechanisms discussed here are also called Assur kinematic chains [132]. An Assur kinematic chain is a planar kinematic chain which can be turned into a minimal zero-mobility chain by locking all its inputs. A minimal zero-mobility chain is made up of a set of links whose relative positions are completely determined by the topology of the chain itself and by the dimensions of its links; moreover, no simpler zero-mobility chains can be found in the given chain. An Assur II kinematic chain, when all its actuated joints are locked, is formed by three binary links. An Assur III kinematic chain, when all its actuated joints are locked, is formed by connecting two ternary links with three binary links in parallel.

**Single-loop spherical components** The single-loop spherical components include the RRR, RRRR and the RRRRR components (Fig. 7.3). The configuration analysis of the above components is equivalent to the displacement analysis of spherical four-bar mechanisms (see [133]).

**Single-loop spatial components** The single-loop spatial components include many types such as the RRRS, RRPS, RPPS, PPPS (Fig. 7.4(a)), RRRRS, RRRSR, PRRRS, PRRSR (Fig. 7.4(b)), RRRRRS and the RRRRRS (Fig. 7.4(c)) single-loop spatial components. For the configuration analysis of the above single-loop spatial components, see [134].

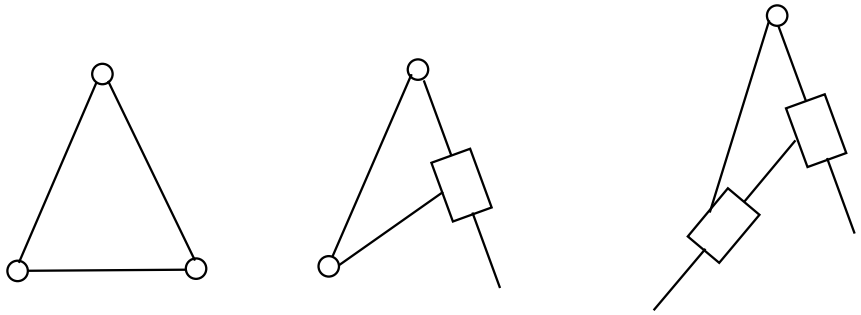

(a) Zero-DOF components

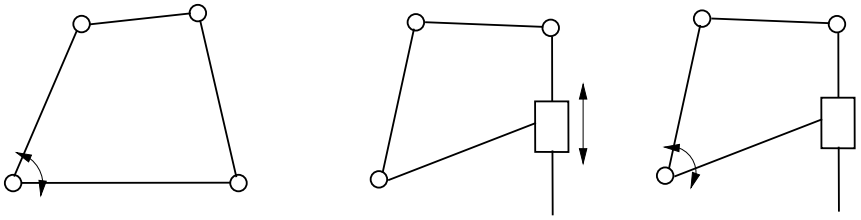

(b) One-DOF components

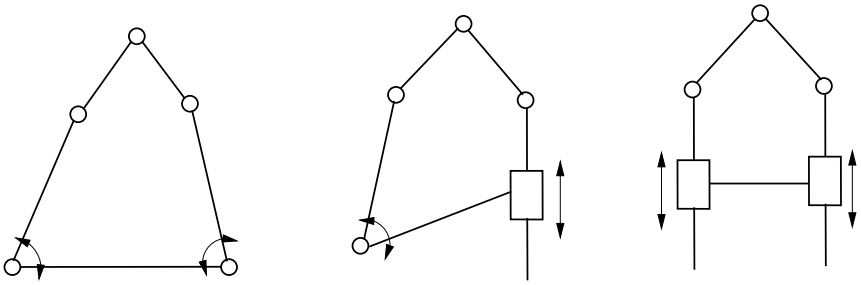

(c) Two-DOF components

Figure 7.2: Single-loop planar components.

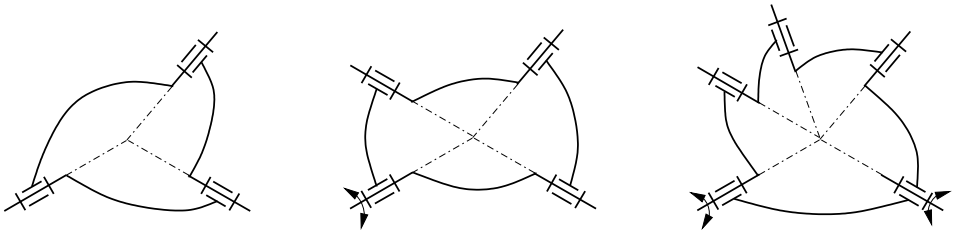

Figure 7.3: Single-loop spherical components.

#### 7.2.2.3 Multi-loop components

**Multi-loop planar components** Theoretically, any known analytic PPMs can be regarded as a component to construct more complex APMs. For example, a 3-RR parallel structure with aligned platforms is an analytic component [39] (Fig. 7.5).

**SS-based components** An SS-based component is composed of two elements connected by SS links or S$\underline{\text{P}}$S legs in which the number of links or legs is equal to the number of relative degrees of freedom between the two elements. Here, points, (straight) line segments, and rigid bodies should be regarded as elements of mechanisms. In the description of the components, the letters P, L, B and b respectively stand for point, line segment, rigid body, and planar rigid body (i.e. a rigid body on which all S joints are coplanar). The parallel components include the PL, PB, LL, Lb component (Fig. 7.6).

### 7.2.3 Composition approach

One way to generate APMs from the analytic components is to assemble several analytic components to form an APM. This form of the component approach is called the composition approach.

In this section, we illustrate the construction of an APM from analytic components by examples. The type synthesis of PMs using the component approach is different from that of mechanisms [132]. The difference lies in that measures should be taken to ensure that the mechanisms generated are PMs.

Let us construct some 3-DOF APMs (Figs. 7.7 – 7.9).

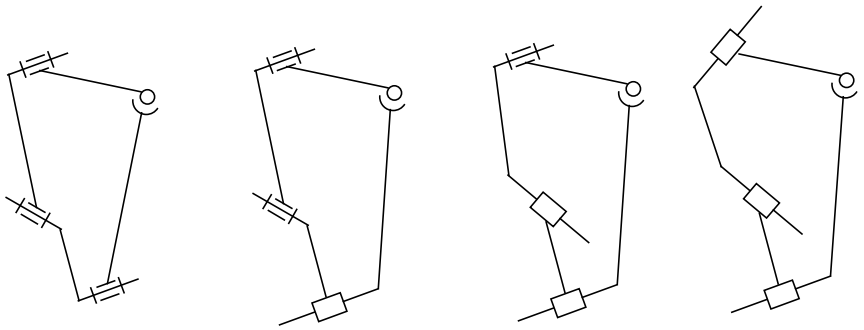

(a) Zero-DOF components

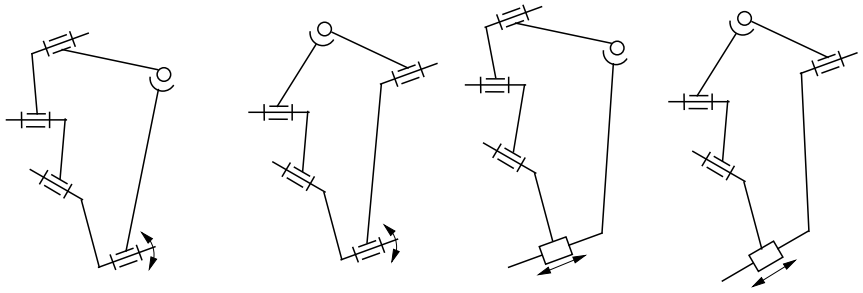

(b) One-DOF components

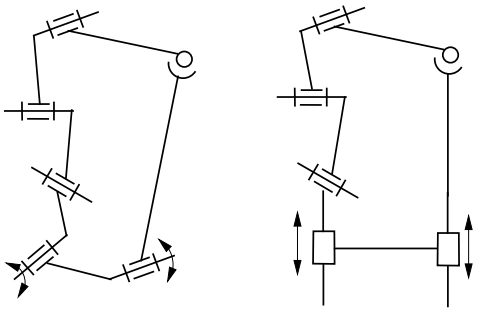

(c) Two-DOF components

Figure 7.4: Single-loop spatial components.

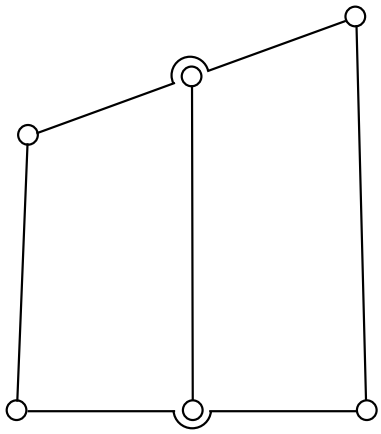

Figure 7.5: 3-RR analytic component.

**Step 1** Select $n$ analytic components and make sure that the total number of actuated joints in the selected analytic components is 3 while the total number of loops in the selected analytic components is 2.

For example, a 1-DOF single-loop analytic component and a 2-DOF single-loop analytic component can be selected. In Fig. 7.7, a 1-DOF planar single-loop analytic component I and a 2-DOF planar single-loop analytic component II are selected. In Fig. 7.8, a 1-DOF spatial single-loop analytic component I and a 2-DOF planar single-loop analytic component II are selected. In Fig. 7.9, a 1-DOF spatial single-loop analytic component I and a 2-DOF spatial single-loop analytic component II are selected.

**Step 2** In a single-loop 2-DOF analytic component, select one link as the base and one link as the connecting link.

In the 2-DOF analytic components shown in Figs. 7.7 – 7.9, links $B_1$ and $B_2$ are selected as the base and the connecting link respectively.

**Step 3** In a single-loop 1-DOF analytic component, select a link and break it into two parts, one of which is connected to the base rigidly, while the other is connected to the connecting link rigidly.

In the 1-DOF analytic components shown in Figs. 7.7 – 7.9, break links B into two parts. Then, connected one part to B1 and another part to to B2 rigidly. Three-DOF

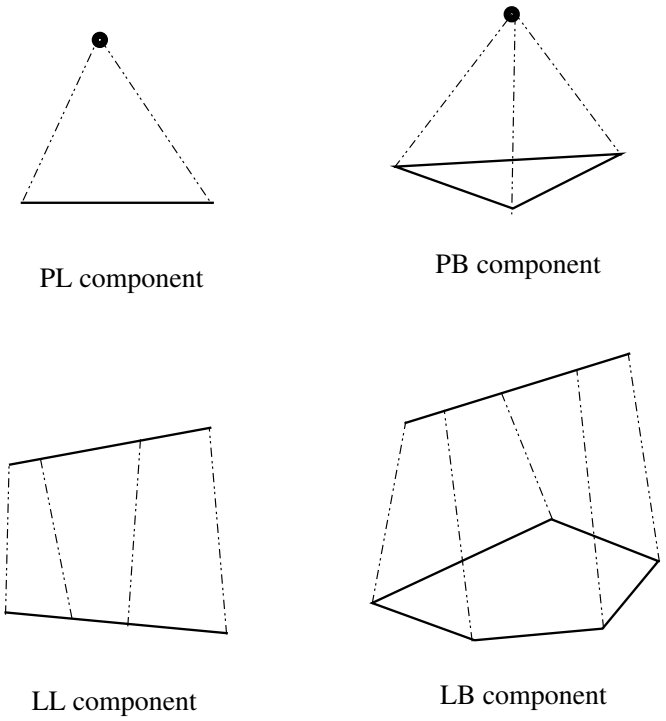


Figure 7.6: SS based components.

mechanisms are obtained.

**Step 4** Change some parameters of the connecting link to guarantee that the mechanism is a PM.

The 3-DOF mechanisms obtained in Step 2 are not PMs. These mechanisms can be turned into PMs in the following way. For the 3-DOF mechanism shown in Fig. 7.7, design the connecting link in such a way that the axis of joint $A_2$ is coaxial with the axis of joint $A_1$. For the 3-DOF mechanism shown in Fig. 7.8, design the moving platform in such a way that the axis of joint $A_2$ is coaxial with the axis of joint $A_1$ and then change the form of the multiple R joints obtained. For the 3-DOF mechanism shown in Fig. 7.9, design the moving platform in such a way that the axis of joint $A_2$ passes through the center of S joint $A_3$ and intersects with the axis of joint $A_1$, then split joint $A_2$ into two coaxial R joints. Of the two coaxial R joints, one is connected to S joint $A_3$ and the other one is connected to R joint $A_1$. Finally, replace the above R joint connected to S joint $A_3$ with S joint $A_3$ itself.

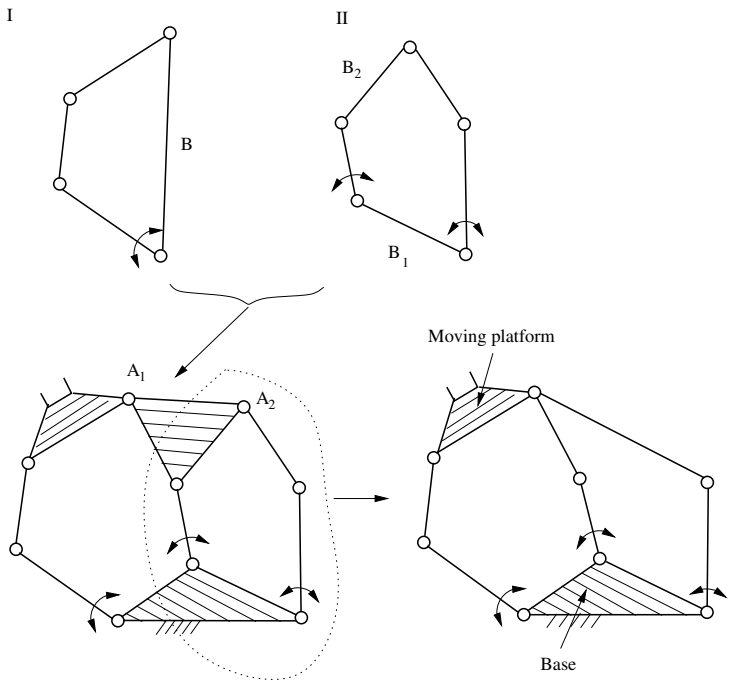


Figure 7.7: Construction of an analytic planar PM.

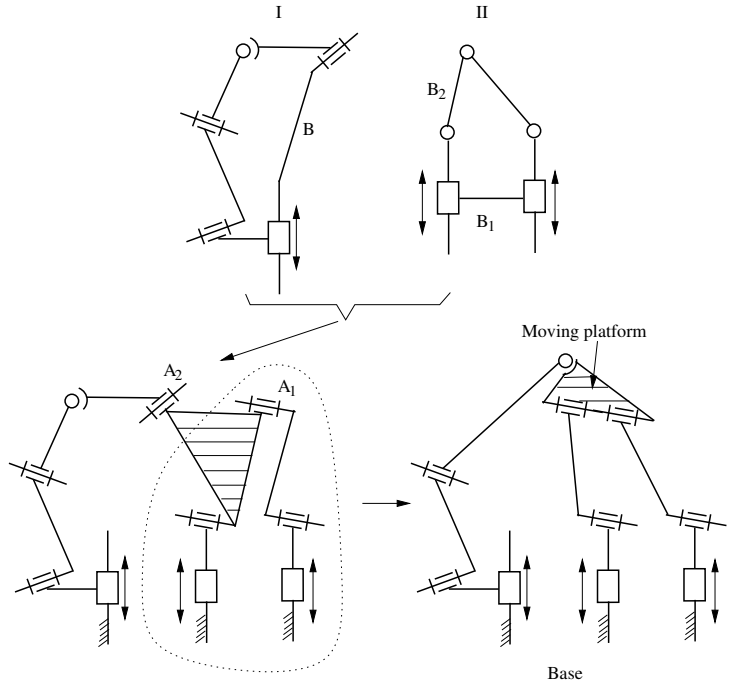


Figure 7.8: Construction of an analytic 3-DOF spatial PM.

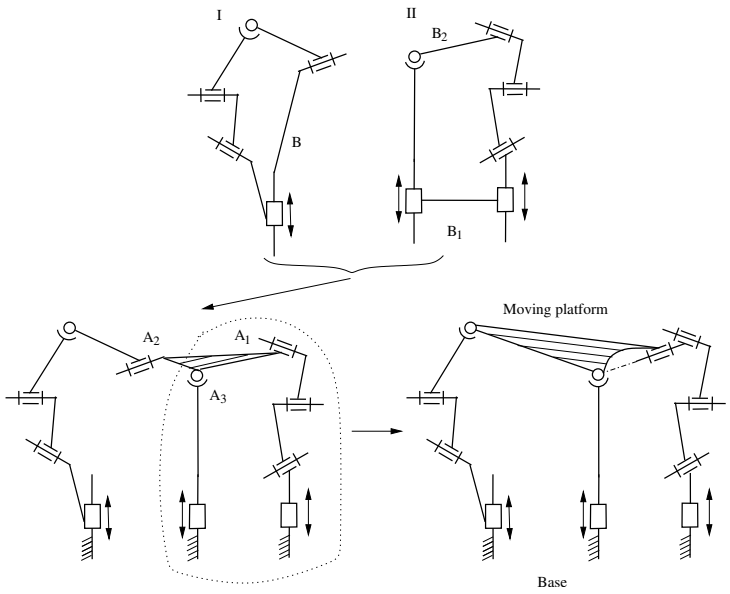


Figure 7.9: Construction of an analytic 3-DOF spatial PM.

### 7.2.4 Decomposition approach

The second way to generate APMs from the analytic components is to change the geometric parameters of platforms of a given PM to ensure that the PM can be decomposed into one or more analytic components (See sections 7.2.4.1 and 7.2.4.2). This form of the component approach is called the decomposition approach.

#### 7.2.4.1 Generation of analytic planar parallel mechanisms

The key point of the decomposition approach to the generation of analytic PPMs (planar parallel mechanisms) is to change the parameters of a given moving platform and/or the base so that the PPM can be decomposed into several analytic components. One sufficient condition to form an analytic component in a PPM is the coincidence of two unactuated R joints on the base or the moving platform. Under the above condition, a 3-legged PPM will be turned into an analytic PPM composed of two single-loop analytic components.

**Generation of analytic 3-R$\underline{P}$R PPMs**

A 3-R$\underline{P}$R PPM is constructed by connecting a moving platform and a base with

three R$\underline{P}$R legs (Fig. 7.10). In general, it is not an analytic PPM.

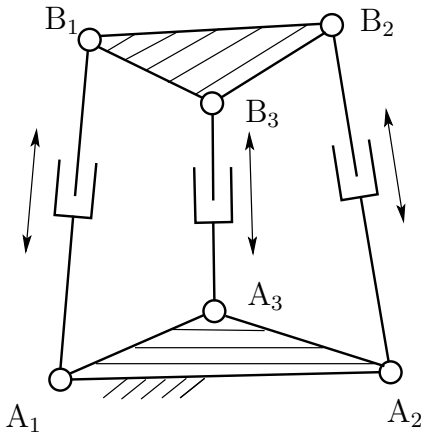


Figure 7.10: General 3-R$\underline{P}$R PPM.

Using the decomposition approach, three types of analytic 3-R$\underline{P}$R PPMs can be obtained (Fig. 7.11). There exist one or two multi-R-joints in each of these analytic PPMs.

(1) Type $\Lambda$ analytic 3-R$\underline{P}$R PPM.

In this type of analytic PPM, there is one double-joint on the moving platform. Its two analytic components are the $A_1$-$A_3$-$B_1$-$A_1$ and $A_2$-$B_1$-$B_2$-$A_2$ analytic components. The FDA of the analytic PPM is reduced to the configuration analysis of the above two analytic components in sequence.

(2) Type V analytic 3-R$\underline{P}$R PPM.

In this type of analytic PPM, there is one double-joint on the base. Its two analytic components are the $A_1$-$B_1$-$B_3$-$A_1$ and $A_1$-$B_2$-$A_2$-$A_1$ analytic components. The FDA of the analytic PPM is reduced to the configuration analysis of the above two analytic components in sequence.

(3) Type N analytic 3-R$\underline{P}$R PPM.

In this type of analytic PPM, there is one double-joint on the base and on the moving platform respectively. Its two analytic components are the $A_1$-$B_1$-$A_2$-$A_1$ and $A_2$-$B_1$-$B_2$-$A_2$ analytic components. The FDA of the analytic PPM is reduced to the

configuration analysis of the above two analytic components. The configuration analysis of the above two analytic components can be performed independently.

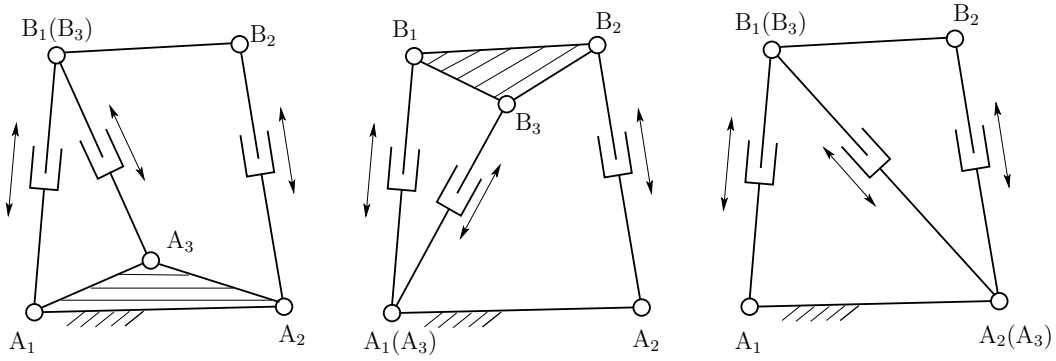


(a) Type Λ (b) Type V (c) Type N

Figure 7.11: Analytic 3-R$\underline{P}$R PPMs.

**Generation of analytic R$\underline{P}$R-PR-R$\underline{P}$R PPMs**

A R$\underline{P}$R-PR-R$\underline{P}$R PPM composed of a moving platform and a base connected by two R$\underline{P}$R legs and one PR leg (Fig. 7.12).

Four types of analytic R$\underline{P}$R-PR-R$\underline{P}$R PPMs (Fig. 7.13) can be generated directly using the decomposition approach. In Types 1 and 2 analytic PPMs, there is one double-joint on the moving platform. In Type 3 analytic PPMs, there is one double-joint on the base. In Type 4 analytic PPMs, there is one double-joint on the base and one double-joint on the moving platform.

Type 1 analytic PPM can be decomposed into two analytic components, namely, the $A$-$B$-$A_2$-$A$ and $A_1$-$B$-$B_1$-$A_1$ analytic components. The FDA of the analytic PPM is reduced to the configuration analysis of the above two analytic components in sequence. Type 2 analytic PPM can be decomposed into two analytic components, namely, the $A_1$-$B_1$-$A_2$-$A_1$ and $A$-$B$-$B_1$-$A_1$-$A$ analytic components. The FDA of the analytic PPM is reduced to the configuration analysis of the above two analytic components in sequence. Type 3 analytic PPM can be decomposed into two analytic components, namely, the $A_1$-$B_1$-$B_2$-$A_1$ and $A$-$A_1$-$B$-$A$ analytic components. The FDA of the analytic PPM is reduced to the configuration analysis of the above two analytic components in sequence. Type 4 analytic PPM can be decomposed into two analytic components, namely, the

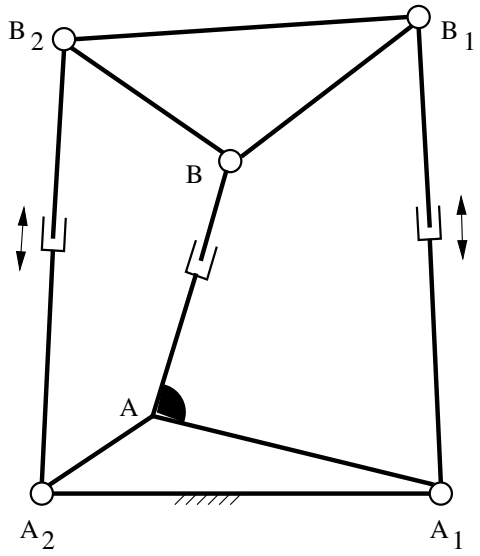


Figure 7.12: General R<u>P</u>R-PR-R<u>P</u>R PPM.

$A$-$B$-$A_1$-$A$ and $A_1$-$B$-$B_1$-$A_1$ analytic components. The FDA of the analytic PPM is reduced to the configuration analysis of the above two analytic components. The configuration analysis of the above two analytic components can be performed independently.

#### 7.2.4.2 Generation of analytic 6-S<u>P</u>S parallel mechanisms

The 6-S<u>P</u>S PM is one of the most typical PMs. It is composed of a moving platform and a base connected by six S<u>P</u>S legs (Fig. 7.14). In Fig. 7.14 and throughout this thesis, each leg is represented by a dash-dot line segment between the centers of its two S joints, each platform is represented by a transparent polygon in thick line whose vertices are the centers of the S joints on the platform. A dotted line within the thick-line polygon is used to represent a non-planar platform. The dotted line separates the vertices of the polygon into two groups. The vertices in the group with three or more vertices are located on one plane, while the other vertices are not located on the plane. For a planar platform, there exists no dotted line because all vertices are on the same plane.

Up to now, nine classes of 6-S<u>P</u>S APMs have been found. The first eight were summarized in [96] while class IX [1] is the 6-S<u>P</u>S PM with linearly-related planar platforms

[1]Here and throughout this section, the class numbers of the 6-S<u>P</u>S APMs refer to the classification

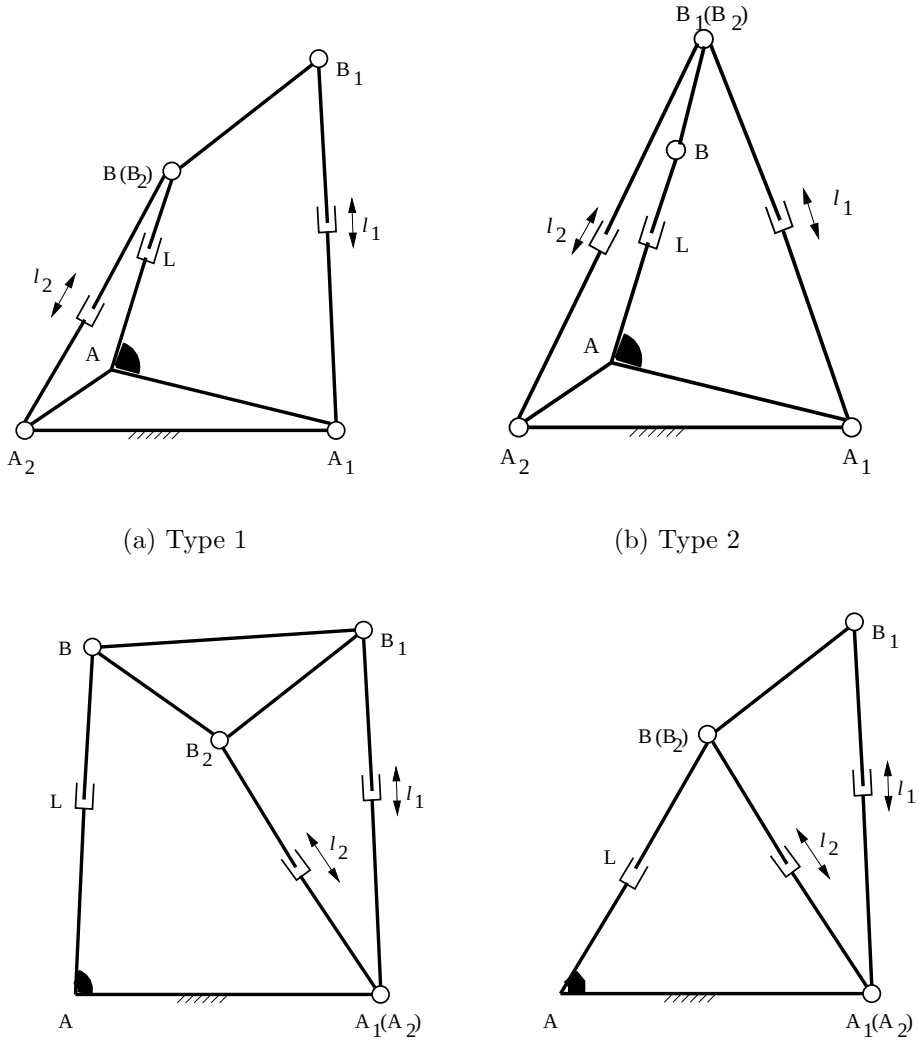


(a) Type 1

(b) Type 2

(c) Type 3.

(d) Type 4

Figure 7.13: Analytic R<u>P</u>R-PR-R<u>P</u>R PPMs composed of Assur II kinematic chains.

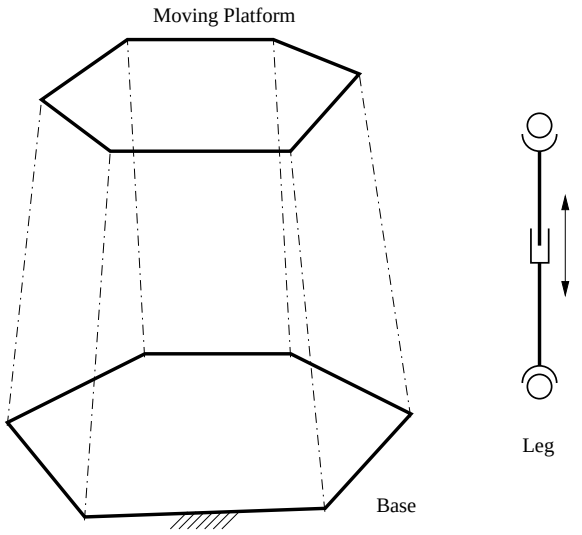


Figure 7.14: 6-S$\underline{P}$S PM.

proposed in [45, 47]. Generating new 6-S$\underline{P}$S APMs is still an open issue.

Using the decomposition approach, two new classes of analytic components for 6-S$\underline{P}$S PMs are first generated. Then, two new classes of 6-S$\underline{P}$S APMs are generated.

**Generation of new classes of analytic LB components**

A 6-S$\underline{P}$S PM can be decomposed into one or more components. A 6-S$\underline{P}$S PM is analytic if all of its components are analytic. Thus, the generation of 6-S$\underline{P}$S PMs is reduced to the generation of analytic components for 6-S$\underline{P}$S PMs.

There are many classes of components for 6-S$\underline{P}$S PMs [40]. The ones related to this section are the $PL$ and $LB$ components. The $PL$ component (Fig. 7.15(a)) is composed of a point ($B_1(B_2)$) and a line segment ($A_1A_2$) connected by two SPS legs ($A_iB_i$), while the $LB$ component (Fig. 7.15(b)) is composed of a line segment ($B_1B_2B_3B_4B_5$) and a rigid body ($A_1A_2A_3A_4A_5$) connected by five SPS legs ($A_iB_i$).

In this section, we focus on the generation of analytic LB components. Up to now, only one class of analytic LB component has been proposed. This is the LB component with a planar base proposed by Zhang and Song [38]. Here and throughout the remainder of this thesis, it is denoted by the Lb component. The configuration

scheme presented in [96].

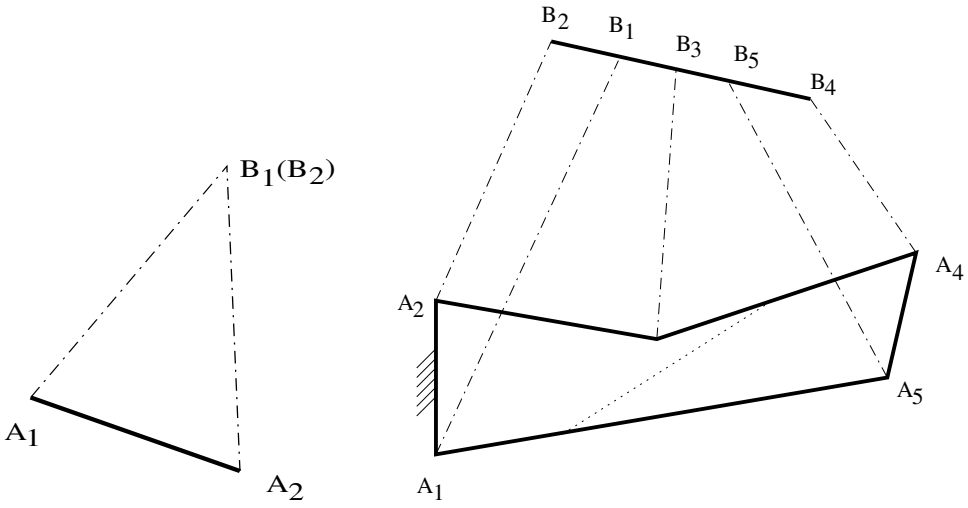


(a) PL component. (b) General LB component.

Figure 7.15: PL and LB components for 6-SPS PMs

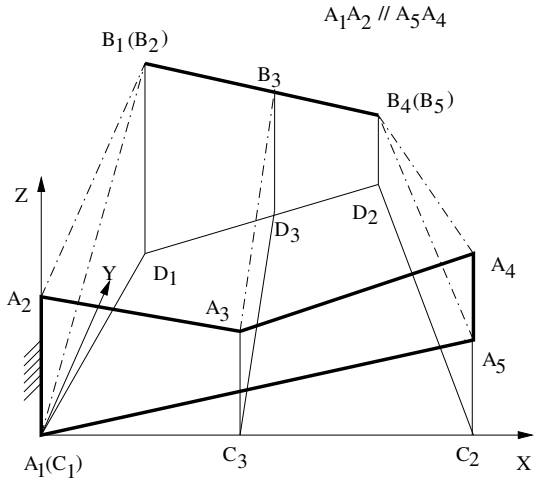


Figure 7.16: Reduction of the $\mathrm{Lb}_{PL//PL}$ component to its equivalent 3-RR planar parallel structure with aligned platforms.

analysis of the Lb component can be performed by solving a univariate quartic equation and a univariate quadratic equation in sequence. There are at most 8 assembly modes for this class of analytic LB component.

To facilitate the generation of new analytic LB components, the geometric conditions, revealed in [39, 41, 135], to reduce the degree of the characteristic polynomial for PMs are reviewed.

It is revealed in [135] that the maximum number of solutions to the FDA of the true Stewart platform (i.e., a specific 6-S$\underline{P}$S PM with three $PL$ components) is 12. The number is smaller than 16, the latter being obtained in the case of a general 6-S$\underline{P}$S PM with three $PL$ components. The reason for this is that the FDA of the true Stewart platform can be reduced to that of a planar parallel structure. The geometric characteristic of the true Stewart platform is that all the straight line segments in its PL components are parallel.

It was shown in [39, 41] that there are two types of 3-RR analytic planar parallel structures with aligned platforms. One is the 3-RR planar parallel structure with non-similar aligned platforms [39], the other is the 3-RR planar parallel structure with similar aligned platforms [41]. The configuration analysis of the former can be performed by solving a cubic univariate equation and a quadratic equation in sequence, while that of the latter can be solved by solving two quadratic univariate equations in sequence.

The above results lead to a natural way of generating analytic LB components. Analytic LB components can be obtained by imposing the following geometric constraints (Fig. 7.16), which are similar to those revealed in [39, 41, 135] for PMs, on the LB component:

(1) There should exist two PL components in the LB component and the line segments in the PL components should be parallel to each other. These conditions ensure that the FDA of the LB component can be reduced to that of a planar parallel structure.

(2) The rigid body in the LB component should be planar. This condition guarantees that the platforms of the planar parallel structure are aligned. An aligned platform of a planar parallel structure or a PM refers to a platform on which all the axes of R

joints are coplanar.

(3) Constraints on the link parameters of the LB component to guarantee that its equivalent planar structure is a 3-RR planar parallel structure with non-similar aligned platforms [39] or a 3-RR planar parallel structure with similar aligned platforms [41].

For convenience, the LB component satisfying the above first two conditions is denoted by $Lb_{PL//PL}$ (Fig. 7.16). In Fig. 7.16, the $Lb_{PL//PL}$ component is projected onto a plane perpendicular to the line segment in a PL component (Fig. 7.16) and a virtual 3-RR planar parallel structure ($C_1C_2C_3 - D_1D_2D_3$) with aligned platforms is obtained. Here, $C_1$, $C_2$, $C_3$, $D_1$, $D_2$ and $D_3$ are respectively the projection of $A_1(A_2)$, $A_4(A_5)$, $A_3$, $B_1(B_2)$, $B_4(B_5)$ and $B_3$. The virtual 3-RR planar parallel structure with aligned platforms is called the equivalent 3-RR analytic planar parallel structure for the $Lb_{PL//PL}$ component (Fig. 7.16). $C_1C_2C_3$ and $D_1D_2D_3$ are called the base and moving platform respectively while $C_iD_i$ is called the leg of the equivalent 3-RR planar structure.

Corresponding with two classes of 3-RR analytic planar parallel structures, two classes of analytic LB components are thus generated. In a class II analytic LB component, its equivalent 3-RR planar structure has non-similar aligned platforms, while in a class III analytic LB component, its equivalent 3-RR planar structure has similar aligned platforms.

**Generation of two new classes of 6-S$\underline{P}$S APMs**

Corresponding to the two new classes, classes II and III, of analytic LB components, two new classes of 6-S$\underline{P}$S APMs can be generated (Fig. 7.17), namely

1. Class X 6-S$\underline{P}$S APM. The class X 6-S$\underline{P}$S APM is the one containing the class II analytic LB component.
2. Class XI 6-S$\underline{P}$S APM. The class XI 6-S$\underline{P}$S APM is the one containing the class III analytic LB component.

Thus, two new classes, X and XI, of 6-S$\underline{P}$S APMs are proposed. The characteristic of the new 6-S$\underline{P}$S APMs is that they contain an analytic LB component with two

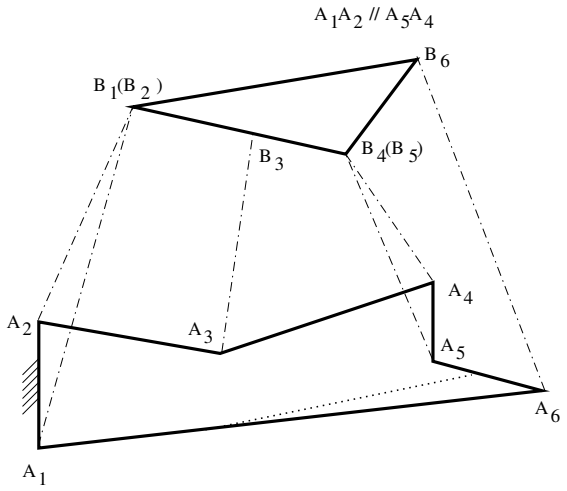


Figure 7.17: New classes of 6-SPS APMs.

PL components, while the characteristic of the analytic LB components with two PL components is that the body is coplanar and the lines in the PL components are parallel to each other. The FDA is reduced to the solution of one univariate cubic equation and two univariate quadratic equations in sequence for the class X 6-SPS APM and to the solution of three univariate quadratic equations in sequence for the class XI 6-SPS APM.

The FDA of these two classes of 6-SPS APMs will be discussed in detail in section 9.3. It will be revealed that both of these two classes of 6-SPS PMs have at most 8 sets of solutions to their FDA problem.

### 7.2.5 Summary

Two component approaches, namely the composition approach and the decomposition approach, have been proposed in this section. The first one is self-contained while the second one starts with PMs which are generated using the general approach to the type synthesis of PMs described in chapter 3. Using these approaches, several new APMs have been obtained.

The work presented in this section is useful in the context of the development of fast 3-RPR, RPR-PR-RPR and 6-SPS PMs.

It should be pointed out that the generation of all possible 6-S$\underline{P}$S APMs is still an open problem.

## 7.3 Geometric approach

Types of TPMs have been obtained in Chapter 4. In this section, we propose a geometric approach to the generation of analytic TPMs from these TPMs. The concept of leg surface is first introduced for TPMs. A geometric interpretation of the FDA of TPMs is given. A geometric approach is then proposed for the type synthesis of analytic TPMs. The characteristics of the geometric approach is that none or less derivation is needed.

### 7.3.1 Linear translational parallel mechanisms

A linear TPM is a TPM for which the FDA can be obtained by solving a set of linear equations. Linear TPMs are the simplest cases of analytic TPMs.

### 7.3.2 Geometric interpretation of the forward displacement analysis of translational parallel mechanisms

When the actuated joint of a given leg of a TPM is locked, the moving platform will be able to translate along a surface with its orientation unchanged. For brevity, the above surface is referred to as the leg-surface (Fig. 7.18) of the leg.

With the introduction of leg-surfaces for TPMs, the FDA of the TPM can be described geometrically as follows: it consists in finding the intersection of three leg-surfaces.

The higher the degree of the leg-surfaces, the more complicated the FDA of the TPM. The simplest cases are TPMs with three planar leg-surfaces. As the intersection of three planes can be obtained by solving a set of linear equations, a TPM is a linear TPM if all of its three leg-surfaces are planes. Thus, type synthesis of linear

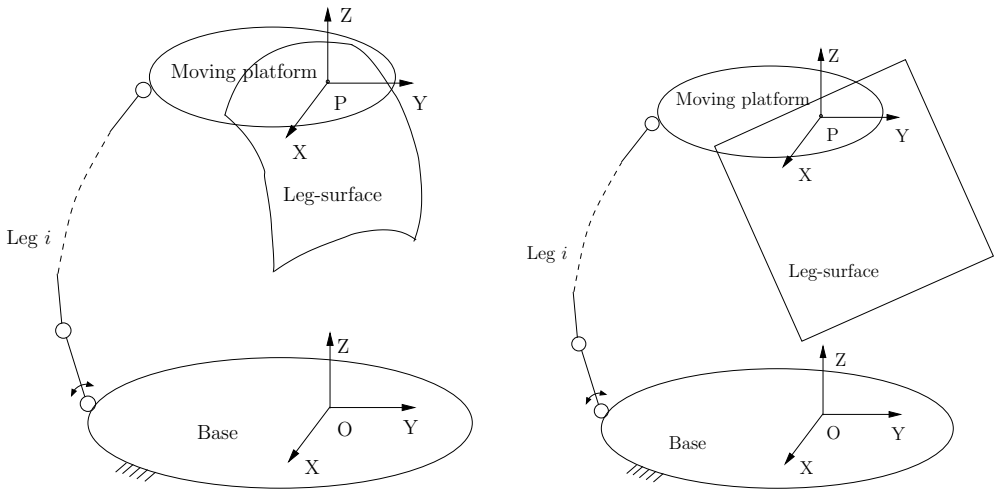


(a) general case. (b) planar case.

Figure 7.18: Leg-surfaces of TPMs.

TPMs is reduced to the type synthesis of legs for TPMs whose leg-surfaces are planes (Fig. 7.18(b)), which are referred to as legs for linear TPMs in the following.

The type synthesis of linear TPMs consists in obtaining linear TPMs from TPMs.

### 7.3.3 Composition characteristics of legs

As the leg-surface of a leg for linear TPMs is a plane, legs for linear TPMs should have the following composition characteristics.

In a leg for linear TPMs, the unactuated joints (Fig. 7.19(a)), except inactive joints, should include (a) two P joints, (b) two R joints with parallel axes and one P joint whose axis is perpendicular to the axes of the R joints with parallel axes, or (c) three R joints with parallel axes. The actuated joint (Fig. 7.19(b)) in a leg may be (a) a $\underline{\text{P}}$ joint or (b) an $\underline{\text{R}}$ joint. It is noted that in a leg with an $\underline{\text{R}}$ joint, there must be an unactuated R joint whose axis is parallel to the axis of the $\underline{\text{R}}$ joint.

Figure 7.20 shows the leg-surface of some legs for linear TPMs.

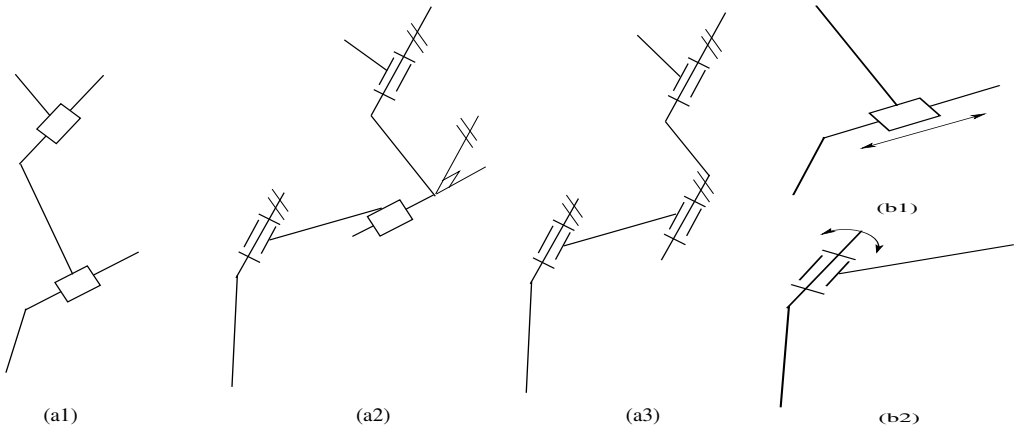


(a) Unactuated joints.

(b) Actuated joints.

Figure 7.19: Characteristics of legs for linear TPMs.

### 7.3.4 Type synthesis

Based on the composition characteristics of legs for linear TPMs, some linear TPMs can be obtained from the list of 3-legged TPMs (Table 4.4).

The TPMs shown in Table 7.1 have three unactuated R joints with parallel axes or two unactuated P joints except for the inactive joints. These TPMs meet the composition characteristics of legs for linear TPMs and are thus linear TPMs.

In the TPMs listed in Table 4.4 except those in Table 7.1, we can impose some geometric constraints on the link parameters to make sure that except for the inactive joints, the axis of the unactuated P joint is perpendicular to the axes of the other two unactuated R joints. The TPMs obtained in this way also meet the composition characteristics of legs for linear TPMs and are thus linear TPMs (Table 7.2).

It is noted that the actuation wrenches of the linear TPMs shown in Table 7.2 are respectively parallel to the axes of the two unactuated R joints other than the inactive joints. The validity condition of actuated joints should be met (Section 4.6.2). These conditions can be described as follows: all the axes of the unactuated R joints, except the inactive joint, should not be parallel to a common plane. These conditions are different from the corresponding conditions obtained with general link geometry.

Table 7.1: Three-legged linear TPMs (part 1)

| Class | No | Type | Geometric condition |
|---|---|---|---|
| 3P | 1 | 3-$\underline{\mathrm{P}}$PP | Three lines each perpendicular to the axes of two unactuated P joints within a leg are not parallel to a plane. |
| 3R-1P | 5 | 3-$\underline{\mathrm{P}}\bar{\mathrm{R}}\bar{\mathrm{R}}\bar{\mathrm{R}}$ | All the axes of $\bar{\mathrm{R}}$ joints are not parallel to a plane. |
| 2R-2P | 6 | 3-$\underline{\bar{\mathrm{R}}}\bar{\mathrm{R}}$PP | The same condition as type 1. |
| | 7-8 | 3-$\underline{\bar{\mathrm{R}}}\mathrm{P}\bar{\mathrm{R}}$P 3-$\underline{\bar{\mathrm{R}}}\mathrm{PP}\bar{\mathrm{R}}$ | |
| 1R-3P | 12-13 | 3-$\underline{\mathrm{P}}\mathrm{PP}\bar{\mathrm{R}}$ 3-$\underline{\mathrm{P}}\mathrm{P}\bar{\mathrm{R}}\mathrm{P}$ | The same condition as type 1. |
| | 14-15 | 3-$\underline{\mathrm{P}}\bar{\mathrm{R}}$PP 3-$\bar{\mathrm{R}}\underline{\mathrm{P}}$PP | |
| 5R | 16 | 3-$\underline{\dot{\mathrm{R}}}\dot{\bar{\mathrm{R}}}\bar{\mathrm{R}}\bar{\mathrm{R}}\bar{\mathrm{R}}$ | The same condition as type 5. |
| | 18 | 3-$\underline{\dot{\mathrm{R}}}\bar{\mathrm{R}}\bar{\mathrm{R}}\bar{\mathrm{R}}\dot{\bar{\mathrm{R}}}$ | |
| 4R-1P | 39-43 | see Table 4.5 | The same condition as type 5. |
| 3R-2P | 51-54 | | The same condition as type 1. |
| | 55-59 | | |
| | 75-79 | | |
| | 80 | | The same condition as type 1. |
| 2R-3P | 81-90 | | |

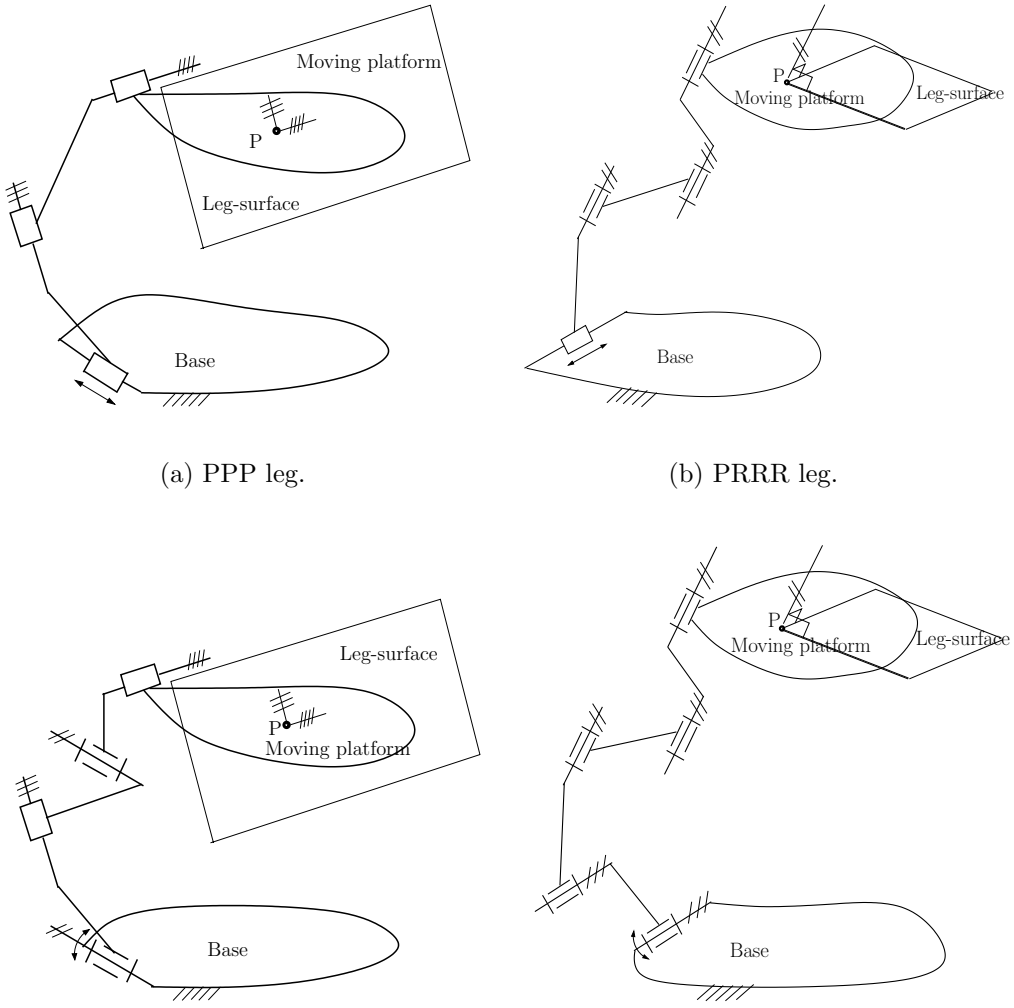


(a) PPP leg.

(b) PRRR leg.

(c) RPRP leg.

(d) RR$\bar{\text{R}}\bar{\text{R}}\bar{\text{R}}$ leg.

Figure 7.20: Some legs for linear TPMs.

Alternatively, the condition can also be obtained using simple geometry. In a general configuration, the three planar leg-surfaces of a TPM have one and only one finite point in common. It is noted that for three planes, the condition for the number of common finite points to be 1 is that the normals of these planes are not parallel to a plane. Detailed conditions can thus be obtained for linear TPMs.

Table 7.2: Three-legged linear TPMs (part 2)

| Class | No | Type | Geometric condition |
|---|---|---|---|
| 2R-2P | 9 | 3-$\underline{\mathrm{P}}\bar{\mathrm{R}}\bar{\mathrm{R}}\mathrm{P}$ | The axis of the unactuated P joint is perpendicular to the $\bar{\mathrm{R}}$ joints within a same leg, not all the axes of the $\bar{\mathrm{R}}$ joints are parallel to a plane. |
| | 10 | 3-$\underline{\mathrm{P}}\bar{\mathrm{R}}\mathrm{P}\bar{\mathrm{R}}$ | |
| | 11 | 3-$\underline{\mathrm{P}}\mathrm{P}\bar{\mathrm{R}}\bar{\mathrm{R}}$ | |
| 4R-1P | 21-22 | 3-$\underline{\dot{\mathrm{R}}}\dot{\mathrm{R}}\bar{\mathrm{R}}\bar{\mathrm{R}}\mathrm{P}$ 3-$\underline{\dot{\mathrm{R}}}\dot{\mathrm{R}}\bar{\mathrm{R}}\mathrm{P}\bar{\mathrm{R}}$ | |
| | 23 | 3-$\underline{\dot{\mathrm{R}}}\dot{\mathrm{R}}\mathrm{P}\bar{\mathrm{R}}\bar{\mathrm{R}}$ | |
| | 27-28 | 3-$\underline{\dot{\mathrm{R}}}\bar{\mathrm{R}}\bar{\mathrm{R}}\mathrm{P}\dot{\mathrm{R}}$ 3-$\underline{\dot{\mathrm{R}}}\bar{\mathrm{R}}\mathrm{P}\bar{\mathrm{R}}\dot{\mathrm{R}}$ | |
| | 29 | 3-$\underline{\dot{\mathrm{R}}}\mathrm{P}\bar{\mathrm{R}}\bar{\mathrm{R}}\dot{\mathrm{R}}$ | |
| 3R-2P | 60-74 | see Table 4.5 | |

### 7.3.5 Variations of linear translational parallel mechanisms

Linear TPMs which are composed of R and P joints only are called the basic types of linear TPMs. Other types of TPMs are variations of the basic types. Variations of linear TPMs can be obtained in one or more of the following ways.

(1) To substitute a combination of one R joint and one P joint along parallel axes with a C joint;

(2) To substitute a combination of two adjacent R joints with unparallel axes with a U (universal) joint;

(3) To substitute an actuated P joint with a $\Pi$ joint, i.e., a parallelogram, whose plane is not parallel to the axes of the two unactuated P joints or not perpendicular to the axes of the unactuated R joints within the same leg;

(4) To substitute an unactuated P joint with a $\Pi$ joint whose plane is parallel to the axes of the two unactuated P joints or perpendicular to the axes of the unactuated R joints within the same leg;

(5) To substitute an actuated R joint with an H (helical) joint whose axis is parallel to the axis of the actuated R joint;

(6) To substitute the only unactuated R joint whose axis is parallel to the axis of an actuated R joint with an H joint whose axis is parallel to the axis of the actuated R joint;

(7) To substitute a pair of unactuated R joints with parallel axes, whose axes are not parallel to the axes of any other R joint in the same leg, with a pair of H joints of the same pitch whose axes are parallel to the axes of the pair of unactuated R joints.

It is noted that in a leg for linear TPMs with an actuated R or H joint, there must be one and only one unactuated R or H joint whose axis is parallel to the axis of the actuated R or H joint. Once the actuated R or H joint is locked, the unactuated R or H joint with parallel axis is also locked by the total constraints on the moving platform of all the legs in a linear TPM. Otherwise, the orientation of the moving platform will change. In the HPPR, HPRP, HRPP, RHPP, RPHP and RPPH legs for linear TPMs, the axes of the H and R joints can be perpendicular to the axes of the two unactuated P joints. In the HHPP, HPHP and HPPH legs for linear TPMs, the axes of the two H joints can also be perpendicular to the axes of the two unactuated P joints if the pitches of the two H joints are different.

### 7.3.6 Summary

A geometric approach has been proposed for the type synthesis of linear TPMs. Linear TPMs have been obtained.

The results of this section have been published in [136, 137, 138, 142]. Concurrently, TPMs with linear-input equations have also been proposed by other researchers in [139, 140, 141, 143, 144]. TPMs with linear-input equations are a subset of linear TPMs. It is noted that the TPMs proposed in [139, 140, 141, 143, 144] are a subset of the TPMs proposed in [136, 138, 137] and that fewer details are given on the type synthesis of TPMs in [139, 140, 141, 143, 144].

The results of this section are of great interest in the development of fast TPMs and parallel kinematic machines with high performance.

## 7.4 Algebraic forward displacement analysis -based approach

This section deals with the type synthesis of analytic R$\underline{P}$R-PR-R$\underline{P}$R PPMs using the algebraic approach proposed in [39]. Six types of analytic R$\underline{P}$R-PR-R$\underline{P}$R PPMs are first generated using the approach based on the structure of the univariate equation. Of the six types, four are composed of analytic components while the other two are composed of Assur III kinematic chains. The forward displacement analysis (FDA) of two types of analytic R$\underline{P}$R-PR-R$\underline{P}$R PPMs composed of Assur III kinematic chains is then performed. The FDA of each of the two types of analytic PPMs composed of Assur III kinematic chains is reduced to the solution of a univariate cubic equation and a quadratic equation in sequence.

### 7.4.1 Introduction

An R$\underline{P}$R-PR-R$\underline{P}$R PPM is constructed by connecting a moving platform and a base with two R$\underline{P}$R legs and one PR leg (Fig. 7.21). A specific R$\underline{P}$R-PR-R$\underline{P}$R PPM has been proposed and applied to an articulated mobile robot in [145]. The R$\underline{P}$R-PR-R$\underline{P}$R PPM proposed by Ridgeway et al. is an analytic PPM as its FDA has been reduced to the solution of a polynomial of degree 3 in $L^2$ [146]. In section 7.2.4.1, several analytic R$\underline{P}$R-PR-R$\underline{P}$R PPMs have been generated using the component approach.

In this section, we perform a systematic study on the generation and the FDA of the analytic R$\underline{P}$R-PR-R$\underline{P}$R PPMs. The algebraic approach proposed for the type synthesis of analytic 3-R$\underline{P}$R PPMs in [39] will be used. Using this approach, APMs can be generated in three steps. The first is to reduce the FDA to the solution of a univariate equation, the second is to find the coefficients whose vanishing will reduce the univariate equation to an equation of degree 4 or lower, and the last is to find the constraints on the base and moving platform which make the above coefficients

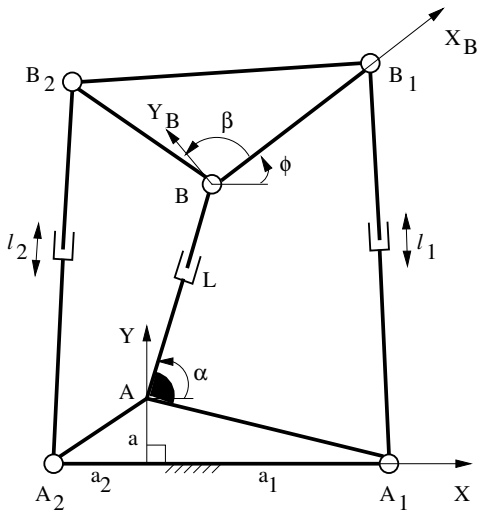


Figure 7.21: R$\underline{\text{P}}$R-PR-R$\underline{\text{P}}$R PPM.

vanishing.

The generation of analytic R$\underline{\text{P}}$R-PR-R$\underline{\text{P}}$R PPMs is first dealt with. The FDA of different types of analytic R$\underline{\text{P}}$R-PR-R$\underline{\text{P}}$R PPMs composed of one Assur III kinematic chain is then performed.

### 7.4.2 Forward displacement analysis of the general R$\underline{\text{P}}$R-PR-R$\underline{\text{P}}$R planar parallel mechanism

The general R$\underline{\text{P}}$R-PR-R$\underline{\text{P}}$R PPM is shown in Fig. 7.21. For purposes of simplification and without loss of generality, two coordinate systems are established. The coordinate system $O-XY$ is attached to the base with the $X$-axis passing through $A_1$ and $A_2$ and the $Y$-axis passing through $A$. The coordinate system $O_B - X_BY_B$ is attached to the moving platform with $O_B$ being coincident with $B$ and the $X_B$-axis passing through $B_1$. The dimensions of the base and the moving platform are denoted by $a_1$, $a_2$, $a$, $\alpha$, $b_1 = BB_1$, $b_2 = BB_2$ and $\beta$. Here, $a_i$ (i=1, 2) designates the coordinate of $A_i$ along the $X$-axis while $a$ denotes the coordinate of $A$ along the $Y$-axis. The inputs of the manipulator are denoted by $l_1 = A_1B_1$ and $l_2 = A_2B_2$. Without loss of generality, we make the assumption that $b_1 \neq 0$.

The FDA of the R$\underline{\text{P}}$R-PR-R$\underline{\text{P}}$R PPM can be stated as follows: for a given set of

inputs $l_1$ and $l_2$, find the pose (position and orientation) of the moving platform $(L, \phi)$. Here, $L = AB$ denotes the joint variable of the passive P joint, and $\phi$ denotes the orientation of the coordinate system of $O_B - X_B Y_B$ with respect to the coordinate system $O - XY$.

The loop closure equations of loops $ABB_1A_1A$ and $ABB_2A_2A$ in complex form are

$$\begin{cases} (ai + Le^{i\alpha} + b_1 e^{i\phi} - a_1)(-ai + Le^{-i\alpha} + b_1 e^{-i\phi} - a_1) = l_1^2 \\ (ai + Le^{i\alpha} + b_2 e^{i(\phi+\beta)} - a_2)(-ai + Le^{-i\alpha} + b_2 e^{-i(\phi+\beta)} - a_2) = l_2^2 \end{cases}$$

Expanding and simplifying the above equations, we have

$$\begin{cases} L^2 + 2Lb_1 \cos(\phi - \alpha) - 2La_1 \cos\alpha - 2a_1 b_1 \cos\phi + 2aL \sin\alpha \\ +2ab_1 \sin\phi + a^2 + s_1 = 0 \\ L^2 + 2Lb_2 \cos(\phi - \alpha + \beta) - 2La_2 \cos\alpha - 2a_2 b_2 \cos(\phi + \beta) \\ +2aL \sin\alpha + 2ab_2 \sin(\phi + \beta) + a^2 + s_2 = 0 \end{cases} \tag{7.1}$$

where

$$s_i = a_i^2 + b_i^2 - l_i^2 \quad i = 1, 2$$

The FDA of the general R$\underline{\text{P}}$R-PR-R$\underline{\text{P}}$R PPM can be obtained by solving Eq. (7.1).

Rearranging Eq. (7.1), we have

$$\begin{cases} L^2 + c_1 L + c_2 = 0 \\ L^2 + d_1 L + d_2 = 0 \end{cases} \tag{7.2}$$

where

$$\begin{aligned} c_1 &= c_{11} \cos\phi + c_{12} \sin\phi + c_{13} \\ c_2 &= c_{21} \cos\phi + c_{22} \sin\phi + c_{23} \\ d_1 &= d_{11} \cos\phi + d_{12} \sin\phi + d_{13} \\ d_2 &= d_{21} \cos\phi + d_{22} \sin\phi + d_{23} \\ c_{11} &= 2b_1 \cos\alpha \\ c_{12} &= 2b_1 \sin\alpha \\ c_{13} &= 2a \sin\alpha - 2a_1 \cos\alpha \\ c_{21} &= -2b_1 a_1 \\ c_{22} &= 2b_1 a \end{aligned}$$

$$
\begin{aligned}
c_{23} &= s_1 + a^2 \\
d_{11} &= 2b_2 \cos\alpha \cos\beta + 2b_2 \sin\alpha \sin\beta \\
d_{12} &= -2\cos\alpha b_2 \sin\beta + 2\sin\alpha b_2 \cos\beta \\
d_{13} &= -2a_2 \cos\alpha + 2a \sin\alpha \\
d_{21} &= -2a_2 b_2 \cos\beta + 2a b_2 \sin\beta \\
d_{22} &= 2a_2 b_2 \sin\beta + 2a b_2 \cos\beta \\
d_{23} &= s_2 + a^2
\end{aligned}
$$

The condition for the existence of a solution for $L$ is [147]

$$
\begin{vmatrix}
1 & c_1 & c_2 & 0 \\
1 & d_1 & d_2 & 0 \\
0 & 1 & c_1 & c_2 \\
0 & 1 & d_1 & d_2
\end{vmatrix} = 0
$$

i.e.,

$$e_6 \cos^3\phi + e_5 \cos^2\phi \sin\phi + e_4 \cos^2\phi + e_3 \cos\phi \sin\phi + e_2 \cos\phi + e_1 \sin\phi + e_0 = 0 \quad (7.3)$$

where the coefficients $e_6$ to $e_0$ are functions of the geometric parameters of links (see Appendix A).

Using the following substitutions in Eq. (7.3)

$$
\begin{cases}
\sin\phi = 2t/(1+t^2) \\
\cos\phi = (1-t^2)/(1+t^2)
\end{cases} \quad (7.4)
$$

where $t = \tan(\phi/2)$, we obtain a polynomial in $t$ of degree 6

$$g_6 t^6 + g_5 t^5 + g_4 t^4 + g_3 t^3 + g_2 t^2 + g_1 t + g_0 = 0 \quad (7.5)$$

where

$$
\begin{aligned}
g_6 &= -e_6 + e_4 - e_2 + e_0 \\
g_5 &= 2e_5 - 2e_3 + 2e_1 \\
g_4 &= 3e_6 - e_4 - e_2 + 3e_0 \\
g_3 &= -4e_5 + 4e_1 \\
g_2 &= -3e_6 - e_4 + e_2 + 3e_0 \\
g_1 &= 2e_5 + 2e_3 + 2e_1 \\
g_0 &= e_6 + e_4 + e_2 + e_0
\end{aligned}
$$

Equation (7.5) is the characteristic polynomial of the general R$\underline{\text{P}}$R-PR-R$\underline{\text{P}}$R PPM. It is of degree six. For each value of $t$ obtained, $\phi$ can be uniquely determined using Eq. (7.4).

Then, $L$ can be obtained from Eq. (7.2) as

$$L = \begin{cases} (d_2 - c_2)/(c_1 - d_1) & \text{if } c_1 \neq d_1 \\ (-c_1 \pm (c_1^2 - 4c_2)^{1/2})/2 & \text{otherwise} \end{cases} \tag{7.6}$$

### 7.4.3 Generation of analytic R$\underline{\text{P}}$R-PR-R$\underline{\text{P}}$R planar parallel mechanisms

Similarly to the generation of analytic 3-R$\underline{\text{P}}$R PPMs [39], analytic R$\underline{\text{P}}$R-PR-R$\underline{\text{P}}$R PPMs can be generated using the method based on the structure of the univariate equation.

It is clear that

(1) if the terms in $\sin\phi$ and $\cos\phi$ of degree 3 in Eq. (7.3) vanish, i.e.

$$\begin{cases} e_6 = 0 \\ e_5 = 0 \end{cases} \tag{7.7}$$

then Eq. (7.3) is reduced to a quadratic equation in $\sin\phi$ and $\cos\phi$ and Eq. (7.5) is reduced to the quartic equation in $t$.

(2) if the terms in $\sin\phi$ in Eq. (7.3) vanish, i.e.

$$\begin{cases} e_5 = 0 \\ e_3 = 0 \\ e_1 = 0 \end{cases} \tag{7.8}$$

then Eq. (7.3) will be reduced into a cubic equation in $\cos\phi$. Analytic PPMs can thus be generated [2].

[2]Theoretically, the work here is not exhaustive as the general condition to generate analytic PPMs is the condition under which Eq.(7.3) may be factored as the product of one linear or quadratic equation in $\sin\phi$ and $\cos\phi$ and one equation in $\cos\phi$ of degree 3 or less.

Equation (7.7) can be re-written in the following form

$$\begin{cases} e_6 = H_0(2H_1H_2\sin\beta + 8H_3H_4) = 0 \\ e_5 = H_0(-H_2H_3\sin\beta + 16H_1H_4) = 0 \end{cases} \tag{7.9}$$

where

$$\begin{aligned} H_0 &= 8b_1b_2(a_1 - a_2) \\ H_1 &= \sin\alpha\cos\alpha \\ H_2 &= -2b_2\cos\beta + b_1 \\ H_3 &= 2\cos^2\alpha - 1 \\ H_4 &= -2b_2\cos^2\beta + b_1\cos\beta + b_2 \end{aligned} \tag{7.10}$$

The solution of Eq. (7.9) yields

$$b_2 = 0 \tag{7.11}$$

or

$$a_1 = a_2 \tag{7.12}$$

or

$$\begin{cases} \beta = 0 \\ b_2 = b_1 \end{cases} \tag{7.13}$$

The PPMs satisfying one or more of Eqs. (7.11), (7.12) and (7.13) are analytic PPMs. These analytic PPMs are actually those generated in section 7.2.4.1 using the component approach (Fig. 7.13).

- (1) The analytic PPM satisfying Eq. (7.11) is the analytic PM shown in Fig. 7.13(a).
- (2) The analytic PPM satisfying Eq. (7.12) is the analytic PM shown in Fig. 7.13(c).
- (3) The analytic PPM satisfying Eq. (7.13) is the analytic PM shown in Fig. 7.13(b).
- (4) The analytic PPM satisfying Eqs. (7.11) and (7.13) is the analytic PPM shown in Fig. 7.13(d).

Equation (7.8) can be re-written in the following form

$$\begin{cases} e_5 = h_{51} b_2 \sin\beta + h_{50} \sin\alpha\cos\alpha = 0 \\ e_3 = h_{33}\cos\alpha a + h_{32} b_2^2 \sin\alpha\cos\alpha\sin^2\beta + h_{31} b_2 \sin\beta + 2h_{30}\sin\alpha\cos\alpha = 0 \\ e_1 = h_{14}\cos^2\alpha\sin\beta b_2 a^2 - 4h_{13}\cos\alpha a + h_{12} b_2^2 \sin\alpha\cos\alpha\sin^2\beta \\ +h_{11} b_2 \sin\beta + h_{10}\sin\alpha\cos\alpha = 0 \end{cases} \tag{7.14}$$

where

$$\begin{aligned} h_{51} &= 2b_1(a_2-a_1)(-1+2\cos^2\alpha)(2b_2\cos\beta - b_1) \\ h_{50} &= -4b_1 b_2 (a_2-a_1)(2b_2\cos^2\beta - b_1\cos\beta - b_2) \\ h_{33} &= 8(a_2-a_1)(b_2^2\cos\alpha\cos^2\beta - b_2^2\cos\alpha\sin^2\beta + 2b_2^2\cos\beta\sin\alpha\sin\beta - b_1^2\cos\alpha) \\ h_{32} &= -2(-s_1 + a_2 a_1) \\ h_{31} &= (2b_2 s_1 - 4b_2 a_1 a_2)\cos^2\alpha\cos\beta - 2b_2 s_1 \sin^2\alpha\cos\beta + (b_1 s_2 + b_1 s_1)\sin^2\alpha \\ &\quad +(-b_1 s_2 - 2b_1 a_1^2 - 2b_1 a_2^2 - b_1 s_1 + 8b_1 a_1 a_2)\cos^2\alpha + 2b_2\cos\beta a_2^2 - 2b_1 a_1 a_2 \\ h_{30} &= (b_1 s_1 b_2 - 4b_1 a_1 b_2 a_2 + b_1 b_2 s_2 + b_1 a_2^2 b_2 + b_1 a_1^2 b_2)\cos\beta \\ &\quad +(-s_1 b_2^2 + a_1 a_2 b_2^2)\cos^2\beta + b_1^2 a_1 a_2 - b_1^2 s_2 \\ h_{14} &= 8(a_1 - a_2) \\ h_{13} &= -2b_1 b_2^2 \sin\alpha\sin\beta\cos\beta + (2a_1^2 b_2 - 2b_2 a_1 a_2 + b_2 s_2 - b_2 s_1)\cos\alpha\cos\beta \\ &\quad +2b_1 b_2^2\cos\alpha\sin^2\beta + (2b_1^2 b_2 + 2a_2^2 b_2 + b_2 s_2 - 2a_1 b_2 a_2 - s_1 b_2)\sin\alpha\sin\beta \\ &\quad +(b_1 s_1 - b_1 s_2 + 2b_1 a_2^2 - 2b_1 a_1 a_2)\cos\alpha \\ h_{12} &= -2b_1 a_2 \\ h_{11} &= 2a_2 b_1 b_2 \sin^2\alpha\cos\beta + (2a_2^2 a_1 - 2a_1^2 a_2 - 2s_1 a_2 + a_1 s_2 + a_1 s_1)\cos^2\alpha \\ &\quad -2b_1^2 a_2 \sin^2\alpha - a_2 s_2 + a_2 s_1 \\ h_{10} &= (2b_2 a_2 s_1 - b_2 a_1 s_2 - a_1 s_1 b_2)\cos\beta - b_1 a_2 s_2 + 2b_1 a_1 s_2 - b_1 s_1 a_2 \end{aligned} \tag{7.15}$$

From Eq. (7.14), two conditions which lead to the vanishing of the terms in $\sin\phi$ in Eq. (7.3) can be obtained as

$$\begin{cases} \sin\beta = 0 \\ \cos\alpha = 0 \end{cases} \tag{7.16}$$

or

$$\begin{cases} \sin\beta = 0 \\ \sin\alpha = 0 \\ a = 0 \end{cases} \tag{7.17}$$

Thus, two types of analytic R$\underline{P}$R-PR-R$\underline{P}$R PPMs composed of Assur III kinematic chains can be generated. They are

1. The analytic R$\underline{P}$R-PR-R$\underline{P}$R PPM with one orthogonal platform and one aligned platform (Fig. 7.22), i.e., a R$\underline{P}$R-PR-R$\underline{P}$R PPM which satisfies Eq. (7.16). Without loss of generality and for the purpose of simplification, the above equation can be reduced to

$$\begin{cases} \beta = \pi \\ \alpha = \pi/2 \\ a = 0 \end{cases} \tag{7.18}$$

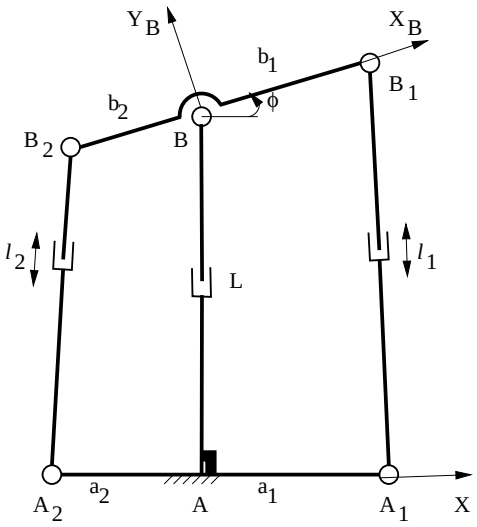


Figure 7.22: Analytic R$\underline{P}$R-PR-R$\underline{P}$R PPM with one aligned platform and one orthogonal platform.

2. The analytic R$\underline{P}$R-PR-R$\underline{P}$R PPM with two aligned platforms (Fig. 7.23), i.e., a R$\underline{P}$R-PR-R$\underline{P}$R PPM which satisfies Eq. (7.17). Without loss of generality and for the purpose of simplification, the above equation can be reduced to

$$\begin{cases} \beta = \pi \\ \alpha = 0 \\ a = 0 \end{cases} \tag{7.19}$$

It is clear that the analytic R$\underline{P}$R-PR-R$\underline{P}$R PPM proposed in [145] is just the symmetric case ($b_2 = b_1$ and $a_2 = -a_1$) of the analytic R$\underline{P}$R-PR-R$\underline{P}$R PPM with one orthogonal platform and one aligned platform proposed here.

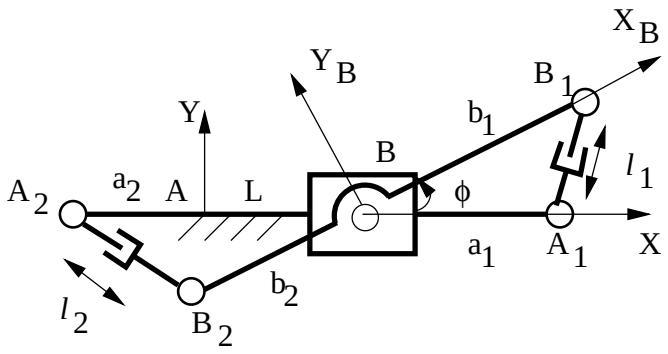


Figure 7.23: Analytic R$\underline{P}$R-PR-R$\underline{P}$R PPM with two aligned platforms.

### 7.4.4 Forward displacement analysis of analytic R$\underline{P}$R-PR-R$\underline{P}$R planar parallel mechanisms

In the previous section, six types of analytic R$\underline{P}$R-PR-R$\underline{P}$R PPMs have been generated. The first four types of analytic R$\underline{P}$R-PR-R$\underline{P}$R PPMs are composed of Assur II kinematic chains. Their FDA is actually the same as the well-documented displacement analysis of planar linkages composed of Assur II kinematic chains (see [132] for example). The last two types of analytic R$\underline{P}$R-PR-R$\underline{P}$R PPMs are composed of Assur III kinematic chains, the FDA of which is more difficult to perform. In the following, we focus on the FDA of the two types of analytic R$\underline{P}$R-PR-R$\underline{P}$R PPMs composed of Assur III kinematic chains.

#### 7.4.4.1 Planar parallel mechanism with one orthogonal platform and one aligned platform

The substitution of Eq. (7.18) into Eq.(7.3) leads to a cubic equation in $\cos\phi$.

$$p_3\cos^3\phi + p_2\cos^2\phi + p_1\cos\phi + p_0 = 0 \tag{7.20}$$

where

$$\begin{aligned}
p_3 &= -8b_2^2b_1a_1 + 8b_1^2b_2a_2 - 8b_1^2b_2a_1 + 8b_2^2b_1a_2 \\
p_2 &= -8b_2a_2b_1a_1 + 4b_1b_2s_1 + 4b_2b_1s_2 + 4b_1^2s_2 - 4b_1^2a_1^2 - 4b_2^2a_2^2 + 4b_2^2s_1 \\
p_1 &= 8b_2^2b_1a_1 - 8b_1^2b_2a_2 + 8b_1^2b_2a_1 + 4b_1a_1s_1 - 4b_2a_2s_2 + 4b_2a_2s_1 \\
&\quad -4s_2b_1a_1 - 8b_2^2b_1a_2 \\
p_0 &= -s_1^2 - 4b_1^2s_2 - 4b_2^2s_1 - s_2^2 + 2s_2s_1 - 4b_1b_2s_1 - 4b_2b_1s_2
\end{aligned}$$

For each value of $\cos\phi$, we have

$$\sin\phi = \pm(1-\cos^2\phi)^{1/2} \tag{7.21}$$

From Eq. (7.6), L can be calculated using

$$L = \begin{cases} ((a_1b_1 + a_2b_2)\cos\phi + (s_2 - s_1)/2)/((b1 + b2)\sin\phi) & \text{if } \sin\phi \neq 0 \\ \pm(2a_1b_1\cos\phi - s_1)^{1/2} & \text{otherwise} \end{cases} \tag{7.22}$$

It has been found in [146] that there are only 4 real solutions to the FDA of the specific symmetric case of the analytic R$\underline{\text{P}}$R-PR-R$\underline{\text{P}}$R PPM with one orthogonal platform and one aligned platform. In fact, the maximum number of real solutions to the FDA is 4 for all the analytic R$\underline{\text{P}}$R-PR-R$\underline{\text{P}}$R PPMs with one orthogonal platform and one aligned platform. This will be proven in Section 9.2 using Sturm's theorem.

#### 7.4.4.2 Planar parallel mechanism with two aligned platforms

The substitution of Eq. (7.19) into Eq. (7.3) yields a cubic equation in $\cos\phi$.

$$q_3\cos^3\phi + q_2\cos^2\phi + q_1\cos\phi + q_0 = 0 \tag{7.23}$$

where

$$\begin{aligned}
q_3 &= -2b_2^2b_1a_2 + 2b_2^2b_1a_1 - 2b_1^2b_2a_2 + 2b_1^2a_1b_2 \\
q_2 &= -b_2b_1s_2 + 2b_2^2a_1a_2 - 2b_1b_2a_2^2 + 2b_1^2a_1a_2 - b_1s_1b_2 - 2b_1a_1^2b_2 + 6b_2b_1a_1a_2 \\
&\quad -b_1^2s_2 - b_1^2a_1^2 - b_2^2a_2^2 - b_2^2s_1 \\
q_1 &= b_2a_1s_2 - b_2s_1a_2 - a_2b_1s_2 + 2a_1b_2a_2^2 + 2b_1a_1a_2^2 - b_2a_2s_2 + s_2b_1a_1 \\
&\quad -b_1s_1a_2 - 2a_1^2b_2a_2 - 2b_1a_1^2a_2 + a_1s_1b_2 + b_1a_1s_1 \\
q_0 &= b_2a_1s_2 - b_2s_1a_2 - a_2b_1s_2 + 2a_1b_2a_2^2 + 2b_1a_1a_2^2 - b_2a_2s_2 + s_2b_1a_1 \\
&\quad -b_1s_1a_2 - 2a_1^2b_2a_2 - 2b_1a_1^2a_2 + a_1s1b_2 + b_1a_1s_1
\end{aligned}$$

For each value of $\cos\phi$, $\sin\phi$ can be calculated using Eq. (7.21). From Eq. (7.6), $L$ can be calculated as

$$L = \begin{cases} (-(a_1b_1 + a_2b_2)\cos\phi + (s1 - s2)/2)/(a_1 - a_2 - (b_1 + b_2)\cos\phi) \\ \qquad\qquad \text{if } a_1 - a_2 - (b_1 + b_2)\cos\phi \neq 0 \\ a_1 - b_1\cos\phi \pm [(a_1 - b_1\cos\phi)^2 - s_1^2 + 2a_1b_1\cos\phi]^{1/2} \\ \qquad\qquad \text{otherwise} \end{cases} \tag{7.24}$$

### 7.4.5 Summary

The generation and the FDA of analytic R$\underline{P}$R-PR-R$\underline{P}$R PPMs have been investigated. Six types of analytic R$\underline{P}$R-PR-R$\underline{P}$R PPMs have been generated. Of the six types, four are composed of Assur II kinematic chains while the other two are composed of Assur III kinematic chains. For each type of the analytic R$\underline{P}$R-PR-R$\underline{P}$R PPMs composed of Assur III kinematic chains, the FDA is reduced to the solution of one univariate cubic equation and one quadratic equation in sequence.

As one of the reviewers of [148] pointed out, the approach based on the geometric features of the coupler curves of four-bar linkages can also be used to generate the analytic PPMs proposed in this section.

This analysis is useful in the context of the development of fast R$\underline{P}$R-PR-R$\underline{P}$R PPMs.

## 7.5 Conclusions

Several approaches to the type synthesis of APMs have been developed in this chapter and several new types of APMs have been proposed.

Using the decomposition approach, the geometric approach and the algebraic FDA-based approach, APMs can be generated from PMs obtained in Chapters 3–6. Almost no derivation is needed when the component approach or the geometric approach is applied. Using the geometric approach, a class of APMs can be generated. However, not all APMs corresponding to a PM can be obtained using the decomposition approach. The geometric approach can only be applied to PMs generating limited motion patterns. The algebraic FDA-based approach is theoretically general. Unfortunately, it is difficult to guarantee, in practice, that all the APMs corresponding to a general PM can be obtained.

The composition approach is self-contained. Using this approach, APMs are obtained directly from analytic components. Like the decomposition approach, almost

no derivation is needed when the composition approach is applied. The drawback of this approach is that the motion pattern of the moving platform is unforeseen in the process of type synthesis.

An approach to the FDA of APMs is readily obtained in the process of type synthesis. If a given APM can be generated using either the component approach or the method based on the structure of univariate equations, the method for the FDA implicitly obtained by the component approach is simpler than the one obtained by the latter approach.

This Chapter contributes to the type synthesis of APMs.

# Chapter 8

# Type synthesis and kinematics of LTPMs: translational parallel mechanisms with linear input-output relations and without constraint singularity

This chapter deals with the type synthesis, kinematic analysis and kinematic synthesis of LTPMs (TPMs with linear input-output relations and without constraint singularity). LTPMs are a subset of linear TPMs we have obtained in Section 7.3. LTPMs are first generated. The proposed LTPMs may or may not contain some inactive joints or redundant DOFs. Constraint singularity analysis, inverse kinematics, forward kinematics and kinematic singularity analysis are then performed. It is proven that an LTPM is free of forward kinematic singularity. Conditions for the LTPMs to be isotropic are revealed. Two additional kinematic merits

exist for the isotropic LTPMs. The first is that an isotropic LTPM is isotropic in any of its configurations within its workspace. The second is that fewer calculations are needed in order to pre-determine the inverse of the Jacobian matrix. Its workspace analysis is performed. Finally, kinematic synthesis of LTPMs is performed.

## 8.1 Introduction

Recently, [136, 142] revealed the condition for all the translational degrees of freedom of the C (cylindrical) joints of the 3-$\underline{\bar{C}}\bar{R}\bar{R}$ TPKC, which is proposed in [13], to be actuated and thus proposed a 3-$\underline{\bar{C}}\bar{R}\bar{R}$ TPM with linear actuators. It has been revealed that the 3-$\underline{\bar{C}}\bar{R}\bar{R}$ TPM has linear input-out equations. In addition, the TPM has no constraint singularity and forward kinematic singularity.

LTPMs are LIO-TPMs (3-legged TPMs with linear input-output relations) without constraint singularity. LIO-TPMs are a subset of linear TPMs we have obtained in Section 7.3 and LTPMs are a subset of LIO-TPMs.

This chapter attempts to perform a systematic study on LTPMs based on the results of type synthesis of TPKCs [13, 14, 17, 18] as well as our previous work [142]. In Section 8.2, the type synthesis of LTPMs is first dealt with. The inverse kinematics and the forward kinematics are performed in Sections 8.3 and 8.4 respectively. In Section 8.5, the kinematic singularity analysis of the LTPMs is investigated. The geometric condition for the LTPMs to be isotropic is revealed in Section 8.6. The workspace analysis of LTPMs is discussed in Section 8.7 while the kinematic design of the isotropic LTPMs is performed in Section 8.8. Finally, conclusions are drawn.

Table 8.1: Three-legged LIO-TPMs (part 1)

| Class | No | Type | Geometric condition |
|---|---|---|---|
| 3P | 1 | 3-$\underline{P}$PP | Three lines each perpendicular to the axes of two unactuated P joints within a leg are not parallel to a plane. |
| 3R-1P | 5 | 3-$\underline{P}\bar{R}\bar{R}\bar{R}$ | All the axes of $\bar{R}$ joints are not parallel to a plane. |
| 1R-3P | 12-13<br>14-15 | 3-$\underline{P}$PP$\bar{R}$ 3-$\underline{P}$P$\bar{R}$P<br>3-$\underline{P}\bar{R}$PP 3-$\bar{R}\underline{P}$PP | The same condition as type 1. |
| 4R-1P | 39-43 | see Table 4.5 | The same condition as type 5. |
| 2R-3P | 81-90 | | |

## 8.2 Type synthesis of LTPMs

### 8.2.1 Type synthesis of translational parallel mechanisms with linear input-output relations

Recalling the geometric interpretation of the FDA of TPMs (Section 7.3), a linear TPM is a LIO-TPM if and only if the position of each of its leg-surfaces is controlled by an actuated joint linearly. This implies that LIO-TPMs are those linear TPMs with $\underline{P}$ joints. From the list of linear TPMs (Tables 7.1 and 7.2), LIO-TPMs can be obtained directly and are listed in Tables 8.1 and 8.2. Tables 8.1 and 8.2 are obtained from Tables 7.1 and 7.2 and the numbering in these tables is not changed. Figure 8.1 shows some LIO-TPMs.

Table 8.2: Three-legged LIO-TPMs (part 2)

| Class | No | Type | Geometric condition |
|---|---|---|---|
| 2R-2P | 9<br>10<br>11 | 3-$\underline{P}\bar{R}\bar{R}$P<br>3-$\underline{P}\bar{R}$P$\bar{R}$<br>3-$\underline{P}$P$\bar{R}\bar{R}$ | The axis of the unactuated P joint is perpendicular to the $\bar{R}$ joints within a same leg, not all the axes of the $\bar{R}$ joints are parallel to a plane. |
| 3R-2P | 60-74 | see Table 4.5 | |

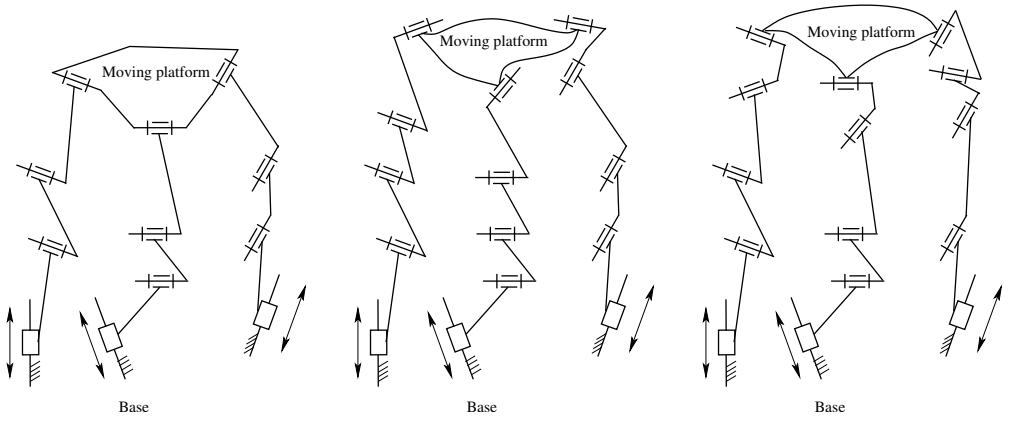


(a) 3-$\underline{\mathrm{P}}\bar{\mathrm{R}}\bar{\mathrm{R}}\bar{\mathrm{R}}$ TPM. (b) 3-$\underline{\mathrm{P}}\bar{\mathrm{R}}\bar{\mathrm{R}}\bar{\mathrm{R}}\dot{\mathrm{R}}$ TPM. (c) 3-$\underline{\mathrm{P}}\bar{\mathrm{R}}\bar{\mathrm{R}}\dot{\mathrm{R}}\bar{\mathrm{R}}$ TPM.

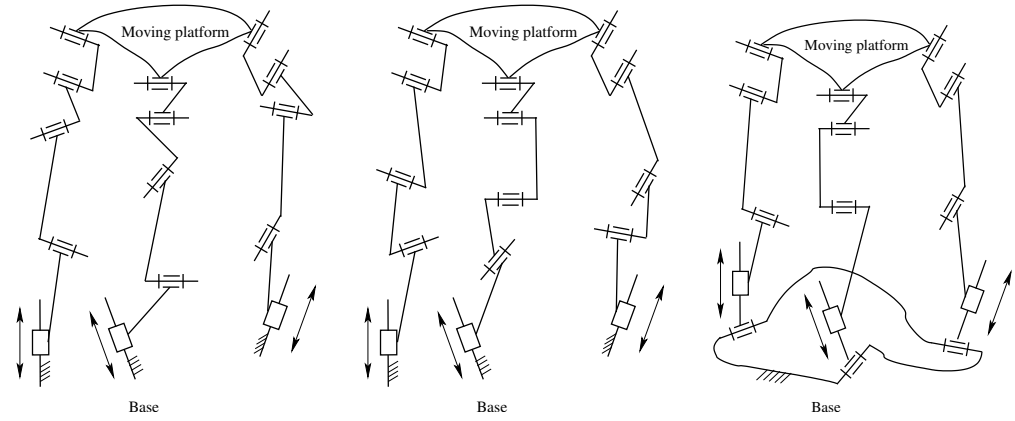


(d) 3-$\underline{\mathrm{P}}\bar{\mathrm{R}}\dot{\mathrm{R}}\bar{\mathrm{R}}\bar{\mathrm{R}}$ TPM. (e) 3-$\underline{\mathrm{P}}\dot{\mathrm{R}}\bar{\mathrm{R}}\bar{\mathrm{R}}\bar{\mathrm{R}}$ TPM. (f) 3-$\dot{\mathrm{R}}\underline{\mathrm{P}}\bar{\mathrm{R}}\bar{\mathrm{R}}\bar{\mathrm{R}}$ TPM.

Figure 8.1: Some LIO-TPMs without redundant DOFs.

It is noted that Tables 8.1 and 8.2 only show the LIO-TPMs without redundant DOFs. LIO-TPMs with redundant DOFs can be obtained from LIO-TPMs without redundant DOFs by adding one or more R joints with axes perpendicular to the leg-surfaces or a P joint parallel to the leg-surface within a same leg (Fig. 8.2).

### 8.2.2 Constraint singularity analysis of the translational parallel mechanisms with linear input-output relations

The constraint singularity [114] occurs when the moving platform of a TPM can rotate instantaneously. The constraint singularity occurs for a TPM if and only if its wrench system (a 3-system of $\infty$-pitch) degenerates into a 2-system or a 1-system.

For those LIO-TPMs with no inactive joints and those LIO-TPMs in which all the inactive joints are connected to the moving platform or the base through a P joint or located on the moving platform or the base, the wrench system of a leg for LTPMs is invariant. The order of the wrench system of these LIO-TPM is thus a constant. Thus, the moving platform cannot rotate at any instant. That is to say, there is no constraint singularity for these LIO-TPMs.

For other LIO-TPMs, the wrench system of a leg for LIO-TPMs is not invariant. When the three lines, each of which is perpendicular to the axes of all the R joints within one leg, are parallel to a plane, the constraint singularity occurs.

### 8.2.3 Generation of LTPMs

An LTPM is a LIO-TPM for which all the inactive joints are connected to the moving platform or the base through a P joint or located on the moving platform or the base. From the list of LIO-TPMs (Tables 8.1 and 8.2) LTPMs can be obtained directly. In fact, all the LIO-TPMs shown in Tables 8.1 and 8.2 except for the types 39, 40 and 71–74 are LTPMs. Based on the above LTPMs, LTPMs with redundant DOF can also be obtained.

For practical reasons, LTPMs should satisfy the following conditions.

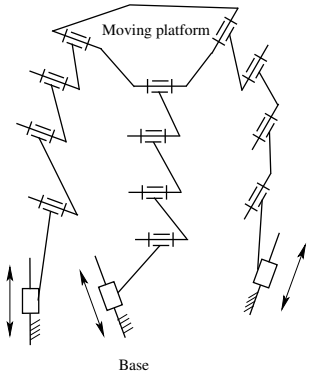


(a) 3-$\underline{\mathrm{P}}\bar{\mathrm{R}}\bar{\mathrm{R}}\bar{\mathrm{R}}\bar{\mathrm{R}}$ TPM.

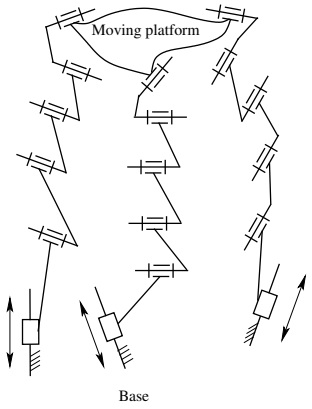


(b) 3-$\underline{\mathrm{P}}\bar{\mathrm{R}}\bar{\mathrm{R}}\bar{\mathrm{R}}\bar{\mathrm{R}}\dot{\mathrm{R}}$ TPM.

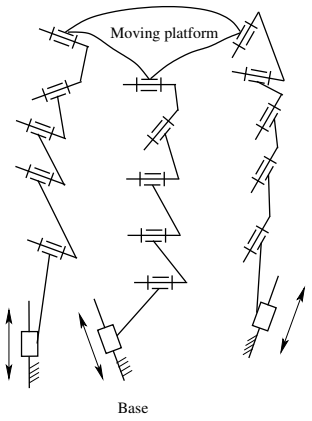


(c) 3-$\underline{\mathrm{P}}\bar{\mathrm{R}}\bar{\mathrm{R}}\bar{\mathrm{R}}\dot{\mathrm{R}}\bar{\mathrm{R}}$ TPM.

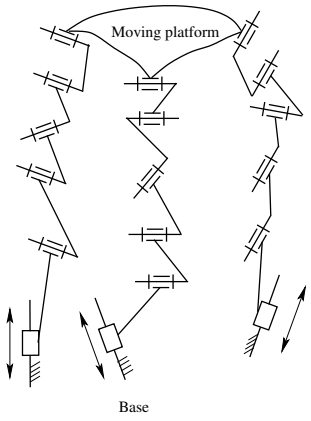


(d) 3-$\underline{\mathrm{P}}\bar{\mathrm{R}}\bar{\mathrm{R}}\dot{\mathrm{R}}\bar{\mathrm{R}}\bar{\mathrm{R}}$ TPM.

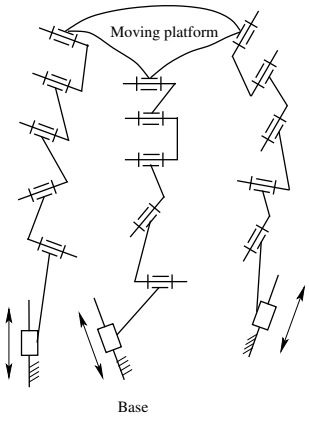


(e) 3-$\underline{\mathrm{P}}\bar{\mathrm{R}}\dot{\mathrm{R}}\bar{\mathrm{R}}\bar{\mathrm{R}}\bar{\mathrm{R}}$ TPM.

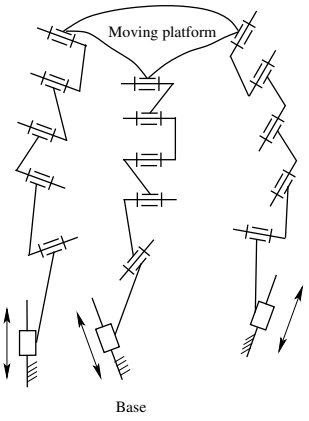


(f) 3-$\underline{\mathrm{P}}\dot{\mathrm{R}}\bar{\mathrm{R}}\bar{\mathrm{R}}\bar{\mathrm{R}}\bar{\mathrm{R}}$ TPM.

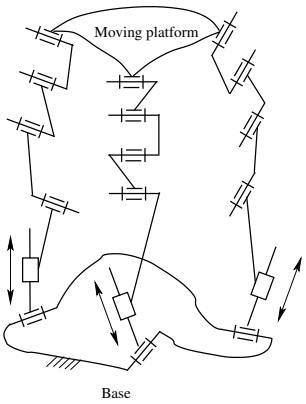


(g) 3-$\dot{\mathrm{R}}\underline{\mathrm{P}}\bar{\mathrm{R}}\bar{\mathrm{R}}\bar{\mathrm{R}}\bar{\mathrm{R}}$ TPM.

Figure 8.2: Some LIO-TPMs with redundant DOFs.

(1) Each of the actuators is located on or connected through an inactive joint to the base.

(2) The number of redundant DOF of a leg is not greater than 1.

(3) The number of inactive joint of a leg is not greater than 1.

All the LTPMs satisfying the above conditions are shown in Fig. 8.3. The number of inactive joints, the redundant DOF and the number of over-constraints of these LTPMs are listed in Table 8.3.

Table 8.3: Three-legged LTPMs

| No | Type | Number of inactive joints | Redundant DOFs | Number of over-constraints |
|---|---|---|---|---|
| 1 | 3-$\underline{\mathrm{P}}\bar{\mathrm{R}}\bar{\mathrm{R}}\bar{\mathrm{R}}$ | 0 | 0 | 3 |
| 2 | 3-$\underline{\mathrm{P}}\bar{\mathrm{R}}\bar{\mathrm{R}}\bar{\mathrm{R}}\dot{\mathrm{R}}$ | 3 | 0 | 0 |
| 3 | 3-$\underline{\mathrm{P}}\dot{\mathrm{R}}\bar{\mathrm{R}}\bar{\mathrm{R}}\bar{\mathrm{R}}$ | 3 | 0 | 0 |
| 4 | 3-$\dot{\mathrm{R}}\underline{\mathrm{P}}\bar{\mathrm{R}}\bar{\mathrm{R}}\bar{\mathrm{R}}$ | 3 | 0 | 0 |
| 5 | 3-$\underline{\mathrm{P}}\bar{\mathrm{R}}\bar{\mathrm{R}}\bar{\mathrm{R}}\bar{\mathrm{R}}$ | 0 | 3 | 3 |
| 6 | 3-$\underline{\mathrm{P}}\bar{\mathrm{R}}\bar{\mathrm{R}}\bar{\mathrm{R}}\bar{\mathrm{R}}\dot{\mathrm{R}}$ | 3 | 3 | 0 |
| 7 | 3-$\underline{\mathrm{P}}\dot{\mathrm{R}}\bar{\mathrm{R}}\bar{\mathrm{R}}\bar{\mathrm{R}}\bar{\mathrm{R}}$ | 3 | 3 | 0 |
| 8 | 3-$\dot{\mathrm{R}}\underline{\mathrm{P}}\bar{\mathrm{R}}\bar{\mathrm{R}}\bar{\mathrm{R}}\bar{\mathrm{R}}$ | 3 | 3 | 0 |

When a combination of one R joint and one P joint with parallel axes arises, or a combination of two R joints with intersecting non-parallel axes arises, they can be replaced with a C joint and U (universal) joint, respectively. Many specific cases of practical LTPMs can be obtained in this way. For reasons of brevity, we only give the specific cases of LTPMs when necessary.

### 8.2.4 Equivalent LTPM

It is clear that the removal of the inactive joints and redundant joints from an LTPM does not affect the input-output relations of the LTPM. The LTPM thus obtained from

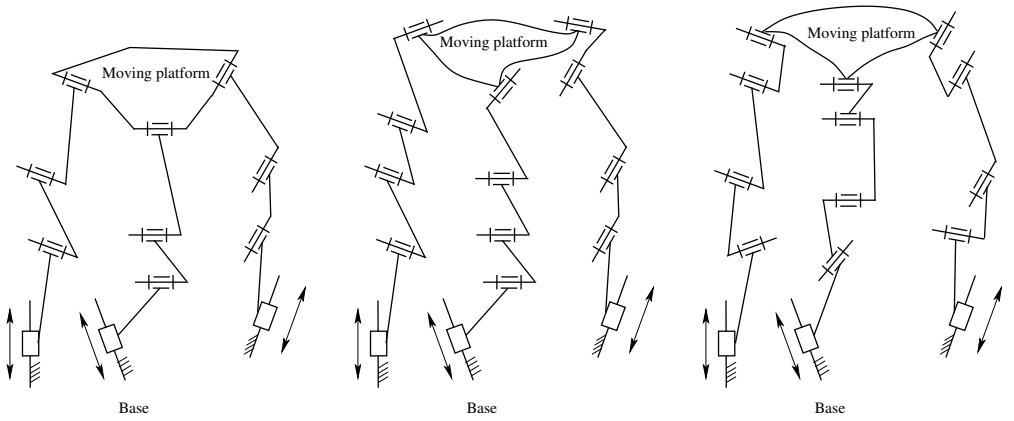


(a) 3-$\underline{\mathrm{P}}\bar{\mathrm{R}}\bar{\mathrm{R}}\bar{\mathrm{R}}$ TPM. (b) 3-$\underline{\mathrm{P}}\bar{\mathrm{R}}\bar{\mathrm{R}}\bar{\mathrm{R}}\dot{\mathrm{R}}$ TPM. (c) 3-$\underline{\mathrm{P}}\dot{\mathrm{R}}\bar{\mathrm{R}}\bar{\mathrm{R}}\bar{\mathrm{R}}$ TPM.

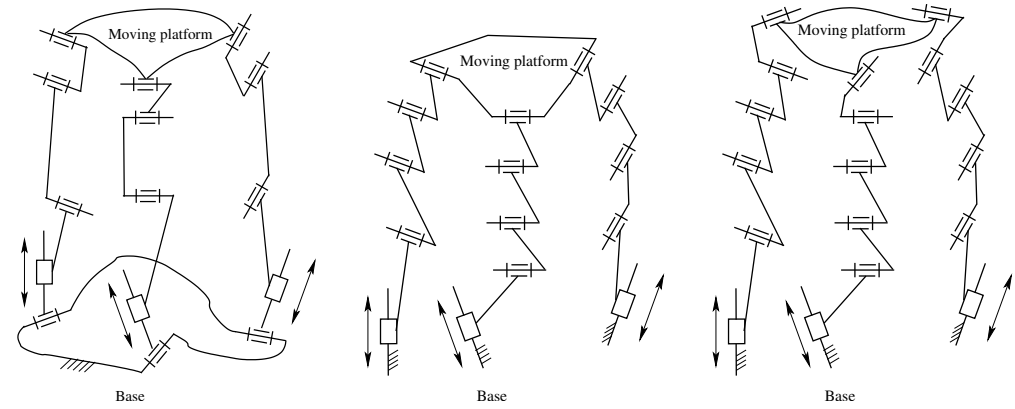


(d) 3-$\dot{\mathrm{R}}\underline{\mathrm{P}}\bar{\mathrm{R}}\bar{\mathrm{R}}\bar{\mathrm{R}}$ TPM. (e) 3-$\underline{\mathrm{P}}\bar{\mathrm{R}}\bar{\mathrm{R}}\bar{\mathrm{R}}\bar{\mathrm{R}}$ TPM. (f) 3-$\underline{\mathrm{P}}\bar{\mathrm{R}}\bar{\mathrm{R}}\bar{\mathrm{R}}\bar{\mathrm{R}}\dot{\mathrm{R}}$ TPM.

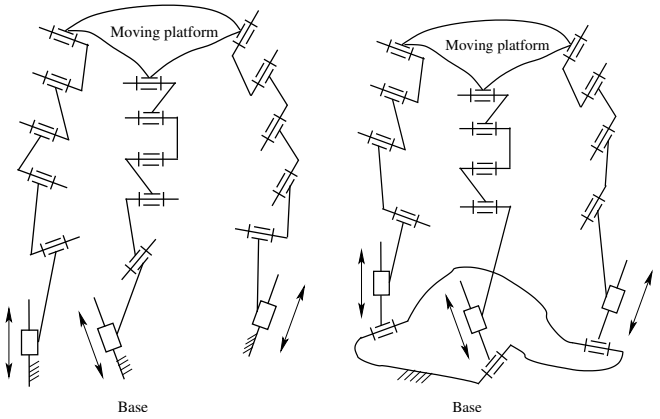


(g) 3-$\underline{\mathrm{P}}\dot{\mathrm{R}}\bar{\mathrm{R}}\bar{\mathrm{R}}\bar{\mathrm{R}}\bar{\mathrm{R}}$ TPM. (h) 3-$\dot{\mathrm{R}}\underline{\mathrm{P}}\bar{\mathrm{R}}\bar{\mathrm{R}}\bar{\mathrm{R}}\bar{\mathrm{R}}$ TPM.

Figure 8.3: Proposed LTPMs.

an LTPM by removing all the inactive joints and redundant joints is kinematically equivalent to the original LTPM and is thus termed an equivalent LTPM of the original LTPM.

It is found that the LTPMs proposed above (Fig. 8.3) have the same equivalent LTPM, namely, the 3-$\underline{\text{P}}\bar{\text{R}}\bar{\text{R}}\bar{\text{R}}$ LTPM [1] described above (Fig. 8.3(a)).

## 8.3 Inverse kinematics of the 3-$\underline{\text{P}}\bar{\text{R}}\bar{\text{R}}\bar{\text{R}}$ LTPM

As all the LTPMs are kinematically equivalent to the 3-$\underline{\text{P}}\bar{\text{R}}\bar{\text{R}}\bar{\text{R}}$ LTPM (Section 8.2.4), the kinematic analysis of all the LTPMs can be performed in the same way as that of the 3-$\underline{\text{P}}\bar{\text{R}}\bar{\text{R}}\bar{\text{R}}$ LTPM.

### 8.3.1 Geometric description

To study the kinematics of the 3-$\underline{\text{P}}\bar{\text{R}}\bar{\text{R}}\bar{\text{R}}$ LTPM, two coordinate systems, $P - X_P Y_P Z_P$ and $O - XYZ$, are attached to its moving platform and base respectively (see Fig. 8.4). In leg $i$ (denoted by the subscript $i$), let $B_i$ denote a point on the axis of the R joint on the moving platform, $C_i$ denote a point on the axis of the R joint adjacent to the P joint, $A_i$ denote a point on the axis of the P joint on the link connected to the base by the P joint, $A_{i0}$ denote the point on the base which is coincident with the initial position of $A_i$, $\mathbf{s}_{i2}$ denote the unit vector along the R joint, $\mathbf{s}_{i1}$ denote the unit vector along the P joint, $\mathbf{b}_{Pi}$ denote the vector from $P$ to $B_i$, $\mathbf{c}_{Ai}$ denote the vector from $A_i$ to $C_i$, $\mathbf{a}_i$ and $\mathbf{a}_{i0}$ denote respectively the position vectors of $A_i$ and $A_{i0}$ in the coordinate system $O - XYZ$, and $S_i$ denote the input $i$ of the 3-$\underline{\text{P}}\bar{\text{R}}\bar{\text{R}}\bar{\text{R}}$ LTPM.

For the purpose of simplification and without loss of generality, the $X_P$-, $Y_P$-, $Z_P$-axes of the coordinate system $P - X_P Y_P Z_P$ are, respectively, parallel to the $X$-, $Y$-, $Z$-axes of the coordinate system $O - XYZ$, while $B_i$ and $C_i$ are chosen in such a way that $A_i C_i$ is perpendicular to $\mathbf{s}_{i2}$.

[1] The 3-P$\bar{\text{R}}\bar{\text{R}}\bar{\text{R}}$ TPKC was implicitly proposed in [13].

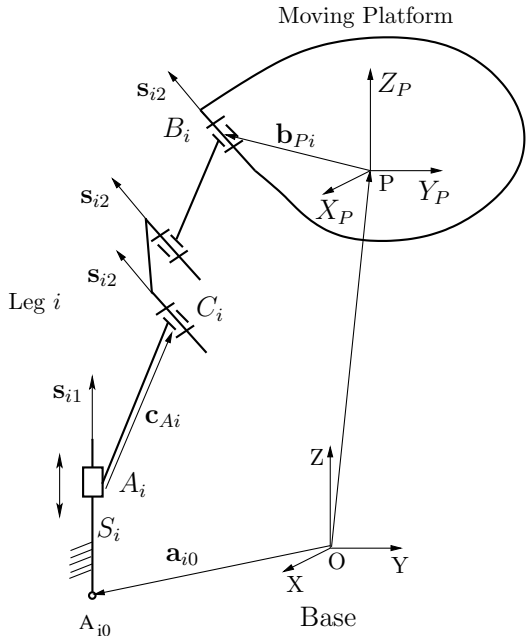


Figure 8.4: $\underline{\text{P}}\bar{\text{R}}\bar{\text{R}}\bar{\text{R}}$ leg for an LTPM.

### 8.3.2 Inverse displacement analysis

The inverse displacement analysis of the 3-$\underline{\text{P}}\bar{\text{R}}\bar{\text{R}}\bar{\text{R}}$ LTPM consists in determining the required inputs, $S_i$ ($i$=1, 2, 3), for a given position, $\mathbf{p}$, of the moving platform, where $\mathbf{p}$ is the vector directed from point $O$ to point $P$.

As there exists no constraint singularity for the 3-$\underline{\text{P}}\bar{\text{R}}\bar{\text{R}}\bar{\text{R}}$ LTPM, $C_iB_i$ ($i$=1, 2, 3) is perpendicular to the axis of the R joint $i$ at any instant, i.e.,

$$\mathbf{s}_{i2}^T[\mathbf{p} + \mathbf{b}_{Pi} - (\mathbf{a}_{i0} + S_i\mathbf{s}_{i1} + \mathbf{c}_{Ai})] = 0 \quad i=1,\ 2,\ 3 \tag{8.1}$$

Expanding Eq. (8.1), we have

$$\mathbf{s}_{i2}^T\mathbf{s}_{i1}S_i = \mathbf{s}_{i2}^T(\mathbf{p} + \mathbf{b}_{Pi} - \mathbf{a}_{i0} - \mathbf{c}_{Ai}) \quad i=1,\ 2,\ 3 \tag{8.2}$$

For a 3-$\underline{\text{P}}\bar{\text{R}}\bar{\text{R}}\bar{\text{R}}$ LTPM, we have $\mathbf{s}_{i2}^T\mathbf{s}_{i1} \neq 0$. From Eq. (8.2), we obtain the solution to the inverse displacement analysis

$$S_i = \mathbf{s}_{i2}^T(\mathbf{p} + \mathbf{b}_{Pi} - \mathbf{a}_{i0} - \mathbf{c}_{Ai})/\mathbf{s}_{i2}^T\mathbf{s}_{i1} \quad i=1,\ 2,\ 3 \tag{8.3}$$

For any $\mathbf{p}$ located inside the workspace, the distance between points $B_i$ and $C_i$ is not greater than the sum of the lengths of all the RR binary links in leg $i$. In the case

that the distance between points $B_i$ and $C_i$ is greater than the sum of the lengths of all the RR binary links in leg $i$, the set of inputs is invalid, as the LTPM cannot be assembled.

Let $\Delta\mathbf{p}$ denote an increment of $\mathbf{p}$, and $\Delta S_i$ denote the corresponding increment of $S_i$. From Eq. (8.3), we have

$$S_i + \Delta S_i = \mathbf{s}_{i2}^T(\mathbf{p} + \Delta\mathbf{p} + \mathbf{b}_{Pi} - \mathbf{a}_{i0} - \mathbf{c}_{Ai})/\mathbf{s}_{i2}^T\mathbf{s}_{i1} \quad i=1,\, 2,\, 3 \tag{8.4}$$

Subtracting Eq. (8.3) from Eq. (8.4), we obtain the solution to the inverse displacement analysis in incremental form

$$\Delta S_i = \mathbf{s}_{i2}^T\Delta\mathbf{p}/\mathbf{s}_{i2}^T\mathbf{s}_{i1} \quad i=1,\, 2,\, 3 \tag{8.5}$$

### 8.3.3 Inverse velocity analysis

The inverse velocity analysis of the 3-$\underline{\text{P}}\bar{\text{R}}\bar{\text{R}}\bar{\text{R}}$ LTPM consists in determining the required velocities of the actuators, $\dot{S}_i(=dS_i/dt)$, for a given velocity, $\mathbf{v}(=d\mathbf{p}/dt)$, of the moving platform in a given configuration.

Differentiating Eq. (8.3) with respect to time, we obtain the solution to the inverse velocity analysis

$$\dot{S}_i = \mathbf{s}_{i2}^T\mathbf{v}/\mathbf{s}_{i2}^T\mathbf{s}_{i1} \quad i=1,\, 2,\, 3 \tag{8.6}$$

## 8.4 Forward kinematics of the 3-$\underline{\text{P}}\bar{\text{R}}\bar{\text{R}}\bar{\text{R}}$ LTPM

### 8.4.1 Forward displacement analysis

The FDA of the 3-$\underline{\text{P}}\bar{\text{R}}\bar{\text{R}}\bar{\text{R}}$ LTPM consists in determining the position, $\mathbf{p}$, of the moving platform for a given set of inputs, $S_i$.

From Eq. (8.1), we have

$$\mathbf{s}_{i2}^T\mathbf{p} = \mathbf{s}_{i2}^T(\mathbf{a}_{i0} + \mathbf{c}_{Ai} + S_i\mathbf{s}_i - \mathbf{b}_{Pi}) \quad i=1,\, 2,\, 3 \tag{8.7}$$

When absolute position control is used to control the motion of the LTPM, the FDA can can be performed as follows.

Rewriting Eq. (8.7) in matrix form, we have

$$\mathbf{J}_1\mathbf{p} = \begin{bmatrix} \mathbf{s}_{12}^T(\mathbf{a}_{10} + \mathbf{c}_{A1} + S_1\mathbf{s}_{11} - \mathbf{b}_{P1}) \\ \mathbf{s}_{22}^T(\mathbf{a}_{20} + \mathbf{c}_{A2} + S_2\mathbf{s}_{21} - \mathbf{b}_{P2}) \\ \mathbf{s}_{32}^T(\mathbf{a}_{30} + \mathbf{c}_{A3} + S_3\mathbf{s}_{31} - \mathbf{b}_{P3}) \end{bmatrix} \tag{8.8}$$

where

$$\mathbf{J}_1 = \begin{bmatrix} \mathbf{s}_{12}^T \\ \mathbf{s}_{22}^T \\ \mathbf{s}_{32}^T \end{bmatrix} \tag{8.9}$$

From Eq. (8.8), we obtain the solution to the FDA

$$\mathbf{p} = \mathbf{J}_1^{-1} \begin{bmatrix} \mathbf{s}_{12}^T(\mathbf{a}_{10} + \mathbf{c}_{A1} + S_1\mathbf{s}_{11} - \mathbf{b}_{P1}) \\ \mathbf{s}_{22}^T(\mathbf{a}_{20} + \mathbf{c}_{A2} + S_2\mathbf{s}_{21} - \mathbf{b}_{P2}) \\ \mathbf{s}_{32}^T(\mathbf{a}_{30} + \mathbf{c}_{A3} + S_3\mathbf{s}_{31} - \mathbf{b}_{P3}) \end{bmatrix} \tag{8.10}$$

It should be pointed out that for a vector $\mathbf{p}$ obtained using Eq. (8.10) with a set of valid inputs, the distance between points $B_i$ and $C_i$ is not greater than the sum of the lengths of all the RR binary links in leg $i$. In the case that the distance between points $B_i$ and $C_i$ is greater than the sum of the lengths of all the RR binary links in leg $i$, the set of inputs is invalid as the LTPM cannot be assembled.

In the case that relative position control is used, the FDA can be performed in the following way.

Rewriting Eq. (8.5) in matrix form, we have

$$\mathbf{J}\Delta\mathbf{p} = \begin{bmatrix} \Delta S_1 \\ \Delta S_2 \\ \Delta S_3 \end{bmatrix} \tag{8.11}$$

where

$$\begin{aligned}\mathbf{J} &= \begin{bmatrix} \mathbf{s}_{12}^T/\mathbf{s}_{12}^T\mathbf{s}_{11} \\ \mathbf{s}_{22}^T/\mathbf{s}_{22}^T\mathbf{s}_{21} \\ \mathbf{s}_{32}^T/\mathbf{s}_{32}^T\mathbf{s}_{31} \end{bmatrix} \\ &= \begin{bmatrix} 1/\mathbf{s}_{12}^T\mathbf{s}_{11} & 0 & 0 \\ 0 & 1/\mathbf{s}_{22}^T\mathbf{s}_{21} & 0 \\ 0 & 0 & 1/\mathbf{s}_{32}^T\mathbf{s}_{31} \end{bmatrix} \mathbf{J}_1 \end{aligned} \tag{8.12}$$

From Eq. (8.11), we obtain the solution to the FDA in incremental form

$$\Delta\mathbf{p} = \mathbf{J}^{-1} \begin{bmatrix} \Delta S_1 \\ \Delta S_2 \\ \Delta S_3 \end{bmatrix} \tag{8.13}$$

where

$$\mathbf{J}^{-1} = \mathbf{J}_1^{-1} \begin{bmatrix} \mathbf{s}_{12}^T\mathbf{s}_{11} & 0 & 0 \\ 0 & \mathbf{s}_{22}^T\mathbf{s}_{21} & 0 \\ 0 & 0 & \mathbf{s}_{32}^T\mathbf{s}_{31} \end{bmatrix} \tag{8.14}$$

### 8.4.2 Forward velocity analysis

The forward velocity analysis of the 3-$\underline{\text{P}}\bar{\text{R}}\bar{\text{R}}\bar{\text{R}}$ LTPM consists in determining the velocity, $\mathbf{v}$, of the moving platform for a given set of velocities of the actuators, $\dot{S}_i$, in a given configuration.

Rewriting Eq. (8.6) in matrix form, we have

$$\begin{bmatrix} \dot{S}_1 \\ \dot{S}_2 \\ \dot{S}_3 \end{bmatrix} = \mathbf{J}\mathbf{v} \tag{8.15}$$

Solving Eq. (8.15), we obtain the solution to the forward velocity analysis

$$\mathbf{v} = \mathbf{J}^{-1} \begin{bmatrix} \dot{S}_1 \\ \dot{S}_2 \\ \dot{S}_3 \end{bmatrix} \tag{8.16}$$

### 8.4.3 Discussion on the Jacobian Matrix

From Eq. (8.12), it can be found that each row of the Jacobian matrix, **J**, is proportional to the unit vectors along the axes of the R joints within one leg. As the unit vector along the axes of all the R joints are invariant, the Jacobian matrix, **J**, is constant.

For a given 3-$\underline{\text{P}}\bar{\text{R}}\bar{\text{R}}\bar{\text{R}}$ LTPM, the inverse of **J** is therefore also constant and can be pre-calculated. Thus, there is no need to calculate $\mathbf{J}^{-1}$ repeatedly in performing the forward position analysis and forward velocity analysis of the 3-$\underline{\text{P}}\bar{\text{R}}\bar{\text{R}}\bar{\text{R}}$ LTPM. This simplifies to a great extent the real-time control of the 3-$\underline{\text{P}}\bar{\text{R}}\bar{\text{R}}\bar{\text{R}}$ LTPM.

As **J** and $\mathbf{J}^{-1}$ are constant, it is evident from Eqs. (8.11) and (8.13) that there will be a same $\Delta\mathbf{p}$ corresponding to a given set of $\Delta S_i$ in any configuration of an LTPM, and vice visa. Thus, both the inverse displacement analysis and the FDA will be further simplified if the LTPM is used with relative position control.

## 8.5 Kinematic singularity analysis of LTPMs

### 8.5.1 Inverse kinematic singularity analysis

The inverse kinematic singularities occur for a PM when the order of the twist system of any one of the legs decreases instantaneously. For a leg in an LTPM, an inverse kinematic singularity occurs if and only if the axes of all the R joints with parallel axes are coplanar. In this case, the distance between points $B_i$ and $C_i$ is equal to the sum of the lengths of all the RR binary links in leg $i$. These configurations correspond to a boundary of the workspace. The inverse kinematic singularities at the boundary of the workspace can be eliminated by limiting the range of motion of the actuated joints.

### 8.5.2 Forward kinematic singularity analysis

When forward kinematic singularities occur for a PM, the moving platform can undergo infinitesimal or finite motion when the inputs are specified. It will be proved below that there exist no forward kinematic singularities for the LTPMs.

From Section 8.2.2, it is known that there exists no constraint singularity for the LTPMs. Thus, Eq. (8.15) is always satisfied. Forward kinematic singularities for the LTPMs occur if and only if $\mathbf{J}$ is singular.

From Section 8.4.3, it is known that each row of the Jacobian matrix, $\mathbf{J}$, is proportional to the unit vector along the axes of the R joints of the group of R joints with parallel axes of one leg. As the axes of the R joints belong to the groups of R joints with parallel axes are not all parallel to a common plane (see Section 8.2), $\mathbf{J}$ is always non-singular. There thus exist no forward kinematic singularities for the LTPMs.

### 8.5.3 Discussion on the choice of working mode

The concept of working mode of a PM was introduced in [149] for a better control and application of PMs. However, the definition of working mode given in [149] does not apply to the LTPMs proposed here, since it is defined based on the input-output velocity equation and the unactuated joint variables are neglected. In this section, the working mode of PMs is generalized to cover the LTPMs with no redundant DOF. The choice of working mode of LTPMs is also discussed.

In performing the inverse displacement analysis of a PM, any one of its legs can be treated as a serial manipulator. The concept of postures of serial manipulator can also be applied to a leg in a PM. A working mode of a PM is defined as a combination of the postures of all its legs. For a PM having multiple solutions to its inverse displacement analysis, there are multiple working modes. The postures of at least one leg are different in different working modes of a PM.

Consider an LTPM with no redundant DOFs. For a given position of the moving platform, there usually exist two sets of solutions to the joint variables of the unactuated

joints for each leg and eight solutions to the inverse displacement analysis of the LTPM. The LTPM has thus 8 working modes. The joint variables of the unactuated joints in at least one leg are different between two working modes while the inputs are the same for a given position of the moving platform. Different working modes are separated by the inverse singularity of one or more legs. If link interference is neglected and the motion ranges of the joints are not limited, the workspace of the manipulator under the different working modes is the same.

In practice, the assembly mode with higher stiffness and in which link interference can be easily avoided should be selected to perform a desired task. If the inverse kinematic singularities at the boundary of the workspace are eliminated by limiting the range of motion of the actuated joints, an LTPM will always remain in the working mode in which it was first assembled.

## 8.6 Isotropic LTPM

An isotropic manipulator [69] is a manipulator whose Jacobian matrix has a condition number equal to 1 in at least one of its configurations. In isotropic configurations, the manipulator performs very well with regard to the force and motion transmission. Except for the 3-$\underline{\bar{C}}\bar{R}\bar{R}$ TPM proposed in [142], isotropic manipulators proposed so far are isotropic only in a small portion of their workspace. In the following, the geometric condition which renders the LTPMs isotropic will be revealed and it will be proved that the isotropic LTPMs are isotropic in their whole workspace.

As each row of the Jacobian matrix, $\mathbf{J}$, is proportional with the unit vector along the axes of R joints in the group of R joints with parallel axes of one leg (Section 8.4.3), it can be easily verified that when the axes of the three R joints are orthogonal and $\|\mathbf{s}_{i2}^T\mathbf{s}_{i1}\|$ for all three legs are equal, the LTPM is isotropic, i.e., the condition number of the Jacobian matrix is 1. As the Jacobian matrix, $\mathbf{J}$, of the LTPM is constant (Section 8.4.3), the isotropic LTPM is isotropic in its whole workspace.

In this case, $\mathbf{J}_1$ (see Eq. (8.9)) is an orthogonal matrix. One has

$$\mathbf{J}_1^{-1} = \mathbf{J}_1^T \tag{8.17}$$

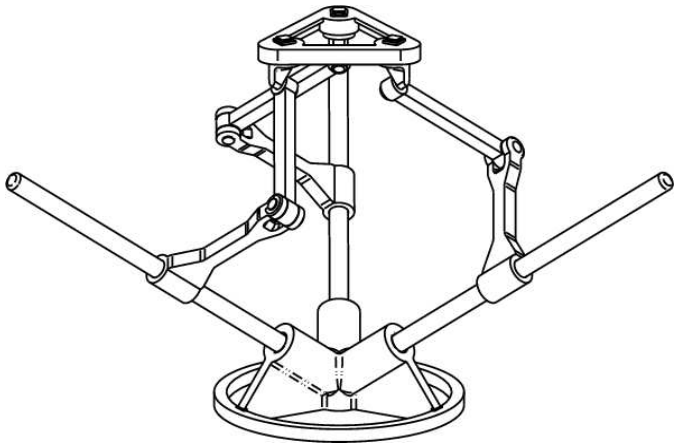

Figure 8.5: Isotropic 3-$\underline{\bar{C}}\bar{R}\bar{R}$ TPM.

The substitution of Eq. (8.17) into Eq. (8.14) yields

$$\mathbf{J}^{-1} = \begin{bmatrix} \mathbf{s}_{12}^T\mathbf{s}_{11}\mathbf{s}_{12} & \mathbf{s}_{22}^T\mathbf{s}_{21}\mathbf{s}_{22} & \mathbf{s}_{32}^T\mathbf{s}_{31}\mathbf{s}_{32} \end{bmatrix} \tag{8.18}$$

Thus, fewer calculations are needed in obtaining the inverse of the Jacobian matrix when performing the forward kinematic analysis of isotropic LTPM. Moreover, if the coordinate system $O-XYZ$ fixed to the base is defined such that vectors $\mathbf{s}_{12}$, $\mathbf{s}_{22}$, and $\mathbf{s}_{32}$ are respectively aligned with the $X$-, $Y$-, and $Z$-axes of $O-XYZ$, then the Jacobian matrix becomes a constant diagonal matrix with identical elements. Hence the inverse displacement analysis as well as the FDA and the associated velocity problems are further simplified.

Figures 8.5 and 8.6 show two isotropic LTPMs. In the 3-$\underline{\bar{C}}\bar{R}\bar{R}$ LTPM shown in Fig. 8.5, the directions of the $\underline{P}$ joints are orthogonal to one another. Its kinematic analysis is the same as a gantry robot. In the case shown in Fig. 8.6, all the axes of $\underline{P}$ are parallel. It is therefore called the parallel version of isotropic 3-$\underline{P}\bar{R}\bar{R}\bar{R}$ LTPM. The translations of the moving platform along the direction parallel to the direction of the P joints is unlimited as long as the strokes of all the $\underline{P}$ joints are not limited.

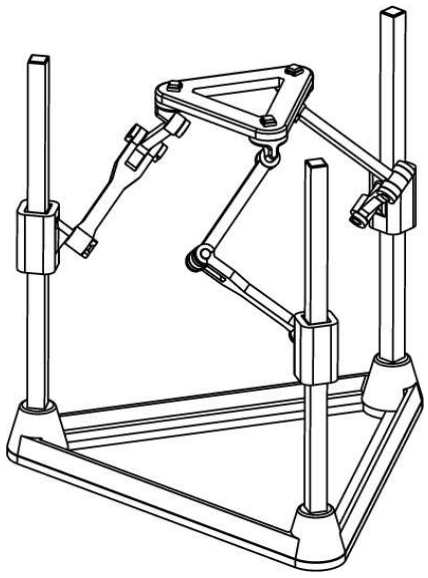

Figure 8.6: Isotropic 3-$\underline{\text{P}}\bar{\text{R}}\bar{\text{R}}\bar{\text{R}}$ TPM (parallel version).

## 8.7 Workspace analysis of the 3-$\underline{\text{P}}\bar{\text{R}}\bar{\text{R}}\bar{\text{R}}$ LTPM

### 8.7.1 Geometric approach to determine the workspace of a parallel mechanism

The workspace of the 3-$\underline{\text{P}}\bar{\text{R}}\bar{\text{R}}\bar{\text{R}}$ TPM can be determined using a geometric approach. The geometric approach was proposed in [105] to determine the workspace of the Stewart platform. For a general PM, the geometric approach can be stated as follows: the workspace of a PM is the intersection of all its leg-spaces. Here, the leg-space is a mobility region permitted by a leg under the action of the wrench system of the moving platform. For example, a leg-space of a TPM is the mobility region permitted by a leg with the orientation of the moving platform kept constant.

### 8.7.2 Workspace of the 3-$\underline{\text{P}}\bar{\text{R}}\bar{\text{R}}\bar{\text{R}}$ LTPM

For a $\underline{\text{P}}\bar{\text{R}}\bar{\text{R}}\bar{\text{R}}$ TPM, each leg-space is bounded by two concentric cylinders whose axes are parallel to the axis of the P joint and two planes which are perpendicular to the axes of the R joints (Fig. 8.7), if joint limits and link interference are neglected. The

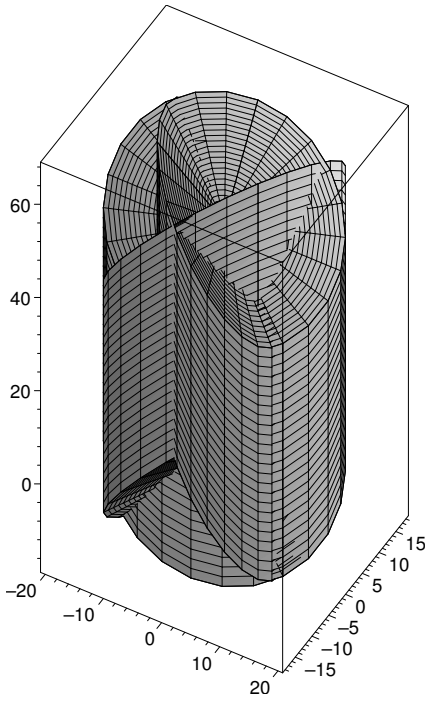


Figure 8.7: Workspace determination of a 3-$\underline{\mathrm{P}}\bar{\mathrm{R}}\bar{\mathrm{R}}\bar{\mathrm{R}}\dot{\mathrm{R}}$ TPM (parallel version).

two concentric cylinders are formed by moving two concentric circles along the axis of the P joints. The radius of the outer circle is equal to the sum of the lengths of the two RR links in the same leg, while the radius of the inner circle is equal to the absolute value of the difference between the lengths of the two RR links.

## 8.8 Kinematic design of isotropic 3-$\underline{\mathrm{P}}\bar{\mathrm{R}}\bar{\mathrm{R}}\bar{\mathrm{R}}$ LTPMs

### 8.8.1 Workspace consideration

In the following, we will discuss two specific versions of the 3-$\underline{\mathrm{P}}\bar{\mathrm{R}}\bar{\mathrm{R}}\bar{\mathrm{R}}$ TPM. The first is the 3-$\underline{\bar{\mathrm{C}}}\bar{\mathrm{R}}\bar{\mathrm{R}}$ TPM (Fig. 8.5), and the second is the parallel version (Fig. 8.6). In the first case, the direction of each P joint is parallel to the axes of the R joints within the same leg. The reduction ratio thus takes the maximum value of 1. In the second case, the workspace will increase proportionally with the increasing of the strokes of the P joints.

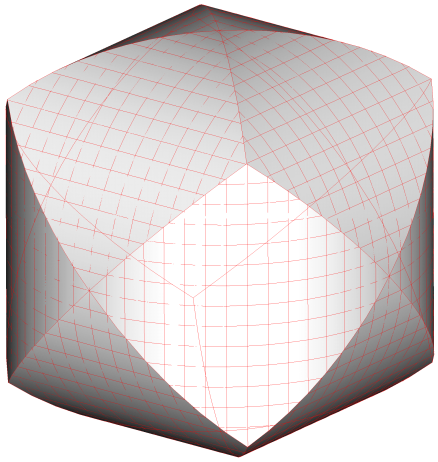

Figure 8.8: The maximal workspace of the isotropic 3-$\underline{\bar{C}}\bar{R}\bar{R}$ TPM.

#### 8.8.1.1 The 3-$\underline{\bar{C}}\bar{R}\bar{R}$ LTPM

For the 3-$\underline{\bar{C}}\bar{R}\bar{R}$ TPM, each leg-space is bounded by two concentric cylinders whose axes are parallel to the axis of the C joint, if joint limits and link interference are neglected. The radius of the outer cylinder is equal to the sum of the lengths of the two links in the same leg, while the radius of the inner cylinder is equal to the absolute value of the difference between the lengths of the two links.

The maximum workspace of the isotropic 3-$\underline{\bar{C}}\bar{R}\bar{R}$ TPM is a tricylinder (Fig. 8.8), which is formed by the intersection of three outer cylinders intersecting at right angles. In this case, the radius of the inner cylinder is equal to zero (the lengths of the two links in a leg are equal). The volume $V$ of the maximum workspace is $8(2-\sqrt{2})r^3$ [150], where $r$ is the radius of the outer cylinder. The stroke of the C joints should be equal to $r$ in order to optimize the manipulator. Further increasing of the stroke will not increase the workspace.

#### 8.8.1.2 3-$\underline{P}\bar{R}\bar{R}\bar{R}$ LTPM (parallel version)

For a 3-$\underline{P}\bar{R}\bar{R}\bar{R}$ TPM (parallel version), each leg-space is bounded by two concentric cylinders whose axes are parallel to the axis of the C joint, if the limitation on joint motions and link interference are neglected. The radius of the outer cylinder is equal to the sum of the lengths of the two links in the same leg while the radius of the inner cylinder is equal to the absolute value of the difference between the lengths of the latter

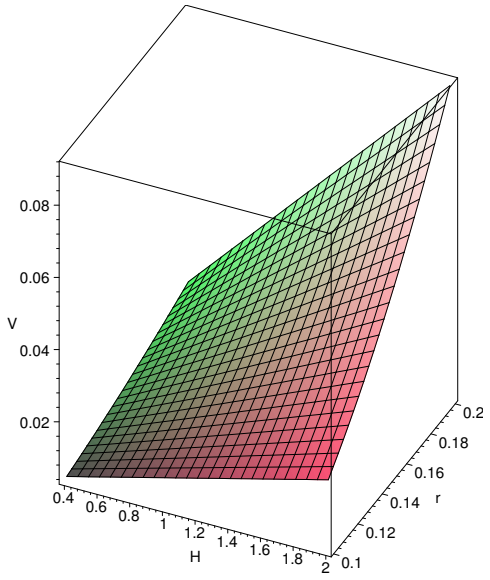


Figure 8.9: Variation of maximal workspace of the isotropic 3-$\underline{\mathrm{P}}\bar{\mathrm{R}}\bar{\mathrm{R}}\bar{\mathrm{R}}$ TPM (parallel version).

two links.

The maximum workspace of the isotropic 3-$\underline{\mathrm{P}}\bar{\mathrm{R}}\bar{\mathrm{R}}\bar{\mathrm{R}}$ TPM (parallel version) is formed by the intersection of the three concentric outer cylinders. For an isotropic 3-$\underline{\mathrm{P}}\bar{\mathrm{R}}\bar{\mathrm{R}}\bar{\mathrm{R}}$ TPM with a maximum workspace, the inner cylinder degenerates into a line (The lengths of the two links in a leg are equal). The variation of the volume $V$ of the maximum workspace with the change of $H$ and $r$ is shown in Fig. 8.9, where $r$ and $H$ are the radius of the outer cylinder and the strokes of all the $\underline{\mathrm{P}}$ joints, respectively.

### 8.8.2 Constraint consideration

For the 3-$\underline{\bar{\mathrm{C}}}\bar{\mathrm{R}}\bar{\mathrm{R}}\dot{\mathrm{R}}$ and 3-$\underline{\mathrm{P}}\bar{\mathrm{R}}\bar{\mathrm{R}}\bar{\mathrm{R}}\dot{\mathrm{R}}$ TPM, it is desirable that they are equivalent to the cases given in the previous section. Simultaneously, the optimal arrangement of the axes of the inactive joints should be dealt with.

Consider the matrix, termed here as the constraint matrix, which maps the couples exerted by the three legs on the moving platform to the external couples acted on the moving platform. Each column in the constraint matrix corresponds to a unit vector which is perpendicular to all the axes of the R joints within a leg. It is desirable to

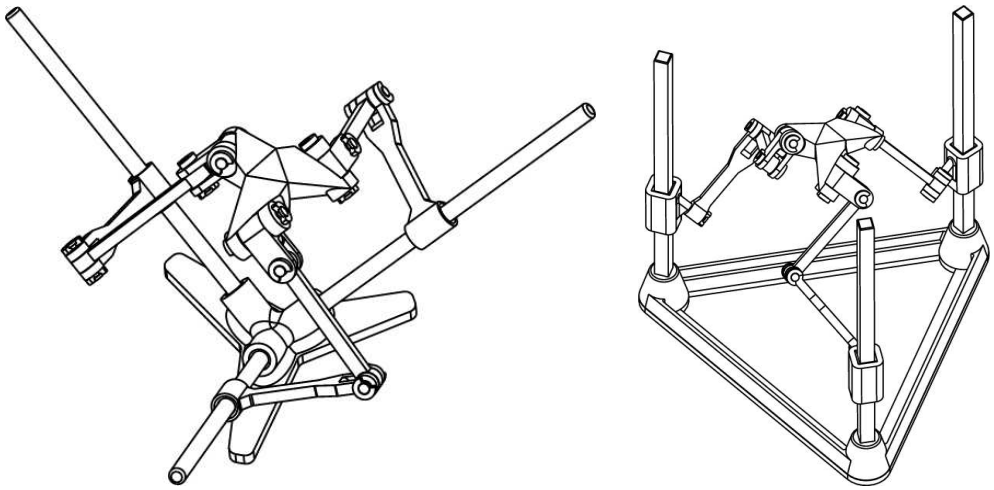

(a) 3-$\underline{\bar{C}}\bar{R}\bar{R}\dot{R}$ LTPM (b) 3-$\underline{P}\bar{R}\bar{R}\bar{R}\dot{R}$ LTPM.

Figure 8.10: Some isotropic LTPMs with an isotropic constraint matrix.

make the constraint matrix isotropic. The isotropic TPM with an isotropic constraint matrix is the isotropic TPM in which the axes of the inactive joints are respectively parallel to the axes of non-inactive R joints in the adjacent link and no pair of such axes are parallel to each other.

In order to make a comprehensive comparison of the LTPMs, several prototypes are being developed in the Robotics Laboratory at Laval University. In addition to the isotropic 3-$\underline{\bar{C}}\bar{R}\bar{R}$ LTPM (Fig. 8.5) and the isotropic 3-$\underline{P}\bar{R}\bar{R}\bar{R}$ LTPM (parallel version) with the axes of actuated joints arranged in parallel (Fig. 8.6), the 3-$\underline{P}\bar{R}\bar{R}\bar{R}\dot{R}$ LTPMs (parallel version) and the isotropic 3-$\underline{\bar{C}}\bar{R}\bar{R}\dot{R}$ both with isotropic constraint matrix (Fig. 8.10) are other potential candidates. As compared with the isotropic 3-$\underline{\bar{C}}\bar{R}\bar{R}$ and 3-$\underline{P}\bar{R}\bar{R}\bar{R}$ LTPMs, the isotropic 3-$\underline{\bar{C}}\bar{R}\bar{R}\dot{R}$ and 3-$\underline{P}\bar{R}\bar{R}\bar{R}\dot{R}$ LTPM are not overconstrained. As compared with the 3-$\underline{\bar{C}}\bar{R}\bar{R}$ and 3-$\underline{\bar{C}}\bar{R}\bar{R}\dot{R}$ LTPMs, the 3-$\underline{P}\bar{R}\bar{R}\bar{R}$ and 3-$\underline{P}\bar{R}\bar{R}\bar{R}\dot{R}$ LTPM have a larger workspace along the direction parallel to the axes of the P joints.

## 8.9 Conclusions

The type synthesis of LTPMs (TPMs with linear input-output relations and without constraint singularity) has been performed in this chapter. The LTPMs may or may not contain some inactive joints and/or redundant DOFs. The inverse kinematics, the forward kinematics, and the kinematic singularity analysis of the LTPMs have been performed. It has been shown that the proposed LTPMs have the following kinematic merits, namely: (1) The Jacobian matrix of the LTPMs is constant. The inverse of the Jacobian matrix can be pre-calculated, and there is no need to calculate repeatedly the inverse of the Jacobian matrix in performing the FDA and forward velocity analysis; (2) There exist no forward kinematic singularities.

The results of this chapter have been published in [136, 137, 138, 142]. Concurrently, isotropic TPMs with linear-input equations have also been proposed by other researchers in [139, 140, 141, 143, 144]. In additions to the results published in [139, 140, 141, 143, 144], TPMs with and without inactive and/or redundant joints are also covered in [136, 138, 142].

Two approaches have been adopted in the kinematic analysis in this section, i.e., the approach based on screw theory and the method based on the differentiation of the constraint equations. The first approach is used in the constraint singularity analysis and the inverse singularity analysis while the second approach is used in the velocity analysis and the forward kinematic singularity analysis. In this way, the above problems are solved in the most concise manner. The geometric condition which makes the LTPMs isotropic has also been revealed. Two additional kinematic merits exist for the isotropic LTPMs. The first is that an isotropic LTPM is isotropic in its whole workspace. The second is that fewer calculations are needed to pre-determine the inverse of the Jacobian matrix. A geometric approach has been proposed for the workspace analysis of LTPMs. Some preferred kinematic designs of the isotropic LTPMs have been revealed. The concept of isotropic design of constraint has also been proposed.

The results of this chapter should be of great interest in the development of fast TPMs and high-performance parallel kinematic machines.

# Chapter 9

# Forward displacement analysis of analytic parallel mechanisms

In this chapter, we deal with the FDA of several APMs, most of which have been proposed in Chapter 7. The FDA of these APMs is more complex than the LTPMs discussed in Chapter 8. For a class of analytic 3-R$\underline{P}$R PPMs, the FDA of the PM is reduced to a univariate equation in $x$ of degree three, which is reported to be six in the literature, in conjunction with a univariate quadratic equation. For the analytic R$\underline{P}$R-PR-R$\underline{P}$R PPMs, an alternative approach to the FDA is proposed and the maximum number of real solutions for one type is revealed. For a class of 6-S$\underline{P}$S APM with an analytic LB component, the FDA is dealt with in detail. It is revealed that both of these classes of 6-S$\underline{P}$S PMs have at most eight sets of solutions to their FDA problem. The FDA is reduced to the solution of one univariate cubic equation and two univariate quadratic equations in sequence for the class IX 6-S$\underline{P}$S APM, and to the solution of three univariate quadratic equations in sequence for the class X 6-S$\underline{P}$S APM.

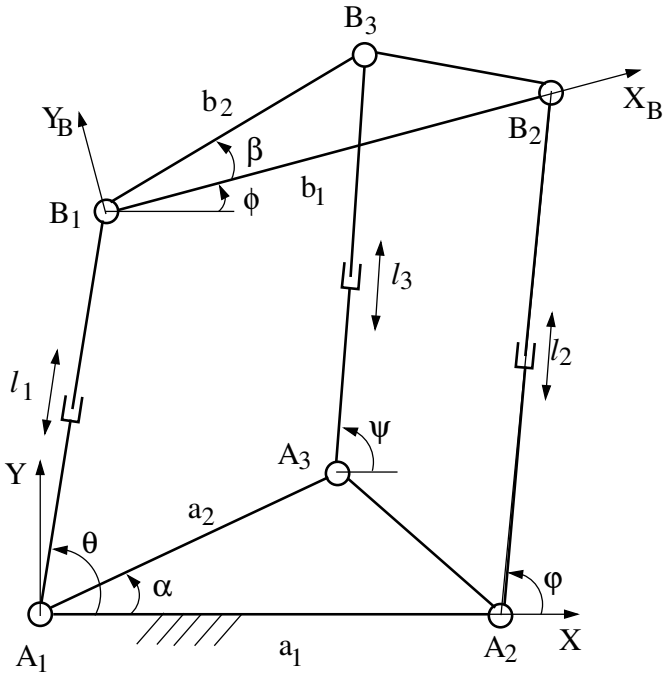


Figure 9.1: General 3-R<u>P</u>R PPM.

## 9.1 Analytic 3-R<u>P</u>R planar parallel mechanisms

A general 3-R<u>P</u>R PPM is shown in Fig. 9.1. It is composed of a moving platform and a base connected by three R<u>P</u>R sub-chains. In addition to the analytic 3-R<u>P</u>R PPMs composed of two Assur II components (Fig. 7.11), three types of analytic PPMs of high-class have been proposed: (a) PPMs with aligned platforms for which the R joints on the base and on the moving platform respectively are collinear [39], b) PPMs with similar platforms for which the base and moving platform triangles are similar [39], and (c) PPMs with similar aligned platforms [41].

In [39], the FDA of the PPM with aligned platforms has been reduced to the solution of polynomials of degree six in $x$, $y$ or $T = \tan(\phi/2)$, where $x$, $y$ and $\phi$ are the parameters denoting the pose (position and orientation) of the moving platform (for details, see Section 9.1.1). In the latter two cases, a cascaded form of the FDA allowing for closed-form solutions is obtained, while none of the coefficients of the polynomial of degree six in $x$ vanishes. The FDA of the PPM with similar platforms has been reduced to the solution of a cubic equation and a quadratic equation in sequence. As the cubic could be factored as a quadratic and a linear equation, and the solution to the linear equation has no physical meaning, the problem can be further reduced to the solution

of two quadratic equations in sequence. In [41], the FDA of the PPM with similar aligned platforms was reduced to the solution of two univariate quadratic equations in sequence.

In this section, we try to complete the FDA of third-class analytic PPMs. A third-class mechanism is a mechanism which contains one third-class Assur kinematic chain [151]. The classification of analytic PPMs is first established. The FDA of different types of third-class analytic PPMs is then performed[1].

### 9.1.1 Classification

A general 3-R$\underline{\text{P}}$R PPM is shown in Fig. 9.1. The dimensions of the base and the moving platform are denoted by $a_1 = A_1A_2$, $a_2 = A_1A_3$, $\alpha = \angle A_2A_1A_3$, $b_1 = B_1B_2$, $b_2 = B_1B_3$ and $\beta = \angle B_2B_1B_3$. The inputs of the manipulator are denoted by $l_1 = A_1B_1$, $l_2 = A_2B_2$, and $l_3 = A_3B_3$.

For the purpose of simplification and without loss of generality, two coordinate systems are established. The coordinate system $O - XY$ is attached to the base with $O$ being coincident with $A_1$ and the $X$-axis passing through $A_2$. The coordinate system $O_B - X_BY_B$ is attached to the moving platform with $O_B$ being coincident with $B_1$ and the $X_B$-axis passing through $B_2$.

The FDA of the PPM can be stated as follows: for a given set of inputs $l_1$, $l_2$ and $l_3$, find the pose (position and orientation) of the moving platform $(x, y, \phi)$. Here, $[x \;\; y]^T$ denotes the position vector of $O_B$ in the coordinate system $O - XY$, and $\phi$ denotes the orientation of the coordinate system of $O_B - X_BY_B$ with respect to the coordinate system $O - XY$. The FDA of third-class analytic PPMs follows the general procedure presented below.

The loop closure equations of loops $A_1B_1B_2A_2A_1$ and $A_1B_1B_3A_3A_1$ in complex form

[1]After the submission of this work to a journal, the publication of [152] was noticed, in which results similar to the ones presented here are obtained with a different approach based on a planar quaternion formulation

are

$$\begin{cases} l_1 e^{i\theta} + b_1 e^{i\phi} - a_1 = l_2 e^{i\varphi} \\ l_1 e^{i\theta} + b_2 e^{i(\phi+\beta)} - a_2 e^{i\alpha} = l_3 e^{i\psi} \end{cases}$$

Multiplying the two members of each of the above equations with their complex conjugates, respectively, we have

$$\begin{cases} l_1 b_1 \cos(\phi - \theta) - l_1 a_1 \cos\theta - a_1 b_1 \cos\phi = d_1 \\ l_1 b_2 \cos(\phi - \theta + \beta) - l_1 a_2 \cos(\theta - \alpha) - a_2 b_2 \cos(\phi + \beta - \alpha) = d_2 \end{cases} \tag{9.1}$$

where

$$d_i = \frac{1}{2}(l_{i+1}^2 - l_1^2 - a_i^2 - b_i^2) \qquad i = 1, 2$$

From the above definitions, it is clear that

$$\begin{cases} x = l_1 \cos\theta \\ y = l_1 \sin\theta \end{cases} \tag{9.2}$$

The FDA of a third-class analytic PPM can be obtained by solving Eqs. (9.1) and (9.2) in conjunction with the corresponding condition given below.

As the complexity of the FDA of different types of analytic PPMs varies to some extent, analytic PPMs can be classified into the following four types, namely:

1. The analytic PPM for which two of the joints on the base or the moving platform coincide (Fig. 7.11).

2. The analytic PPM with non-similar aligned platforms, i.e., PPMs which satisfy

$$\begin{cases} b_1/a_1 \neq b_2/a_2 \\ \alpha = \beta = 0 \end{cases} \tag{9.3}$$

3. The analytic PPM with similar triangular platforms, i.e., PPMs which satisfy

$$\begin{cases} b_1/a_1 = b_2/a_2 = k \neq 0 \\ \alpha = \beta \neq 0 \end{cases} \tag{9.4}$$

4. The analytic PPMs with similar aligned platforms, i.e., PPMs which satisfy

$$\begin{cases} b_1/a_1 = b_2/a_2 = k \neq 0 \\ \alpha = \beta = 0 \end{cases} \tag{9.5}$$

The first type of analytic PPM is of the second-class. As this type of manipulator can be decomposed into two second-class Assur groups, the FDA can be performed using the well-documented component method for position analysis of second-class planar multi-loop linkages (see Section 7.2.4 or [153] for example). The last three types of PPMs are of the third-class. The FDA of third-class analytic PPMs can make use of the methods presented in [39] or the alternative approaches presented in the following sections.

Unlike what was presented in [39], a PPM for which two of the joints on the base or the moving platform coincide is not regarded to be a PPM with aligned platforms in this section.

### 9.1.2 Planar parallel mechanism with non-similar aligned platforms

The FDA of the PPMs with non-similar aligned platforms can be performed as follows.

Substituting Eq. (9.3) into Eq. (9.1), we obtain

$$\begin{cases} l_1 b_1 \cos(\phi - \theta) - l_1 a_1 \cos\theta - a_1 b_1 \cos\phi = d_1 \\ l_1 b_2 \cos(\phi - \theta) - l_1 a_2 \cos\theta - a_2 b_2 \cos\phi = d_2 \end{cases} \tag{9.6}$$

Multiplying the first equation in Eq. (9.6) by $a_2 b_2$ and then subtracting from it the second equation in Eq. (9.6) multiplied by $a_1 b_1$, we obtain

$$l_1 b_1 b_2 (a_2 - a_1) \cos(\phi - \theta) - l_1 a_1 a_2 (b_2 - b_1) \cos\theta = a_2 b_2 d_1 - a_1 b_1 d_2 \tag{9.7}$$

Multiplying the second equation in Eq. (9.6) by $b_1$ and then subtracting from it the first equation in Eq. (9.6) multiplied by $b_2$, we get

$$-b_1 b_2 (a_2 - a_1) \cos\phi + l_1 (a_1 b_2 - a_2 b_1) \cos\theta = b_1 d_2 - b_2 d_1 \tag{9.8}$$

The substitution of Eq. (9.2) into Eqs. (9.7) and (9.8) then yields

$$z_2 x \cos\phi + z_2 y \sin\phi - z_1 x = z_5 \tag{9.9}$$

where

$$\begin{aligned} z_1 &= a_1 a_2 (b_2 - b_1) \\ z_2 &= b_1 b_2 (a_2 - a_1) \\ z_5 &= a_2 b_2 d_1 - a_1 b_1 d_2 \end{aligned}$$

and

$$z_2 \cos\phi = z_3 x - z_4 \tag{9.10}$$

where

$$z_3 = a_1 b_2 - a_2 b_1$$
$$z_4 = b_1 d_2 - b_2 d_1$$

From the substitution of Eq. (9.10) in Eq. (9.9), we get

$$z_2 y \sin\phi = z_5 + z_1 x - x(z_3 x - z_4) \tag{9.11}$$

It is known that

$$\sin^2\phi + \cos^2\phi = 1 \tag{9.12}$$

Moreover, from Eq.(9.2), we have

$$x^2 + y^2 = l_1^2 \tag{9.13}$$

Substituting Eqs. (9.10), (9.11) and (9.13) into Eq. (9.12) multiplied by $z_2^2 y^2$, we get

$$c_0 x^3 + c_1 x^2 + c_2 x + c_3 = 0 \tag{9.14}$$

where

$$c_0 = -2 z_1 z_3$$
$$c_1 = l_1^2 z_3^2 - z_4^2 + z_2^2 - 2 z_3 z_5 + (z_4 + z_1)^2$$
$$c_2 = 2[-l_1^2 z_3 z_4 + z_5 (z_4 + z_1)]$$
$$c_3 = l_1^2 z_4^2 + z_5^2 - l_1^2 z_2^2$$

For each value of $x$ obtained by solving Eq. (9.14), $y$ can be calculated as

$$y = \pm (l_1^2 - x^2)^{1/2} \tag{9.15}$$

For a given set of $x$ and $y$, $\phi$ can be derived from Eqs. (9.10) and (9.11) as

$$\begin{cases} \cos\phi = (z_3 x - z_4)/z_2 \\ \sin\phi = [(z_5 + z_1 x - x(z_3 x - z_4)]/(z_2 y) \end{cases} \quad \text{if } y \neq 0 \tag{9.16}$$

$$\begin{cases} \cos\phi = (z_3 x - z_4)/z_2 \\ \sin\phi = \pm(1 - \cos^2\phi)^{1/2} \end{cases} \quad \text{if } y = 0 \tag{9.17}$$

The FDA of the PPMs with non-similar aligned platforms is reduced to the solution of a cubic equation in $x$ (Eq. (9.14)) and a quadratic equation (Eq. (9.15)), instead of the polynomial equation of degree six in $x$ as derived in [39]. Moreover, the method proposed here is more concise than that presented in [39] since fewer special cases arise.

Similar to the process proposed in [39], it can be proved that there are at most two solutions to Eq. (9.14) in the interval $[-l_1, l_1]$. Thus there are at most four solutions to the FDA of the PPM with non-similar aligned platforms.

### 9.1.3 Planar parallel mechanism with similar triangular platforms

The FDA of the PPMs with similar triangular platforms can be performed as follows.

The substitution of Eq. (9.4) into Eq. (9.1) yields

$$\begin{cases} kl_1a_1\cos(\phi-\theta) - l_1a_1\cos\theta - ka_1^2\cos\phi = d_1 \\ kl_1a_2\cos(\phi-\theta+\alpha) - l_1a_2\cos(\theta-\alpha) - ka_2^2\cos\phi = d_2 \end{cases} \tag{9.18}$$

Substituting Eq. (9.2) into Eq. (9.18) and solving for $x$ and $y$, we then have

$$\begin{cases} x = w_x/w \\ y = w_y/w \end{cases} \tag{9.19}$$

where

$$\begin{aligned} w &= a_1a_2\sin\alpha(k^2+1-2k\cos\phi) \\ w_x &= \{a_2u_1[k\sin(\phi+\alpha)-\sin\alpha] - ka_1u_2\sin\phi\} \\ w_y &= -\{a_2u_1[k\cos(\phi+\alpha)-\cos\alpha] - a_1u_2(k\cos\phi-1)\} \\ u_i &= ka_i^2\cos\phi + d_i \end{aligned}$$

As singularities occur when $\sin\phi = 0$, we assume that $\sin\phi \neq 0$ and hence we have $w \neq 0$. The substitution of Eq. (9.19) into Eq. (9.13) yields

$$(a_2^2u_1^2 + a_1^2u_2^2 - 2a_1a_2u_1u_2\cos\alpha)/(a_1a_2w\sin\alpha) = l_1^2 \tag{9.20}$$

Equation (9.20) can then be turned into a quadratic equation in $\cos\phi$

$$e_0\cos^2\phi + e_1\cos\phi + e_2 = 0 \tag{9.21}$$

where

$$e_0 = k^2 a_1^2 a_2^2 (a_1^2 + a_2^2 - 2a_1 a_2 \cos\alpha)$$
$$e_1 = 2ka_1 a_2 [a_1 a_2 (d_1 + d_2 + l_1^2 \sin^2\alpha) - \cos\alpha (a_1^2 d_2 + a_2^2 d_1)]$$
$$e_2 = a_2^2 d_1^2 + a_1^2 d_2^2 - 2a_1 a_2 d_1 d_2 \cos\alpha - a_1^2 a_2^2 l_1^2 \sin^2\alpha (k^2 + 1)$$

Solution of Eq. (9.21) yields

$$\cos\phi = (-e_1 \pm w_1^{1/2})/(2e_0) \tag{9.22}$$

where

$$w_1 = e_1^2 - 4e_0 e_2 \tag{9.23}$$

For each solution of $\cos\phi$, $\sin\phi$ can be calculated as

$$\sin\phi = \pm(1 - \cos^2\phi)^{1/2} \tag{9.24}$$

For each value of $\phi$, $x$ and $y$ can be obtained using Eq. (9.19).

The FDA of PPMs with similar triangular platforms is reduced to the solution of two quadratic equations in sequence. It can be easily seen from Eqs. (9.21), (9.24) and (9.19) that the maximum number of solutions to the FDA of PPM with similar triangular platforms is four. The above result is consistent with the one obtained in [39] and the formulation presented here is elegant and more concise. In [39], the problem is reduced to the solution of a cubic (Eq. (73) in [39]) and a quadratic in sequence. As the cubic could be factored as a quadratic and a linear equation, and the solution to the linear equation has no physical meaning, the problem can be further reduced to the solution of two quadratic equations in sequence. The difference results from the fact that the cubic presented in [39] has an extraneous solution, i.e., the solution to the linear equation (Eq.(75) in [39]), which is generated by an improper formulation.

### 9.1.4 Planar parallel mechanism with similar aligned platforms

The FDA of the PPMs with similar aligned platforms can be performed as follows. Substituting Eq. (9.5) into Eq. (9.1), we have

$$\begin{cases} kl_1 a_1 \cos(\phi - \theta) - l_1 a_1 \cos\theta - ka_1^2 \cos\phi = d_1 \\ kl_1 a_2 \cos(\phi - \theta) - l_1 a_2 \cos\theta - ka_2^2 \cos\phi = d_2 \end{cases} \tag{9.25}$$

Multiplying the second equation in Eq. (9.25) by $a_1$ and then subtracting from it the first equation multiplied by $a_2$, we get

$$-kt_1 \cos\phi = t_2 \tag{9.26}$$

where

$$t_1 = a_1 a_2 (a_2 - a_1)$$
$$t_2 = a_1 d_2 - a_2 d_1$$

Solving Eq. (9.26), we obtain the value for $\cos\phi$

$$\cos\phi = -t_2/(kt_1) \tag{9.27}$$

Thus, two solutions for $\phi$ can be obtained using Eqs. (9.24) and (9.27).

Multiplying the first equation in Eq. (9.25) by $a_2^2$ and then subtracting from it the second equation in Eq. (9.25) multiplied by $a_1^2$, we have

$$kl_1 a_1 a_2 (a_2 - a_1)\cos(\phi - \theta) - l_1 a_1 a_2 (a_2 - a_1)\cos\theta = a_2^2 d_1 - a_1^2 d_2 \tag{9.28}$$

The substitution of Eq. (9.2) into Eq. (9.28) yields

$$kt_1 x \cos\phi + kt_1 \sin\phi - t_1 x = t_3 \tag{9.29}$$

where

$$t_3 = a_2^2 d_1 - a_1^2 d_2$$

For a given value of $\phi$ obtained, the corresponding values of $x$ and $y$ can be obtained as follows. As singularities occur when $\sin\phi = 0$, we assume that $\sin\phi \neq 0$.

Substituting Eq. (9.27) into Eq. (9.29), we have

$$kt_1 y \sin\phi = t_3 + (t_1 + t_2)x \tag{9.30}$$

The substitution of Eqs. (9.30), (9.24) and (9.27) into Eq. (9.13) multiplied by $k^2 t_1^2 \sin^2\phi$ gives a quadratic in $x$

$$f_0 x^2 + f_1 x + f_2 = 0 \tag{9.31}$$

where

$$f_0 = (k^2 + 1)t_1^2 + 2t_1 t_2$$
$$f_1 = 2t_3(t_1 + t_2)$$
$$f_2 = t_3^2 - l_1^2(k^2 t_1^2 - t_2^2)$$

Table 9.1: Solutions to Example 1

| No | x | y | $\phi(^\circ)$ |
|---|---|---|---|
| 1 | -1 | 0 | 41.41 |
| 2 | -1 | 0 | -41.41 |
| 3 | -0.25 | 0.9682 | -75.52 |
| 4 | -0.25 | -0.9682 | 75.52 |

The solution of Eq. (9.31) gives

$$x = [-f_1 \pm (w_2)^{1/2}]/(2f_0) \tag{9.32}$$

where

$$w_2 = f_1^2 - 4f_0f_2$$

Then, from Eq. (9.30), we get

$$y = [t_3 + (t_1 + t_2)x]/(kt_1 \sin\phi) \tag{9.33}$$

It can be easily seen from Eqs. (9.24), (9.27), (9.32) and (9.33) that the maximum number of solutions to the FDA of PPMs with similar aligned platforms is four. The approach of solution presented here is more robust than the one obtained in [41] and more concise than the one presented in [39]. No spurious roots need to be computed.

### 9.1.5 Examples

Numerical examples are now presented in order to illustrate the application of the method proposed in the previous section.

Example 1. The dimensions of the base and the moving platform of the PPM with non-similar aligned platforms are: $a_1 = 1$, $a_2 = 2$, $b_1 = 3$, $b_2 = 2$. The inputs of the manipulator are $l_1 = 1.5$, $l_2 = 2$, $l_3 = 2$. The four sets of solutions obtained are shown in Table 9.1.

Example 2. The dimensions of the base and the moving platform of the PPM with similar triangular platforms are: $a_1 = 40$, $a_2 = 20$, $\alpha = 30(^\circ)$, $k = 0.5$. The inputs of

Table 9.2: Solutions to Example 2

| No | x | y | $\phi(^\circ)$ |
|---|---|---|---|
| 1 | 1.0160 | 1.7227 | 87.9571 |
| 2 | -0.7943 | 1.8355 | -87.9571 |
| 3 | 1.9805 | -0.2787 | 93.8293 |
| 4 | 1.4501 | 1.3774 | -93.8293 |

Table 9.3: Solutions to Example 3

| No | x | y | $\phi(^\circ)$ |
|---|---|---|---|
| 1 | 30.6353 | 9.2457 | 30.82 |
| 2 | 13.4469 | -29.0376 | 30.82 |
| 3 | 13.4469 | 29.0376 | -30.82 |
| 4 | 30.6353 | -9.2457 | -30.82 |

the manipulator are $l_1 = 2$, $l_2 = 44$, $l_3 = 21$. The four sets of solutions we obtained are shown in Table 9.2.

Example 3. The dimensions of the base and the moving platform of the PPM with similar aligned platforms are: $a_1 = 40$, $a_2 = 20$, $k = 0.5$. The inputs of the manipulator are $l_1 = 32$, $l_2 = 21$, $l_3 = 24$. The four sets of solutions we obtained are shown in Table 9.3.

### 9.1.6 Summary

A classification of analytic 3-R$\underline{\text{P}}$R PPMs has been proposed. New approaches have been proposed to the FDA of the three types of third-class analytic PPMs. The FDA of the PPM with non-similar aligned platforms is reduced to the solution of a cubic equation in $x$ and a quadratic equation in sequence, instead of the polynomial equation of degree six in $x$ as derived in [39]. The FDA of PPMs with similar triangular platforms is reduced to the solution of two quadratic equations in sequence. The FDA of PPMs with similar aligned platforms is reduced here to the solutions of two quadratic equations in sequence, with no spurious root. The method proposed here is more concise than that presented in [39] as fewer special cases occur.

It should be pointed out that a PPM with congruent base and moving platform will be architecturally singular (undergo finite motion) when $\phi = 0$.

This section together with [39] completes the FDA of third-class analytic 3-R$\underline{P}$R PPMs. This analysis is useful in the context of the development of fast 3-R$\underline{P}$R PPMs.

## 9.2 Analytic R$\underline{P}$R-PR-R$\underline{P}$R planar parallel mechanisms

In section 7.4, the analytic R$\underline{P}$R-PR-R$\underline{P}$R PPMs of high class have been generated, an approach to the FDA of the analytic R$\underline{P}$R-PR-R$\underline{P}$R PPMs has also been implicitly proposed. In this section, an alternative method is first given for the FDA of analytic R$\underline{P}$R-PR-R$\underline{P}$R PPMs (Figs. 7.22 and 7.23) composed of Assur III kinematic chains. The difference between these two methods for the FDA lies in that unknowns are eliminated in different orders. The maximum number of real solutions to the FDA is then revealed based on this alternative method.

### 9.2.1 Planar parallel mechanism with one orthogonal platform and one aligned platform

Substituting Eq. (7.18) into Eq. (7.1), we obtain

$$\begin{cases} -2a_1b_1\cos\phi + 2Lb_1\sin\phi + L^2 + s_1 = 0 \\ 2a_2b_2\cos\phi - 2Lb_2\sin\phi + L^2 + s_2 = 0 \end{cases} \tag{9.34}$$

The elimination of $\phi$ then yields a cubic equation in $z = L^2$, i.e.,

$$u_3z^3 + u_2z^2 + u_1z + u_0 = 0 \tag{9.35}$$

where

$$\begin{aligned}
u_3 &= (b_1+b_2)^2 \\
u_2 &= 2b_1^2s_2 + 2b_1s_2b_2 + 2s_1b_2b_1 + 2s_1b_2^2 + b_1^2a_1^2 + 2b_1a_1b_2a_2 + b_2^2a_2^2 \\
u_1 &= b_1^2s_2^2 + 2b_1s_2s_1b_2 + s_1^2b_2^2 + 2b_1^2a_1^2s_2 + 2b_1a_1s_2b_2a_2 + 2s_1b_2a_2b_1a_1 + 2s_1b_2^2a_2^2 - 4b_1^2a_1^2b_2^2 \\
&\quad +8b_1^2a_1b_2^2a_2 - 4b_1^2b_2^2a_2^2 \\
u_0 &= (b_1a_1s_2 + s_1b_2a_2)^2
\end{aligned}$$

Once $z = L^2$ is obtained by solving the above equation, $L$ can be determined using

$$L = \pm z^{1/2} \tag{9.36}$$

For each value of $L$, $\phi$ can be determined using Eq. (9.37) if $L \neq 0$ or Eq. (9.38) if $L = 0$, i.e.,

$$\begin{cases} \cos\phi = [b_2(L^2+s_1) + b_1(L^2+s_2)]/[2b_1b_2(a_1-a_2)] \\ \sin\phi = [a_1b_1(L^2+s_2) - a_2b_2(L^2+s_1)]/[2Lb_1b_2(a_1-a_2)] \end{cases} \tag{9.37}$$

if $L \neq 0$, or

$$\begin{cases} \cos\phi = s_1/(2a_1b_1) = -s_2/(2a_2b_2) \\ \sin\phi = \pm(1-\cos^2\phi)^{1/2} \end{cases} \tag{9.38}$$

otherwise.

In order to obtain the maximum number of real solutions to the FDA of the analytic R$\underline{\text{P}}$R-PR-R$\underline{\text{P}}$R PPM with one orthogonal platform and one aligned platform, the maximum number of real roots of Eq. (9.35) will now be investigated. In fact, only non-negative roots of this polynomial are valid, since $z$ is defined as $L^2$. Hence, Sturm's theorem [147] will be used on the interval given by $z \in [0, \infty)$. Let

$$f(z) = u_3z^3 + u_2z^2 + u_1z + u_0$$

It is obvious that

$$\begin{aligned}
f(0) &\geq 0 \\
f(+\infty) &> 0
\end{aligned}$$

Following the procedure proposed on pages 1087-1088 in [39], it can be proved using Sturm's theorem that the maximum number of solutions of Eq. (9.35) on the interval of [0, $+\infty$) is 2. We can thus conclude that there are at most four real solutions to the FDA of the analytic R$\underline{\text{P}}$R-PR-R$\underline{\text{P}}$R PPM with one orthogonal platform and one aligned platform.

### 9.2.2 Planar parallel mechanism with two aligned platforms

Substitution of Eq. (7.19) into Eq.(7.1) leads to

$$\begin{cases} (2b_1L - 2a_1b_1)\cos\phi + L^2 - 2a_1L + s_1 = 0 \\ (-2b_2L + 2a_2b_2)\cos\phi + L^2 - 2a_2L + s_2 = 0 \end{cases} \tag{9.39}$$

Eliminating $\cos\phi$ from the above equation, we obtain a cubic equation in $L$

$$v_3L^3 + v_2L^2 + v_1L + v_0 = 0 \tag{9.40}$$

where

$$\begin{aligned} v_3 &= b_1 + b_2 \\ v_2 &= -b_1a_1 - 2b_1a_2 - 2a_1b_2 - b_2a_2 \\ v_1 &= 2b_1a_1a_2 + b_1s_2 + s_1b_2 + 2a_1b_2a_2 \\ v_0 &= -b_1a_1s_2 - s_1b_2a_2 \end{aligned}$$

For each value of $L$ obtained, $\cos\phi$ can be determined by solving the first or second equation in Eq. (9.39)

$$\cos\phi = \begin{cases} (L^2 - 2a_1L + s_1)/[2b_1(a_1 - L)] & \text{if } a_1 \neq L \\ (L^2 - 2a_2L + s_2)/[2b_2(L - a_2)] & \text{if } a_2 \neq L \end{cases} \tag{9.41}$$

and $\sin\phi$ can be calculated using Eq. (7.21). Thus, there are at most six solutions to the FDA of the analytic R$\underline{\text{P}}$R-PR-R$\underline{\text{P}}$R PPM with two aligned platforms.

For both the analytic R$\underline{\text{P}}$R-PR-R$\underline{\text{P}}$R PPM with one orthogonal platform and one aligned platform (see Eqs. (9.36), (9.37) and (9.38)) and the analytic R$\underline{\text{P}}$R-PR-R$\underline{\text{P}}$R PPM with two aligned platforms (see Eqs. (9.41) and (7.21)), the assembly modes corresponding to a given set of inputs appear in pairs. The two assembly modes in each pair are symmetric about the $X$-axis. It is noted that in addition to the four sets of real solutions to the FDA of the analytic R$\underline{\text{P}}$R-PR-R$\underline{\text{P}}$R PPM with one orthogonal platform and one aligned platform, there are always two sets of complex solutions.

### 9.2.3 Examples

Numerical examples are given here to verify the above results on the FDA of the analytic R$\underline{\text{P}}$R-PR-R$\underline{\text{P}}$R PPMs composed of Assur III groups.

Example 1. The dimensions of the base and the moving platform of the analytic R$\underline{P}$R-PR-R$\underline{P}$R PPM with one orthogonal platform and one aligned platform are (see Fig. 7.22): $a_1 = 15$, $a_2 = -15$, $\alpha = \pi/2$, $b_1 = 10$, $b_2 = 12$, $\beta = \pi$. The inputs of the manipulator are $l_1 = 30$, $l_2 = 35$. The four sets of real solutions obtained are shown in Table 9.4.

Table 9.4: Solutions to Example 1.

| No | $L$ | $\phi$ |
|---|---|---|
| 1 | 19.6601 | 2.8808 |
| 2 | -19.6601 | 3.4024 |
| 3 | 31.9425 | .2438 |
| 4 | -31.9425 | 6.0394 |

Example 2. The dimensions of the base and the moving platform of the analytic R$\underline{P}$R-PR-R$\underline{P}$R PPM with two aligned platforms are (see Fig. 7.23): $a_1 = 15$, $a_2 = -15$, $\alpha = 0$, $b_1 = 20$, $b_2 = 20$, $\beta = \pi$. The inputs of the manipulator are $l_1 = 20$, $l_2 = 25$. The six sets of real solutions obtained are shown in Table 9.5.

Table 9.5: Solutions to Example 2.

| No | $L$ | $\phi$ |
|---|---|---|
| 1 | -5.49041 | 1.3308 |
| 2 | -5.4904 | 4.9524 |
| 3 | -15.0000 | 0.9734 |
| 4 | -15.0000 | 5.3098 |
| 5 | 20.4904 | 0.4794 |
| 6 | 20.4904 | 5.8038 |

## 9.3 Analytic 6-S$\underline{P}$S parallel mechanisms

Two new classes, X and XI, of 6-S$\underline{P}$S APMs have been generated in Section 7.2.4.2 using the decomposition approach. A method for the FDA has also been implicitly proposed in the process of generation. The FDA of the new 6-S$\underline{P}$S APMs is performed in detail in this section. The FDA is reduced to the solution of one univariate cubic

equation and two univariate quadratic equations in sequence for the class X 6-SPS APM and to the solution of three univariate quadratic equations in sequence for the class XI 6-SPS APM. It is shown that both classes X and XI of 6-SPS PMs have at most eight sets of solutions to the FDA problem.

### 9.3.1 General steps for the forward displacement analysis

For the purpose of simplification and without loss of generality, two coordinate systems are established (Fig. 9.2). The coordinate system $O - XYZ$ is attached to the base with $O$ being coincident with $A_1$, the $Z$-axis coinciding with $A_1A_2$ and the $X$-axis intersecting $A_4A_5$. The coordinate system $O_B - X_BY_BZ_B$ is attached to the moving platform with $O_B$ being coincident with $B_1(B_2)$ and the $X_B$-axis passing through $B_3$ and $B_4(B_5)$. $Y_B$ is chosen to keep $B_6$ located on the coordinate plane $O_B - X_BY_B$. The geometric parameters for the platforms of the 6-SPS PM are [2] $z_{A2}$, $x_{A3}$, $z_{A3}$, $x_{A4}$, $z_{A4}$, $z_{A5}$, $x_{A6}$, $y_{A6}$, $z_{A6}$, $x_{B3}^{(B)}$, $x_{B4}^{(B)}$, $x_{B6}^{(B)}$ and $y_{B6}^{(B)}$. $y_{A3} = 0$ as the base of the Lb component is planar and located on the O-XZ plane. Here, $\mathbf{a}_i = [x_{Ai} \;\; y_{Ai} \;\; z_{Ai}]^T$ and $\mathbf{b}_i = [x_{Bi} \;\; y_{Bi} \;\; z_{Bi}]^T$ denote the position vector of $A_i$ and $B_i$ in the coordinate system $O - XYZ$, while $\mathbf{b}_i^{(B)} = [x_{Bi}^{(B)} \;\; y_{Bi}^{(B)} \;\; z_{Bi}^{(B)}]^T$ denotes the position vector of $B_i$ in the coordinate system $O - X_BY_BZ_B$.

The FDA of the 6-SPS PM can be stated as follows: for a given set of inputs $L_i = \parallel A_iB_i \parallel (i = 1, 2, \cdots, 6)$, find the pose (position and orientation) of the moving platform. Here, the position vector of $O_B$, $\mathbf{o}_B = [x \;\; y \;\; z]^T$, in the coordinate system $O - XYZ$ is used to denote the position of the moving platform, the direction cosine matrix

$$[\mathbf{R}] = \begin{bmatrix} i_x & j_x & k_x \\ i_y & j_y & k_y \\ i_z & j_z & k_z \end{bmatrix} \tag{9.42}$$

of the coordinate system of $O_B - X_BY_BZ_B$ with respect to the coordinate system $O - XYZ$ is used to denote the orientation of the moving platform.

The set of equations for the FDA of the 6-SPS PM is

$$(\mathbf{o}_B + [\mathbf{R}]\mathbf{b}_i^{(B)} - \mathbf{a}_i)^T(\mathbf{o}_B + [\mathbf{R}]\mathbf{b}_i^{(B)} - \mathbf{a}_i) = L_i^2 \quad i = 1, \; 2, \; \cdots, \; 6 \tag{9.43}$$

[2] $y_{A3} = 0$ as the base of the Lb component is planar and located on the O-XZ plane

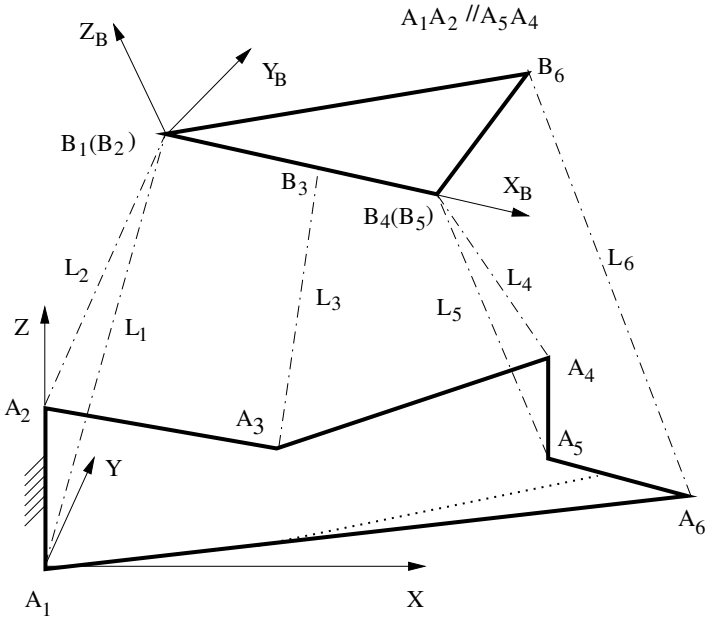


Figure 9.2: Classes X and XI of 6-S$\underline{P}$S APMs.

The FDA of the two new classes of 6-S$\underline{P}$S APMs follows the same general steps presented below.

Step 1 Perform the configuration analysis of the LB component to obtain $x$, $y$, $z$, $i_x$ $i_y$ and $i_z$.

The configuration analysis of the LB component consists in solving the first five equations in Eq. (9.43) which is actually Eq. (9.44). It can be performed following the procedure presented in section 9.3.2.

Step 2 Calculate the remaining orientation parameters $j_x$, $j_y$, $j_z$, $k_x$, $k_y$ and $k_z$.

### 9.3.2 Step 1: Configuration analysis of the $Lb_{PL//PL}$ component

For clarity, the $\mathrm{Lb}_{PL//PL}$ component is shown separately in Fig. 9.3. Its configuration analysis can be stated as follows: for a given set of inputs $L_i = \| A_iB_i \|$ $(i = 1, 2, \cdots, 5)$, find the pose (position and orientation) of the moving line. Here, the position of the moving line is denoted by the position vector of $O_B$, $\mathbf{o}_B = [x \quad y \quad z]^T$, in the

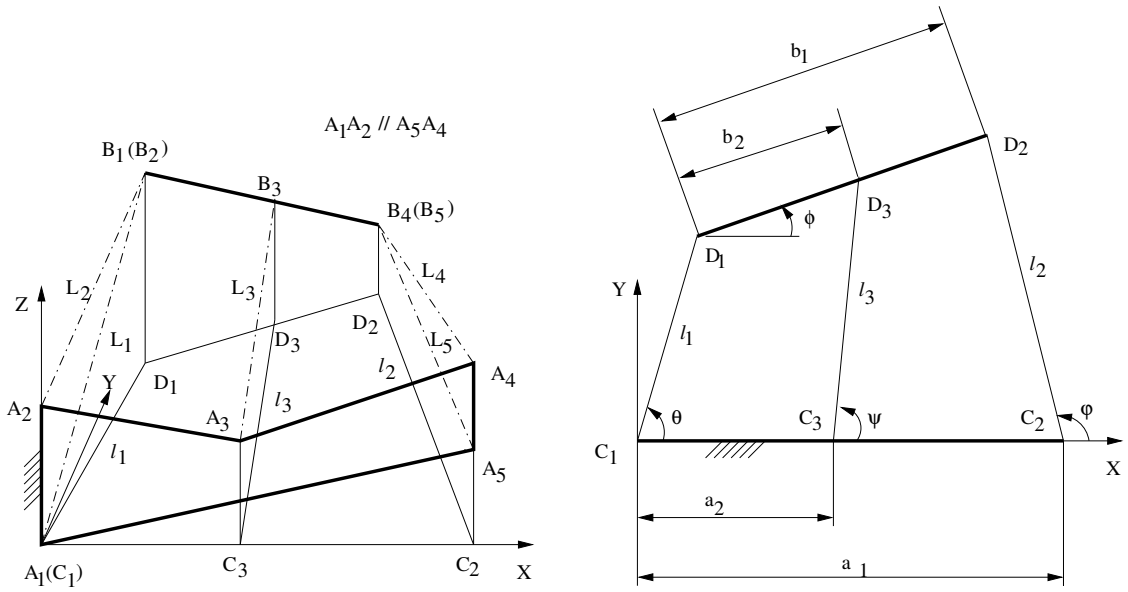


(a) Reduction of the $\mathrm{Lb}_{PL//PL}$ component to its equivalent 3-RR planar parallel structure with aligned platforms.

(b) Equivalent 3-RR planar parallel structure with aligned platforms.

Figure 9.3: Configuration analysis of the $\mathrm{Lb}_{PL//PL}$ component

coordinate system $O-XYZ$, and the orientation of the moving line by the unit vector, $\mathbf{x}_i = [i_x \;\; i_y \;\; i_z]^T$ along the moving line with respect to the coordinate system $O-XYZ$.

The configuration analysis can be performed by solving the following equations.

$$(\mathbf{o}_B + x_{Bi}^{(B)}\mathbf{x}_i - \mathbf{a}_i)^T(\mathbf{o}_B + x_{Bi}^{(B)}\mathbf{x}_i - \mathbf{a}_i) = L_i^2 \quad i = 1,\ 2,\ \cdots,\ 5 \tag{9.44}$$

Equation (9.44) is actually the set of the first five equations in Eq. (9.43).

As pointed out in Section 7.2.4.2, the LB component is consisted of three components. The first is the $B_1$-$A_1A_2$ PL component, the second is the $B_4$-$A_4A_5$ PL component and the last is an equivalent 3-RR planar parallel structure with aligned platforms. The equivalent 3-RR planar parallel structure ($C_1C_2C_3 - D_1D_2D_3$) is obtained by projecting the $Lb_{PL//PL}$ component onto the O-XY coordinate plane (Fig. 9.3(a)). Here, $C_1$, $C_2$, $C_3$, $D_1$, $D_2$ and $D_3$ are respectively the projections of $A_1(A_2)$, $A_4(A_5)$, $A_3$, $B_1(B_2)$, $B_4(B_5)$ and $B_3$ on the O-XY plane. $C_1C_2C_3$ and $D_1D_2D_3$ are called the base and moving platform respectively while $C_iD_i$ is called a leg of the equivalent 3-RR planar parallel structure.

The configuration analysis of the $Lb_{PL//PL}$ component can be performed following the steps below.

**Step 1a** Perform the configuration analysis of the first PL component to calculate $z$ and $i_z$.

**Step 1b** Perform the configuration analysis of the second PL component to compute the geometric parameters for the equivalent 3-RR planar parallel structure.

**Step 1c** Perform the configuration analysis of the equivalent 3-RR planar parallel structure to calculate $x$, $y$, $i_x$ and $i_y$.

#### 9.3.2.1 Step 1a: Configuration analysis of the first PL component

By performing the configuration analysis of the first PL component, $z$ and $i_z$ can be obtained.

The solution of the first two equations, corresponding to LB component $A_1B_1A_2$, in Eq. (9.44) yields

$$z = (L_1^2 - L_2^2 + z_{A2}^2)/(2z_{A2}) \tag{9.45}$$

The solution of the fourth and fifth equations in Eq. (9.44), corresponding to PL component $B_4$-$A_4A_5$, gives the coordinate of $B_4$ along the Z-axis

$$z_{B4} = (L_4^2 - L_5^2 + z_{A5}^2 - z_{A4}^2)/[2(z_{A5} - z_{A4})] \tag{9.46}$$

$i_z$ can then be obtained as

$$i_z = (z_{B4} - z)/x_{B4}^{(B)} \tag{9.47}$$

#### 9.3.2.2 Step 1b: Configuration analysis of the second PL component

By performing the configuration analysis of the second PL component, the geometric parameters for the equivalent 3-RR planar parallel structure can be obtained.

The dimensions of the base and the moving platform of the equivalent 3-RR planar parallel structure are denoted by $a_1 = C_1C_2$, $a_2 = C_1C_3$, $b_1 = D_1D_2$ and $b_2 = D_1D_3$.

The leg lengths of the 3-RR planar parallel structure are denoted by $l_1 = C_1D_1$, $l_2 = C_2D_2$ and $l_3 = C_3D_3$.

Solving Eq. (9.45) and the first equation in Eq. (9.44), we have

$$l_1 = (L_1^2 - z^2)^{1/2} \tag{9.48}$$

Solving Eq. (9.46) and the fourth equation in Eq. (9.44), we have

$$l_3 = [L_4^2 - (z_{B4} - z_{A4})^2]^{1/2} \tag{9.49}$$

It is obvious that

$$a_1 = x_{A4} \tag{9.50}$$

$$a_2 = x_{A3} \tag{9.51}$$

$$b_1 = [x_{B4}^{(B)2} - (z_{B4} - z)^2]^{1/2} \tag{9.52}$$

$$b_2 = b_1 x_{B3}^{(B)} / x_{B4}^{(B)} \tag{9.53}$$

The coordinate of $B_3$ along the z-axis is

$$z_{B3} = z + x_{B3}^{(B)}(z_{B4} - z)/x_{B4}^{(B)} \tag{9.54}$$

Thus, $l_2$ can be calculated as

$$l_2 = [L_3^2 - (z_{B3} - z_{A3})^2]^{1/2} \tag{9.55}$$

It can be seen that once the inputs $L_i$ of the $Lb_{PL//PL}$ component are given, the geometric parameters, $a_i$, $b_i$ and $l_i$, for the equivalent 3-RR planar parallel structure can be uniquely determined.

#### 9.3.2.3 Step 1c: Configuration analysis of the equivalent 3-RR planar parallel structure

By performing the configuration analysis of the equivalent 3-RR planar parallel structure, $x$, $y$, $i_x$ and $i_y$ can be determined.

For clarity, the equivalent 3-RR planar parallel structure $C_1C_2C_3-D_1D_2D_3$ is shown separately in Fig. 9.3(b). Two coordinate systems are established in order to perform the configuration analysis of the 3-RR planar parallel structure. The coordinate system $O-XY$ is attached to the base with $O$ being coincident with $C_1$ and the $X$-axis passing through $C_2$ and $C_3$. The coordinate system $O_D - X_DY_D$ is attached to the moving platform with $O_D$ being coincident with $D_1$ and the $X_D$-axis passing through $D_2$ and $D_3$.

The configuration analysis of the 3-RR planar parallel structure can be stated as follows: for a given set of leg lengths $l_i =\| C_iD_i \|$ (i=1, 2, 3), find the pose of the moving platform. Here, the position vector of $O_D$ ,$[x \quad y]^T$, in the coordinate system $O - XY$ is used to denote the position of the moving platform, and the unit vector $[i_x \quad i_y]^T$ along the $X_i$ axis with respect to the coordinate system $O - XY$ is used to denote the orientation of the moving platform.

The configuration analysis of 3-RR planar parallel structures has been dealt with in Sections 9.1.2 and 9.1.4, where $\phi$ is used to denote the angle between the axes $X$ and $X_D$. It is clear that

$$\begin{cases} i_x = \cos\phi \\ i_y = \sin\phi \end{cases} \tag{9.56}$$

In the following, we re-list the formulae to perform the configuration analysis of the 3-RR planar parallel structures to facilitate the reading of this section.

**Case 1**

The 3-RR planar parallel structure with non-similar aligned platforms, i.e., a 3-RR planar parallel structure satisfies

$$b_1/a_1 \neq b_2/a_2 \tag{9.57}$$

Solving $x$ first using

$$c_0x^3 + c_1x^2 + c_2x + c_3 = 0 \tag{9.58}$$

where

$$c_0 = -2z_1z_3$$

$$c_1 = l_1^2 z_3^2 - z_4^2 + z_2^2 - 2z_3 z_5 + (z_4 + z_1)^2$$

$$c_2 = 2[-l_1^2 z_3 z_4 + z_5(z_4 + z_1)]$$

$$c_3 = l_1^2 z_4^2 + z_5^2 - l_1^2 z_2^2$$

$$z_1 = a_1 a_2 (b_2 - b_1)$$

$$z_2 = b_1 b_2 (a_2 - a_1)$$

$$z_3 = a_1 b_2 - a_2 b_1$$

$$z_4 = b_1 d_2 - b_2 d_1$$

$$z_5 = a_2 b_2 d_1 - a_1 b_1 d_2$$

$$d_i = \frac{1}{2}(l_{i+1}^2 - l_1^2 - a_i^2 - b_i^2) \quad i = 1, 2$$

Then, calculate $y$ for each value of $x$ obtained using

$$y = \pm(l_1^2 - x^2)^{1/2} \tag{9.59}$$

Finally, calculate $i_x$ and $i_y$ using

$$\begin{cases} i_x = \cos\phi = (z_3 x - z_4)/z_2 \\ i_y = \sin\phi = [(z_5 + z_1 x - x(z_3 x - z_4)]/(z_2 y) \end{cases} \quad \text{if } y \neq 0 \tag{9.60}$$

$$\begin{cases} i_x = \cos\phi = (z_3 x - z_4)/z_2 \\ i_y = \sin\phi = \pm(1 - i_x^2)^{1/2} \end{cases} \quad \text{if } y = 0 \tag{9.61}$$

The configuration analysis of the 3-RR planar parallel structure with non-similar aligned platforms is thus reduced to the solution of one univariate cubic equation and one univariate quadratic equation in sequence.

Similar to the process proposed in [39], it can be proved that there are at most two solutions to Eq. (9.58) in the interval $[-l_1, l_1]$. Thus, there are at most four solutions

to the configuration analysis of the 3-RR planar parallel structure with non-similar aligned platforms.

**Case 2**

The 3-RR planar parallel structure with similar aligned platforms, i.e., a 3-RR planar parallel structure which satisfies

$$b_1/a_1 = b_2/a_2 = k \neq 0 \tag{9.62}$$

The configuration analysis of the 3-RR planar parallel structure with similar aligned platforms can be performed as follows. Firstly, calculate $i_x$ using

$$i_x = \cos\phi = -t_2/(kt_1) \tag{9.63}$$

where

$$t_1 = a_1 a_2 (a_2 - a_1)$$

$$t_2 = a_1 d_2 - a_2 d_1$$

$$d_i = \frac{1}{2}(l_{i+1}^2 - l_1^2 - a_i^2 - b_i^2) \quad i = 1, 2$$

Secondly, calculate $i_y$ using

$$i_y = \sin\phi = \pm(1 - i_x^2)^{1/2} \tag{9.64}$$

Thirdly, obtain $x$ by using

$$x = [-f_1 \pm (f_1^2 - 4f_0 f_2)^{1/2}]/(2f_0) \tag{9.65}$$

which are obtained by solving

$$f_0 x^2 + f_1 x + f_2 = 0 \tag{9.66}$$

where

$$f_0 = (k^2 + 1)t_1^2 + 2t_1 t_2$$

$$f_1 = 2t_3(t_1 + t_2)$$

$$f_2 = t_3^2 - l_1^2(k^2 t_1^2 - t_2^2)$$

$$t_3 = a_2^2 d_1 - a_1^2 d_2$$

Finally, calculate $y$ using (As singularities occur when $i_y = 0$, we assume that $i_y \neq 0$.)

$$y = [t_3 + (t_1 + t_2)x]/(kt_1 i_y) \tag{9.67}$$

It can be easily seen from Eqs. (9.64), (9.63), (9.65) and (9.67) that the configuration analysis of the 3-RR planar parallel structure with similar aligned platforms is reduced to the solution of two univariate quadratic equations in sequence. The maximum number of solutions to the configuration analysis of the 3-RR planar parallel structure with similar aligned platforms is four.

### 9.3.3 Step 2: Calculation of the remaining orientation parameters

The remaining unknowns are $j_x$, $j_y$, $j_z$, $k_x$, $k_y$, $k_z$. These orientation parameters $j_x$, $j_y$, $j_z$, $k_x$, $k_y$, $k_z$ can be obtained following the procedure below.

It is evident that

$$i_x j_x + i_y j_y + i_z j_z = 0 \tag{9.68}$$

$$j_x^2 + j_y^2 + j_z^2 = 1 \tag{9.69}$$

The 6th equation of Eq. (9.43) is

$$\begin{aligned}(x_{B6}^{(B)} i_x + y_{B6}^{(B)} j_x + x - x_{A6})^2 + (x_{B6}^{(B)} i_y + y_{B6}^{(B)} j_y + y - y_{A6})^2 \\ +(x_{B6}^{(B)} i_z + y_{B6}^{(B)} j_z + z - z_{A6})^2 = L_6^2\end{aligned} \tag{9.70}$$

Manipulation of Eqs. (9.68)-(9.70) gives

$$\begin{cases} j_z = [-F_6 \pm (F_6^2 - E_6 Q_6)^{1/2}]/E_6 \\ j_x = G_5 j_z + H_5 \\ j_y = G_6 j_z + H_6 \end{cases} \tag{9.71}$$

where

$$E_6 = G_5^2 + G_6^2 + 1$$

$$F_6 = G_5 H_5 + G_6 H_6$$

$$Q_6 = H_5^2 + H_6^2 - 1$$

$$G_5 = (B_6 i_z - C_6 i_y)/w_6$$

$$H_5 = -D_6 i_y / w_6$$

$$G_6 = (C_6 i_x - A_6 i_z)/w_6$$

$$H_6 = D_6 i_x / w_6$$

$$w_6 = A_6 i_y - B_6 i_x$$

$$A_6 = 2y_{B6}^{(B)}(x - x_{A6})$$

$$B_6 = 2y_{B6}^{(B)}(y - y_{A6})$$

$$C_6 = 2y_{B6}^{(B)}(z - z_{A6})$$

$$\begin{aligned} D_6 = x_{B6}^{(B)2} + y_{B6}^{(B)2} + (x - x_{A6})^2 + (y - y_{A6})^2 + (z - z_{A6})^2 - L_6^2 \\ + 2x_{B6}^{(B)}[i_x(x - x_{A6}) + i_y(y - y_{A6}) + i_z(z - z_{A6})] \end{aligned}$$

For any set of $i_x$, $i_y$, $i_z$, $j_x$, $j_y$ and $j_z$, $k_x$, $k_y$, $k_z$ can be obtained as

$$\begin{cases} k_x = i_y j_z - j_y i_z \\ k_y = i_z j_x - j_z i_x \\ k_z = i_x j_y - j_x i_y \end{cases} \tag{9.72}$$

The analysis presented above shows that the FDA was reduced to the solution of one univariate cubic equation and two univariate quadratic equations in sequence for the class IX and to the solution of three univariate quadratic equations in sequence for the class X. Both of these two classes of 6-S$\underline{\text{P}}$S PMs have at most eight sets of solutions to their FDA problem.

### 9.3.4 Examples

Numerical examples are now presented in order to illustrate the application of the method proposed in the previous sections.

**Example 1**. The dimensions of the base and the moving platform of the class X 6-S$\underline{P}$S APM are (see Fig. 2): $z_{A2} = 5$, $x_{A3} = 7$, $z_{A3} = 4$, $x_{A4} = 10$, $z_{A4} = 1$, $z_{A5} = 7$, $x_{A6} = 6$, $y_{A6} = 8$, $z_{A6} = 2$, $x_{B3}^{(B)} = 3$, $x_{B4}^{(B)} = 6$, $x_{B6}^{(B)} = 3$, $y_{B6}^{(B)} = 3$. The inputs of the manipulator are $L_1 = 12.2$, $L_2 = 9.7$, $L_3 = 10.4$, $L_4 = 13.2$, $L_5 = 11.3$, $L_6 = 6.8$. Of the eight sets of solutions we obtained, four sets are real (Table 1).

Table 9.6: Real solutions for Example 1

| No | $i_x$ | $i_y$ | $i_z$ | $j_x$ | $j_y$ | $j_z$ | $k_x$ | $k_y$ | $k_z$ | $x$ | $y$ | $z$ |
|---|---|---|---|---|---|---|---|---|---|---|---|---|
| 1 | -0.1530 | -0.9882 | -0.0160 | 0.9777 | - 0.1490 | -0.1477 | 0.1436 | -0.0382 | 0.9890 | 0.1472 | 9.2313 | 7.9750 |
| 2 | -0.1530 | - 0.9882 | -0.0160 | 0.1489 | -0.0071 | - 0.9888 | 0.9771 | -0.1537 | 0.1483 | 0.1472 | 9.2313 | 7.9750 |
| 3 | 0.8393 | 0.5437 | -0.0160 | 0.5432 | -0.8362 | 0.0752 | 0.0275 | - 0.0718 | -0.9972 | 4.6118 | 7.9982 | 7.9750 |
| 4 | 0.8393 | 0.5437 | -0.0160 | -0.5377 | 0.8247 | -0.1754 | -0.0822 | 0.1558 | 0.9845 | 4.6118 | 7.9982 | 7.9750 |

**Example 2**. The dimensions of the base and the moving platform of class XI 6-S$\underline{P}$S APM are (see Fig. 2): $z_{A2} = 5$, $x_{A3} = 5$, $z_{A3} = 4$, $x_{A4} = 10$, $z_{A4} = 1$, $z_{A5} = 7$, $x_{A6} = 6$, $y_{A6} = 8$, $z_{A6} = 2$, $x_{B3}^{(B)} = 3$, $x_{B4}^{(B)} = 6$, $x_{B6}^{(B)} = 3$, $y_{B6}^{(B)} = 3$. The inputs of the manipulator are $l_1 = 1.5$, $l_2 = 2$, $l_3 = 2$, $l_4 = 1.5$, $l_5 = 2$, $l_6 = 2$. Of the eight sets of solutions we obtained, two sets are real (Table 2).

Table 9.7: Real solutions for Example 2

| No | $i_x$ | $i_y$ | $i_z$ | $j_x$ | $j_y$ | $j_z$ | $k_x$ | $k_y$ | $k_z$ | $x$ | $y$ | $z$ |
|---|---|---|---|---|---|---|---|---|---|---|---|---|
| 1 | 0.6887 | 0.7251 | -0.0160 | -0.7243 | 0.6887 | 0.0324 | 0.03450 | -0.0107 | 0.9995 | 6.1196 | 6.9131 | 7.9750 |
| 2 | 0.6887 | 0.7251 | -0.0160 | 0.7006 | -0.6708 | -0.2434 | -0.1872 | 0.1564 | -0.9699 | 6.1196 | 6.9131 | 7.9750 |

### 9.3.5 Summary

It has been shown that both the classes X and XI of 6-S$\underline{P}$S APMs have at most eight sets of solutions to their FDA problem. The FDA has been reduced to the solution of one univariate cubic equation and two univariate quadratic equations in sequence for the class X 6-S$\underline{P}$S APM and to the solution of three univariate quadratic equations in sequence for the class XI 6-S$\underline{P}$S APM.

It should be pointed out that the 6-SPS APM of class X will undergo finite motion once it reaches a configuration in which its equivalent 3-RR planar parallel structure has a finite degree of freedom. Also, it should be mentioned that the generation of all possible 6-SPS APMs is still an open problem.

## 9.4 Conclusion

The FDA of analytic 3-RPR and RPR-PR-RPR PPMs as well as the 6-SPS APM has been performed. It has been verified that these PMs are APMs. The maximum number of real solutions has been found for some cases which is smaller than the maximum number of solutions in the complex domain. Care should be taken to avoid extraneous roots when the elimination approach is used.

The work presented in this section is useful in the context of the development of fast 3-RPR and RPR-PR-RPR PPMs as well as 6-SPS PMs.

# Chapter 10

# Forward kinematic singularity analysis of parallel mechanisms

In this chapter, the singularity analysis of several typical PMs is dealt with. First, we discuss the singularity analysis of the analytic 3-R$\underline{P}$R PPM with similar platforms. It is shown that the singularity surfaces divide its workspace into four singularity-free regions. It is also proved that there exists a one-to-one correspondence between the analytic expressions for the four solutions to the FDA and the four singularity-free regions. This further simplifies the FDA of the PPM since we can obtain directly the only solution to its FDA once the singularity-free region in which the PM works is specified. Finally, the singularity analysis of a class of PMs with a 3-XS structure is performed based on the instability analysis of structures. Here, X denotes a generalized joint with one degree of freedom. The geometric characteristic is revealed using a method based on linear algebra.

## 10.1 Analytic 3-R$\underline{P}$R parallel mechanisms

The singularity analysis of the 3-R$\underline{P}$R manipulator with similar platforms is first performed. It is shown that the singularity surfaces divide its workspace into four singularity-free regions. It is also proved that the four solutions in analytic expression form to the forward displacement analysis correspond to different singularity-free regions for the 3-R$\underline{P}$R manipulator with similar platforms. This simplifies further the FDA in this case as the unique solution to the FDA can be found without the need to compute all the four solutions as long as the singularity-free region in which the manipulator works is given.

### 10.1.1 Introduction

Extensive work has been done in the singularity analysis of the 3-R$\underline{P}$R manipulator [79, 154, 155, 156]. Three types of singularities may exist for PMs [79]. For the analytic 3-R$\underline{P}$R planar PPM, architecture singularities are well known and can be easily avoided, and inverse kinematic singularities are known to happen at the boundary of the Cartesian workspace. The forward kinematic singularities (also type II or uncertainty singularities) are more elusive to geometric analysis and have been investigated in detail in [154, 155, 156]. The 3-R$\underline{P}$R PMs are classified into three classes according to the types of singularity loci in Cartesian workspace [154, 155]. The first is the 3-R$\underline{P}$R manipulators, such as the general case, for which the singular loci for a given orientation of the moving platform can be either a hyperbola, an ellipse, or a parabola. The second is the 3-R$\underline{P}$R manipulators, such as the 3-R$\underline{P}$R manipulator with aligned platforms, for which the singularity loci for a given orientation of the moving platform always form a hyperbola. The third is the 3-R$\underline{P}$R manipulators, such as the 3-R$\underline{P}$R manipulator with symmetrical aligned platforms, for which the singularity loci for a given orientation of the moving platform form a straight line. In [156], the singularity analysis of the 3-R$\underline{P}$R manipulator is performed using the Clifford algebra of the projective plane. In [41], it is shown using numerical examples that for a 3-R$\underline{P}$R manipulator with similar aligned platforms, the four solutions to its FDA fall into different singularity-free regions respectively. The uniqueness domains of the general 3-R$\underline{P}$R PPM is introduced and studied in [157]. It is also revealed that singularity-free trajectory-planning is time-consuming for the general case.

This section aims at revealing the relationship between the solutions in analytic form and the different singularity-free regions for 3-R$\underline{\text{P}}$R manipulator with similar platforms in order to simplify the control of the PM.

### 10.1.2 Geometric description

An analytic 3-R$\underline{\text{P}}$R PPM with similar platforms is shown in Fig. 10.1. It is constructed by connecting a base platform and a moving platform, which is similar to the base platform, with three R$\underline{\text{P}}$R sub-chains. The dimensions of the base platform and the moving platform are denoted by $a_1 = A_1A_2$, $a_2 = A_1A_3$, $\alpha = \angle A_2A_1A_3 = \angle B_2B_1B_3$, $b_1 = B_1B_2$, $b_2 = B_1B_3$. The inputs of the manipulator are denoted by $l_1 = A_1B_1$, $l_2 = A_2B_2$, and $l_3 = A_3B_3$. For the analytic 3-R$\underline{\text{P}}$R PPM with similar platforms, one has

$$b_i = ka_i \qquad i = 1, 2, 3 \tag{10.1}$$

with $k \neq 0$. In addition to Eq. (10.1), one also has for analytic 3-R$\underline{\text{P}}$R PPM with similar aligned platforms

$$\alpha = 0 \tag{10.2}$$

For the purpose of simplification and without loss of generality, two coordinate systems are established. The coordinate system $O{-}XY$ is attached to the base platform with $O$ being coincident with $A_1$ and the $X$-axis passing through $A_2$. The coordinate system $O_B - X_BY_B$ is attached to the moving platform with $O_B$ being coincident with $B_1$ and the $X_B$-axis passing through $B_2$.

### 10.1.3 Singularity analysis

Let $(x, y, \phi)$ denote the pose of the moving platform. Here, $[x \;\; y]^T$ denotes the position vector of $O_B$ in the coordinate system $O - XY$, and $\phi$ denotes the orientation of the coordinate system of $O_B - X_BY_B$ with respect to the coordinate system $O - XY$.

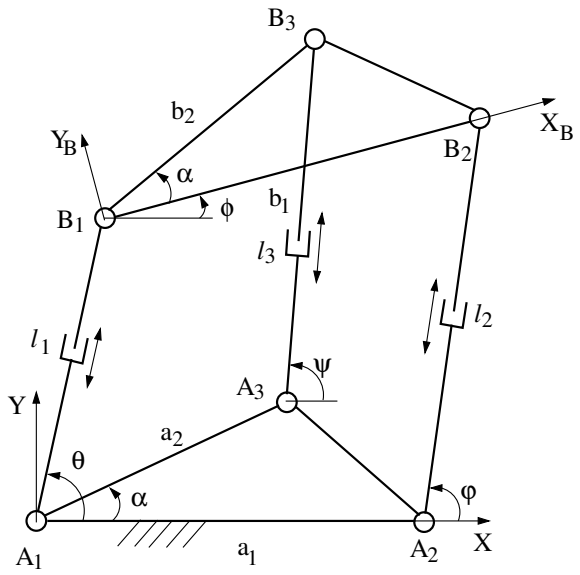


Figure 10.1: Analytic 3-RPR PPM with similar platforms.

The inverse displacement analysis equation of the analytic 3-RPR PPM with similar platforms is

$$\begin{cases} x^2 + y^2 = l_1^2 \\ (x + b_1 \cos\phi - a_1)^2 + (y + b_1 \sin\phi)^2 = l_2^2 \\ p^2 + q^2 = l_3^2 \end{cases} \tag{10.3}$$

where

$$p = x + b_2 \cos(\phi + \alpha) - a_2 \cos\alpha$$

and

$$q = y + b_2 \sin(\phi + \alpha) - a_2 \sin\alpha$$

Differentiating Eq. (10.3) with respect to time yields

$$\mathbf{J}_2 \begin{Bmatrix} \dot{\phi} \\ \dot{x} \\ \dot{y} \end{Bmatrix} = \mathbf{J}_1 \begin{Bmatrix} \dot{l}_1 \\ \dot{l}_2 \\ \dot{l}_3 \end{Bmatrix} \tag{10.4}$$

where

$$\mathbf{J}_2 = \begin{bmatrix} 0 & x & y \\ J_{223} & x + b_1 \cos\phi - a_1 & y + b_1 \sin\phi \\ J_{233} & p & q \end{bmatrix} \tag{10.5}$$

with

$$J_{223} = -b_1(x - a_1)\sin\phi + b_1 y\cos\phi$$

$$\begin{aligned} J_{233} = &-b_2(x - a_2\cos\alpha)\sin(\phi + \alpha) \\ &+b_2(y - a_2\sin\alpha)\cos(\phi + \alpha) \end{aligned}$$

and

$$\mathbf{J}_1 = \begin{bmatrix} l_1 & 0 & 0 \\ 0 & l_2 & 0 \\ 0 & 0 & l_3 \end{bmatrix} \tag{10.6}$$

The forward kinematic singularities occur [79, 154, 155] when

$$|\mathbf{J}_2| = 0 \tag{10.7}$$

#### 10.1.3.1 Planar parallel mechanism with similar triangular platforms

The substitution of Eqs. (10.1) and (10.5) into Eq. (10.7) yields

$$ka_1a_2[-(x^2 + y^2)\sin\alpha + c_1 y + c_2 x]\sin\phi = 0$$

Since $ka_1a_2 \neq 0$, the above equation can be reduced to

$$[-(x^2 + y^2)\sin\alpha + c_1 y + c_2 x]\sin\phi = 0 \tag{10.8}$$

where

$$c_1 = a_2 - a_1\cos\alpha - ka_2\cos\phi + ka_1\cos(\alpha + \phi) \tag{10.9}$$

$$c_2 = a_1\sin\alpha + ka_2\sin\phi - ka_1\sin(\alpha + \phi) \tag{10.10}$$

Equation (10.8) can be decomposed into the following two equations

$$\sin\phi = 0 \tag{10.11}$$

and

$$(x^2 + y^2)\sin\alpha - c_1 y - c_2 x = 0 \tag{10.12}$$

Equation (10.12) can be rearranged as

$$(x - x_0)^2 + (y - y_0)^2 = r_0^2 \tag{10.13}$$

where

$$\begin{cases} x_0 = c_2/(2\sin\alpha) \\ y_0 = c_1/(2\sin\alpha) \\ r_0 = (c_1^2 + c_2^2)^{1/2}/(2\sin\alpha) \end{cases} \tag{10.14}$$

which represents a circle of radius $r_0$ with its center at $(x_0, y_0)$.

The remarkable fact that can be verified is

$$(x_0 - x_{00})^2 + (y_0 - y_{00})^2 = r_{00}^2 \tag{10.15}$$

where

$$\begin{cases} x_{00} = (a_2 - a_1\cos\alpha)/(2\sin\alpha) \\ y_{00} = a_1/2 \\ r_{00} = k(a_1^2 + a_2^2 - 2a_1a_2\cos\alpha)^{1/2}/(2\sin\alpha) \end{cases} \tag{10.16}$$

which means that the projections of the centers of the singular circles on the O-XY plane form a circle of radius $r_{00}$ with its center at $(x_{00}, y_{00})$.

It is clear that for the 3-R$\underline{\text{P}}$R manipulator with similar triangular platforms, the forward kinematic singularity loci in the X-Y coordinate plane for a specified orientation $\phi$ of the moving platform is a circle (Eq. (10.13)) if $\sin\phi \neq 0$ or a whole plane if $\sin\phi = 0$ (Eq. (10.11)).

Apparently, the forward kinematic singularity loci are much simpler and easier to detect for the 3-R$\underline{\text{P}}$R manipulator with similar triangular platforms when compared with the general 3-R$\underline{\text{P}}$R manipulator [155].

If the restrictions on the range of the inputs of the manipulator are neglected, the workspace of the manipulator is divided into four singularity-free regions by its singularity surface (Fig. 10.2. For clarity, the three singularity planes, $\phi = -\pi$ $\phi = 0$, and $\phi = \pi$, corresponding with Eq. (10.11) are omitted). The four singularity-free regions are shown in Fig. 10.2 and discussed below.

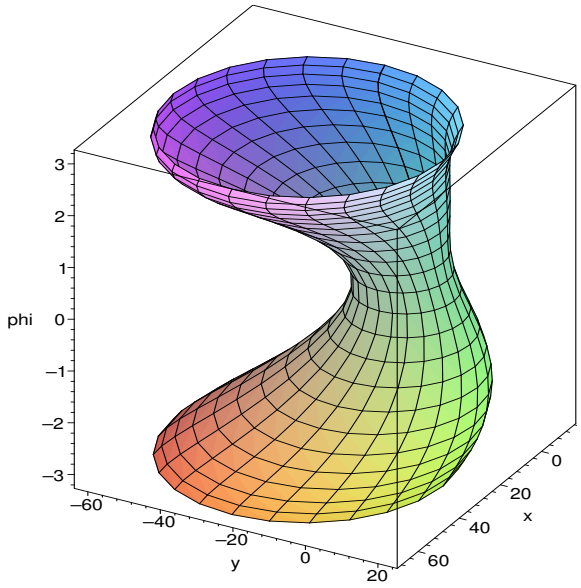


Figure 10.2: Singular surface of analytic 3-RPR PPM with similar triangular platforms (planes at $\phi = -\pi,\ \ 0,\ \ \pi$ are omitted).

(1) Singularity-free region I. The conditions for the singularity-free region I are

$$\begin{cases} 0 < \phi < \pi \\ (x - x_0)^2 + (y - y_0)^2 - r_0^2 < 0 \end{cases} \tag{10.17}$$

(2) Singularity-free region II. The conditions for the singularity-free region II are

$$\begin{cases} 0 < \phi < \pi \\ (x - x_0)^2 + (y - y_0)^2 - r_0^2 > 0 \end{cases} \tag{10.18}$$

(3) Singularity-free region III. The conditions for the singularity-free region III are

$$\begin{cases} -\pi < \phi < 0 \\ (x - x_0)^2 + (y - y_0)^2 - r_0^2 < 0 \end{cases} \tag{10.19}$$

(4) Singularity-free region IV. The conditions for the singularity-free region IV are

$$\begin{cases} -\pi < \phi < 0 \\ (x - x_0)^2 + (y - y_0)^2 - r_0^2 > 0 \end{cases} \tag{10.20}$$

#### 10.1.3.2 Planar parallel mechanism with similar aligned platforms

The substitution of Eqs.(10.1), (10.2) and (10.5) into Eq. (10.7) yields

$$ka_1a_2(a_2 - a_1)[kx\sin\phi - (k\cos\phi - 1)y]\sin\phi = 0$$

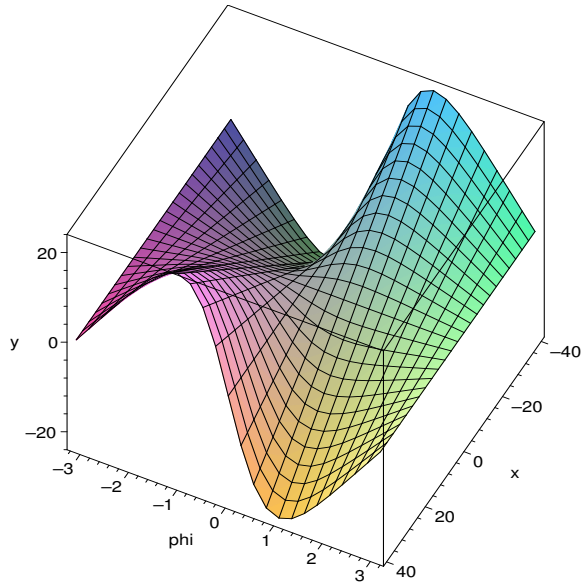


Figure 10.3: Singular surface of analytic 3-R$\underline{P}$R PPM with similar aligned platforms (planes at $\phi = -\pi,\ \ 0,\ \ \pi$ are omitted).

i.e.,

$$[kx\sin\phi - (k\cos\phi - 1)y]\sin\phi = 0 \tag{10.21}$$

Equation (10.21) can be decomposed into the following two equations

$$\sin\phi = 0 \tag{10.22}$$

and

$$kx\sin\phi - (k\cos\phi - 1)y = 0 \tag{10.23}$$

It is clear that for the 3-R$\underline{P}$R manipulator with similar aligned platforms, the forward kinematic singularity loci in the X-Y coordinate plane for a specified orientation $\phi$ of the moving platform form a straight line (Eq. (10.23)) if $\sin\phi \neq 0$, or a whole plane if $\sin\phi = 0$ (Eq. (10.22)).

Apparently, the forward kinematic singularity loci are much simpler and easier to detect for the 3-R$\underline{P}$R manipulator with similar aligned platforms when compared with those of the general 3-R$\underline{P}$R manipulator [155].

If the restrictions on the range of the inputs of the manipulator are neglected, the workspace of the manipulator is divided into four singularity-free regions by its

singularity loci (Fig. 10.3. For clarity, the three singularity planes, $\phi = -\pi$, $\phi = 0$ and $\phi = \pi$, corresponding with Eq. (10.22) are omitted). The four singularity-free regions are

(1) Singularity-free region I. The conditions for the singularity-free region I are

$$\begin{cases} 0 < \phi < \pi \\ kx \sin\phi - (k\cos\phi - 1)y > 0 \end{cases} \tag{10.24}$$

(2) Singularity-free region II. The conditions for the singularity-free region II are

$$\begin{cases} 0 < \phi < \pi \\ kx \sin\phi - (k\cos\phi - 1)y < 0 \end{cases} \tag{10.25}$$

(3) Singularity-free region III. The conditions for the singularity-free region III are

$$\begin{cases} -\pi < \phi < 0 \\ kx \sin\phi - (k\cos\phi - 1)y > 0 \end{cases} \tag{10.26}$$

(4) Singularity-free region IV. The conditions for the singularity-free region IV are

$$\begin{cases} -\pi < \phi < 0 \\ kx \sin\phi - (k\cos\phi - 1)y < 0 \end{cases} \tag{10.27}$$

### 10.1.4 Distribution of the solutions to the forward displacement analysis into singularity-free regions

In Section 10.1.3, it has been shown that the workspace of the 3-R$\underline{\text{P}}$R manipulator with similar platforms is divided into four singular-free regions. Moreover, it has been shown in Section 9.1 that the maximum number of assembly modes of the 3-R$\underline{\text{P}}$R manipulator with similar platforms is four. That is to say that the number of singularity-free regions is equal to the number of assembly modes for the 3-R$\underline{\text{P}}$R manipulator with similar platforms. This section will reveal the relationship between the solutions to the FDA and the four singularity-free regions.

Table 10.1: Distribution of the solutions to FDA into singularity-free regions of analytic 3-R$\underline{P}$R PPMs with similar triangular platforms.

| Singularity-free region | Solution to FDA |
|---|---|
| I | $\cos\phi = C\phi^+$, $\sin\phi = S\phi$ |
| II | $\cos\phi = C\phi^-$, $\sin\phi = S\phi$ |
| III | $\cos\phi = C\phi^+$, $\sin\phi = -S\phi$ |
| IV | $\cos\phi = C\phi^-$, $\sin\phi = -S\phi$ |

where $C\phi^+ = [-e_1 + (w_1)^{1/2}]/(2e_0)$, $C\phi^- = [-e_1 - (w_1)^{1/2}]/(2e_0)$
$x = w_x/w$, $y = w_y/w$

#### 10.1.4.1 Planar parallel mechanism with similar triangular platforms

Using Eqs. (9.13) and (9.19), we have

$$[(x^2 + y^2)\sin\alpha - c_1 y - c_2 x] = \sin\alpha(e_0\cos\phi + 0.5e_1)/k \tag{10.28}$$

Substituting Eq. (9.22) into Eq. (10.28), we have

$$[(x^2 + y^2)\sin\alpha - c_1 y - c_2 x] = \pm w_1^{1/2}\sin\alpha/k \tag{10.29}$$

Equation (10.29) shows that singularities occur when $w_1 = 0$. In addition, we can conclude that there exists a one-to-one correspondence — shown in Table 10.1 — between the four solutions to the FDA and the four singularity-free regions of the 3-R$\underline{P}$R manipulator with similar triangular platforms in non-singular configurations.

#### 10.1.4.2 Planar parallel mechanism with similar aligned platforms

Using Eqs. (9.30), (9.26) and (9.24), we have

$$\begin{aligned} & kx\sin\phi - (k\cos\phi - 1)y \\ &= [(kx\sin\phi - (k\cos\phi - 1)y)(kt_1^2\sin\phi)]/(kt_1^2\sin\phi) \\ &= (f_0 x + 0.5f_1)/(kt_1^2\sin\phi) \end{aligned} \tag{10.30}$$

Substituting Eqs. (9.32) and (9.24) into Eq. (10.30), we have

$$\begin{aligned} & kx\sin\phi - (k\cos\phi - 1)y \\ &= \pm w_2^{1/2}/(kt_1^2\sin\phi) \end{aligned} \tag{10.31}$$

Table 10.2: Distribution of the solutions to FDA into singularity-free regions of analytic 3-R$\underline{P}$R PPMs with similar aligned platforms.

| Singularity-free region | Solution to FDA |
|---|---|
| I | $\cos\phi = C\phi$, $\sin\phi = S\phi$, $x = x^+$, $y = y^+$ |
| II | $\cos\phi = C\phi$, $\sin\phi = S\phi$, $x = x^-$, $y = y^-$ |
| III | $\cos\phi = C\phi$, $\sin\phi = -S\phi$, $x = x^-$, $y = -y^-$ |
| IV | $\cos\phi = C\phi$, $\sin\phi = -S\phi$, $x = x^+$, $y = -y^+$ |

where $C\phi = -t_2/(kt_1)$, $S\phi = (1 - C^2\phi)^{1/2}$
$x^+ = [-f_1 + w_2^{1/2}]/(2f_0)$, $x^- = [-f_1 - w_2^{1/2}]/(2f_0)$
$y^+ = [t_3 - (t_1 + t_2)x^+]/(kt_1 S\phi)$, $y^- = [t_3 - (t_1 + t_2)x^-]/(kt_1 S\phi)$

Equation (10.31) shows that singularities occur when $w_2 = 0$. In addition, we can conclude that there exists a one-to-one correspondence — shown in Table 10.2 — between the four solutions to the FDA and the four singularity-free regions of the 3-R$\underline{P}$R manipulator with similar aligned platforms in non-singular configurations.

We can conclude from the above result that each singularity-free region of the 3-R$\underline{P}$R manipulator with similar platforms corresponds to one assembly mode of the manipulator. Thus, the singularity-free regions of the 3-R$\underline{P}$R manipulator with similar platforms can be easily determined using Eqs. (10.17), (10.18), (10.19), and (10.20) for the 3-R$\underline{P}$R manipulator with similar triangular platforms or Eqs. (10.24), (10.25), (10.26), and (10.27) for the 3-R$\underline{P}$R manipulator with similar aligned platforms.

When changing from one assembly mode to another, the 3-R$\underline{P}$R manipulator with similar platforms must run into singularities. This is different from the case of the general 3-R$\underline{P}$R manipulator [160], which can change from one assembly mode to another without running into singularities.

Once the singularity-free region in which the 3-R$\underline{P}$R manipulator with similar platforms works is chosen, the unique solution to the FDA can be computed directly according to Table 10.1 or 10.2. There is no need to calculate all the four solutions to the FDA first and then chose the correct solution from the four solutions. This further simplifies the FDA of the 3-R$\underline{P}$R manipulator with similar aligned platforms.

Table 10.3: Solutions to the FDA and singularity-free regions of Example 1.

| No | x | y | $\phi(^\circ)$ | singularity-free region |
|---|---|---|---|---|
| 1 | 1.0160 | 1.7227 | 87.9571 | II |
| 2 | -0.7943 | 1.8355 | -87.9571 | IV |
| 3 | 1.9805 | -0.2787 | 93.8293 | I |
| 4 | 1.4501 | 1.3774 | -93.8293 | III |

### 10.1.5 Numerical examples

Two numerical examples are given to verify the results obtained in the previous sections. It is shown that different solutions to the forward displacement analysis of 3-R$\underline{\text{P}}$R manipulators with similar platforms indeed correspond to different singularity-free regions of the manipulator.

Example 1. The dimensions of the base platform and the moving platform of the 3-R$\underline{\text{P}}$R manipulator with similar triangular platforms are (see Fig. 1): $a_1 = 40$, $a_2 = 20$, $\alpha = 30^\circ$), $k = 0.5$. The inputs of the manipulator are $l_1 = 2$, $l_2 = 44$, $l_3 = 21$. The four sets of solutions to the FDA we obtained and their corresponding singularity-free regions are shown in Table 10.3 and Fig. 10.4. It is clear that different solutions fall into different singularity-free regions for the 3-R$\underline{\text{P}}$R manipulator with similar triangular platforms.

Example 2. The dimensions of the base platform and the moving platform of the analytic PPMs with similar aligned platforms are (see Fig. 1): $a_1 = 40$, $a_2 = 20$, $k = 0.5$, $\alpha = 0$. The inputs of the manipulator are $l_1 = 32$, $l_2 = 21$, $l_3 = 24$. The four sets of solutions to the FDA we obtained and their corresponding singularity-free regions are shown in Table 10.4 and Fig. 10.5. It is clear that different solutions fall into different singularity-free regions for the 3-R$\underline{\text{P}}$R manipulator with similar aligned platforms.

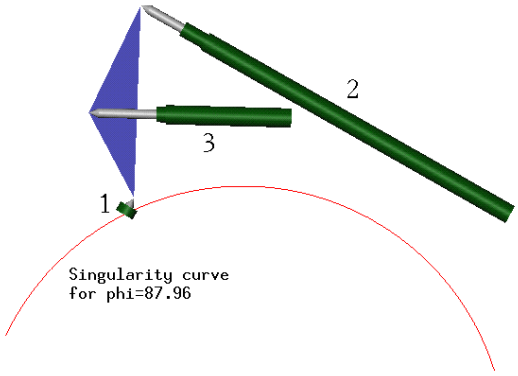


(a) Solution 1 in singularity-free region II.

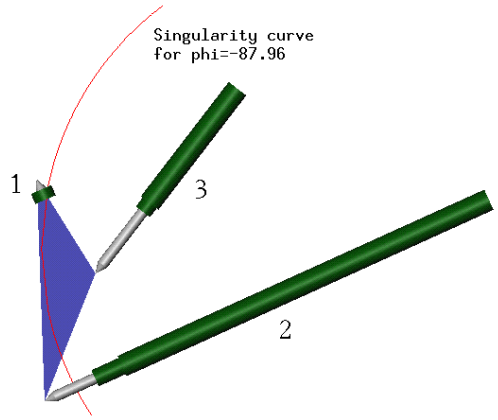


(b) Solution 2 in singularity-free region IV.

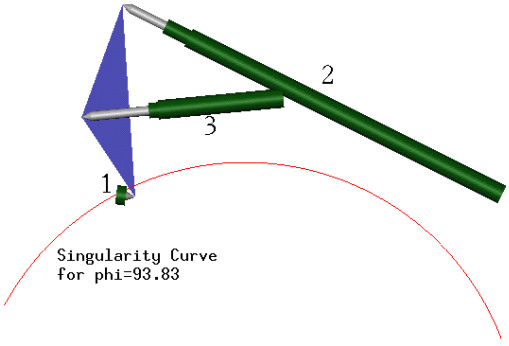


(c) Solution 3 in singularity-free region I.

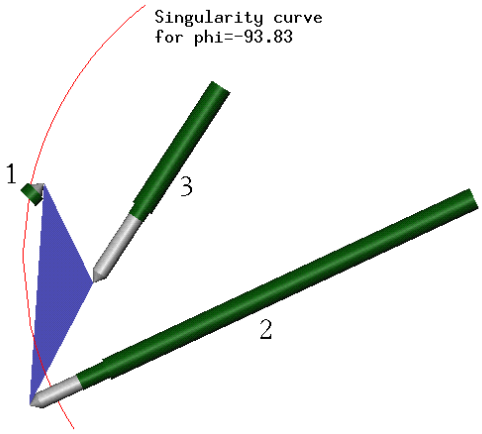


(d) Solution 4 in singularity-free region III.

Figure 10.4: Distribution of solutions to the FDA into the singularity-free regions (Example 1).

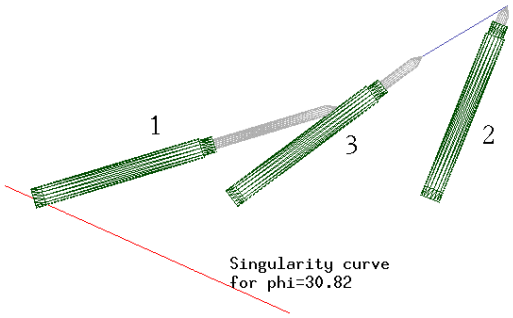


(a) Solution 1 in singularity-free region I.

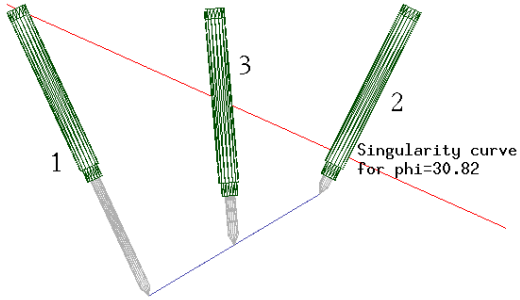


(b) Solution 2 in singularity-free region II.

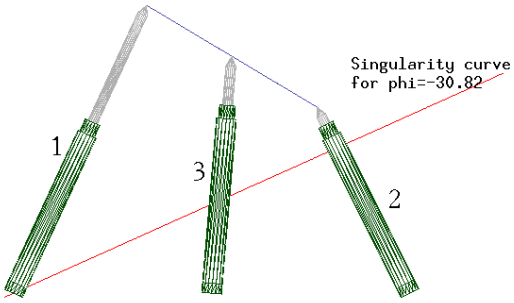


(c) Solution 3 in singularity-free region III.

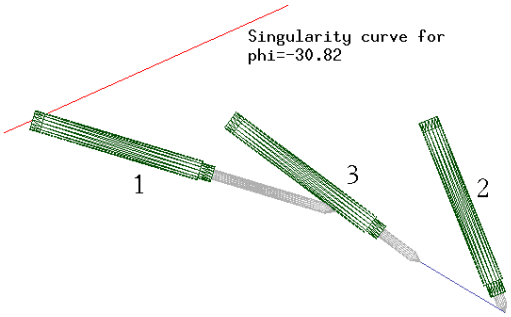


(d) Solution 4 in singularity-free region IV.

Figure 10.5: Distribution of solutions to the FDA into the singularity-free regions (Example 2).

Table 10.4: Solutions to the FDA and singularity-free regions of Example 2.

| No | x | y | $\phi(^\circ)$ | singularity-free region |
|---|---|---|---|---|
| 1 | 30.63525 | 9.2457 | 30.82 | I |
| 2 | 13.4469 | -29.0376 | 30.82 | II |
| 3 | 13.4469 | 29.0376 | -30.82 | III |
| 4 | 30.63525 | -9.2457 | -30.82 | IV |

## 10.2 An approach to the forward kinematic singularity analysis based on the instability analysis of structures

In this section, we propose a method for the forward kinematic singularity analysis of parallel mechanisms based on the instability analysis of structures. We focus on the forward kinematic singularity analysis of a class of PMs with a 3-XS structure. Here, X denotes a generalized joint with one degree of freedom. The geometric characteristic is also revealed using a method based on linear algebra.

### 10.2.1 Introduction

The forward kinematic singularity analysis of PMs is a difficult problem and has received much attention from many researchers over the past two decades. Different approaches have been proposed for the forward kinematic singularity analysis of PMs, for example, the method based on line geometry or screw theory [84, 85, 86, 87, 88, 89, 90, 81, 83, 91, 92, 71], the algebraic method based on the Jacobian matrix [79, 80, 93], the method based on a differentiation of the closure equations [94, 95] and the component approach [96, 97]. Some results have also been obtained on the generation of architecturally singular Gough-Stewart PMs [97, 98, 99, 100, 101].

This section presents a unified and simplified approach to the forward kinematic singularity analysis of PMs with a 3-XS structure. A 3-XS structure is composed of two platforms connected by three XS legs in-parallel. Here, X denotes a generalized joint with one degree of freedom. An X joint can take the form of any kinematic joint

with one degree of freedom such as an R joint or a P joint or the form of any closed kinematic chain with one degree of freedom such as a parallelogram. This class of PMs covers many PMs which have been proposed in the literature. For example, the true Stewart platform, the 6-3 Gough-Stewart PMs, the 6-DOF PM with three pantographs [86], the 3-RRRS PMs [69, 95] and the following PMs listed in [32]: the 3-PRS PM by Merlet, the 3-PRS PM by Carretaro, the 3-RPS PM by Lee, the 3-RSR PM by Lambert and Hui, The Carpal wrist by Canfield, the CaPaman PM by Ceccarelli, the 6-RUS PM by Hunt, the 3-RRPS PM by Alizade, the 3-PRPS PM by Behi, the 3-PRPS PM by Kohli, the 3-PPSR PM by Ben-Horin, the 3-PPSP PM by Byun and the 6-DOF PM with three parallelograms by Ebert-Uphoff as well as the Turin PM by Romiti and Sorli.

### 10.2.2 Proposed approach

A PM is usually turned into a structure when its actuated joints are locked. As a PM is consisted of one or more components [96, 59], the structure is consisted of one or more substructures each of which is obtained by locking the actuated joints within a component of the PM.

For example, the 6-3 Gough-Stewart PM (Fig. 10.6) is consisted of three PL components[1] ($A_1A_2$-$B_1$, $A_3A_4$-$B_2$ and $A_5A_6$-$B_3$) and one 3-RS component [59]. When all the actuated joints are locked, the PM is reduced to a $PL^3$ 6-US structure. The $PL^3$ 6-US structure is consisted of three PL substructures and one 3-RS substructure (Fig. 10.7). For simplicity reasons, a 6-3 Gough-Stewart PM and a $PL^3$ 6-US structure are represented by the same figure. A dotted line is used to represent a UPS leg in representing the 6-3 Gough-Stewart PM or a US leg in representing the $PL^3$ 6-US structure. A joint in the 3-XS structure is represented by a small circle.

Considering that the forward kinematic singularity of the PM occurs if one or more of its components is in a forward kinematic singularity [96, 97], the forward kinematic singularity analysis of PMs is thus reduced to finding the instability conditions for their substructures. The latter can usually be obtained by differentiating the constraint

[1] In [59], the 6-3 Gough-Stewart PM is referred to as the $PL^3$ 6-UPS PM based on the classification of Gough-Stewart PMs according to their components. A PL component is composed of a point and a straight line segment connected by two UPS legs in-parallel.

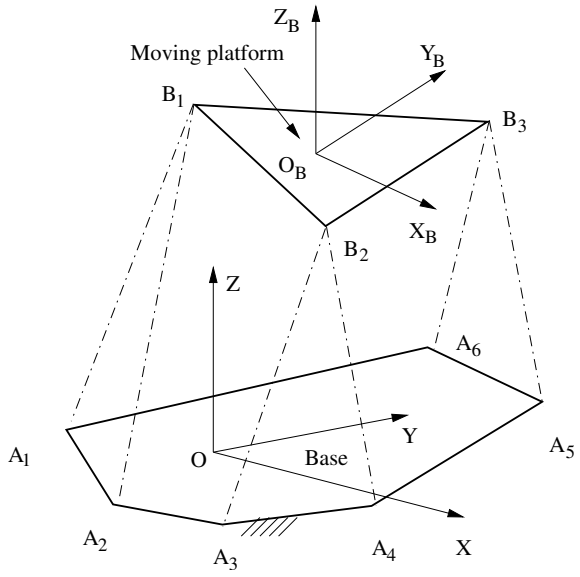


Figure 10.6: 6-3 Gough-Stewart PM or $PL^3$ 6-US structure.

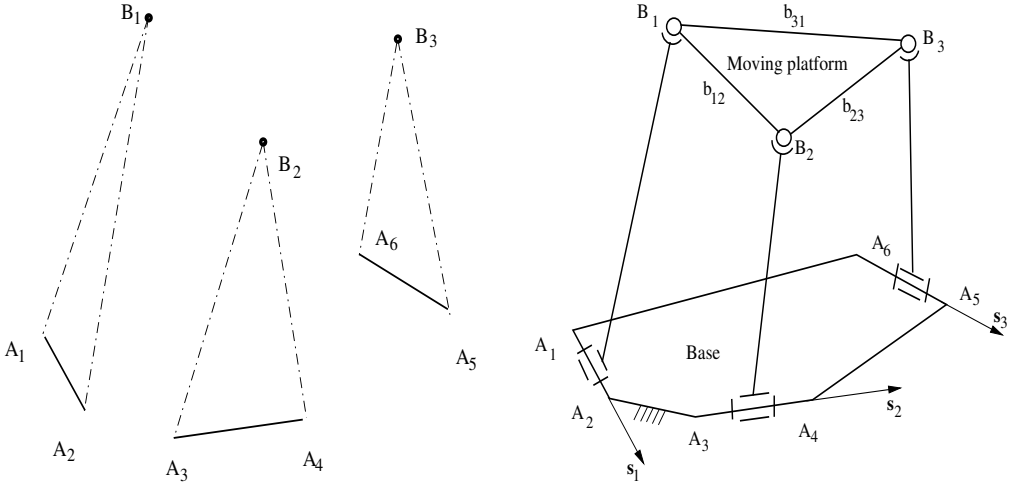


(a) PL components or substructures.

(b) 3-RS structure.

Figure 10.7: Composition of the 6-3 Gough-Stewart PM or $PL^3$ 6-US structure.

equations.

### 10.2.3 Instability conditions for a 3-XS structure

There exist many types of structures. Among those, the structures corresponding to many PMs are the 3-XS structures. For example, the 3-RS, RS-RS-PS, RS-PS-PS, 3-PS (Fig. 10.8) and the 3-ΠS structures. Here, Π denotes a parallelogram.

The instability conditions for a 3-XS structure can be obtained by differentiating its constraint equations. The set of constraint equations should be set up with a minimum number of unknowns in order to reduce the number of operations in the elimination procedure.

Let $\mathbf{b}_i$ $(i = 1, 2, 3)$ denote the position vector of the center of the $i$-th S joint $B_i$ $(i = 1, 2, 3)$ on a 3S platform (Fig. 10.8) and let $b_{12}$, $b_{23}$ and $b_{31}$ denote the link parameters of the 3S platform, i.e., let $b_{ij}$ denote the distance between point $B_i$ and $B_j$. The constraint equations for the 3-XS structure are (Figs. 10.8 and 10.9)

$$\begin{cases} (\mathbf{b}_2 - \mathbf{b}_1) \cdot (\mathbf{b}_2 - \mathbf{b}_1) = b_{12}^2 \\ (\mathbf{b}_3 - \mathbf{b}_2) \cdot (\mathbf{b}_3 - \mathbf{b}_2) = b_{23}^2 \\ (\mathbf{b}_1 - \mathbf{b}_3) \cdot (\mathbf{b}_1 - \mathbf{b}_3) = b_{31}^2 \end{cases} \tag{10.32}$$

with

$$\mathbf{b}_i = f(q_i) \tag{10.33}$$

where $q_i$ denotes the joint variable associated with the X joint. Variable $q_i$ is equal to $\theta_i$ if the X joint is an R joint or to $S_i$ if the X joint is a P joint.

Equations (10.32) and (10.33) are respectively the rigid body condition of the moving platform and the constraint equation of the legs. Differentiating Eqs. (10.32) and (10.33), one obtains

$$\begin{cases} (\mathbf{b}_2 - \mathbf{b}_1) \cdot (d\mathbf{b}_2 - d\mathbf{b}_1) = 0 \\ (\mathbf{b}_3 - \mathbf{b}_2) \cdot (d\mathbf{b}_3 - d\mathbf{b}_2) = 0 \\ (\mathbf{b}_1 - \mathbf{b}_3) \cdot (d\mathbf{b}_1 - d\mathbf{b}_3) = 0 \end{cases} \tag{10.34}$$

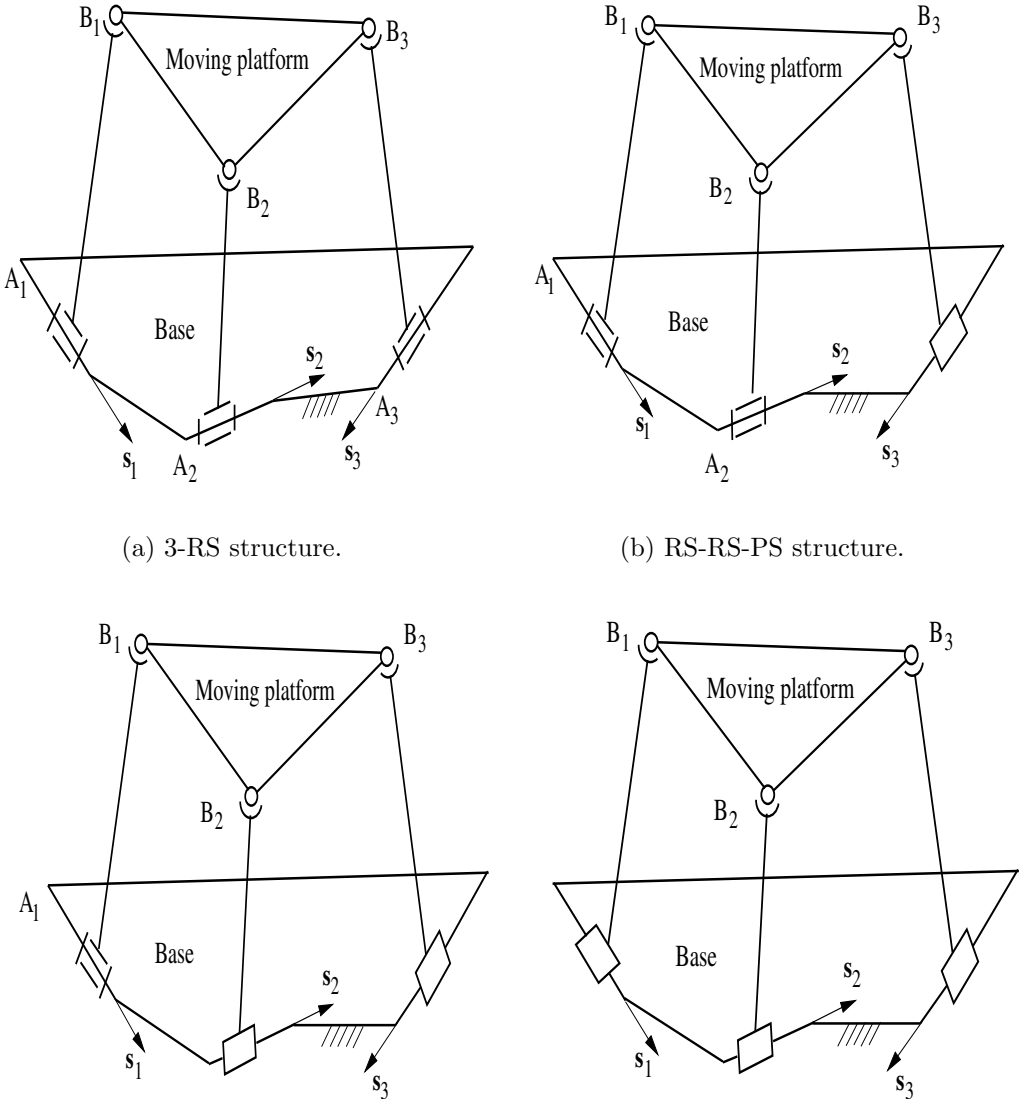


(a) 3-RS structure.

(b) RS-RS-PS structure.

(c) PS-PS-RS structure.

(d) 3-PS structure.

Figure 10.8: 3-XS structures.

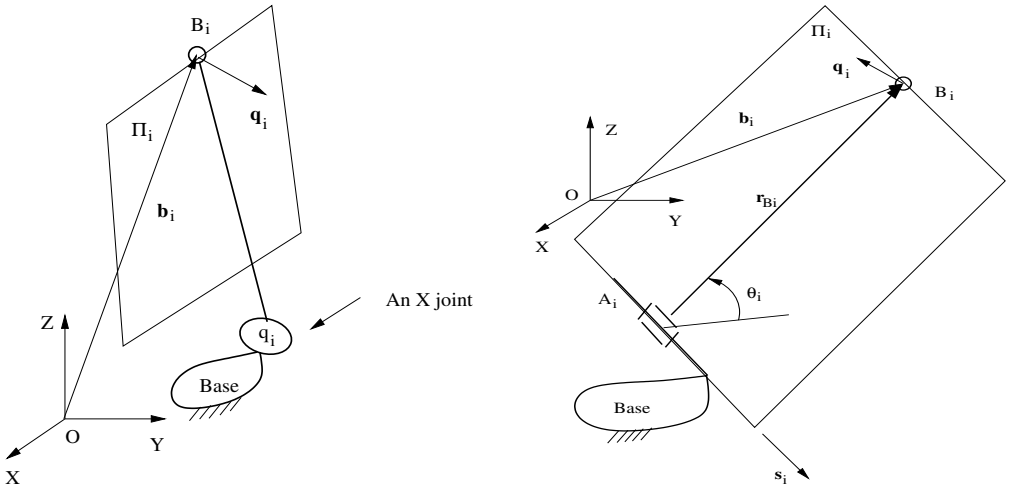


(a) XS leg.

(b) RS leg.

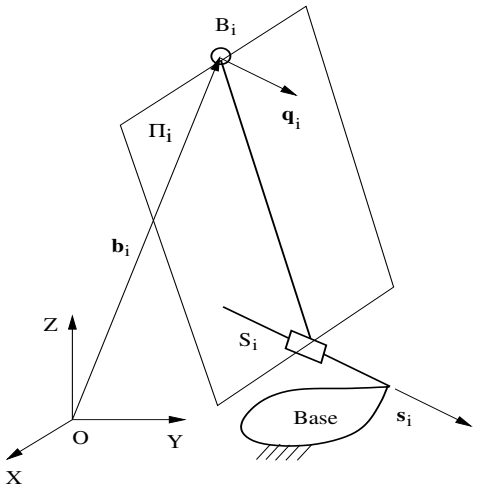


(c) PS leg.

Figure 10.9: XS legs.

with

$$d\mathbf{b}_i = \mathbf{q}_i dq_i \tag{10.35}$$

where

$$\mathbf{q}_i = d\mathbf{b}_i/dq_i \tag{10.36}$$

Vector $\mathbf{q}_i$ can be found without difficulty (Fig. 10.9). For example, one has

$$\mathbf{q}_i = \begin{cases} \mathbf{s}_i \times \mathbf{r}_{Bi} & \text{for an RS leg} \\ \mathbf{s}_i & \text{for a PS leg} \end{cases} \tag{10.37}$$

Here, $\mathbf{s}_i$ denotes the unit vector along the R or P joint in the RS or PS leg while $\mathbf{r}_{Bi}$ denotes a vector directed from a point on the axis of the R joint to the center of the S joint. The substitution of Eq. (10.35) into Eq. (10.34) yields

$$\begin{bmatrix} -(\mathbf{b}_2 - \mathbf{b}_1)\cdot\mathbf{q}_1 & (\mathbf{b}_2 - \mathbf{b}_1)\cdot\mathbf{q}_2 & 0 \\ 0 & -(\mathbf{b}_3 - \mathbf{b}_2)\cdot\mathbf{q}_2 & (\mathbf{b}_3 - \mathbf{b}_2)\cdot\mathbf{q}_3 \\ (\mathbf{b}_1 - \mathbf{b}_3)\cdot\mathbf{q}_1 & 0 & -(\mathbf{b}_1 - \mathbf{b}_3)\cdot\mathbf{q}_3 \end{bmatrix} \begin{Bmatrix} dq_1 \\ dq_2 \\ dq_3 \end{Bmatrix} = 0 \tag{10.38}$$

The 3-XS structure is unstable if and only if one or more of the $dq_i$'s can be different from zero. From Eq. (10.38), we get

$$\begin{vmatrix} -(\mathbf{b}_2 - \mathbf{b}_1)\cdot\mathbf{q}_1 & (\mathbf{b}_2 - \mathbf{b}_1)\cdot\mathbf{q}_2 & 0 \\ 0 & -(\mathbf{b}_3 - \mathbf{b}_2)\cdot\mathbf{q}_2 & (\mathbf{b}_3 - \mathbf{b}_2)\cdot\mathbf{q}_3 \\ (\mathbf{b}_1 - \mathbf{b}_3)\cdot\mathbf{q}_1 & 0 & -(\mathbf{b}_1 - \mathbf{b}_3)\cdot\mathbf{q}_3 \end{vmatrix} = 0 \tag{10.39}$$

i.e.,

$$\begin{aligned} &-[(\mathbf{b}_2 - \mathbf{b}_1)\cdot\mathbf{q}_1][(\mathbf{b}_3 - \mathbf{b}_2)\cdot\mathbf{q}_2][(\mathbf{b}_1 - \mathbf{b}_3)\cdot\mathbf{q}_3] \\ &+[(\mathbf{b}_2 - \mathbf{b}_1)\cdot\mathbf{q}_2][(\mathbf{b}_3 - \mathbf{b}_2)\cdot\mathbf{q}_3][(\mathbf{b}_1 - \mathbf{b}_3)\cdot\mathbf{q}_1] = 0 \end{aligned} \tag{10.40}$$

Equation (10.40) is the instability condition for a 3-XS structure or the forward kinematic singularity condition for PMs with a 3-XS structure. When Eq. (10.40) is satisfied, one or more links in the 3-XS structure will undergo infinitesimal or finite motion with respect to the 3X platform, and the 3S platform will undergo infinitesimal or finite motion with respect to the 3X platform.

The following specific case should be noted: If $\mathbf{q}_i = \mathbf{0}$ for the XS leg $i$, Eq. (10.40) is always satisfied. In this case, the satisfaction of Eq. (10.40) does not mean that the

3S platform will undergo infinitesimal or finite motion with respect to the 3X platform. As the above-mentioned specific case occurs only when an inverse kinematic singularity occurs for leg $i$, we make the assumption that $\mathbf{q}_i \neq 0$ in the following discussion. In the case of the RS leg, we assume that the S joint is not located on the axis of the R joint of the same RS leg.

The above-mentioned derivation of the forward kinematic singularity conditions for PMs with a 3-XS structure only requires the expansion of a $3 \times 3$ determinant, whereas the derivation in [84] starts from six equations, and the calculation of a $6 \times 6$ or $4 \times 4$ determinant is needed in [93] and [86, 90, 158] respectively. As compared to the works of [94, 95, 159], the formulation proposed here is more concise as no input velocities are involved in the derivation. Hence, the singularity analysis of PMs with the same structure can be performed in a unified way instead of on a case-by-case basis, as in the current literature.

### 10.2.4 Geometric interpretation of the instability condition for the 3-XS structure

From Eq. (10.40), one has

$$\begin{aligned}&[(\mathbf{b}_2-\mathbf{b}_1)\cdot\mathbf{q}_1][(\mathbf{b}_3-\mathbf{b}_2)\cdot\mathbf{q}_2][(\mathbf{b}_1-\mathbf{b}_3)\cdot\mathbf{q}_3]\\ +&[(\mathbf{b}_1-\mathbf{b}_2)\cdot\mathbf{q}_2][(\mathbf{b}_2-\mathbf{b}_3)\cdot\mathbf{q}_3][(\mathbf{b}_3-\mathbf{b}_1)\cdot\mathbf{q}_1]=0\end{aligned} \tag{10.41}$$

The above equation can be rewritten as

$$\begin{vmatrix} 0 & (\mathbf{b}_2-\mathbf{b}_1)\cdot\mathbf{q}_1 & (\mathbf{b}_3-\mathbf{b}_1)\cdot\mathbf{q}_1 \\ (\mathbf{b}_1-\mathbf{b}_2)\cdot\mathbf{q}_2 & 0 & (\mathbf{b}_3-\mathbf{b}_2)\cdot\mathbf{q}_2 \\ (\mathbf{b}_1-\mathbf{b}_3)\cdot\mathbf{q}_3 & (\mathbf{b}_2-\mathbf{b}_3)\cdot\mathbf{q}_3 & 0 \end{vmatrix} = 0 \tag{10.42}$$

Thus, there exist non-vanishing solutions to the following equations.

$$\begin{bmatrix} 0 & (\mathbf{b}_2-\mathbf{b}_1)\cdot\mathbf{q}_1 & (\mathbf{b}_3-\mathbf{b}_1)\cdot\mathbf{q}_1 \\ (\mathbf{b}_1-\mathbf{b}_2)\cdot\mathbf{q}_2 & 0 & (\mathbf{b}_3-\mathbf{b}_2)\cdot\mathbf{q}_2 \\ (\mathbf{b}_1-\mathbf{b}_3)\cdot\mathbf{q}_3 & (\mathbf{b}_2-\mathbf{b}_3)\cdot\mathbf{q}_3 & 0 \end{bmatrix} \begin{Bmatrix} k_1 \\ k_2 \\ k_3 \end{Bmatrix} = 0 \tag{10.43}$$

Let $\{k_1 \;\; k_2 \;\; k_3\}$ denote any one set of non-zero solutions to the above equation. Two cases may occur:

Case $a$)

$$k = k_1 + k_2 + k_3 \neq 0 \tag{10.44}$$

Case $b$)

$$k = k_1 + k_2 + k_3 = 0 \tag{10.45}$$

In order to facilitate the derivation of the geometric interpretation of the instability condition for a 3-XS structure or the forward kinematic singularity conditions for PMs with a 3-XS structure, Eq. (10.43) is rewritten as

$$\begin{cases} (k_2(\mathbf{b}_2 - \mathbf{b}_1) + k_3(\mathbf{b}_3 - \mathbf{b}_1)) \cdot \mathbf{q}_1 = 0 \\ (k_1(\mathbf{b}_1 - \mathbf{b}_2) + k_3(\mathbf{b}_3 - \mathbf{b}_2)) \cdot \mathbf{q}_2 = 0 \\ (k_1(\mathbf{b}_1 - \mathbf{b}_3) + k_2(\mathbf{b}_2 - \mathbf{b}_3)) \cdot \mathbf{q}_3 = 0 \end{cases} \tag{10.46}$$

Let us consider Case $a$) first. In Case $a$), one has $k \neq 0$ (see Eq. (10.44)). Let $k'_i = k_i/k$, $(i = 1, 2, 3)$. One obtains

$$k'_1 + k'_2 + k'_3 = 1 \tag{10.47}$$

Equation (10.46) divided by $k$ yields

$$\begin{cases} (k'_2(\mathbf{b}_2 - \mathbf{b}_1) + k'_3(\mathbf{b}_3 - \mathbf{b}_1)) \cdot \mathbf{q}_1 = 0 \\ (k'_1(\mathbf{b}_1 - \mathbf{b}_2) + k'_3(\mathbf{b}_3 - \mathbf{b}_2)) \cdot \mathbf{q}_2 = 0 \\ (k'_1(\mathbf{b}_1 - \mathbf{b}_3) + k'_2(\mathbf{b}_2 - \mathbf{b}_3)) \cdot \mathbf{q}_3 = 0 \end{cases} \tag{10.48}$$

From Eq. (10.48), one obtains

$$\begin{cases} (\mathbf{b}_1 + k'_2(\mathbf{b}_2 - \mathbf{b}_1) + k'_3(\mathbf{b}_3 - \mathbf{b}_1) - \mathbf{b}_1) \cdot \mathbf{q}_1 = 0 \\ (\mathbf{b}_2 + k'_1(\mathbf{b}_1 - \mathbf{b}_2) + k'_3(\mathbf{b}_3 - \mathbf{b}_2) - \mathbf{b}_2) \cdot \mathbf{q}_2 = 0 \\ (\mathbf{b}_3 + k'_1(\mathbf{b}_1 - \mathbf{b}_3) + k'_2(\mathbf{b}_2 - \mathbf{b}_3) - \mathbf{b}_3) \cdot \mathbf{q}_3 = 0 \end{cases} \tag{10.49}$$

Now, letting

$$\begin{cases} \mathbf{c}_1 = \mathbf{b}_1 + k'_2(\mathbf{b}_2 - \mathbf{b}_1) + k'_3(\mathbf{b}_3 - \mathbf{b}_1) \\ \mathbf{c}_2 = \mathbf{b}_2 + k'_1(\mathbf{b}_1 - \mathbf{b}_2) + k'_3(\mathbf{b}_3 - \mathbf{b}_2) \\ \mathbf{c}_3 = \mathbf{b}_3 + k'_1(\mathbf{b}_1 - \mathbf{b}_3) + k'_2(\mathbf{b}_2 - \mathbf{b}_3) \end{cases} \tag{10.50}$$

and substituting Eq. (10.47) into Eq. (10.50), one obtains

$$\mathbf{c}_1 = \mathbf{c}_2 = \mathbf{c}_3 \tag{10.51}$$

Let

$$\mathbf{c} = \mathbf{c}_1 = \mathbf{c}_2 = \mathbf{c}_3 \tag{10.52}$$

Equation (10.49) can therefore be rewritten as

$$\begin{cases} (\mathbf{c} - \mathbf{b}_1) \cdot \mathbf{q}_1 = 0 \\ (\mathbf{c} - \mathbf{b}_2) \cdot \mathbf{q}_2 = 0 \\ (\mathbf{c} - \mathbf{b}_3) \cdot \mathbf{q}_3 = 0 \end{cases} \tag{10.53}$$

From Eqs. (10.50–10.52), we learn that $\mathbf{c}$ is the position vector of a point C on the $B_1B_2B_3$ plane. The $i$-th equation in Eq. (10.53) indicates that $\mathbf{c}$ is also a point on the plane $\Pi_i$ (Fig. 10.9) through $B_i$ and perpendicular to $\mathbf{q}_i$. Thus, Eq. (10.53) shows that for any set of non-zero solutions to Eq. (10.43) with $k \neq 0$, four planes, the $B_1B_2B_3$ plane and planes $\Pi_i$ $(i = 1, 2, 3)$, have a common point C.

Now, let us consider Case *b*). In this case, there are no less than two non-zero $k_i$'s. Otherwise, all $k_i$'s will be zero. Without loss of generality, one can make the assumption that $k_1$ and $k_2$ are non-zero. Eliminating $k_3$ in Eq. (10.46) using Eq. (10.45), one obtains

$$\begin{cases} (k_1(\mathbf{b}_1 - \mathbf{b}_3) + k_2(\mathbf{b}_2 - \mathbf{b}_3)) \cdot \mathbf{q}_1 = 0 \\ (k_1(\mathbf{b}_1 - \mathbf{b}_3) + k_2(\mathbf{b}_2 - \mathbf{b}_3)) \cdot \mathbf{q}_2 = 0 \\ (k_1(\mathbf{b}_1 - \mathbf{b}_3) + k_2(\mathbf{b}_2 - \mathbf{b}_3)) \cdot \mathbf{q}_3 = 0 \end{cases} \tag{10.54}$$

The vector $[k_1(\mathbf{b}_1 - \mathbf{b}_3) + k_2(\mathbf{b}_2 - \mathbf{b}_3)]$ is parallel to the $B_1B_2B_3$ plane. Equation (10.54) indicates that all the planes $\Pi_i$ $(i = 1, 2, 3)$ are parallel to the vector $[k_1(\mathbf{b}_1 - \mathbf{b}_3) + k_2(\mathbf{b}_2 - \mathbf{b}_3)]$. Thus, the four planes, the $B_1B_2B_3$ plane and planes $\Pi_i$ $(i = 1, 2, 3)$, have one common point for the set of non-zero solutions to Eq. (10.43) with $k = 0$. The common point is the point at infinity in the direction of $(k_1(\mathbf{b}_1 - \mathbf{b}_3) + k_2(\mathbf{b}_2 - \mathbf{b}_3))$.

In summary, the non-zero solutions to Eq. (10.43) will lead to the following geometric condition: the four planes, the $B_1B_2B_3$ plane and planes $\Pi_i$ $(i = 1, 2, 3)$, have one or more common points. This is the geometric interpretation of the instability condition of the 3-XS structure or the forward kinematic singularity conditions of PMs with a 3-XS structure.

Although the geometric interpretation of the forward kinematic singularity conditions of PMs with a 3-XS structure can also be obtained using screw theory [90] or line geometry [84], the formulation here is the simplest.

### 10.2.5 General steps for the forward kinematic singularity analysis of parallel mechanisms with a 3-XS structure

The general steps which are required in order to perform the forward kinematic singularity analysis of PMs with a 3-XS structure can be stated as follows:

**Step 1.** Calculate the unknown position vectors, $\mathbf{b}_i$, of the centers of the S joints located on the 3S platform from the pose (position and orientation) of the moving platform.

**Step 2.** Calculate the unknown unit vectors, $\mathbf{s}_i$, along the axes of the X joints located on the 3X platform from the pose of the moving platform in the cases of the RS or the PS legs.

**Step 3.** Calculate the unknown position vectors of points $A_i$, on the axes of the X joints located on the 3X platform from the pose of the moving platform in the case of the RS legs.

**Step 4.** Determine the vectors $\mathbf{q}_i$, using Eq. (10.36) or Eq. (10.37).

**Step 5.** Perform the forward kinematic singularity analysis numerically or symbolically using Eq. (10.40).

In performing the forward kinematic singularity analysis of PMs with a 3-XS structure, one or two steps of Steps 1 – 3 can usually be omitted as there may be no unknown to be calculated in these steps. See the forward kinematic singularity analysis of 6-3 Gough-Stewart PMs given in Section 10.2.6 for example.

### 10.2.6 Forward kinematic singularity analysis of 6-3 Gough-Stewart parallel mechanisms

The 6-3 Gough-Stewart PM is one typical PM of the broad class of PMs with a 3-XS structure. In the following, we deal with the forward kinematic singularity analysis of a 6-3 Gough-Stewart PM using the proposed approach. To perform the forward kinematic singularity analysis of a 6-3 Gough-Stewart PM, two coordinate frames are

first defined (Fig. 10.6). The coordinate frame O-XYZ is attached to the base. The coordinate frame $O_B$-$X_BY_BZ_B$ is attached to the moving platform with points $B_1$, $B_2$ and $B_3$ located in the $O_B$-$X_BY_B$ plane.

The structures corresponding to the 6-3 Gough-Stewart PM are three PL structures and one 3-RS structure (Fig. 10.7). Forward kinematic singularities occur for the 6-3 Gough-Stewart PM if and only if one or more of its structures are unstable.

The PL structure is unstable if and only if it degenerates into a line. Considering that the above case cannot be achieved due to the limits of joint motion, the forward kinematic singularities due to the instability of the PL structure are omitted in the discussion below. In the following, we perform a detailed study of the forward kinematic singularities of the 6-3 Gough-Stewart PM due to the instability of the 3-RS structure.

For the 3-RS structure of the 6-3 Gough-Stewart PM, the unit vectors, $\mathbf{s}_i$, along the axes of the R joints located on the 3R platform, i.e., the base, as well as the position vectors of the points ($A_1$, $A_3$ and $A_5$) on the three R joints are all known. Steps 2 and 3 are thus omitted.

**Step 1.** Calculate the unknown position vectors, $\mathbf{b}_i$, of the centers of the S joints located on the 3S platform, i.e., the moving platform.

Let $\mathbf{p} = \{x \quad y \quad z\}^T$ and $\mathbf{R} = [R_{i,j}]_{3\times 3}$ denote the position and direction cosine matrix of the moving platform. The position vector of $B_i$ can be calculated as

$$\mathbf{b}_i = \mathbf{p} + \mathbf{R}\mathbf{b}_i^P \tag{10.55}$$

where, $\mathbf{b}_i^P = \{x_{Bi} \quad y_{Bi} \quad z_{Bi}\}^T$ is the position vector of $B_i$ in the coordinate frame $O_B$-$X_BY_BZ_B$.

**Step 4.** Determine the vectors $\mathbf{q}_i$ using Eq. (10.37).

**Step 5.** Perform the forward kinematic singularity analysis numerically or symbolically using Eq. (10.40).

The forward kinematic singularity equation obtained is

$$(y_{B1}x_{B3} - y_{B3}x_{B1} - y_{B1}x_{B2} + y_{B2}x_{B1} - y_{B2}x_{B3} + y_{B3}x_{B2})f(\mathbf{p}, \mathbf{R}) = 0 \tag{10.56}$$

From Eq. (10.56), one has

$$(y_{B1}x_{B3} - y_{B3}x_{B1} - y_{B1}x_{B2} + y_{B2}x_{B1} - y_{B2}x_{B3} + y_{B3}x_{B2}) = 0 \tag{10.57}$$

and

$$f(\mathbf{p}, \mathbf{R}) = 0 \tag{10.58}$$

Equation (10.57) is in fact the condition for the collinearity of the three points $B_i$. This means that when points $B_i$ are collinear, the PM is architecturally singular. It is clear that under the condition given by Eq. (10.57), the platform $B_1B_2B_3$ can rotate about the line through all $B_i$'s. In the following, we make the assumption that $B_1$, $B_2$ and $B_3$ are not collinear.

Equation (10.58) is a six-dimensional manifold. It is very complex to investigate how this manifold separates the workspace of the PM.

In the remaining parts of this section, we will investigate the singularity surface for a given orientation of the moving platform for a 6-3 Gough-Stewart PM.

#### 10.2.6.1 Forward kinematic singularity surface for a given orientation

The forward kinematic singularity surface for a given orientation of the moving platform for the general 6-3 Gough-Stewart PM can be expressed using Eq. (10.56) or (10.58) as

$$\begin{aligned} & e_{300}x^3 + e_{030}y^3 + e_{003}z^3 + e_{210}x^2y + e_{201}x^2z + e_{120}xy^2 + e_{021}y^2z \\ + \; & e_{102}xz^2 + e_{012}yz^2 + e_{111}xyz + e_{200}x^2 + e_{020}y^2 + e_{002}z^2 \\ + \; & e_{110}xy + e_{101}xz + e_{011}yz + e_{100}x + e_{010}y + e_{001}z + e_{000} = 0 \end{aligned} \tag{10.59}$$

Here, $e_{ijk}$ is used to denote the coefficient of the term $x^iy^jz^k$ in the equations of the forward kinematic singularity surfaces. This result is similar to what was obtained in [93] for the singularity analysis of the Gough-Stewart PM, whereas the results in [93] were obtained by calculating a $6 \times 6$ determinant.

#### 10.2.6.2 Some 6-3 Gough-Stewart parallel mechanisms with a forward kinematic singularity surface of reduced degree

In general, the forward kinematic singularity surface of a PM has a very complex shape, which makes it very difficult to perform singularity-free path planning [35]. The study of PMs with simple forward kinematic singularity surfaces is of interest as their path planning may be easier than in the general case. Several cases of PMs with a forward kinematic singularity surface of reduced degree are proposed in the following.

**The decoupled case:** For the decoupled case, $A_1A_2$ and $A_3A_4$ are both collinear to the X-axis. The forward kinematic singularity equation then becomes

$$\begin{aligned} & (g_{010}y + g_{001}z + g_{000})(f_{020}y^2 + f_{002}z^2 + f_{110}xy + f_{101}xz + f_{011}yz \\ + \quad & f_{100}x + f_{010}y + f_{001}z + f_{000}) = 0 \end{aligned} \tag{10.60}$$

**The decoupled orthogonal case:** For the decoupled orthogonal case, $A_1A_2$ and $A_3A_4$ are collinear to the X-axis while $A_5A_6$ is parallel to the Y-axis. The forward kinematic singularity equation is then

$$\begin{aligned} & (g_{010}y + g_{001}z + g_{000})(f_{002}z^2 + f_{101}xz + f_{011}yz + f_{100}x + f_{010}y \\ + \quad & f_{001}z + f_{000}) = 0 \end{aligned} \tag{10.61}$$

**The decoupled parallel case:** For the decoupled parallel case, $A_1A_2$ and $A_3A_4$ are both collinear to the X-axis while $A_5A_6$ is parallel to the X-axis and located in the O-XY plane. The forward kinematic singularity equation is then written as

$$R_{1,3}(g_{010}y + g_{001}z + g_{000})(z + h_{000}) = 0 \tag{10.62}$$

**The decoupled spherical case:** For the decoupled spherical case, $A_1A_2$, $A_3A_4$ and $A_5A_6$ intersect at the origin O while $A_1A_2$ and $A_3A_4$ are both collinear to the X-axis and $A_5A_6$ is located in the O-XY plane.

The forward kinematic singularity equation then becomes

$$(ax + by + cz)(g_{010}y + g_{001}z + g_{000})(z + h_{000}) = 0 \tag{10.63}$$

**The spherical case:** For the spherical case, $A_1A_2$, $A_3A_4$ and $A_5A_6$ intersect at the origin O. The forward kinematic singularity equation is then

$$\begin{aligned} & (ax+by+cz)(f_{200}x^2+f_{020}y^2+f_{002}z^2+f_{110}xy+f_{101}xz+f_{011}yz \\ + \quad & f_{100}x+f_{010}y+f_{001}z+f_{000})=0 \end{aligned} \tag{10.64}$$

**The orthogonal spherical case:** For the orthogonal spherical case, $A_1A_2$, $A_3A_4$ and $A_5A_6$ are coincident with the X-, Y- and Z-axes respectively. The forward kinematic singularity equation is then written as

$$(ax+by+cz)(f_{110}xy+f_{101}xz+f_{011}yz+f_{100}x+f_{010}y+f_{001}z+f_{000})=0 \tag{10.65}$$

**The orthogonal case:** For the orthogonal case, $A_1A_2$, $A_3A_4$ and $A_5A_6$ are parallel to the X-, Y- and Z-axes respectively. The forward kinematic singularity equation then becomes

$$\begin{aligned} & e_{210}x^2y+e_{201}x^2z+e_{120}xy^2+e_{021}y^2z+e_{102}xz^2+e_{012}yz^2 \\ + \quad & e_{111}xyz+e_{200}x^2+e_{020}y^2+e_{002}z^2+e_{110}xy+e_{101}xz+e_{011}yz \\ + \quad & e_{100}x+e_{010}y+e_{001}z+e_{000}=0 \end{aligned} \tag{10.66}$$

**The parallel-to-a-line case:** For the parallel-to-a-line case, $A_1A_2$, $A_3A_4$ and $A_5A_6$ are all parallel to the X-axis. The forward kinematic singularity equation is then

$$R_{1,3}(e_{020}y^2+e_{002}z^2+e_{011}yz+e_{010}y+e_{001}z+e_{000})=0 \tag{10.67}$$

**The parallel planar case:** For the parallel planar case, $A_1A_2$, $A_3A_4$ and $A_5A_6$ are all parallel to the X-axis and located on the O-XY plane. The forward kinematic singularity equation is then written as

$$R_{1,3}(e_{002}z^2+e_{011}yz+e_{010}y+e_{001}z+e_{000})=0 \tag{10.68}$$

**The parallel-to-a-plane case:** For the parallel-to-a-plane case, $A_1A_2$, $A_3A_4$ and $A_5A_6$ are all parallel to the O-XY plane. The forward kinematic singularity equation then becomes

$$\begin{aligned} & e_{003}z^3+e_{201}x^2z+e_{021}y^2z+e_{102}xz^2+e_{012}yz^2+e_{111}xyz+e_{200}x^2+e_{020}y^2 \\ + \quad & e_{002}z^2+e_{110}xy+e_{101}xz+e_{011}yz+e_{100}x+e_{010}y+e_{001}z+e_{000}=0 \end{aligned} \tag{10.69}$$

**The partially-parallel-to-a-line case:** For the partially-parallel-to-a-line case, $A_1A_2$ and $A_3A_4$ are both parallel to the X-axis. The forward kinematic singularity equation is then

$$\begin{aligned} & e_{030}y^3 + e_{003}z^3 + e_{120}xy^2 + e_{021}y^2z + e_{102}xz^2 + e_{012}yz^2 + e_{111}xyz + e_{020}y^2 \\ + \quad & e_{002}z^2 + e_{110}xy + e_{101}xz + e_{011}yz + e_{100}x + e_{010}y + e_{001}z + e_{000} = 0 \end{aligned} \tag{10.70}$$

**The partially-parallel and orthogonal case:** For the partially-parallel and orthogonal case, $A_1A_2$ and $A_3A_4$ are parallel to the X-axis and $A_5A_6$ is parallel to the Y-axis. The forward kinematic singularity equation is then written as

$$\begin{aligned} & e_{003}z^3 + e_{021}y^2z + e_{102}xz^2 + e_{012}yz^2 + e_{111}xyz + e_{020}y^2 + e_{002}z^2 + e_{110}xy \\ + \quad & e_{101}xz + e_{011}yz + e_{100}x + e_{010}y + e_{001}z + e_{000} = 0 \end{aligned} \tag{10.71}$$

#### 10.2.6.3 Geometric interpretation of the forward kinematic singularity condition of the decoupled parallel case and the decoupled spherical case

Although the geometric interpretation of the forward kinematic singularity conditions has been proposed for the general 6-3 Gough-Stewart PM, it is still of interest to reveal the geometric characteristics of the forward kinematic singularity conditions for the cases with forward kinematic singularity surfaces of a reduced degree. In this subsection, the geometric interpretation of the forward kinematic singularity conditions of the decoupled parallel case and the decoupled spherical case presented in the previous subsection will be investigated.

From Eqs. (10.60) – (10.63), we learn that a common forward kinematic singularity condition

$$g_{010}y + g_{001}z + g_{000} = 0 \tag{10.72}$$

exists for the decoupled case, the decoupled orthogonal case, the decoupled parallel case and the decoupled spherical case. When Eq. (10.72) is met, points $B_1$ and $B_2$ and the axes $A_1A_2$ ($A_3A_4$) are coplanar.

From Eqs. (10.62) and (10.63), we learn that a common forward kinematic singularity condition

$$z + h_{000} = 0 \tag{10.73}$$

exists for the decoupled parallel case and the decoupled spherical case. When Eq. (10.73) is met, point $B_3$ is located in the $A_1A_2A_3A_4A_5A_6$ plane.

From Eqs. (10.62), (10.67) and (10.68), we learn that a common forward kinematic singularity condition

$$R_{1,3} = 0 \tag{10.74}$$

exists for the decoupled parallel case, the parallel-to-a-line case and the parallel planar case. When Eq. (10.74) is met, the $Z_B$-axis is perpendicular to the X-axis. In other words, the $B_1B_2B_3$ plane is parallel to the X-axis.

From Eqs. (10.63)–(10.65), we learn that a common forward kinematic singularity condition

$$ax + by + cz = 0 \tag{10.75}$$

exists for the decoupled spherical case, the spherical case and the orthogonal spherical case. When Eq. (10.75) is met, the $B_1B_2B_3$ plane passes through the origin O.

Thus, from Eq. (10.62), we obtain that forward kinematic singularities occur for the decoupled parallel case if and only if (1) the $B_1B_2B_3$ plane is parallel to the X-axis; (2) points $B_1$ and $B_2$ and the axes $A_1A_2$ ($A_3A_4$) are coplanar and/or (3) point $B_3$ is located in the $A_1A_2A_3A_4A_5A_6$ plane.

From Eq. (10.63), we obtain that forward kinematic singularities occur for the decoupled spherical case if and only if (1) the $B_1B_2B_3$ plane passes through the origin O; (2) points $B_1$ and $B_2$ and the axes $A_1A_2$ ($A_3A_4$) are coplanar and/or (3) point $B_3$ is located in the $A_1A_2A_3A_4A_5A_6$ plane.

## 10.3 Conclusions

It has been shown that the singularity surfaces divide the workspace into four singularity-free regions for an analytic 3-R$\underline{P}$R PPM with similar platforms. The boundary of the singularity-free regions for a given orientation of the moving platform is a circle in the case of the 3-R$\underline{P}$R manipulator with similar triangular platforms or a straight line in

the case of a manipulator with similar aligned platforms. The one-to-one correspondence between the solutions to the FDA and the singularity-free regions is revealed for the analytic 3-R$\underline{P}$R PPMs with similar platforms. This simplifies further the FDA of the 3-R$\underline{P}$R manipulator with similar platforms.

In addition to the three classes of analytic 3-R$\underline{P}$R PPMs classified according to the singularity loci in Cartesian workspace for a given orientation of the platform, a fourth class of analytic PPM is found. For this class of 3-R$\underline{P}$R manipulator, such as the 3-R$\underline{P}$R manipulator with similar triangular platforms, the singularity loci for a given orientation always form a parabola. The condition for the analytic 3-R$\underline{P}$R PPM for which the singularity loci for a given orientation of the moving platform always form a straight line is also generalized.

Unlike the general analytic 3-R$\underline{P}$R PPM [160], the analytic 3-R$\underline{P}$R PPMs with similar platforms must meet singularities when changing from one assembly mode to another.

A unified and simplified approach has also been proposed in this section to perform the forward kinematic singularity analysis of PMs with a 3-XS structure. This approach is general enough to cover several PMs proposed in the literature. The problem has been reduced to the instability analysis of structures. The geometric interpretation has been revealed for the instability condition of the 3-XS structure using a method based on linear algebra. The forward kinematic singularity analysis of the 6-3 Gough-Stewart PM has been performed in detail in order to illustrate the application and the efficiency of the proposed approach. Specific cases of 6-3 Gough-Stewart PMs with forward kinematic singularity surfaces of reduced degree for a given orientation of the moving platform have also been proposed. The geometric interpretation of the singularity conditions for some of the specific cases has also been revealed.

As compared to the existing methods for the forward kinematic singularity analysis of PMs, the characteristics of the proposed approach are:

1. The forward kinematic singularity analysis of a PM is reduced to the instability analysis of its equivalent structure and no input velocities are involved in the derivation.

2. The forward kinematic singularity analysis of PMs with the same structure can be performed in a unified and simplified way. The instability condition of a structure is formulated by differentiating its constraint equations with the minimum number of unknowns.

3. The component approach is useful and has been applied for the simplification of the singularity analysis of PMs with two or more components and the investigation on PMs with a singularity surface of reduced degree.

4. The proposed formulation involves the expansion of a $3\times3$ determinant as opposed to $6 \times 6$ or $4 \times 4$ determinants in most of the other methods.

This work will be useful in the design and control of analytic 3-R$\underline{P}$R PPMs and PMs with a 3-XS structure.

# Chapter 11

# Conclusions

In this chapter, the results obtained in the previous chapters are summarized. The contributions are highlighted. Issues needing more attention in the future are suggested.

## 11.1 Summary

In this thesis, a systematic study has been presented on the type synthesis and kinematics of general PMs (parallel mechanisms) and APMs (analytic PMs). APMs refer to PMs with a characteristic polynomial of fourth degree or lower. The forward displacement analysis (FDA) of APMs can be performed analytically and efficiently since the

roots of a polynomial equation of fourth degree or lower can be obtained as algebraic functions of its coefficients.

In Chapter 1, an overview of the literature has been presented. The research on the type synthesis and kinematics of PMs at its current state of development cannot meet the needs in developing new PMs with a specified motion pattern and PMs with simple kinematics. Therefore, this thesis sets out to (1) provide a unified and systematic approach to the type synthesis of PMs, (2) devote considerable attention to the type synthesis of PMs with relatively simple kinematics, (3) perform a comprehensive kinematic study of a class of APMs of great potential application, and (4) simplify the forward kinematic singularity analysis of PMs and reveal the characteristics of certain APMs from the perspective of kinematic singularities. These issues have been addressed and the identified problems have been solved.

The tools needed for the accomplishment of the goals have been provided in Chapter 2. In particular, screw theory was reviewed because it has been selected among different approaches as the basis of most works reported in this thesis. A new approach to the mobility analysis of parallel kinematic chains, as well as a method to verify the validity of the selection of actuated joints in PMs using screw theory have also been proposed.

A general procedure for the type synthesis of PMs based on screw theory has been proposed in Chapter 3. This procedure takes both the synthesis of the kinematic chain and the selection of actuated joints into consideration. Four main steps have been identified. In the first step, the combinations of the wrench systems of the legs are derived from the desired motion pattern and the specified number of overconstraints. In the second step, the type synthesis of the legs satisfying the demands resulting from step one is performed. Subsequently, in step three several of the generated legs are put together to form parallel kinematic chains. Finally, in step four, a valid set of joints is selected to be actuated, thus completing the synthesis of the PM. For use in the last step, the concept of dependent joint groups has been introduced.

In Chapter 4, the proposed general procedure has been exemplified for the class of 3-DOF translational PMs (TPMs). All possible legs for translational parallel kinematic chains have been derived. The same results have been found using the small-finite-motion approach and the virtual joint approach. TPMs with and without inactive joints have been obtained. Of all possible TPMs found, the 90 TPMs with three

identical legs have been given. Variations using helical and parallelogram joints have also been indicated.

The proposed general procedure has been exemplified for the class of 3-DOF spherical PMs (SPMs) in Chapter 5. Many legs with P and R joints have been generated using the virtual S-joint approach. Seventy-six spherical kinematic chains with three identical legs have been given, from which 27 SPMs with identical legs are identified. As compared to the Agile Eye [44], some of the new SPMs have the advantage of a more flexible arrangement of the actuated joints on the base, for instance in a parallel arrangement, but they are more complex in structure.

In Chapter 6, the proposed general procedure has been exemplified for the class of PMs with three rotational and one translational degree of freedom (3T1R-PMs). All possible legs for 3T1R-PMs have been derived. The same results have been found using both the small-finite-motion approach and the virtual joint approach. 3T1R-PMs with and without inactive joints have been obtained. Of all possible 3T1R-PMs found, the 11 3T1R-PMs with four identical legs have been given. Variations using helical and parallelogram joints have also been indicated.

The type synthesis of APMs has been dealt with in Chapter 7. Several approaches have been proposed for the type synthesis of APMs. These approaches are the component approach, the geometric approach and the algebraic FDA-based approach. Within the component approach, a further distinction was made between the composition approach and the decomposition approach. The decomposition approach, the geometric approach and the algebraic FDA-based approach extend the general procedure for the type synthesis of PMs with an additional fifth step, which constitutes a condition for the PM generated in the first four steps to be an APM. The composition approach in fact circumvents the five-step procedure by making use of analytic components to construct PMs which will then automatically be APMs. Among the new APMs generated, linear TPMs — i.e. TPMs whose FDA can be solved by linear equations — are the most promising ones.

In Chapter 8, the type synthesis, kinematic analysis and kinematic synthesis of LTPMs have been performed. An LTPM is a TPM with linear input-output relations and without constraint singularities. Several types of LTPMs have been generated. The proposed LTPMs may or may not contain some inactive joints and/or redundant

joints. The constraint singularity analysis, inverse kinematics, forward kinematics and kinematic singularity analysis have also been performed. It has been proved that an LTPM is free of forward kinematic singularities. Isotropic conditions for the LTPMs have been revealed. Two additional kinematic merits exist for the isotropic LTPM. The first is that an isotropic LTPM is isotropic in any of its configurations within its workspace. The second is that fewer calculations are needed in order to pre-determine the inverse of the Jacobian matrix. Its workspace analysis has been performed. The kinematic synthesis of LTPMs has also been performed.

In Chapter 9, the FDA of several APMs has been performed. For a class of analytic 3-R$\underline{P}$R planar PMs, the FDA has been reduced to a univariate equation in $x$ of degree 3 — which is reported to be six in the literature — in conjunction with a univariate quadratic equation. For the FDA of analytic R$\underline{P}$R-PR-R$\underline{P}$R planar PMs, an alternative approach to the FDA has been proposed and the maximum number of real solutions for one type has been revealed. For a class of 6-S$\underline{P}$S APMs with an analytic LB component, the FDA has been dealt with in details. It has been revealed that both of these classes of 6-S$\underline{P}$S APMs have at most eight sets of solutions to their FDA. The FDA has been reduced to the solution of one univariate cubic equation and two univariate quadratic equations in sequence for the class X 6-S$\underline{P}$S APM and to the solution of three univariate quadratic equations in sequence for the class XI 6-S$\underline{P}$S APM.

In Chapter 10, the forward kinematic singularity analysis of several typical PMs has been dealt with. The forward kinematic singularity analysis of the 3-R$\underline{P}$R APM with similar base and moving platform has first been performed. It has been shown that the singularity surfaces divide its workspace into four singularity-free regions. It has also been proved that there exists a one-to-one correspondence between the analytic expressions for the four solutions to the FDA and the four singularity-free regions. This result further simplifies the FDA since one can obtain directly the only solution to the FDA once the singularity-free region in which the PM works has been specified. An approach has been proposed based on the instability analysis of structures for the forward kinematic singularity analysis of a broad class of PMs with a 3-XS structure. The characteristic of this approach is that the forward kinematic singularity analysis of PMs with the same structures can be performed in a unified way. For PMs with a 3-XS structure, the forward kinematic singularity analysis has been reduced to a $3 \times 3$ determinant in the most concise manner. The geometric characteristic of singular configurations has been revealed using a method based on linear algebra. Although the

geometric interpretation has been revealed using Grassmann geometry or screw theory before, the approach proposed here seems to be the simplest.

## 11.2 Major contributions

The major contributions are highlighted below.

1. The approach to the type synthesis of PMs based on screw theory.

   The approach is more general than the other current approaches. In the first step, the combinations of the leg wrench systems are derived from the desired motion pattern and the specified number of overconstraints. In the second step, the type synthesis of the legs satisfying the demands resulting from step one is performed. Subsequently, in step three several of the generated legs are put together to form parallel kinematic chains. Finally, in step four, a valid set of joints is selected to be actuated, thus completing the synthesis of the PM.

2. Type synthesis of PMs generating 3-DOF translation, spherical motion and 3T1R motion.

   The full-cycle mobility conditions and the validity conditions for the actuated joints have been revealed for these cases. All the types of TPMs and 3T1R-PMs involving R and P joints have been obtained while many types of SPMs involving R and P joints have been obtained. The results cover all those PMs generating the same motion pattern in the literature as well as some new types.

3. Several approaches to the type synthesis of APMs.

   Comparing the component approach, the geometric approach and the algebraic FDA-based approach, it is found that the algebraic FDA-based approach is more general. However, the derivation needed is very complex, whereas nearly no derivation is needed when the component approach and the geometric approach are used.

4. Linear TPMs and LTPMs.

   Linear TPMs and LTPMs are suitable for fast PM design from the kinematic point of view since the FDA can be performed by solving a set of linear equations.

(a) The presented types of linear TPMs and LTPMs include all the types of LTPMs proposed concurrently by others as well as several additional types.

(b) It is revealed that there are no forward kinematic singularities for the proposed LTPMs.

(c) Globally isotropic LTPMs have been found. The kinematic design issues have been discussed.

5. The approach based on the instability analysis of structures for the forward kinematic singularity analysis of PMs.

   The characteristic of this approach is that the forward kinematic singularity analysis of PMs with the same structure can be performed in a unified way. For a broad class of PMs with a 3-XS structure, the forward kinematic singularity analysis is reduced to a $3 \times 3$ determinant in the most concise manner. The geometric interpretation of singular configurations is revealed simply using linear algebra, although the geometric interpretation has been revealed using Grassmann geometry or screw theory before.

6. The forward kinematic singularity characteristics of an APM have been investigated.

   For a class of analytic planar PMs, it has been proved that there is a one-to-one correspondence between the analytic expressions for the four solutions to the FDA and the four singularity-free regions. This further simplifies the FDA since we can obtain directly the only solution to the FDA once the singularity-free region in which the PM works has been specified.

## 11.3 Future research

The following issues may deserve more attention in the future.

1. To determine other motion patterns for practical applications, such as each of the parallel modules of a hybrid machine tool, and then perform the type synthesis of PMs. In addition to TPMs, SPMs and 3T1R-PMs, the type synthesis of PMs generating other motion patterns with 3, 4 or 5 DOFs has also been performed

and some new PMs have been obtained. These results have not been presented here because (1) the potential application of these PMs is not as clear as TPMs, SPMs and 3T1R-PMs, and (2) the application of the general procedure has been well illustrated using the type synthesis of TPMs, SPMs, and 3T1R-PMs, and (3) the inclusion of these results would further increase the number of pages, which is already greater than that of most theses. Some possible limitations on the proposed approach to the type synthesis of PMs are expected to be found in the progress of the research on motion patterns in practice or in theory.

2. To study the kinematics of PMs with a characteristic polynomial of degree 2 and then degree 3 and 4. It has been shown in Chapter 10 that for an APM with a characteristic polynomial of degree 2, there is a one-to-one correspondence between the analytic expressions for four solutions to the FDA and the four singularity-free regions. This result further simplifies the FDA since one can obtain directly the only solution to the FDA once the singularity-free region in which the PM works is specified. The questions to be answered in this aspect are: (a) Do similar characteristics exist for all APMs with a characteristic polynomial of degree 2? (b) What are the characteristics of APMs with a characteristic polynomial of degree 3? (c) What are the characteristics of APMs with a characteristic polynomial of degree 4?

3. To perform a comprehensive study of new PMs, like the linear TPMs, of great potential application. The comprehensive study will include the constraint singularity analysis, the forward kinematics, the inverse kinematics, the kinematic error analysis, the workspace analysis and the kinematic design.

4. To build prototypes of LTPMs for certain applications and to make a practical comparison between overconstrained and non-overconstrained PMs.

5. To use the concept of the instability of structures to analyze the forward kinematic singularities of PMs with a structure different from the 3-XS structure.

# Bibliography


[1] Merlet J.-P., 2002, *Parallel Robots: Open Problems*, http://www-sop.inria.fr/coprin/equipe/merlet/Problemes/isrr99-html.html.

[2] Rolland L., 2002, *About parallel robots*, http://www.loria.fr/~rolland/apropos_eng.html.

[3] Brumson B., 2002, *Parallel Kinematic Robots*, http://www.robotics.org/public/articles /archivedetails.cfm?id=797.

[4] Bonev I., 2002, *Delta Parallel Robot - the Story of Success*, http://www.parallemic.org/Reviews/Review002.html.

[5] Bonev I., 2002, *What is going on with parallel robots?*, http://www.robotics.org/public/articles/archivedetails.cfm?id=798.

[6] Birglen L., Gosselin C., Pouliot N., Monsarrat B. and Laliberté T., 2002, "SHaDe, a new 3-DOF haptic device," *IEEE Transactions on Robotics and Automation*, **18**(2), pp. 166–175.

http://www.parallemic.org/Reviews/Review003.html.

[7] Vorndran S., 2002, *Low-Inertia Parallel-Kinematics Systems for Submicron Alignment and Handling*, http://www.parallemic.org/Reviews/Review012.html.

[8] Merlet J. P., 2002, "An initiative for the kinematics study of parallel manipulators," *Proceedings of the Workshop on Fundamental Issues and Future Research Directions for Parallel Mechanisms and Manipulators*, Québec, Québec, October 3–4, pp. 2–9.

[9] Brogårdh T., 2002, "PKM research - important issues, as seen from a product development perspective at ABB," *Proceedings of the Workshop on Fundamental Issues and Future Research Directions for Parallel Mechanisms and Manipulators*, Québec, Québec, October 3–4, pp. 68–82.

[10] Hunt K. H., 1973, "Constant-velocity shaft couplings: a general theory, " *ASME Journal of Engineering for Industry*, **95B**, May, pp. 455–464.

[11] Hunt K. H., 1983, "Structural kinematics of inparallel-actuated robot-arms," *ASME Journal of Mechanical Design*, **105**(4), pp. 705–712.

[12] Earl C.F. and Rooney J., 1983, "Some kinematic structures for robot manipulator design," *Journal of Robotic Systems*, **18**(5), pp. 213–219.

[13] Hervé J. M. and Sparacino F., 1991, "Structural synthesis of parallel robots generating spatial translation," *Proceedings of the fifth International Conference on Advanced Robotics*, Pisa, Italy, June 19-22, **1**, 808–813.

[14] Hervé J. M., 1995, "Design of parallel manipulators via the displacement group," *Proceedings of the 9th World Congress on the Theory of Machines and Mechanisms*, Milan, Italy, **3**, pp. 2079–2082.

[15] Tsai L. W., 1999, "The enumeration of a class of three-DOF parallel manipulators," *Proceedings of the 10th World Congress on the Theory of Machines and Mechanisms*, Oulu, Finland, **3**, pp. 1121–1126.

[16] Karouia K. and Hervé J. M., 2000, "A three-DOF Tripod for generating spherical rotation," *Advances in Robot Kinematics*, J. Lenarčič and M. M. Stanišič (eds.), Kluwer Academatic Publishers, pp. 395–402.

[17] Frisoli A., Checcacci D., Salsedo F. and Bergamasco M., 2000, "Synthesis by screw algebra of translating in-parallel actuated mechanisms," *Advances in Robot Kinematics*, J. Lenarčič and M. M. Stanišič (eds.), Kluwer Academatic Publishers, pp. 433–440.

[18] Kong X. and Gosselin C. M., 2001, "Generation of parallel manipulators with three translational degrees of freedom using screw theory," *Proceedings of the CCToMM Symposium on Mechanisms, Machines, and Mechatronics*, Montreal, Canada. June 1.

[19] Zlatonov D. and Gosselin C.M., 2001, "A new parallel architecture with four degrees of freedom," *Proceedings of the 2nd Workshop on Computational Kinematics*, Seoul, Korea, pp. 57-66.

[20] Yang T.-L., Jin Q., Liu A.-X. Yao F.-H. and Luo Y., 2001, "Structure synthesis of 4-DOF (3-translation and 1-rotation) parallel robot mechanisms based on the units of single-opened-chain," *Proceedings of the 2001 ASME Design Engineering Technical Conference and Computers and Information in Engineering Conference*, Pittsburgh, PA, September 9-12, DETC2001/DAC-21152.

[21] Jin Q., Yang T.-L., Liu A.-X. Shen H.-P. and Yao F.-H., 2001, "Structure synthesis of a class of 5-DOF parallel robot mechanisms based on single-opened-chain units," *Proceedings of 2001 ASME Design Engineering Technical Conferences and Computers and Information in Engineering Conference*, Pittsburgh, PA, September 9-12, DETC2001/DAC-21153.

[22] Carricato M. and Parenti-Castelli V., 2001, "A family of 3-DOF translational parallel manipulators," *Proceedings of the 2001 ASME Design Engineering Technical Conferences & Computers and Information in Engineering Conference*, Pittsburgh, PA, September 9-12, DETC2001/DAC-21035.

[23] Huang Z. and Li Q.C., 2001, "Two novel symmetrical 5-DOF parallel mechanisms," *Journal of Yanshan University*, 2001, **25**(4), pp. 283-286.

[24] Huang Z. and Li Q.C., 2002, "Construction and kinematic properties of 3-UPU parallel mechanisms," *Proceedings of the 2002 ASME Design Engineering Technical Conferences & Computers and Information in Engineering Conference*, Montreal, DETC2002/MECH-34321.

[25] Huang Z. and Li Q.C., 2002, "Some novel lower-mobility parallel mechanisms," *Proceedings of the 2002 ASME Design Engineering Technical Conferences & Computers and Information in Engineering Conference*, Montreal, DETC2002/MECH-34299.

[26] Huang Z. and Li Q.C., 2002, "On the type synthesis of lower-mobility parallel manipulators," *Proceedings of the Workshop on Fundamental Issues and Future Research Directions for Parallel Mechanisms and Manipulators*, Québec, Québec, October 3–4, pp. 272–283.

[27] Huang Z. and Li Q.-C., 2002, "General Methodology for the type synthesis of lower-mobility symmetrical parallel manipulators and several novel manipulators," *International Journal of Robotics Research*, **21**(2), pp. 131–145.

[28] Kong X. and Gosselin C. M., 2002, "Type synthesis of 3-DOF spherical parallel manipulators based on screw theory," *Proceedings of the 2002 ASME Design Engineering Technical Conferences and Computers and Information in Engineering Conference*, Montreal, Canada, September 29–October 2, DETC2002/MECH-21152.

[29] Tsai L.W., 2002, "Type synthesis of parallel manipulators with lower-mobility," *Keynote presented at the 2002 ASME Design Engineering Technical Conferences and Computers and Information in Engineering Conference*, Montreal, Canada, September 29-October 2.

[30] Hervé J. M., 1999, "The Lie group of rigid body displacements, a fundamental tool for mechanisms design," *Mechanism and Machine Theory*, **34**(5), pp. 719–730.

[31] Angeles J., 2002, "The qualitative synthesis of parallel manipulators," *Proceedings of the Workshop on Fundamental Issues and Future Research Directions for Parallel Mechanisms and Manipulators*, Québec, Québec, October 3–4, pp. 160–169.

[32] Merlet J. P., 2002, *Parallel Robots*, Kluwer Academic Publishers, Dordrecht.

[33] Bonev I., 2002, *Bibliography on Parallel Mechanisms*, http://www.robotics.org.

[34] Raghavan M., 1993, "The Stewart platform of general geometry has 40 configurations," *ASME Journal of Mechanical Design*, **115**(2), pp. 277–282.

[35] Dasgupta B. and Mruthyunjaya T.S., 1998, "Singularity-free path planning for the Stewart platform manipulator," *Mechanism and Machine Theory*, **33**(6), pp. 711–725.

[36] Clavel R., 1990, "Device for the movement and positioning of an element in space", *United States Patent*, No. 4976582.

[37] Wang G., 1992, "Forward displacement analysis of a class of the 6-6 Stewart platforms," *Proceedings of the 1992 ASME Design Technical Conferences*, DE-Vol. 45, pp. 113–117.

[38] Zhang C.D. and Song S. M., 1992, "Forward kinematics of parallel (Stewart) platforms with closed form solutions," *Journal of Robotic Systems*, 1992, **9**(4), pp. 93–112.

[39] Gosselin C. M. and Merlet J. P., 1994, "The direct kinematics of planar parallel manipulators: special architectures and number of solutions," *Mechanism and Machine Theory*, **29**(8), pp. 1083–1097.

[40] Kong X., and Yang T. 1994, "Generation and forward displacement analyses of two new classes of analytic 6-SPS parallel manipulators," *Proceedings of the 1994 ASME Design Technical Conferences*, Minneapolis, MN, DE-Vol. 72, pp. 323–330.

[41] Kong X., 1995, "Forward displacement and singularity analysis a class of analytic 3-RPR planar parallel manipulator," *Proceedings of Advanced Manufacturing Technology* (in Chinese), Beijing, China, pp. 103-104.

[42] Merlet J. P., 1996, "Direct kinematics of planar parallel manipulators," *Proceedings of the 1996 IEEE International Conference on Robotics and Automation*, San Diego, **4**, pp. 3744-3749.

[43] Gosselin C. M., and Gagné M., 1995, "A closed-form solution for the direct kinematics of a special class of spherical three-degree-of-freedom parallel manipulators," *Proceedings of the Second Workshop on Computational Kinematics*, September 4–6, INRIA, Sophia-Antipolis, France, pp. 231–240.

[44] Gosselin C. M. and Hamel J.-F., 1996, "The agile eye: a high-performance three-degree-of-freedom camera-orienting device", *Proceeding of the 1996 IEEE International Conference on Robotics and Automation*, San Diego, pp. 781–786.

[45] Bruyninckx H. and De Schutter J., 1996, "A class of fully parallel manipulators with closed-form forward kinematics," *Recent Advances in robot kinematics*, J. Lenarčič and V. Parenti-Castelli (eds.), Kluwer Academic Publishers, pp. 411-420.

[46] Kong X., 1998, "Forward displacement analysis of three new classes of analytic spherical parallel manipulators," *Proceedings of the 1998 ASME Design Engineering Technical Conferences*, September 13-16, Atlanta, GA, DETC98/MECH-5953.

[47] Yang J. and Geng Z. J., 1998, "Closed form forward kinematics solution to a class of Hexapod robots," *IEEE Transactions on Robotics and Automation*, **14**(3), pp. 503-508.

[48] Weisstein E. W., 2002, "Algebraic Equations," *Eric Weisstein's World of Mathematics*, http://mathworld.wolfram.com/topics/AlgebraicEquations.html.

[49] Erdman A. G., 1993, "Modern Kinematics: Developments in the Last Forty Years," John Wiley & Sons Inc., Chap 3.

[50] Yang T.-L., 1983, "Structural analysis and number synthesis of spatial mechanisms," *Proceedings of the 6th World Conference on the Theory of Machines and Mechanism*, New Dehli, Vol. **1**, pp. 280–283.

[51] Yang T.-L. and Yao H.-F., 1992, "Topological characteristics and automatic generation of structural synthesis of spatial mechanisms: Part II – Automatic generation of structural types of kinematic chains," *Proceedings of the 1992 ASME Design Technical Conference*, Scottsdale, AZ, USA, DE-Vol. 47, pp. 187–190.

[52] Kong X. and Yang T.-L., 1994, "Detection of improper general spatial kinematic chains involving deferent types of joints," *Proceedings of the 1994 ASME Design Technical Conferences*, DE-Vol. 70, pp. 323–328.

[53] Kong X., 1994, *A study on the theory of kinematic analysis of multi-loop spatial linkages* (in Chinese), Ph.D. Thesis, Southeast University, Nanjing, China.

[54] Luo Y., Yang T. and Seireg A., 1998, "Structural types synthesis of multi-loop spatial kinematic chains with general variable constraints ," *Proceedings of the 1998 ASME Design Engineering Technical Conferences*, September 13-16, Atlanta, GA, DETC98/MECH-5895.

[55] Kong X., 1999, "Detection of input interference in spatial linkages," *Journal of Mechanical Transmission* (in Chinese), **23**(4), pp. 23–25.

[56] Agrawal S. K., 1990, "Rate kinematics of in-parallel manipulators systems," *Proceedings of the 1990 IEEE International Conference on Robotics and Automation*, Cincinnati, USA, pp. 104–109.

[57] Huang Z. and Zhao T.S., 2000, "Theory and application of selecting components of spatial mechanisms," *Chinese Journal of Mechanical Engineering* (in Chinese), 2000, **36**(10), pp. 81-85.

[58] Huang Z., Fang Y.F., 1996, "Kinematic characteristics analysis of 3-DOF in-parallel actuated pyramid mechanisms," *Mechanism and Machine Theory*, **31**(8), pp. 1009-1018.

[59] Kong X. and Gosselin C. M., 2000, "Classification of 6-SPS parallel manipulators according to their components," *Proceedings of the 2000 ASME Design Engineering Technical Conferences & Computers and Information in Engineering Conference*, Baltimore, MD, Sept. 10-13, DETC2000/MECH-14105.

[60] Innocenti C. and Parenti-Castelli V., 1990, "Direct position analysis of the Stewart platform mechanism," *Mechanism and Machine Theory*, **25**(6), pp. 611–621.

[61] Husty M., 1996, "An algorithm for solving the direct kinematic of Stewart-Gough-type platforms," *Mechanism and Machine Theory*, **31**(4), pp. 365–380.

[62] Wampler C. W., 1996, "Forward displacement analysis of general six-in-parallel SPS (Stewart) platform manipulators using soma coordinates," *Mechanism and Machine Theory*, **31**(3), pp. 331-337.

[63] Baron L. and Angeles J., 1995, "A linear algebraic solution of the direct kinematics of parallel manipulators using a camera," *Proceedings of the ninth World Congress on the Theory of Machines and Mechanisms*, Milan, Italy, **3**, pp. 1925–1929.

[64] Parenti-Castelli V. and Di Gregorio R., 1998, "Real time computation of the actual posture of the general geometry 6-6 fully-parallel mechanism using two extra sensors," *ASME Journal of Mechanical Design*, **120**(4), pp. 549–554.

[65] Parenti-Castelli V. and Di Gregorio R., 1999, "Determination of the actual posture of the general Stewart platform using only one extra sensor," *ASME Journal of Mechanical Design*, **121**(1), pp. 21–25.

[66] Innocenti C., 1998, "Closed-form determination of the location of the rigid body by seven in-parallel linear-transducers," *ASME Journal of Mechanical Design*, **120**(2), pp. 293–298.

[67] Tancredi L. and Teillaud M., 1999, "Application de la géometrie synthétique au problème de modélisation géométrique directe des robots parallèles," *Mechanism and Machine Theory*, **34**(2), pp. 255–269.

[68] Bonev I. A. and Ryu J., 1999, "A new method for solving the direct kinematics of general 6-6 Stewart platforms using three linear extra sensors," *Mechanism and Machine Theory*, **35**(3), pp. 423–436.

[69] Angeles J., 1997, *Fundamentals of Robotic Mechanical Systems*, Springer-Verlag New York.

[70] Agrawal S. K., 1991, "Study of an in-parallel mechanism using reciprocal screws," *Proceedings of the Ninth World Congress on the Theory of Machines and Mechanisms*, Prague, August 26-31, **2**, pp. 405–408.

[71] Tsai L.-W., 1999, *Robot analysis: The Mechanics of Serial and Parallel Manipulators*, John Wiley & Sons Inc.

[72] Kumar V., Waldron K. J., Chrikjian G. and Lipkin H., 2000, "Applications of screw system system theory and Lie theory to spatial kinematics: A Tutorial," *Proceedings of the 2000 ASME Design Engineering Technical Conferences & Computers and Information in Engineering Conference*. Baltimore.

[73] Huang Z. and Tesar D., 1985, "Modeling formulation of six-DOF parallel multiloop manipulators," *Proceedings of the Fourth IFToMM Symposium on Linkage and CAD Design Methods: Part 1*, Bucharest, Romania, July 4-9, Paper No. 20.

[74] Freeman R. A. and Tesar D., 1988, "Dynamic modeling of serial and parallel mechanisms/robotic systems: part I – Methodology," *Proceedings of 1988 ASME Design Technical Conferences*, Kissimee, Florida, September 25-28, pp. 7-18.

[75] Freeman R. A. and Tesar D., 1988, "Dynamic modeling of serial and parallel mechanisms/robotic systems: part I – Applications," *Proceedings of 1988 ASME Design Technical Conferences*, Kissimee, Florida, September 25-28, pp. 19-27.

[76] Kong X., 1990, *Kinematic influence coefficients method for the analysis of spatial linkages* (in Chinese), Master's Thesis, Yanshan University, Qinhuangdao, China.

[77] Huang Z. and Wang H.B, 1992, "Dynamic force analysis of n-DOF multi-Loop complex spatial mechanisms," *Mechanism and Machine Theory*, 1992, **27**(1), pp. 97-105.

[78] Huang Z., Kong L. F. and Fang Y.F., 1997, *Mechanism Theory of Parallel Robotic Manipulators and Control* (in Chinese), China Machinery Press, Beijing, China.

[79] Gosselin C. M. and Angeles J., 1990, "Singularity analysis of closed-loop kinematic chains," *IEEE Transactions on Robotics and Automation*, **6**(3), pp. 281–290.

[80] Ma O. and Angeles J., 1991, "Architecture singularities of platform manipulators," *Proceedings of the 1991 IEEE International Conference on Robotics and Automation*, Sacramento, CA, April 9-11, **2**, pp. 1542–1547.

[81] Zlatanov D., Fenton R. G. and Benhabib B., 1994, "Analysis of the instantaneous kinematics and singular configurations of hybrid chain manipulators," *Proceedings of the 1994 ASME Design Technical Conferences*, Minneapolis, MN, DE-Vol. 72, pp. 467–476.

[82] Zlatonov D., Fenton R. G. and Benhabib B., 1994, "Singularity analysis of mechanisms and robots via a motion-space model of the instantaneous kinematics," *Proceedings of the 1994 IEEE International Conference on Robotics and Automation*, pp. 980–991.

[83] Park F. C. and Kim J. M., 1999, "Singularity analysis of closed kinematic chains," *ASME Journal of Mechanical Design*, **121**(1), pp. 32–38.

[84] Merlet J. P., 1988, "Parallel manipulators - Part 2: Singular configurations and Grassmann geometry," *Technical Report*, INRIA, Sophia Antipolis, France.

[85] Merlet J. P., 1989, "Singular configurations of parallel manipulators and Grassmann geometry," *The International Journal of Robotics Research*, **8**(5), pp. 45–56.

[86] Collins C. L. and Long G. L., 1994, "Line geometry and the singularity analysis of an in-parallel hand controller for force-reflected teleoperation," *Proceedings of the 1994 ASME Design Technical Conferences*, Minneapolis, MN, DE-Vol. 72, pp. 361–369.

[87] Notash L., 1998, "Uncertainty configurations of parallel manipulators," *Mechanism and Machine Theory*, **33**(1/2), pp. 123–138.

[88] Kumar V., 1992, "Instantaneous kinematics of parallel chain mechanisms," *ASME Journal of Mechanical Design*, **114**(3), pp. 349–358.

[89] Agrawal S. K. and Roth B., 1992, "Statics of in-parallel manipulator systems," *ASME Journal of Mechanical Design*, **114**(4), pp. 564–468.

[90] Ebert-Uphoff I, Lee J-K and Lipkin H., 2000, "Characteristic tetrahedron of wrench singularities for parallel manipulators with three legs," *Proceedings of a Symposium Commemorating the Legacy, Works, and Life of Sir Robert Stawell*

*Ball upon the 100th Anniversary of A Treatise on theory of Screws*, Cambridge, UK, July 9-11.

[91] Huang Z., Zhao Y.S., Wang J. and Yu J. J., 1999, "Kinematic principle and geometrical condition of general-linear-complex special configuration of parallel manipulators," *Mechanism and Machine Theory*, **34**(8), pp. 1171-1186.

[92] Angeles J., Yang G. and Chen I.-M., 2001, "Singularity analysis of three-legged, six-DOF platform manipulators with RRRS legs," *Proceedings of the 2001 IEEE/ASME International Conference on Advanced Intelligent Mechatronics*, Como, Italy, July 8-12, pp. 32–36.

[93] Mayer St-Onge B. and Gosselin C. M., 2000, "Singularity analysis and representation of the general Gough-Stewart platform," *The International Journal of Robotics Research*, **19**(3), pp. 271–288.

[94] Basu D. and Ghosal A., 1997, "Singularity analysis of platform-type multi-loop spatial mechanisms," *Mechanism and Machine Theory*, 1997, **32**(3), pp. 375–389.

[95] Yang G., Chen I.-M., Lin W. and Angeles J., 2001, "Singularity analysis of three-legged parallel robots based on the passive-joint velocities," *Proceedings of the 2001 IEEE International Conference on Robotics and Automation*, Seoul, Korea. May 21-26, pp. 2407-2412.

[96] Kong X. and Yang T., 1996, "Dimensional type synthesis and special configuration analysis of analytic 6-SPS parallel manipulators," *High-Tech Letters* (in Chineses), **6**(6), pp. 17-20.

[97] Kong X., 1998, "Generation of singular 6-SPS parallel manipulators," *Proceedings of the 1998 ASME Design Engineering Technical Conferences*, Atlanta, GA, Sept. 13-16, DETC98/MECH-5952.

[98] Karger A. and Husty M., 1997, "Singularities and self-motions of Stewart-Gough platforms," *Proceedings of the NATO Advanced Study Institute on Computational Methods in Mechanisms*, Angeles J. and Zakhariev E. (Eds.), Varna, Bulgaria, June 16-28, **II**, pp. 279–288.

[99] Karger A. and Husty M., 1998, "Architecture singular parallel manipulators," *Advances in Robotic Kinematics: Analysis and Control*, J. Lenarcic and M. Husty (eds.), Kluwer Academic Publishers, pp. 445–454.

[100] Karger A. and Husty M., 2000, "Self-motions of Griffis-Duffy Type parallel manipulators," *Proceedings of the 2000 IEEE International Conference on Robotics and Automation*, San Francisco, CA, April 24-28, **2**, pp. 7–12.

[101] Roschel Ö. and Mick S., 1998, "Characterization of architecturally shaky platforms," *Advances in Robotic Kinematics: Analysis and Control*, J. Lenarcic and M. Husty(eds.), Kluwer Academic Publishers, pp. 465–474.

[102] Wohlhart, K., 2002, "Synthesis of architecturally mobile double-planar platforms," *Advances in Robot Kinematics – Theory and Applications*, Lenarčič J. and Thomas F. (Eds.), Kluwer Academic Publishers, pp. 473–483.

[103] McAree P. R. and Daniel R.W., 1999, "Explanation of never-special assembly changing motions for 3-3 parallel manipulators," *International Journal of Robotics Research*, **18**(6), pp. 556–574.

[104] Merlet J. P., Gosselin C. M. and Mouly N., 1998, "Workspaces of planar parallel manipulators," *Mechanism and Machine Theory*, **33**(1/2), pp. 7–20.

[105] Gosselin C. M., 1990, "Determination of the workspace of 6-DOF parallel manipulators," *ASME Journal of Mechanisms, Transmissions, and Automation in Design*, **112**(3), pp. 331–336.

[106] Gosselin C. M. and Angeles J., 1989, "The optimum kinematic design of a spherical three-degree-of-freedom parallel manipulator," *ASME Journal of Mechanisms, Transmission and Automation in Design*, **111**(2), pp. 202–207.

[107] Boudreau R. and Gosselin C. M., 2001, "La synthèse d'une plate-forme de Gough-Stewart pour un espace atteignable prescrit," *Mechanism and Machine Theory*, **36**(3), pp. 327–342.

[108] Hay A. M. and Snyman J. A, 2002, "Design of parallel manipulators for optimal conditioning throughout a prescribed workspace," *Proceedings of the Workshop on Fundamental Issues and Future Research Directions for Parallel Mechanisms and Manipulators*, Québec, Québec, October 3–4, pp. 267–271.

[109] Laliberté T., Gosselin C. M. and Côté G., 1999, "Rapid prototyping of mechanisms," *Proceedings of 10th World Congress on the Theory of Machines and Mechanisms*, Oulu, Finland, **3**, pp. 959-964.

[110] Hunt K. H., 1990, *Kinematic Geometry of Mechanisms*, Cambridge University Press.

[111] Bruyninckx H., 1998, "Unified kinematics for serial, parallel and mobile robots," *Advances in Robotic Kinematics: Analysis and Control*, J. Lenarcic and M. Husty (eds.), Kluwer Academic Publishers, pp. 343–352.

[112] Waldron K. J., 1967, "Hybrid overconstrained linkages," *Journal of Mechanisms*, **3**, pp. 73-78.

[113] Yang T. L., 1986, "Kinematic structural analysis and spatial single-loop chains," *Proceedings of the 1986 ASME Design Technical Conferences*, Columbus, OH, ASME paper 86-DET-181.

[114] Zlatanov D., Bonev I. and Gosselin C. M., 2002, "Constraint singularities of parallel mechanisms," *Proceedings of the 2002 IEEE International Conference on Robotics and Automation*, Washington DC, May, pp. 496–502.

[115] Di Gregorio R. and Parenti-Castelli V., 1999, "Mobility analysis of the 3-UPU parallel mechanism assembled for a pure translational motion," *Proceedings of the 1999 IEEE/ASME International Conference on Advanced Intelligent Mechatronics*, pp. 520-525.

[116] Appleberry W. T., 1992, "Anti-Rotation Positioning Mechanism," *United States Patent*, No. 5156062.

[117] Di Gregorio R. and Parenti-Castelli V., 1998, "A translational 3-DOF parallel manipulator," *Advances in Robot Kinematics: Analysis and Control*, J. Lenarčič and M. Husty (eds.), Kluwer Academatic Publishers, pp. 49–58.

[118] Zhao T. S. and Huang Z., 2000, "A novel three DOF translational platform mechanism and its kinematics," *Proceedings of the 2000 ASME Design Engineering Technical Conferences & Computers and Information in Engineering Conference*, DETC2000/MECH-14101.

[119] Jin Q., and Yang T.-L., 2001, "Position analysis for a class of novel 3-DOF translational parallel robot mechanisms," *Proceedings of the 2001 ASME Design Engineering Technical Conferences & Computers and Information in Engineering Conference*, Pittsburgh, PA, Sept. 10-12, DETC2001/DAC-21151

[120] Carricato M. and Parenti-Castelli V., 2001, "Position Analysis of a New Family of 3-DOF Translational Parallel Robot Manipulators," *Proceedings of the 2000 ASME Design Engineering Technical Conferences & Computers and Information in Engineering Conference*, Sept. 10-12, DETC2001/DAC-21036,

[121] Cox D. J. and Tesar D., 1989, "The dynamic model of a three-degree-of-freedom parallel robotic shoulder module," *Proceedings of the Fourth International Conference on Advanced Robotics*, Columbus.

[122] Craver W. M., 1989, *Structural analysis and design of a three-degree-of-freedom robotic shoulder module*. Master's Thesis, The University of Texas at Austin.

[123] Di Gregorio R., 2001, "A new parallel wrist using only revolute pairs: the 3-RUU wrist," *Robotica*, **19**(3), pp. 305–309.

[124] Vischer P. and Clavel R., 2000, "Argos: A novel 3-DOF parallel wrist mechanism," *The International Journal of Robotics Research*, **19**(1), pp. 5–11.

[125] Di Gregorio R., 2001, "Kinematics of a new spherical parallel manipulator with three equal legs: the URC wrist," *Journal of Robotic Systems*, **18**(5), pp. 213–219.

[126] Phillips J., 1984, *Freedom in Machinery: Volume 2 Screw Theory Exemplified*, Cambridge University Press, pp.164–165

[127] Karouia M. and Hervé J. M., 2002a, "A family of novel orientational 3-DOF parallel robots," *Proceedings of RomanSy'2002*, Udine, Italy, July 1–4.

[128] Hervé J. M. and Karouia M., 2002b, "The novel 3-RUU wrist with no idle pair," *Proceedings of the Workshop on Fundamental Issues and Future Research Directions for Parallel Mechanisms and Manipulators*, Québec, Québec, October 3–4, pp. 284–285.

[129] Rolland L. H., 1999, "The Manta and the Kanuk: Novel 4-DOF parallel mechanisms for industrial handling," *Proceedings of 1999 International Mechanical Engineering Congress and Exposition*, November 14-19, Nashville, USA.

[130] Pierrot F., Marquet F., Company O., and Gil T., 2001, "H4 parallel robot: modeling, design and preliminary experiments," *Proceedings of the 2001 IEEE International Conference on Robotics & Automation*, Seoul, Korea, May 21–26, pp. 3256–3261.

[131] Li S., Huang Z. and Zuo R., 2002, "Kinematics of a special 3-DOF, 3-TPT parallel manipulator," *Proceedings of the 2002 ASME Design Engineering Technical Conferences & Computers and Information in Engineering Conference*, Montreal, DETC2002/MECH-34322.

[132] Ceresole E., Fanghella P. and Galletti C., 1996, "Assur's groups, AKCS, basic trusses, SOCS, etc.: modular kinematics of planar linkages," *Proceedings of the 1996 ASME Design Engineering Technical Conferences*, 96-DETC/MECH-1027.

[133] Chiang C. H., 1996, *Kinematics of spherical mechanisms*, McGraw-Hill Inc.

[134] Duffy J., 1980, *Analysis of Mechanisms and Robot Manipulators*, John Wiley & Sons.

[135] Lazard D. and Merlet J. P., 1994, "The (true) Stewart platform has 12 configurations," *Proceedings of the 1994 IEEE International Conference on Robotics and Automation*, **3**, pp. 2160–2165.

[136] Kong X. and Gosselin C. M., 2001, "Analytical manipulators with three translational degrees of freedom", *United States Patent application*, Filed on May 31.

[137] Kong X. and Gosselin C. M., 2002, "Type synthesis of linear translational parallel manipulators," *Advances in Robot Kinematics – Theory and Applications*, Lenarčič J. and Thomas F. (Eds.), Kluwer Academic Publishers, pp. 411–420.

[138] Kong X. and Gosselin C. M., 2002, "A class of 3-DOF translational parallel manipulators with linear input-output equations," *Proceedings of the Workshop on Fundamental Issues and Future Research Directions for Parallel Mechanisms and Manipulators*, Québec, Québec, October 3–4, pp. 25–32.

[139] Carricato M., 2001, "Singularity-free fully-isotropic translational parallel manipulators," Ph.D. Thesis, University of Bologna, Italy.

[140] Carricato M. and Parenti-Castelli V., 2002, "Singularity-free fully-isotropic translational parallel mechanisms" *The International Journal of Robotics Research*, **21**(2), pp. 161–174.

[141] Kim H. S. and Tsai L.-W. 2002, "Evaluation of a Cartesian parallel manipulator", *Advances in Robot Kinematics – Theory and Applications*, Lenarčič J. and Thomas F. (Eds.), Kluwer Academic Publishers, pp. 21–28.

[142] Kong X. and Gosselin C. M., 2002, "Kinematics and singularity analysis of a novel type of 3-CRR 3-DOF translational parallel manipulator," *The International Journal of Robotics Research*, (in press).

[143] Carricato M. and Parenti-Castelli V., 2002, "Singularity-free fully-isotropic translational parallel manipulators", *Proceedings of the 2002 ASME Design Engineering Technical Conferences & Computers and Information in Engineering Conference*, Montreal, Canada, Sept. 29-Oct. 2, DETC2001/MECH-34301.

[144] Kim H. S. and Tsai L.-W., 2002, "Design optimization of a Cartesian parallel manipulator," *Proceedings of the 2002 ASME Design Engineering Technical Conferences & Computers and Information in Engineering Conference*, Montreal, Canada, Sept. 29-Oct. 2, DETC2001/MECH-34323.

[145] Ridgeway S., Crane III C. D., Adist P. and Harrell R., 1992, "The mechanical design of a parallel actuated joint for an articulated mobile robot," *Proceedings of the 1992 ASME Design Technical Conferences*, Scottsdale, AZ, DE-Vol. 45, pp. 591-597.

[146] Ridgeway S. C., Crane C. D. and Duffy J., 1996, "A forward analysis of a two degree of freedom parallel manipulator," *Recent advances in robot kinematics*, Lenarčič J. and Parenti-Castelli V.(eds.), Kluwer Academic Publishers, pp. 431-440.

[147] Barbeau E. J., 1989, *Polynomials*, Springer, New York.

[148] Kong X. and Gosselin C. M., 2002, "Generation and forward displacement analysis of RPR-PR-RPR analytic planar parallel manipulators," *ASME Journal of Mechanical Design*, **124**(2), pp. 294-300.

[149] Chablat D. and Wenger Ph., 1998, "Working modes and aspects in fully parallel manipulators," *Proceedings of the 1998 IEEE International Conference on Robotics & Automation*, Leuven, Belgium, pp. 1964–1969.

[150] Weisstein E. W., 2001, "Steinmetz Solid," *Eric Weisstein's World of Mathematics*, http://mathworld.wolfram.com/SteinmetzSolid.html.

[151] Mlynarski T., 1996, "Position analysis of planar linkages using the method of modification of kinematic units," *Mechanism and Machine Theory*, **31**(6), pp. 831–838.

[152] Collins C. L., 1999, "Classification and forward kinematics of planar parallel manipulators," *Proceedings of the International Workshop on Parallel Kinematic Machines PKM'99*, Milan, Italy, November.

[153] Shen H.-P. and Yang T.-L., 1994, "A new method and automatic generation for kinematic analysis of complex planar mechanisms based on the ordered single-opened-chains," *Proceedings of the 1994 ASME Design Technical Conferences*, DE-Vol. 70, 493–500.

[154] Sefrioui J. and Gosselin C.M., 1992, "Singularity analysis and representation of planar parallel manipulators," *Robotics and Autonomous Systems*, **10**(4), pp. 209–224.

[155] Sefrioui J. and Gosselin C.M., 1995, "On the quadratic nature of the singularity curves of planar three-degree-of-freedom parallel manipulators," *Mechanism and Machine Theory*, **30**(4), pp. 533–551.

[156] Collins C. L. and McCarthy J. M., 1998, "The quartic singularity surfaces of planar platforms in the Clifford algebra of the projective plane," *Mechanism and Machine Theory*, **33**(7), pp. 931-944.

[157] Wenger Ph. and Chablat D., 1998, "Workspace and assembly modes in fully-parallel manipulators: A descriptive study," *Advances in Robot Kinematics: Analysis and Control*, J. Lenarčič and M. Husty (eds.), Kluwer Academatic Publishers, pp. 117–126.

[158] Zhao X. and Peng S., 2001, "Research on the singular configuration of parallel manipulators," *Chinese Journal of Mechanical Engineering* (in Chinese), 2001, **36**(5), pp. 35–37.

[159] Shi X., and Fenton R. G., 1992, "Structural instabilities of in platform type parallel manipulators due to singular configurations," *Proceedings of the 1992 ASME Design Technical Conferences*, Scottsdale, AZ, DE-Vol. 45, pp. 347–352.

[160] Innocenti C. and Parenti-Castelli V., 1998, "Singularity-free evolution from one configuration to another in serial and fully-parallel manipulators," *ASME Journal of Mechanical Design*, **120**(1), pp. 73–79.

# Appendix A

# Coefficients of Eq. (7.3)

$$
\begin{aligned}
e_6 &= d_{11}c_{11}d_{21} - d_{12}c_{11}d_{22} - d_{11}c_{12}d_{22} - d_{12}c_{12}d_{21} + c_{12}^2 d_{21} - c_{11}c_{22}d_{12} \\
&\quad -c_{12}c_{21}d_{12} + d_{12}^2 c_{21} - c_{12}c_{22}d_{11} + c_{11}c_{21}d_{11} + 2d_{11}c_{22}d_{12} - c_{11}^2 d_{21} \\
&\quad +2c_{11}c_{12}d_{22} - d_{11}^2 c_{21}
\end{aligned}
$$

$$
\begin{aligned}
e_5 &= c_{11}c_{22}d_{11} + d_{12}^2 c_{22} + c_{12}^2 d_{22} - c_{12}c_{22}d_{12} + d_{11}c_{11}d_{22} + c_{12}c_{21}d_{11} \\
&\quad -d_{12}c_{12}d_{22} - 2c_{11}c_{12}d_{21} - d_{11}^2 c_{22} - 2d_{11}c_{21}d_{12} + c_{11}c_{21}d_{12} \\
&\quad +d_{12}c_{11}d_{21} - c_{11}^2 d_{22} + d_{11}c_{12}d_{21}
\end{aligned}
$$

$$
\begin{aligned}
e_4 &= -2d_{22}c_{22} - c_{11}^2 d_{23} + d_{13}c_{11}d_{21} - 2d_{11}c_{21}d_{13} + d_{11}c_{13}d_{21} \\
&\quad +d_{11}c_{11}d_{23} - 2c_{11}c_{13}d_{21} + c_{13}c_{21}d_{11} + c_{11}c_{23}d_{11} + c_{11}c_{21}d_{13} \\
&\quad -d_{12}c_{13}d_{22} - d_{12}c_{12}d_{23} - d_{13}c_{12}d_{22} - c_{13}c_{22}d_{12} - c_{12}c_{22}d_{13} - c_{12}c_{23}d_{12} \\
&\quad +2d_{12}c_{22}d_{13} + 2c_{12}c_{13}d_{22} + 2d_{21}c_{21} - d_{11}^2 c_{23} + d_{12}^2 c_{23} + c_{12}^2 d_{23} \\
&\quad -d_{21}^2 + d_{22}^2 - c_{21}^2 + c_{22}^2
\end{aligned}
$$

$$
\begin{aligned}
e_3 &= d_{12}c_{11}d_{23} + d_{12}c_{13}d_{21} + c_{11}c_{23}d_{12} - 2c_{11}c_{12}d_{23} + c_{13}c_{21}d_{12} + c_{13}c_{22}d_{11} \\
&\quad + d_{11}c_{13}d_{22} + 2d_{22}c_{21} + d_{13}c_{11}d_{22} + c_{12}c_{23}d_{11} - 2c_{12}c_{13}d_{21} + c_{11}c_{22}d_{13} \\
&\quad - 2c_{11}c_{13}d_{22} + 2d_{21}c_{22} + c_{12}c_{21}d_{13} + d_{11}c_{12}d_{23} + d_{13}c_{12}d_{21} - 2c_{21}c_{22} \\
&\quad - 2d_{11}c_{22}d_{13} - 2d_{11}c_{23}d_{12} - 2d_{12}c_{21}d_{13} - 2d_{21}d_{22}
\end{aligned}
$$

$$
\begin{aligned}
e_2 &= c_{11}c_{22}d_{12} - c_{12}^2 d_{21} - c_{21}d_{13}^2 + d_{11}c_{12}d_{22} + c_{12}c_{22}d_{11} + 2d_{21}c_{23} - 2c_{11}c_{12}d_{22} \\
&\quad + c_{12}c_{21}d_{12} - c_{13}^2 d_{21} + d_{12}c_{12}d_{21} + d_{11}c_{13}d_{23} - 2d_{11}c_{22}d_{12} - d_{12}^2 c_{21} \\
&\quad + d_{13}c_{13}d_{21} + d_{12}c_{11}d_{22} + d_{13}c_{11}d_{23} + c_{11}c_{23}d_{13} - 2c_{21}c_{23} - 2d_{11}c_{23}d_{13} \\
&\quad - 2c_{11}c_{13}d_{23} - 2d_{21}d_{23} + c_{13}c_{23}d_{11} + c_{13}c_{21}d_{13} + 2d_{23}c_{21}
\end{aligned}
$$

$$
\begin{aligned}
e_1 &= d_{12}c_{12}d_{22} - 2c_{22}c_{23} - c_{22}d_{13}^2 + c_{12}c_{23}d_{13} + c_{12}c_{22}d_{12} + d_{13}c_{12}d_{23} - c_{12}^2 d_{22} \\
&\quad + 2d_{23}c_{22} + 2d_{22}c_{23} - 2d_{12}c_{23}d_{13} + c_{13}c_{22}d_{13} - 2d_{22}d_{23} + d_{13}c_{13}d_{22} \\
&\quad - d_{12}^2 c_{22} - c_{13}^2 d_{22} - 2c_{12}c_{13}d_{23} + c_{13}c_{23}d_{12} + d_{12}c_{13}d_{23}
\end{aligned}
$$

$$
\begin{aligned}
e_0 &= -c_{23}d_{13}^2 + 2d_{22}c_{22} + c_{13}c_{23}d_{13} + d_{13}c_{13}d_{23} + d_{12}c_{13}d_{22} + d_{12}c_{12}d_{23} \\
&\quad + d_{13}c_{12}d_{22} + c_{13}c_{22}d_{12} + c_{12}c_{22}d_{13} + c_{12}c_{23}d_{12} - 2d_{12}c_{22}d_{13} - 2c_{12}c_{13}d_{22} \\
&\quad - d_{23}^2 - c_{22}^2 - c_{12}^2 d_{23} + 2d_{23}c_{23} - c_{13}^2 d_{23} - d_{12}^2 c_{23} - d_{22}^2 - c_{23}^2
\end{aligned}
$$